

Lipid pathways in Huntington's disease

by

Luis Carlos Morales Burbano

A thesis submitted in partial fulfillment of the requirements for the degree of

Doctor of Philosophy

Department of Pharmacology
University of Alberta

© Luis Carlos Morales Burbano, 2018

Abstract

Huntington's disease (HD) is a monogenic neurodegenerative disorder characterized by progressive choreic movements, dystonia, motor incoordination, cognitive decline and behavioural changes. HD is caused by an abnormal increase in the number of CAG repeats in the exon 1 of the huntingtin (*HTT*) gene, leading to an expanded polyglutamine stretch in the HTT protein. Mutant huntingtin (muHTT) is prone to misfold into toxic conformations and to aggregate, impairing vesicular transport, mitochondrial metabolism, cell signalling and gene transcription, and leading to neuronal dysfunction and death in various brain regions.

Our laboratory and others have shown that two distinct lipid biosynthetic pathways, the mevalonate pathway and the pathway for the synthesis of gangliosides, are also impaired in HD, potentially contributing to disease pathogenesis.

The mevalonate pathway is responsible for the production of cholesterol and isoprenoids. Isoprenoids are used for the prenylation of small GTPases, a crucial post-translational modification that regulates small GTPases activity and a wide range of downstream cell processes, including vesicular traffic and autophagy. Several studies have investigated the synthesis of cholesterol in HD models, but whether impairment of the mevalonate pathway could also lead to defective protein prenylation was not known, and has been investigated in the first part of this thesis.

I showed that steady-state prenylation of various representative small GTPases is not affected in a wide range of cell and animal HD models, in spite of downregulation of the mevalonate pathway. However, levels of one of these small GTPases, RAB7, a protein involved in vesicular transport and selective autophagy, were significantly decreased across models of HD.

Together with cholesterol, gangliosides are another class of lipids that are highly enriched in the brain and are crucial for neuronal functions. Studies in our laboratory showed that gangliosides

levels are decreased in HD models and that administration of one ganglioside in particular, GM1, has profound therapeutic effects in HD mouse models. The underlying mechanisms were in part, investigated in this thesis.

I demonstrated that GM1 decreases accumulation of protein aggregates in HD cells, as well in a second model of proteotoxic stress represented by pharmacological inhibition of the ubiquitin-proteasome system, thus alleviating cellular stress.

Surprisingly, the beneficial effects of GM1 were not mediated by an increase in autophagy, a cellular process known to degrade muHTT aggregates and to be modulated by gangliosides in other model systems. Instead, I showed that administration of GM1 promotes the secretion of muHTT, as well as components of the aggresome, within extracellular vesicles (EVs). These are membrane-delimited vesicles that form within the multivesicular bodies (MVB) or that bud from the plasma membrane, carrying a wide array of proteins and nucleic acids, including toxic misfolded proteins. These data suggest that the neuroprotective activity of GM1 in HD models might be mediated, at least partially, by the secretion of toxic muHTT towards the extracellular space, thus relieving intracellular proteotoxic load in susceptible neurons.

Preface

This thesis is an original work by Luis Morales.

Part of the data shown in Chapter 3 was generated in collaboration with Dr. Amany Mohamed, a former Ph.D. student of the Department of Pharmacology, under the supervision of Dr. Elena Posse de Chaves (Department of Pharmacology, University of Alberta).

Data presented in chapter 6 have been generated in collaboration with Ms. Vaibhavi Kadam, a current student of the graduate program in Neuroscience (Neuroscience and Mental Health Institute, University of Alberta), under the supervision of Dr. Simonetta Sipione. Additionally, some of the analyses performed by electron microscopy were done by Dr. Nasser Tahbaz (Department of Cell Biology, University of Alberta).

Part of the data presented in Appendix I was generated in collaboration with Mrs. Alba Di Pardo, a former student in Dr. Sipione laboratory, and will be submitted for publication as a co-authored paper, which is currently in preparation. I contributed with experimental data, as well as with the preparation of the manuscript.

Chapters 4, 5 and 7 are my original work.

Acknowledgements

First, I would like to thank my Ph.D. supervisor, Dr. Simonetta Sipione, the person who has guided me through this long journey that has finally come to an end. I sincerely appreciate all the hard work you have been doing as my mentor during all these years. Your advice and feedback have helped me to become a better researcher every day. I am immensely grateful for giving me the opportunity to work with you. For sure, you will not be forgotten.

I would also like to thank Dr. Elena Posse de Chaves. More than once you have been emotional support, as well as the voice of reason.

To Dr. Luc Berthiaume, for your advice, comments and suggestions.

To all the current and past members of the Sipione laboratory, especially to Diego Ordóñez who worked by my side in order to standardize new techniques and methodologies that were the basis of much of this thesis. Of course, I'd like to thank Melanie Alpaugh, Sabine Schmelz, Mel Horkey, Danny Galleguillos, Mel Horkey and Qian Wang. I would also like to say thank you to our younger members of the laboratory, Vaibhavi Kadam, John Monyror and Aislinn Maguire. You have given me the opportunity to be part of your growth as future researchers.

To my little family here in Canada, Lina Parra, Libardo Estupiñán, and many other amazing people who have contributed to my happiness in one way or another. Hundreds of stories and adventures will be remembered forever.

To my parents who have given me everything I ever needed and more. Mom and Dad who are the pillars of my life, and my brother, who has been my role model since my infancy.

To my friends Edwin Insuasty and Heler Romero, two wonderful people I had the opportunity to grow with, both professionally and personally. In the case I did not say it before, I want to express how proud I am of both of you. Thanks for teaching me that friendship is forever.

Importantly, I'd like to thank Colciencias and the government of Colombia for providing me with the financial support for my Ph.D. studies.

And finally, to Adriana Briones, the person whose existence made all this possible. I will never have enough words to express my gratitude towards you.

Table of contents

Chapter 1: General background	1
1.1. General introduction.....	2
1.2. Epidemiology	3
1.3. Clinical Features.....	4
1.3.1. Diagnosis	4
1.3.2. Motor abnormalities	5
1.3.3. Non-motor abnormalities.....	6
1.4. Neuropathology.....	8
1.4.1. Neuronal pathways of the basal ganglia	9
1.4.2. Macroscopic alterations.....	10
1.4.3. Microscopic findings	12
1.5. Huntingtin functions and mutant huntingtin dysfunctions.....	16
1.5.1. The Huntingtin gene and protein	16
1.5.2. Function(s) of Huntingtin protein.....	19
1.5.3. Pathophysiology of HD: The loss and gain-of-function of mutant HTT	21
1.5.3.1. Cleavage, misfolding and aggregation of muHTT	22
1.5.3.2. Mitochondrial dysfunction.....	25
1.5.3.3. Transcriptional dysregulation	27
1.5.3.4. Impairment in protein clearance systems.....	29
1.6. Animal and cell models of HD.....	33
1.6.1. Non-mammalian models of HD	33
1.6.2. Mouse models of HD.....	33
1.6.3. Cell models of HD.....	35
1.7. Therapeutic approaches.....	36
1.8. General hypotheses and objectives of the thesis	38
1.9. Figures	40
Chapter 2: Materials and methods	42
2.1. Chemicals and reagents.....	43
2.2. Administration of GM1	43
2.3. Cell models.....	43

2.4. Animal models	47
2.5. Gene expression analysis	47
2.6. Preparation of Lipoprotein-Deficient Serum (LPDS)	48
2.7. Immunoblotting.....	48
2.8. Triton X114 fractionation.....	50
2.9. Cell transfection	51
2.10. Generation of stably-transfected cell lines.....	53
2.11. Immunocytochemistry.....	54
2.12. Lysosome staining.....	54
2.13. Image analysis	55
2.14. Protein p62 soluble/insoluble fractionation.....	56
2.15. Preparation of extracellular vesicle-depleted serum (EVDS)	56
2.16. Purification of extracellular vesicles from conditioned media.....	57
2.17. Fluorescent staining of extracellular vesicles.....	58
2.18. Transmission electron microscopy of extracellular vesicles.....	58
2.19. Detection and quantification of ganglioside GM1 in lysates and extracellular vesicles..	59
2.20. Filter trap assay	60
2.21. Statistical analysis	60
Chapter 3: The role of the mevalonate pathway in Huntington’s disease	61
3.1. Introduction	62
3.1.1. The mevalonate pathway: the biosynthesis of cholesterol, isoprenoids and more.....	62
3.1.2. The mevalonate pathway and Huntington’s disease.....	67
3.1.3. Small GTPases and HD	71
3.2. Results	76
3.2.1. Triton X114 fractionation of RAS and RAB7 is not affected in immortalized HD striatal cells	76
3.2.2. Triton X114 fractionation of RAS and RAB7 is not affected in HD neurons nor astrocytes	77
3.2.3. Triton X114 fractionation of RAS, RAB7 and RAB11 is not affected in brains of HD mice	78
3.2.4. Total levels of RAB7 are decreased across models of HD.....	79
3.3. Discussion	80
3.4. Figures.....	85

Chapter 4: GM1 reduces protein aggregation in two models of proteotoxic stress.....	99
4.1. Introduction	100
4.1.1. Ganglioside GM1: Synthesis and functions within the CNS	101
4.1.1.1. Synthesis	101
4.1.1.2. Functions of ganglioside GM1.....	103
4.1.2. Ganglioside GM1 and neurodegeneration.....	105
4.1.3. Ganglioside GM1 and HD.....	107
4.1.4. The aggresome: A general response to misfolded proteins and proteotoxic stress...	108
4.2. Results	112
4.2.1. Treatment with ganglioside GM1 reduces the amount of muHTT aggregates in cell models of HD.....	112
4.2.2. Treatment with ganglioside GM1 reduces protein aggregation in striatal cells after inhibition of the proteasome	113
4.3. Discussion	115
4.4. Figures.....	119
Chapter 5: Autophagy is not involved in the reduction of protein aggregates after GM1 treatment	131
5.1. Introduction	132
5.1.1. Autophagy: Molecular basis.....	132
5.1.2. The core machinery of autophagy	134
5.1.2.1. Cargo recognition.....	135
5.1.2.2. Fusion with the lysosome.....	137
5.1.3. Transcriptional regulation of autophagy.....	138
5.1.4. Autophagy in neurodegeneration and in HD.....	139
5.1.5. Autophagy and GM1	142
5.2. Results	143
5.2.1. Ganglioside GM1 does not affect autophagy markers in cells transfected with wtHTT or muHTT	143
5.2.2. GM1 does not affect LC3-II levels in a model of proteotoxic stress induced by MG132	144
5.2.3. GM1 does not affect MG132-induced phosphorylation of p62	145
5.2.4. GM1 treatment does not decrease p62 protein half-life in STHdh Q7/7 cells	146

5.2.5. GM1 treatment prevents upregulation of lysosomal genes and lysosome biogenesis in proteotoxic stress conditions, but not in basal conditions	146
5.3. Discussion	148
5.4. Figures	153
Chapter 6: GM1 increases the secretion of misfolded proteins via extracellular vesicles.....	160
6.1. Introduction	161
6.1.1. Extracellular vesicles: general concepts	161
6.1.2. A brief review of the history of EVs	162
6.1.3. Classification of EVs	162
6.1.4. Mechanisms of formation and secretion of EVs	163
6.1.5. Physiological and pathophysiological role of EVs.....	167
6.2. Results	170
6.2.1. GM1 promotes the secretion of extracellular vesicles from neuronal cells	170
6.2.2. Exogenously administered GM1 is internalized by cells and incorporated into extracellular vesicles.....	171
6.2.3. GM1 promotes the secretion of HTT via extracellular vesicles	172
6.2.4. GM1 promotes the secretion of p62 via extracellular vesicles in cells undergoing proteotoxic stress	174
6.3. Discussion	174
6.4. Figures	179
Chapter 7: General discussion and conclusions.....	193
7.1. Summary of findings.....	194
7.1.1. The mevalonate pathway is impaired in HD models, but protein prenylation is not affected	194
7.1.2. Exogenous supply of ganglioside GM1 reduces accumulation of aggregated proteins in an autophagy-independent manner, and increases misfolded protein secretion via extracellular vesicles	195
7.2. Overall significance of findings and concluding remarks.....	196
7.3. Future directions.....	197
7.4. Figures	198
Bibliography	199

Appendix I: Mutant HTT impairs nuclear transport of mSREBP2 and causes a defective upregulation of transcription of cholesterologenic genes upon culture in lipoprotein-deficient medium	290
Nuclear transport of mature SREBP2 is impaired in HD models.....	291
HD cells have impaired regulation of transcription of cholesterologenic genes upon culture in lipoprotein-deficient medium.....	291
Discussion	292
Figures	295
Appendix II: Tables	300

List of figures

Figure 1.1 The Huntington's disease brain.....	40
Figure 1.2. Simplified representation of the circuitry of the basal ganglia.....	41
Figure 3.1. The mevalonate pathway and Huntington's disease	85
Figure 3.2. Prenylation reactions of small GTPases	86
Figure 3.3. Triton X114 fractionation of RAS and RAB7 is not affected in immortalized HD striatal cells	88
Figure 3.4. Electrophoretic mobility shift assay confirms that prenylation of RAS and RAB7 is normal in HD cells	90
Figure 3.5. Triton X114 fractionation of RAS and RAB7 is not affected in HD neurons nor astrocytes.....	91
Figure 3.6. Triton X114 fractionation of RAS, RAB7 and RAB11 is not affected in brains of HD mice.....	93
Figure 3.7. Total levels of RAB7 are decreased in brain tissue and primary neurons from HD mice.....	95
Figure 3.8. Total levels of RAB7 are decreased across models of HD	97
Figure 4.1. Ganglioside GM1: Structure and synthesis	119
Figure 4.2. Ganglioside GM1 administration reduces the amount of muHTT in the brains of Q140/140 mice.....	121
Figure 4.3. Aggregates formed by muHTT are decorated by p62	122
Figure 4.4. Ganglioside GM1 treatment reduces the amount of muHTT aggregates in cell models	123
Figure 4.5. Ganglioside GM1 treatment reduces accumulation of polyubiquitinated proteins in STHdh Q7/7 cells undergoing proteotoxic stress	125
Figure 4.6. GM1 treatment reduces the number and size of aggresomes in STHdh Q7/7 cells undergoing proteotoxic stress	127
Figure 4.7. Ganglioside GM1 treatment reduces the amount of Triton X100-insoluble p62 in neuronal cells undergoing proteotoxic stress.....	129
Figure 5.1. GM1 does not affect autophagy markers in cells transfected with WT or muHTT. .	153
Figure 5.2. MG132 increases LC3-II levels in neuronal cells. Addition of GM1 does not modify the response to MG132	154

Figure 5.3. GM1 does not affect MG132-induced phosphorylation of p62 at Ser403	155
Figure 5.4. GM1 treatment does not affect p62 protein half-life in STHdh Q7/7 cells.....	156
Figure 5.5. GM1 treatment prevents upregulation of lysosomal genes in proteotoxic stress conditions.....	157
Figure 5.6. Ganglioside GM1 decreases the number of LysoTracker®-positive puncta during proteotoxic stress	158
Figure 6.1. Extracellular vesicles: microvesicles and exosomes	179
Figure 6.2. GM1 promotes the secretion of extracellular vesicles from neuronal cells	180
Figure 6.3. GM1 promotes the secretion of extracellular vesicles from embryonic cortical primary neurons	182
Figure 6.4. Exogenously administered GM1 is internalized by cells and incorporated into extracellular vesicles	184
Figure 6.5. GM1 promotes the secretion of HTT via extracellular vesicles in transiently transfected HeLa cells.....	185
Figure 6.6. GM1 promotes the secretion of HTT in both, microvesicles and exosomes.....	186
Figure 6.7. GM1 promotes the secretion of HTT via extracellular vesicles in transiently transfected N2a cells.....	187
Figure 6.8. GM1 promotes the secretion of muHTT via extracellular vesicles in stably transfected N2a cells.....	189
Figure 6.9. GM1 promotes the secretion of muHTT via extracellular vesicles in stably transfected HeLa cells.....	190
Figure 6.10. GM1 promotes the secretion of p62 via extracellular vesicles in cells undergoing proteotoxic stress	192
Figure 7.1. GM1 effects on the accumulation of protein aggregates: a working model.....	198
Figure A1. Nuclear transport of mature SREBP2 is impaired in HD models	295
Figure A2. HD fibroblasts do not efficiently upregulate the transcription of cholesterologenic genes upon culture in lipoprotein-deficient medium (LPDM)	297
Figure A3. Decreased upregulation of <i>Hmgcr</i> gene in mouse HD astrocytes upon culture in lipoprotein-deficient medium (LPDM).....	299

List of abbreviations

24-OH-Chol	24-hydroxycholesterol
a.a.	Amino acid
AD	Alzheimer's disease
ALIX	ALG-2-interacting protein X
ALS	Amyotrophic lateral sclerosis
APP	Amyloid precursor protein
Aq	Aqueous phase
Atg	Autophagy-related proteins
Atp6v1h	V-type proton ATPase subunit H
A β	Amyloid β
A β 42	Amyloid β 1-42
BDNF	Brain-derived neurotrophic factor
CMA	Chaperone-mediated autophagy
CNS	Central nervous system
CSF	Cerebrospinal fluid
Ctsd	Cathepsin D
D	Detergent
DAPI	4',6-diamidino-2-phenylindole
DiI	(1,1'-dioctadecyl-3,3,3',3'-tetramethyl indocarbocyanine perchlorate
DIV	Days in vitro
EMSA	Electrophoretic mobility shift assay
ERK	Extracellular signal-regulated kinases
ESCRT	Endosomal sorting complex responsible for transport
EVDS	Extracellular vesicle-depleted serum
EVs	Extracellular vesicles
FBS	Fetal bovine serum
FPP	Farnesyl-diphosphate

FTase	Farnesyltransferase
GABA	γ -aminobutyric acid
GDP	Guanosine diphosphate
GFP	Green fluorescence protein
GGPP	Geranylgeranyl-diphosphate
GGTase I	Geranylgeranyl transferase I
GGTase II	Geranylgeranyl transferase II
GTP	Guanosine triphosphate
GTPase	Guanosine triphosphate hydrolase
HAP1	Huntingtin-associated protein 1
HD	Huntington's disease
HMGCoA	3-hydroxy-3-methylglutaryl CoA
HMGCR	HMGCoA reductase
HSP90	Heat Shock protein of 90 KDa
ILVs	Intraluminal vesicles
IPP	Isopentenyl diphosphate
K63	Lysine 63
KI	Knock-in
LPDM	Lipoprotein-deficient media
LPDS	Lipoprotein-deficient serum
MG132	Z-Leu-Leu-Leu-al
mRNA	Messenger ribonucleic acid
mSREBP2	Mature form of SREBP2
mTOR	Mammalian target of rapamycin
muHTT	Mutant huntingtin
MVB/LE	Multivesicular bodies/late endosomes
N2a	Neuro2a
NMDA	N-Methyl-D-aspartate

NPC	Niemann-Pick C
PBS	Phosphate-buffered saline
PD	Parkinson's disease
PrP ^{Sc}	Prion Protein Scrapie
RAB	RAS-related protein
RAS	Rat sarcoma viral oncogene
RM	Regular medium
RT	Room temperature
SCAP	SREBP cleavage-activating protein
SDS	Sodium dodecyl sulphate
SDS-PAGE	SDS - polyacrylamide gel electrophoresis
SRE	Sterol response element
SREBP2	Sterol response element binding protein 2
TDP43	Transactive response DNA binding protein 43
TFEB	Transcription factor EB
TSG101	Tumor susceptibility 101
UHDRS	Unified HD rating scale
ULK	Unc-51-like
UPS	Ubiquitin-proteasome system
WT	Wild-type
wtHTT	Wild-type HTT
YAC128	Yeast artificial chromosome 128
α syn	α -synuclein

Chapter 1: General background

This chapter is my original work.

1.1. General introduction

Huntington's disease (HD) is the most common monogenic neurodegenerative disorder and it is characterized by progressive choreic movements, dystonia, motor incoordination, cognitive decline and behavioural changes (1).

HD is caused by an abnormal increase in the number of CAG repeats in the exon 1 of the huntingtin gene (*HTT*), located on chromosome 4. This mutation leads to an expanded polyglutamine stretch (polyQ) in the N-terminus of HTT protein. HD is a fully penetrant disease in individuals carrying more than 39 CAG repeats, but its penetrance is reduced in carriers of 36-39 CAG repeats (2).

Interestingly, the age of onset is inversely correlated with the number of CAG repeats in the *HTT* gene (3). Anticipation phenomenon, defined as the event in which the offspring has an earlier onset of the disease than the parents, can be observed in families carrying the mutant *HTT* gene, especially in the paternal lineage. This is due to the instability and possible elongation of the CAG stretch in germinal cells, which can lead to the transmission of the mutation to the newer generations with an increased number of CAG repeats (4).

The HTT protein is ubiquitously expressed, but its function remains unclear. However, it is known that mutant huntingtin (muHTT) can acquire misfolded and toxic conformations (5), and through mechanisms that are still under investigation, muHTT impairs vesicular transport, mitochondrial metabolism, cell signaling and gene transcription in HD neurons and glial cells, leading to neuronal dysfunction and death in various regions of the brain, especially, but not limited to the striatum and cortex. The molecular and cellular mechanisms underlying muHTT toxicity will be reviewed in more details in following sections of this document.

1.2. Epidemiology

The prevalence of HD is variable depending on the population studied. Furthermore, there is a big discrepancy in the amount and quality of epidemiologic studies performed in different regions of the world, perhaps contributing to the variability of the numbers reported.

It has been found that Asia has the lowest prevalence of HD in the world, with 0.4 patients per 100,000 inhabitants. Conversely, North America and the United Kingdom have the highest reported prevalence, with 7.33 and 6.68 cases per 100,000 inhabitants, respectively (6).

Moreover, prevalence can be affected by the accuracy of the diagnostic methods, both in the clinic and the laboratory. It has been reported that cases in the United Kingdom have doubled from 1990 to 2010. Researchers claim that better molecular diagnostics, combined with an increase in health coverage may cause this phenomenon, more than an actual increase in the real number of HD patients in the islands (7).

Instead, countries with poor clinical diagnostics and low health coverage may report a lower number of patients. Such is the case of sub-Saharan nations, with a prevalence of 0.2-0.5 cases per 100,000 inhabitants (8), a number that is strikingly different from the prevalence of HD in African-descendent Americans in the United States, at 6.37 per 100,000 inhabitants (9).

Studies of prevalence in Latin America have revealed that certain isolated populations have notoriously different prevalence when compared to the rest of the world. For example, the general prevalence in countries like Mexico and Venezuela is 4 and 0.5 per 100,000 inhabitants, respectively (10,11). However, due to a founder effect, small isolated populations in Venezuela (Lake Maracaibo), Peru, (Cañete-Lima) and Brazil (Feira Grande, Alagoas) have reported prevalence values of 700, 40 and 72 cases per 100,000 inhabitants, respectively (12), which are

several times higher than the world average. Furthermore, the populations of Juan de Acosta and El Dificil in northern Colombia, have been described to be clusters of multiple families with a very high prevalence of possible HD, but the exact number of cases has yet to be determined, mostly due to the difficult access to this geographical zone (12).

1.3. Clinical Features

1.3.1. Diagnosis

The diagnosis of HD is based largely on the anamnesis, followed by genetic testing. HD diagnosis should be considered when there is a family history of the disease, in a patient with motor disturbances such as chorea and dystonia (13). In an attempt to standardize the diagnosis of HD, a unified HD rating scale (UHDRS) has been developed, in which total motor score ranges from 0, where no motor abnormalities are observed, to 4, where the motor impairments are highly suggestive of HD (14). Nonetheless, some minor and subtle motor and non-motor deficits may appear many years before the clinical onset of the disease. This stage is called “premanifest period”, and may span for up to 15 years before the definitive signs and symptoms of HD finally become manifest (15).

Since the discovery of the mutation that causes HD in 1993 (2), and after the vast improvement in molecular biology techniques, nowadays, the diagnosis of HD relies heavily on genetic testing (1). The identification of the mutation in a patient, not only allows for a proper and accurate diagnosis of the patient itself but also provides the information required to perform adequate genetic counselling to the relatives of the patient. Additionally, the possibility of identification of carriers, years before the disease becomes manifest, has opened the door for imaging, behavioural or

biochemical studies before the onset of the neurodegeneration. This has enormous relevance for the design of possible future therapies aimed to stop or slow down the progression of the disease.

1.3.2. Motor abnormalities

The neuronal pathology in the striatum follows a bi-phasic course, first affecting the medium spiny neurons that belong to the indirect pathway, and later in life, the medium spiny neurons of the direct pathway start to be affected as well. Because of this, the motor abnormalities can also be evident in a bi-phasic fashion: a hyperkinetic phase whose main manifestation is chorea at early stages of the disease, followed by a hypokinetic phase, mainly characterized by dystonia and bradykinesia (16,17).

Chorea is the hallmark manifestation of HD, being present in virtually all adult patients with HD, although it is thought to be an intermediate manifestation of the disease. Choreic movements can be very subtle at the beginning of the symptomatic stage. Facial movements such as eyebrow-raising, jaw contractions and winking are examples of these subtle involuntary movements. In more advanced stages of the disease, choreic movements usually involve larger groups of muscles, causing abdominal contractions, head movements, and abduction/adduction of arms and legs (13).

Second to chorea, dystonia is one of the most common manifestations of HD. It usually appears at later stages in adult patients. Foot inversion, internal rotation of the limbs and fist clenching are commonly observed in HD patients (18). Other involuntary movements frequently observed in adult HD patients are tics and myoclonus, however, these latter symptoms appear to be more common in younger patients diagnosed with HD (19-21).

Due to the anticipation phenomenon discussed above, there is a proportion of patients who have an early onset of HD symptomatology. These patients generally carry longer CAG repeats in their

HTT gene. Patients whose symptoms start before the age of 21 are considered to have juvenile-onset HD. It has been reported that patients with juvenile-onset HD are very commonly the offspring of an affected male, rather than a female (22,23).

The differential symptomatology of juvenile-onset HD poses challenges to the diagnosis of the disease. First of all, the parents may appear to be unaffected or may be pre-symptomatic. Not all clinicians would suspect HD if family history of the disease is not clear, or if it is not present at all. Second, the symptomatology may be quite different, compared to adult patients. Most common early symptoms may include poor performance at school, discoordination, and clumsiness, as well as a decline in fine motor functions (22,23). Chorea is mostly absent at the beginning of the disease, but it usually appears as the disease progresses. Dystonia (sustained/repetitive muscle contractions) and myoclonus (spasmodic/fast contraction of muscles) are very common ways of presentation of juvenile-onset HD.

Perhaps the main difference between adult-onset and juvenile-onset HD is the presence of seizures which may affect up to 35% of juvenile patients, but are very rare in adult patients. Seizures are characteristically generalized tonic-clonic (grand mal), but absence (petit mal) or myoclonic seizures are observed as well (24). In some extreme cases, the first manifestation of juvenile-onset HD is a progressive myoclonus epilepsy, that later may be accompanied by intellectual decline and other psychiatric disturbances such as mood instability, agitation and delusion (25).

1.3.3. Non-motor abnormalities

Patients diagnosed with HD do not only show motor disturbances but also suffer from non-motor abnormalities. These non-motor alterations may be divided into two main groups: cognitive and emotional.

Cognitive abnormalities can be detected several years before the onset of the motor symptoms (26). Dementia with relative preservation of memory is the most prominent type of cognitive impairment in HD, conversely to what is observed in other common dementias, such as Alzheimer's disease (AD). This specific kind of dementia is defined as "subcortical type", since it is mostly present in patients with degenerative diseases that are not necessarily characterized by cortical atrophy, including Parkinson's disease (PD) or vascular dementia (27). The typical cognitive profile of an adult HD patient is characterized by cognitive slowing, impaired attention, difficulties in short- and long-term planning, as well as an impaired emotion recognition (28-31).

Language is relatively well preserved in patients with HD. However, some longitudinal studies done in pre-symptomatic HD patients have revealed that verbal episodic memory may be altered, and it progresses as the onset of motor symptoms approaches, and may even correlate with striatal size, measured by magnetic resonance (32).

The multinational prospective observational study TRACK-HD, which observed pre-manifest and early HD patients for over 36 months, reported on the behavioural changes that occur before the disease onset, or in very early stages of the disease. This study revealed that 10 out of 12 cognitive tests had some alteration, or showed deterioration along the period of observation, with respect to healthy controls. Visual attention, visuomotor and spatial integration, as well as psychomotor speed, were amongst the most affected cognitive functions (33-35).

Instead, cognitive changes in juvenile-onset HD are not that well documented, mostly due to the small number of cases. These patients are often misdiagnosed as developmental delayed, or even being attention deficit-hyperactivity disorder patients. Juvenile-onset HD patients have been shown to exhibit various deficits in attention and executive functioning (22,36).

As mentioned earlier, HD patients often show other psychiatric alterations that do not constitute cognitive impairments but rather may be classified as mood disorders. These findings are more difficult to categorize and document due to the lack of specific tests or surveys that could help with the assessment of the progression of these behavioural abnormalities. Depression is the most common comorbidity, accounting for up to half of the patients. Suicidal ideation is very common as well. It has been reported that almost 2% of patients diagnosed with HD have attempted suicide. Other behavioural changes may include apathy and irritability, traits that can severely affect a patient's quality of life (37-39).

1.4. Neuropathology

Muscle contraction and relaxation, hence motor control, is executed via a synchronized concert of signals coming from various regions of the brain, including the primary motor cortex, the basal ganglia and the cerebellum, among others. These signals are highly reverberated and modulated in between and inside these various structures, before reaching their muscle of destination. This enormous complexity and secondary control is what allows us to move large groups of muscles to perform gross movements, such as walking, but at the same time, have a precise and fine control of small muscles that are needed for writing, painting or playing a musical instrument.

Basal ganglia are a group of neuronal nuclei found at the base of the forebrain and midbrain. Parts of the basal ganglia are: the globus pallidus (divided in internal and external), the subthalamic nucleus, the substantia nigra (divided in pars compacta and pars reticulata) and the striatum. The last is composed of two different nuclei: the caudate nucleus and the putamen. The striatum receives its name due to the extensive axonal connexions between both nuclei, giving the appearance of being striated in anatomical specimens (Fig. 1.1) (40,41).

The cell composition of the striatum is very peculiar. Neurons inside the striatum can be roughly divided into two large groups: 1) Projection neurons, whose axons will end in a different region than their soma; 2) Local circuit neurons, whose axons will remain in the striatum. Beyond the division in these two groups, neurons can be classified by their size, neurotransmitter, among other characteristics. By far, the most common type of neuron in the striatum is denominated medium spiny neuron, accounting for up to 95% of all the neurons in the striatum. These cells use γ -aminobutyric acid (GABA) as neurotransmitter, and the majority of their projections are directed to the globus pallidus and to the substantia nigra pars reticulata (42).

1.4.1. Neuronal pathways of the basal ganglia

Due to its importance in the pathophysiology of HD, the following section will be dedicated to summarizing the neuronal pathways that are integrated in the basal ganglia, and particularly in the striatum.

The cortex, including the primary motor cortex, but also other regions dedicated to motor control (e.g. secondary motor cortex), are the origin and the main provider of glutamatergic excitatory signals that enter the striatum (43). Here, the information coming from the cortex flows through two different pathways: direct pathway and indirect pathway.

The direct pathway is constituted by the axons of the medium spiny neurons projecting directly (hence, the name of the pathway) to the internal segment of the globus pallidus and the substantia nigra pars reticulata. These cells and projections do not only carry the GABA neurotransmitter, but also the neuropeptide substance P.

The indirect pathway instead, is composed of inhibitory enkephalin-expressing projections originated in the striatum, directed towards the external segment of the globus pallidus, which

then, convey the information via excitatory synapses to the subthalamic nucleus, which in turn, projects excitatory axons towards the internal segment of the globus pallidus (41,44,45).

From the internal segment of the globus pallidus, where direct and indirect pathways converge, GABAergic neurons project to the thalamus, and from here, thalamic neurons project excitatory axons to the frontal and premotor cortex, which in turn, modulate and have influence in the output of information from the cortex towards the striatum (46). This circular and reverberating flux of information is what is known as the cerebro-cortico/basal ganglia/thalamo/cortical circuit and is the basis of the motor control exerted by the basal ganglia. In some textbooks, this circuitry is referred as to be part of the “extrapyramidal system” (Fig. 1.2) (42).

1.4.2. Macroscopic alterations

Perhaps the most remarkable characteristic of the HD brain is the evident (in most cases) bilateral atrophy of the striatum (47-49). Although striatal atrophy is the most common and striking finding, cerebral cortex, thalamus and general white matter can show significant decrease in volume, ranging from 21-57%, depending on the stage of the disease (Fig.1.1) (50,51).

It has been very well documented that the degeneration appears to follow a caudo-rostral direction, starting in the tail of the caudate nucleus, and slowly progressing towards the head of the caudate and the putamen (48,52). Based on this phenomenon, Vonsattel and collaborators (51), after analyzing >160 autopsy specimens and correlating the macro and microscopic findings with clinical data, created a grading system (from 0 to 4) in an attempt to standardize the stage of degeneration of HD brains.

Brains graded as 0 have no evident atrophy in any of the regions typically affected by HD. Usually, this grade is reserved for patients who are genetically diagnosed with HD but have not reached the

age of onset of the disease, and died of different causes. Grade 1 brains may show reduced size of the tail and the body of the caudate nuclei, but not evident atrophy of its head, or the putamen. Grades 2 and 3 show mild to moderate atrophy of the head of the caudate nuclei but it preserves its convexity towards the ventricle. Finally, in grade 4, the striatal atrophy is such that the striatum appears to be concave, and the neuronal loss has reached more than 95%, compared to healthy controls (42,48,51).

Despite the fact that the Vonsattel grading system is based almost exclusively on the morphology of the striatum, there is a correlation between the degree of atrophy in the striatum and the degeneration in other regions of the brain. Brains graded as 0 or 1 have no evident atrophy in any other regions of the brain, while brains graded as 4 also show extensive atrophy of the cortex (48,51).

Perhaps the area that is most affected in HD after the striatum, is the globus pallidus (Fig. 1.1). Brains that were graded as 3 or 4 showed up to 50% reduction in the size of the globus pallidus compared to control subjects, being the external segment of the globus pallidus the most affected area. After analyzing the specimens under the microscope, it was observed that the number of neurons in the globus pallidus was not affected, but rather there was a reduction in the neuropil, causing the neuronal bodies to be “packed” closer together. Authors interpreted this observation to be evidence that the reduction in size of the globus pallidus was not due to a decline in the number of cells, but rather a decrease in the number of incoming connections from the already degenerated striatum (48,51).

Cerebral cortex has also been shown to be atrophic in HD, especially in brains graded as 3 or 4. However, various reports made by different researchers in various groups of patients have

contradictory results with respect to the presence or absence of neuronal loss, oligodendrocytic loss and/or astrogliosis in the cortex of HD patients (53-56).

Other areas that may present atrophy and/or cellular loss in brains with scores 3-4 are the thalamus, substantia nigra and subthalamic nucleus. These findings are variable among patients and may depend on both, loss of connectivity and loss of neurons (48).

It is generally accepted that the cerebellum is spared from significant atrophy (48,51). The exception to this statement would be the cases of juvenile-onset HD, where cerebellar mass is significantly decreased with respect to control subjects (49,57).

1.4.3. Microscopic findings

The majority of the cellular mass (~95%) in the striatum is made of medium spiny neurons, GABAergic neurons that project towards other nuclei within the basal ganglia. The medium spiny neurons are selectively affected in HD, for reasons that are still under investigation (42,45,49,51,58).

In tissue sections, medium spiny neurons can be identified by immunolabeling against glutamic acid decarboxylase, one of the enzymes in the biochemical pathway for the synthesis of GABA. Other markers commonly used are dynorphin, calbindin, calcineurin and the dopamine-and cAMP-regulate phosphoprotein 32 kDa (DARPP32) (58,59). Moreover, medium spiny neurons projecting to the internal or external globus pallidus, hence, belonging to the direct or indirect pathway, can be identified by immunolabeling against substance P or enkephalin, respectively (42). The development of these set of tools has allowed researchers to identify and pinpoint the specific populations of cells that are lost during the different stages of HD.

Studies using immunolabelling against calbindin, calcineurin and DARPP32 have consistently shown that the number of soma of medium spiny neurons is decreased in the striatum of HD patients compared to healthy controls, and that the amount of neuronal loss correlates positively with motor impairment score (60-62).

Concomitant with the loss of neuronal bodies, the projections from the medium spiny neurons towards the globus pallidus are also significantly decreased, and similarly to what happens to the neuronal somas, the loss of incoming axons into the globus pallidus correlates with motor alterations. It is important to mention that the projections expressing enkephalin, hence being part of the indirect pathway, seem to degenerate first. Conversely, those projections that express substance P and that are directed towards the internal segment of the globus pallidus (direct pathway) are relatively conserved until advanced stages of HD, when eventually both enkephalin- and substance P- expressing axons are significantly loss (59,63,64). This phenomenon is believed to be the cause of the well-known bi-phasic presentation of the disease, starting with a hyperkinetic phase, that later in life seems to transform into a hypokinetic phenotype (42,49).

Cannabinoid receptor type 1 (CB1), which is normally expressed in nearly all sites where the terminal axons of the medium spiny neurons reside, has been shown to be decreased in both segments of the globus pallidus, as well as in the substantia nigra. Interestingly, this decrease is observed even in brains graded as 0, which may suggest that the dysfunction in the cannabinoid system precedes the degeneration in the striatum. Concomitantly, there is an increase in the expression of GABA receptors subunits, which is believed to be a compensatory mechanism that follows the decreased amount of GABAergic afferences coming from the striatum (65-68).

Cortical atrophy has been extensively documented in HD patients. It follows the striatal degeneration and is more evident in brains graded as stage 3 and 4. It has been shown that frontal

lobe atrophy correlates with striatal degeneration, as well as with cognitive impairment in HD patients (69). Although early studies did not show a reduction in the number of cells in HD cortices, but rather an increased density of neurons per unit of volume (48,51), more recent studies indicate that there is significant neuronal loss in the cortex of HD patients. In fact, it is believed that the neuronal loss is layer-specific. Pyramidal neurons in cortical layers III, V and VI are either reduced in number, or their dendritic arborization is affected in samples of HD brains, compared with control subjects (55,70,71).

Some studies focusing on cortical motor areas also found significant reduction in the volume of the primary motor cortex and premotor region of HD patients (72). Moreover, some studies suggested that there is a correlation between the cortical area affected and clinical presentation. For instance, patients in which cortical atrophy was more pronounced in areas such as anterior cingulate cortex, associational cortices in the frontal, parietal and temporal lobes, the psychiatric symptoms were usually more pronounced. Instead, when motor areas were the ones predominantly atrophic, the major symptomatology was motor disability (73-76).

Reactive gliosis, involving astrocytes and microglia, is present in areas where the neuronal loss is more prominent, such as the dorsal striatum. Gliosis also correlates with the grade of neurodegeneration (77). The number of astrocytes is increased, even in brains with lower grades of HD (78). Conversely, a study done in pre-symptomatic HD carriers has shown that there is no evidence of reactive gliosis in the tail of the caudate, usually affected early in HD (79). These findings suggest that reactive gliosis may appear in parallel with neuronal degeneration.

Activated microglia are also abnormally present in brains affected by HD. Autopsy specimens have revealed abnormal activation of microglia that correlates with the degree of neurodegeneration, and that localizes preferentially in areas typically more affected by the disease

(80,81). Excessive microglia activation and correlation with HD symptomatology were later corroborated by studies in living patients using PET scan technology, by utilizing ligands that bind specifically to activated microglial cells (82,83).

An important neuropathological finding in HD brains is the presence of aggregates of muHTT inside the nucleus, cytoplasm and neurites of HD neurons (84-86). Various antibodies against muHTT have been developed, and multiple groups confirmed the presence of intracellular muHTT aggregates in samples from juvenile and adult HD brains (87-89). Even though muHTT aggregates were present unequivocally in at least a fraction of the neurons in HD brains, researchers quickly learned that there was a dissociation between muHTT aggregation and the patterns of neuronal loss in the striata of HD patients. Aggregates of muHTT were more common in spared interneurons, while they were almost absent in medium spiny neurons, the most affected cell type in HD, raising the question whether muHTT aggregation is a predictor of neuronal loss, or instead a cytoprotective mechanism against muHTT toxicity (90), a question that is still not fully answered to this day.

The sequence of events that lead from expression of muHTT to neurodegeneration at molecular and cellular levels are still under investigation, but it is known that the elongation of the polyQ stretch in HTT causes the protein to acquire a noxious misfolded conformation, favours the generation of toxic fragments (gain-of-function mutation), but also interferes with the normal functions of the HTT protein (loss-of-function mutation). In the following sections, I will summarize the more important aspects of the HTT protein structure, normal functions of HTT, and dysfunctions caused by muHTT.

1.5. Huntingtin functions and mutant huntingtin dysfunctions

1.5.1. The Huntingtin gene and protein

The *HTT* gene is located in the chromosome 4 (4p16.3) in human cells. It contains 67 exons that span a total of 180 kb (91). Identity between the human *HTT* gene and its ortholog in mice is 86%. However, while the human gene usually contains 13 to 36 CAG repeats in its exon 1, being highly polymorphic, the mouse ortholog usually contains only 7 CAG repeats (92). Phylogenetic studies have shown that the *HTT* gene is highly conserved amongst various mammals, and that there is evidence of an ancestral polyQ transcript in the sea urchin, which resembles certain regions of the human *HTT* gene, suggesting that the polyQ stretch may have an important role that has been conserved during evolution (93). The *HTT* gene is transcribed ubiquitously throughout the body, but it is mainly expressed in the central nervous system (94,95).

HTT protein is essential for embryonic development since deletion of both alleles of the *Htt* gene in mice results in abnormal gastrulation at day 7.5 and reabsorption of the embryo at day 8.5, before the formation of the central nervous system (96,97). However, there is some controversy regarding the phenotype of the heterozygous mice. While Duyao and collaborators (96) reported that deletion of one allele of *Htt* gene in mice resulted in normal development and no observable phenotype, Nasir and collaborators (97), who disrupted the exon 5 of the mouse *Htt* gene, found that heterozygous mice displayed increased motor activity, cognitive impairment and neuronal loss in the subthalamic nucleus. Inactivation of *Htt* in adult mice leads to reduced lifespan, atrophy of the forebrain and motor disabilities, suggesting that HTT is not only required during development but is also important for neuronal survival in adult animals (98).

Full-length human HTT protein has 3142 amino acids (on average, due to the variability of the CAG stretch) and a predicted molecular weight of 347.67 kDa (UNIPROT entry No. P42858). The large size of this protein has hampered efforts to elucidate its structure until recent work by Guo and collaborators (99) who used cryo-electron microscopy to determine the structure with a resolution of 4 Ångströms. Authors of this study concluded that HTT is largely in an α -helical conformation and contains three major domains: N-terminal and C-terminal domains, both containing multiple HEAT (huntingtin, elongation factor 3, protein phosphatase 2A and lipid kinase TOR) repeats arranged as a solenoid, and a bridge domain.

HTT protein contains at least 36 HEAT repeats, named after the first discovered proteins that share this domain, organized in four clusters. Coincidentally, proteins that contain HEAT repeats are relatively large and usually participate in protein complexes. It has been shown that HEAT repeat domains have a tendency to adopt an α -helix conformation that allows proteins to acquire flexibility, a characteristic that is especially important during protein-protein interaction in multiprotein complexes (100,101).

At its N-terminal region, more specifically between a.a. 174-207, HTT protein contains a karyopherin β 2 type nuclear localization signal (NLS). Interestingly, the NLS found in HTT appears to be atypically larger when compared to other proteins sharing the same kind of NLS. Authors hypothesized that a specific conformation in the N-terminus region of HTT may allow its interaction with karyopherin β 2, favouring its transport into the nucleus (102).

HTT has at least one conserved nuclear export signal (NES) in the protein located at the C-terminus region (103). Furthermore, although there has not been identified a conserved NES in the N-terminal region of the protein, it has been shown that N-terminal fragments (a.a. 1-171) of muHTT interact aberrantly with the nucleoprotein translocated promoter region (TRP), part of the nuclear

pore complex (104). These findings may explain why muHTT accumulates in the cell nucleus of HD patients and HD mouse models (84,85,105).

Post-translational modifications of HTT protein are abundant and widespread across the protein length. Moreover, these modifications regulate toxicity, stability or functions of HTT (106). Sumoylation occurs in three lysine residues located in the first 17 amino acids of HTT, domain known as N17. Sumoylation of HTT at these sites exacerbates muHTT toxicity in a *Drosophila* HD model (107).

Phosphorylation has also been reported in the N17 domain, however, phosphorylation of specific residues within the N17 domain may have different effects on the HTT protein. Phosphorylation of Thr3 is reduced in samples from human and mouse HD brains, compared to their WT counterparts. Concomitantly, it is also known that phosphorylation at this site decreases the aggregation and toxicity of N-terminal muHTT fragments (108-111).

The I κ B kinase (IKK) complex is able to phosphorylate HTT at residues Ser13 and Ser16. These two post-translational modifications have shown to target muHTT for degradation (112). However, in later years it was shown that inhibition of IKK, paradoxically increased the phosphorylation of the N17 domain, while inhibitors of casein kinase 2 (CK2) decreased it (113), suggesting that the modulation of the phosphorylation of the N17 domain is more complex than initially thought.

Phosphomimetic substitutions at Ser13 and Ser16 abolished the neurodegenerative effects of full-length muHTT in an HD mouse model and also prevented muHTT aggregation and amyloid fibril formation *in vitro* (114), suggesting that the phosphorylation at these sites may become an important target for potential future disease-modifying treatments. In fact, our laboratory has

demonstrated that chronic intraventricular infusion of ganglioside GM1 triggers the phosphorylation of muHTT at Ser13 and Ser16, attenuating muHTT toxicity and restoring motor function in a mouse model of HD (115). The role of GM1 in HD will be further discussed in following sections of this document.

Phosphorylation of HTT is not limited to the N17 domain. Other residues (Ser421, Ser536, Ser116, among others) also undergo phosphorylation. Some of these post-translational modifications modulate muHTT cleavage and toxicity (116-122).

Acetylation of muHTT at Lys444 is crucial for its incorporation into autophagosomes for autophagic degradation, improving muHTT clearance in cell and *C. elegans* models of HD (123). Additionally, palmitoylation at Cys214 by huntingtin interacting protein 14 (HIP14) has been shown to be essential for correct localization of HTT within the cell. Additionally, palmitoylation may also modulate the aggregation of muHTT (124).

A myristoylation site at Gly553 has also been reported in a fragment resulting from the proteolytic cleavage of HTT by caspases 3 and 6 (at a.a. 552 and 586, respectively). The myristoylated fragment localizes to the ER and induces the formation of autophagosomes in non-starving cells, suggesting that this post-translational modified fragment may play a role in the initiation of autophagy. Interestingly, it was also shown that the presence of an elongated polyQ resulted in a reduction of myristoylation of this fragment (125).

1.5.2. Function(s) of Huntingtin protein

Since the discovery of the role of HTT in HD, multiple cellular functions and processes have been attributed to the HTT protein. To start, HTT has a role in embryonic development since *Htt*^{-/-} mouse embryos do not develop properly and are non-viable (96,97). HTT protein also has a role

in the regulation of cell survival/apoptosis. Animal models of HD, ischemia, trauma, and spinal cord injury, all models in which apoptosis is abundant, showed reduced levels of wild-type HTT (wtHTT) protein (126). Furthermore, overexpression of wtHTT in striatal cells was protective against various apoptotic stimuli (127-130). Although the mechanism by which HTT is antiapoptotic is not well understood, two hypotheses have been proposed. First, huntingtin interacting protein 1 (HIP1) and its partner huntingtin interacting protein 1 protein interactor (HIPPI) form a protein complex that leads to activation of caspase 8, the release of cytochrome C from the mitochondria, ultimately activating apoptosis (130,131). wtHTT interacts and sequesters HIP1, preventing its binding to HIPPI and thus, protecting the cell against apoptosis. The complex HTT-HIP1 is less stable in the presence of an elongated polyQ stretch (130,132). Additionally, wtHTT can directly interact with and block pro-apoptotic proteins such as caspase 9 (127,128).

There are also reports of the involvement of HTT in gene transcription. For example, HTT can interact and sequester the repression element-1 silencing transcription factor/neuro-restrictive silencer factor (REST/NRSF), which is a negative regulator of the transcription of the brain-derived neurotrophic factor (BDNF), thus promoting its transcription (133,134). Overexpression of wtHTT increases the phosphorylation of cAMP response element-binding element (CREB) in striatal neurons, a well-known positive regulator of the BDNF transcription (135).

One of the most recent functions that has been attributed to HTT is its involvement in vesicular trafficking (136,137). The structure of HTT suggests that it may work as a scaffold protein able to interact with membranes. The N17 domain of HTT can form an amphipathic helix that has been proposed to be a membrane-interacting domain with the endoplasmic reticulum, late endosomes and autophagosomes (138). Also, an N-terminal region located within a cluster of HEAT repeats

(a.a. 172-372) has affinity for phospholipids at the plasma membrane (139). Additionally, the interaction with membranes may also be mediated by HTT palmitoylation at residue Cys214 (124).

Moreover, many of the known interactors of HTT are involved in vesicular trafficking, either by interacting with the microtubule network, or by being a constitutive part of motor protein complexes. Examples of HTT-interacting proteins are huntingtin-associated protein 1 (HAP1), kinesin, dynactin, optineurin, among others. (140-145). Additionally, HTT has been found to stimulate the vesicular transport of BDNF (146). Conversely, HTT containing an expanded polyQ stretch, or depletion of HTT inhibits the vesicular transport of BDNF, among other proteins (146,147).

HTT may also have a function at the level of the synapse. HTT is enriched in the synapses and is also known to interact with post-synaptic density protein 95 (PSD-95), modulating the function of the NMDA and kainate glutamate receptors. Overexpression of wtHTT protects neuronal cell lines against glutamate-dependent excitotoxicity, while expression of muHTT enhances it (148,149).

1.5.3. Pathophysiology of HD: The loss and gain-of-function of mutant HTT

As summarized in the previous section, there are multiple functions that have been attributed to HTT protein, including roles that range from embryonic development to vesicle trafficking.

The elongation of the polyQ stretch interferes with such normal functions of HTT (150), impairing cellular processes such as gene transcription (151), vesicular transport (146,147), anti-apoptotic functions (130,132), autophagy (152), among others. This suggests that elongation of the polyQ stretch leads, at least in part, to a loss of normal HTT functions.

At the same time, the elongation of the polyQ stretch leads to the acquisition of abnormal conformations that make muHTT more prone to cleavage into toxic fragments by different cellular

proteases, and promotes the oligomerization and aggregation of muHTT. This acquisition of toxic properties and the dominant inheritance of the disease suggest that the HD mutation is also a gain-of-function mutation.

Thus, the cellular dysfunctions that eventually lead to neuronal cell death, striatal atrophy and HD symptomatology, may arise from a combination of the acquired toxicity of muHTT, its fragments and aggregates, as well as from the loss of the normal functions of the HTT protein.

In the following section, I will summarize some of the literature regarding what cellular functions are altered by muHTT, and how they might, at least partially, explain the neurodegeneration observed in HD.

1.5.3.1. Cleavage, misfolding and aggregation of muHTT

The full-length wtHTT protein, but more importantly muHTT, can be cleaved by various proteases, including caspases and calpains, among others. Caspase 3 can cleave wtHTT and muHTT at positions 513 and 552, while caspase 2 and caspase 6 cleave the HTT protein at positions 552 and 586, respectively. Two sequences compatible with calpain putative sites are located at positions 469 and 536 (153-160).

Cleavage of muHTT generates N-terminal fragments containing the elongated polyQ stretch, which are more toxic than full-length muHTT protein (153-160). The presence of these N-terminal muHTT fragments has been confirmed in both, brains from HD patients, as well as in brains from mouse HD models (156,157,161,162). The hypothesis of proteolytic cleavage of muHTT and the generation of N-terminal muHTT fragments being major players in HD pathogenesis is supported by studies using either inhibitors of proteases (caspases) or cleavage-resistant mutant versions of

muHTT, in which disease was delayed in HD mice (155,160) or HD cells were protected against apoptotic stimuli (158).

To my knowledge, there is at least one study attributing cellular toxicity to C-terminal non-polyQ HTT fragments through a mechanism dependent on dilation of the endoplasmic reticulum (ER), impairment of dynamin protein functions and ER stress. Since these fragments can be generated from wtHTT as well, authors claim that toxicity may arise from abnormal muHTT proteolysis, or in synergy with N-terminal polyQ-containing muHTT fragments, but not under normal conditions (163).

Fragments of muHTT are not only product of proteolytic cleavage. In fact, Gipson and collaborators (164) found that aberrant splicing of the intron 1 in the *HTT* mRNA occurs in HdhQ150 mice, a knock-in mouse model of HD which expresses the endogenous mouse *Htt* gene with an elongated CAG stretch. This aberrant splicing results in a short poly-adenylated mRNA that is translated into an elongated polyQ muHTT exon 1 protein (164,165) a fragment that is highly pathogenic when expressed in mouse models (105,166). The aberrantly spliced mRNA was also found in a second mouse model expressing the full-length human *HTT* gene, as well as in three samples of human HD tissue, confirming that the aberrant splicing is not only a property of the mouse gene, but also happens with the human *HTT* mRNA (164,165). Further studies have shown that this incorrectly spliced mRNA is present in brain tissue and peripheral cells of HD patients, but is particularly abundant in cells derived from juvenile-onset HD patients (167).

Formation or presence of muHTT oligomers, protofibrils, fibrils and aggregates has been demonstrated *in vitro* (168), as well as in the brains of HD patients and HD mouse models. There is a positive correlation between the length of the polyQ stretch and its propensity to form such oligomers/aggregates (169-174).

Despite the existence of evidence of a direct link between the presence of an elongated polyQ stretch and the formation of aggregates, the role of HTT aggregation in the pathophysiology of the disease is very controversial, and to this date, we are not certain whether aggregation has a role in the neurotoxicity that leads to cellular death, or if it is instead a mechanism by which the cells sequester and isolate toxic proteins, as a potential neuroprotective strategy (175).

For instance, there are studies showing that aggregation-resistant-muHTT variants (phosphomimetics of Thr3, Ser13 and Ser16) have decreased toxicity compared to regular muHTT in *Drosophila* models of HD (176). However, another group reported that a single mutation (M8P) in the N17 domain abolished muHTT aggregation, but also resulted in increased toxicity in a cell model of HD (138).

This ambivalence can also be observed in mouse models of HD, where some researchers have reported an association between aggregates and degeneration, while others have observed the opposite. For example, Yamamoto and collaborators (177), using a conditional mouse model in which an N-terminal (Q94) fragment of muHTT is expressed, demonstrated that turning on the expression of the fragment led to the aggregation of muHTT, as well as to neuronal degeneration and a motor phenotype compatible with HD. Turning off the expression of the gene led to a significant reduction of the muHTT aggregates and an amelioration of the motor phenotype, suggesting that there is a direct correlation between muHTT aggregation, degeneration and motor behaviour. Same observations were made in another mouse model expressing an N-terminal muHTT fragment (a.a. 1-171) with 82 CAG repeats, where neurodegeneration and motor phenotype were correlated with muHTT aggregation (178).

Instead, two different models of HD expressing full-length muHTT, the BACHD and the YAC128 mice, do not show evident aggregation of muHTT in the nucleus of striatal neurons, but showed

striatal neurodegeneration and a motor phenotype compatible with HD (179,180). The dissociation between aggregation and toxicity is also supported by the early studies in human HD brains, where the majority of muHTT aggregates were located in spared neurons, while the medium spiny neurons, the type of neuron that is most affected in HD, contained less to none muHTT aggregates (90).

Studies *in vitro* have shown that aggregation of muHTT is dynamic and variable among cells. In fact, Gong and collaborators (181) using an inducible PC12 cell model of HD and live microscopy imaging, showed that the formation of the muHTT aggregate is time-dependent, but the aggregation onset and size of muHTT aggregates differed dramatically amongst cells, even if induction of the expression of the transgene occurred simultaneously. Cells that initiated the aggregation process earlier were more prone to die sooner after induction, but the size of the aggregate was not a good predictor of cell death. In fact, cells that developed larger muHTT aggregates were less prone to cell death, compared to cells with smaller inclusion bodies.

The controversy whether muHTT aggregation is part of the culprit of the degeneration in HD, or instead is a neuroprotective mechanism, is fueled by the fact that there is a wide variety of structures of muHTT aggregates. Thus, oligomeric structures may be more toxic than big inclusion bodies (182). However, other aggregate structures have also been reported, including globular (183), fibrillar (168) and amorphous (184), all with perhaps different degrees of toxicity, whose proportion may differ amongst the different cell and animal models of HD.

1.5.3.2. Mitochondrial dysfunction

Neurons are cells with a high demand for energy that is required to maintain their basal functions such as neurotransmission and synaptic plasticity. Neurons are characterized by their high usage

of ATP for various neuronal processes, including the maintenance of the membrane potential, cytoskeleton remodelling, release and recycling of neurotransmitters, among others (185,186). Thus, it is no surprise that many neurodegenerative diseases have been linked to mitochondrial dysfunction (187,188).

Mitochondrial fusion and fission are processes by which unhealthy mitochondria undergo “maintenance” to recover their membrane potential (homeostasis) (189). Mutations in two essential proteins involved in fusion and fission of mitochondria, OPA1 and MFN2, have been associated with two monogenic neurodegenerative diseases: Charcot-Marie-Tooth type 2A and dominant optic atrophy (190,191). HTT interacts with various proteins linked to the mitochondrial fission/fusion process, including HIP1, HIP14, endophilin 3, clathrin, and dynamin (192-195).

In HD human striata, there is an imbalance between mitochondrial fission and fusion, with an increased expression of DRP1 and FIS1, two proteins that promote mitochondrial fission, and a decreased expression of MFN1/2, a protein that promotes the fusion of mitochondria. Also, levels of the peroxisome proliferator-activated receptor-co-activator gamma-1 alpha (PGC1 α) protein, a key transcription factor and regulator of mitochondrial biogenesis, as well as mitochondrial proteins in the human HD striata, are decreased compared to controls. These findings correlated with the grade of HD, suggesting that there is a progressive loss of mitochondria in the striata of HD patients (196,197).

It was later shown that muHTT interacts aberrantly with DRP1, increasing its GTPase enzymatic activity. Consequently, mitochondria in HD neurons are excessively fragmented. Also, anterograde mitochondria transport is impaired in HD neurons, accompanied by synaptic loss (198). Some of these phenotypes can be reverted by the expression of a dominant-negative DRP1,

not only suggesting that excessive mitochondrial fission is one of the many players of the neurodegeneration process in HD, but also opening the door for therapeutic intervention (199).

Mitochondria, especially unhealthy ones, are an important source of reactive species of oxygen (ROS). These ROS cause damage by peroxidizing lipids and DNA. Perez-Severiano and collaborators (200) showed excessive lipid peroxidation in the striatum of transgenic mice expressing an N-terminal fragment of muHTT. The oxidative damage paralleled the decline in motor behaviour. These findings were replicated in a second HD mouse model (201), as well as in human HD brain tissue (202).

When mitochondria are damaged, they are normally degraded through a specialized mechanism called mitophagy. When a mitochondrion cannot function properly, it loses its membrane potential. This is detected by a mechanism that includes the proteins PTEN-induced putative kinase (PINK) and the ubiquitin E3 ligase parkin. This complex promotes the ubiquitination of proteins in the mitochondrial outer membrane (e.g. VDAC) that serve as a signal for the delivery of damaged mitochondria towards the autophagosome for degradation (203-207). There is evidence that HD immortalized striatal cells do not properly degrade damaged mitochondria due to a failure in cargo recognition. This accumulation of damaged mitochondria may contribute to the oxidative stress that could ultimately lead to the demise of the neurons in HD (152).

1.5.3.3. Transcriptional dysregulation

Multiple studies regarding the possible effects of muHTT on gene expression have been carried out, both in cultured cells, as well as in brains of mouse models of HD. However, it is a challenge to identify which changes are directly caused by muHTT, and which ones are a secondary response to the multiple metabolic and cellular alterations that occur as a response to the degeneration (208).

Several studies have reported that muHTT is able to bind and sequester various transcription factors including CREB-binding protein (CBP), p53, Sp1, TAFII130 and PQBP-1, interfering with their normal function within the nucleus (209-211). Nucifora and collaborators (151) demonstrated that the nuclei of HD cells in culture, HD transgenic mice and human HD brain samples were depleted of CBP. Instead, CBP protein colocalized with muHTT aggregates in the cytosol. In the presence of muHTT, CBP is not able to bind its promoter, however, this effect can be reversed by overexpression of CBP, suggesting that the sequestration of CBP by muHTT is a saturable phenomenon.

I previously mentioned how wtHTT positively regulates the transcription of *BDNF* gene through its interaction with REST/NRSF, a negative regulator of *BDNF* transcription. In the case of muHTT, this interaction is less effective, thus allowing REST/NRSF to be abnormally translocated into the nucleus, where it inhibits transcription of the *BDNF* gene. Low BDNF levels are believed to contribute to striatal neurodegeneration in HD (134,212).

Mitochondrial biogenesis, as mentioned before, is impaired in various models of HD. Cui and collaborators (213) reported that muHTT represses the transcription of PGC1 α , a key transcriptional regulator of genes associated to mitochondrial biogenesis, by associating with its promoter and with two of the main transcription factors for PGC1 α , CREB and TAF4. The authors of this work also reported that the overexpression of PGC1 α reversed the toxicity of muHTT in cultured striatal neurons, and lentiviral delivery of PGC1 α into the striatum of HD transgenic mice prevented striatal atrophy.

Another approach was used by Sipione and collaborators (214), who studied the early transcriptional changes in an inducible cell model of HD. Cells expressing an N-terminal fragment of muHTT containing polyQ of various lengths under the control of a conditional promoter were

studied using microarray analysis, thus evaluating the global early changes in gene expression occurring upon expression of muHTT. Expression in numerous genes involved in cholesterol synthesis, monounsaturated fatty acid synthesis, and fatty acid oxidation was decreased. This work and subsequent studies on the expression of cholesterologenic genes in HD will be discussed in more detail in Chapter 3 and Appendix I.

1.5.3.4. Impairment in protein clearance systems

Cells, through various mechanisms, exert precise control over the synthesis, localization, and proper degradation of proteins. This balance is known as “proteostasis” (215,216).

The mechanisms that participate in concert to ensure proper cellular proteostasis are many, and include the chaperone-mediated control to ensure the correct folding of nascent polypeptides, as well as the post-translational modifications of proteins (i.e. palmitoylation) that facilitate the right localization of proteins within the cell, and importantly, the mechanisms that are in charge of the elimination of proteins that have become misfolded or damaged (215,216). Degradative proteostatic pathways are particularly relevant in the context of HD (217).

Degradation of misfolded or damaged proteins is achieved, in general, by three main mechanisms: The ubiquitin-proteasome system (UPS), chaperone-mediated autophagy (CMA) and macroautophagy (218) which are briefly reviewed below.

- **Ubiquitin-proteasome system**

Degradation of proteins by the UPS begins with the addition of monomers of ubiquitin (ubiquitination) to lysine residues of the protein to be degraded. After the first ubiquitin monomer has been transferred to the protein, sequential ubiquitin molecules can be added to lysine residues of the previous one. This is known as polyubiquitination (219). The ubiquitin molecule itself

possesses 7 lysine residues that can be subsequently ubiquitinated (K6, K11, K27, K29, K33, K48 and K63), allowing for the branching of polyubiquitin chains in almost infinite combinations (220). At first, it was believed that the UPS selectively degraded proteins marked with poly-K48 ubiquitination, but it was later demonstrated that almost all types of poly-Ub labelled proteins can be recognized and degraded by the UPS (221-224).

Ubiquitination is an active multistep process, carried out sequentially by three groups of enzymes named E1, E2 and E3. Enzymes that belong to the E1 and E2 groups are called ubiquitin-activating enzymes and ubiquitin-conjugating enzymes, respectively. Enzymes that belong to the E3 group are the ubiquitin ligases. These enzymes carry out the final step ubiquitination, and are the enzymes that possess specificity for the target (225).

Once a protein has been “tagged” with polyubiquitin chains, it is recognized and bound by Ub-associated-Ub-like (UBA-UBL) shuttling proteins, which deliver the cargo to the 19S (regulatory) subunit of the proteasome (226-229). Proteins are de-ubiquitinated as they are being unfolded and shuttled into the proteolytic chamber of the 20S subunit, where the protein is subsequently cleaved in an energy-dependent process (230,231). The UPS not only plays a role in the degradation of damaged proteins, but it also participates in development and differentiation, antigen presentation, apoptosis regulation and amino acid recycling (218).

In HD, the UPS is impaired, although the mechanisms by which muHTT inhibits the proteasome are still under investigation. For instance, there have been several reports of inclusion bodies containing muHTT that are also positive for ubiquitin and various components of the proteasome, suggesting that the UPS is engaged in an attempt to eliminate the toxic protein (85,87,232).

Wang and collaborators observed a slower rate of degradation of fluorescent reporter proteins used to determine the activity of the UPS, in primary neurons and in the striatum of transgenic mice expressing an N-terminal fragment of muHTT (R6/2), suggesting decreased activity of the UPS (233). However, in another study, aggregates made of recombinant muHTT peptides did not inhibit the UPS activity *in vitro*, suggesting that the inhibition of the UPS may require prior muHTT ubiquitination or other post-translational modifications (234).

Another hypothesis that has been studied is the possibility of “clogging” of the UPS with polyQ stretches that may be difficult to degrade. Two studies, using different approaches concluded that muHTT, and even polyQ peptides can sequester, and due to a stable interaction, clog the catalytic activity of the proteasome (235,236). Two other studies, however, reached different conclusions and showed that muHTT and polyQ peptides are completely and efficiently degraded by eukaryotic proteasomes (237,238).

- **Chaperone-mediated autophagy**

Chaperone-mediated autophagy is a selective lysosomal-based degradative system in which soluble cytosolic substrates are recognized and delivered directly into the lumen of the lysosome for their degradation (239). Recognition of the cargo is carried out by the cytosolic chaperone heat shock cognate protein of 70 KDa (HSC70), which by interacting with a consensus sequence (KFERQ) shared among the targets of CMA, is able to recruit and deliver the cargo to the lysosomal membrane (240). HSC70, together with the cargo, are then able to interact with the lysosomal-associated membrane protein type 2A (LAMP-2A) for the translocation of the protein into the luminal side of the lysosome, where a luminal form of HSC70 (lys-HSC70) participates in the internalization of the cargo (241). Once the protein is in the lumen of the lysosome, it is quickly degraded by resident proteases.

Although HTT does not contain the KFERQ sequence, it has been hypothesized that phosphorylation at Ser16 provides a negative charge that would mimic a KFERQ-like sequence, which could be recognized by HSC70 (112,242). Two other potential KFERQ-like sequences have been found between amino acids 99-103 and 248-252 of the HTT protein (242).

The work done by Koga and collaborators (243) demonstrated that levels of LAMP-2A and lys-HSC70 are increased in HD striatal cells and in the striatum of STHdh Q111 mice. Furthermore, N-terminal fragments (amino acids 1-82) of wtHTT and muHTT are degraded by CMA, while full-length HTT is not, despite containing the three KFERQ-like sequences mentioned above. The degradation of HTT N-terminal fragments by CMA was further confirmed in a second study, this time using a longer N-terminal fragment of HTT (amino acids 1-552), with wtHTT N-terminal fragments degraded more efficiently than the muHTT counterparts (244).

- **Macroautophagy**

Macroautophagy (hereafter referred simply as autophagy) is also a lysosomal-based degradative system in which the cargo is first recognized and engulfed by a specialized organelle called “autophagosome”. Autophagosomes then fuse with the lysosome in order to expose the cargo to the lysosomal enzymatic machinery and thus achieve the degradation of the cargo. Contrary to CMA, autophagy can degrade non-soluble material such as organelles, pathogens, and aggregated proteins (i.e. muHTT) (245-249). Autophagy and its role in HD will be further reviewed in Chapter 5.

1.6. Animal and cell models of HD

After the discovery of the HD causative mutation by the Huntington's Disease Research Collaborative Group in 1993 (2), various groups around the world have created animal and cell models of HD, which are briefly reviewed below.

1.6.1. Non-mammalian models of HD

Non-mammalian organisms have some advantages including the rapid generation of offspring and the low cost of maintenance. HD models have been developed in *Drosophila*, *C. elegans* and *Danio Rerio* (250-254), in which many features of the disease can be replicated and studied, including a reduced life-span, progressive neuronal degeneration, aggregation of muHTT, among others (208). The rapid development of the phenotypes and the low cost make these models ideal for the initial study of new pathways, high-throughput screening of drugs or genetic manipulation for the study of disease modifiers. Nevertheless, as for any other disease modelled in a non-mammalian organism, it is sometimes hard to predict the extent to which findings in these models do reflect the human pathology (208).

1.6.2. Mouse models of HD

Mouse models have allowed researchers to study the early pathological, cellular and molecular dysfunctions caused by muHTT. Several mouse models of HD have been developed to date, including transgenic mice expressing either N-terminal fragments or the full-length muHTT gene, as well as knock-in models, created more recently in an attempt to closely reproduce the human pathology. Below I will briefly describe the most important characteristics of the mouse models that were used during my thesis work. For a recent review of the mouse models of HD developed so far, please refer to (255).

Yeast Artificial Chromosome (YAC) transgenic mice express the full-length human *HTT* gene, under the control of the human *HTT* promoter region. YAC46 and YAC72 mice, with 46 and 72 CAG repeats, respectively, were created first (256). These mice show electrophysiological abnormalities (impaired long-term potentiation) at 6 months of age. By 12 months of age, selective degeneration of the medium spiny neurons associated with muHTT accumulation in the nucleus is observed. Interestingly, these mice do not show any muHTT aggregation in any of the brain regions examined (256).

Years later, using the same principles, YAC128 mice expressing muHTT with 128 CAG repeats were created (179). These mice have less inter-individual variability and an earlier onset of the disease compared with the YAC72 mice. Hyperkinesia appears at 3 months of age followed by motor deficit on the rotarod at 6 months, and striatal and cortical atrophy at 9 and 12 months of age. No inclusion bodies of muHTT were detected, but researchers reported “micro-aggregates” detected only by immunogold and observable only under an electron microscope (179).

Knock-in (KI) HD mice were created in order to overcome the potential damage done to other genes during the insertion of the transgene into a random position in the genome. Furthermore, by using KI animals, it is possible to study the differences between homozygous or heterozygous mice for the HD mutation, allowing us to understand better the potential gene-dose effects caused by the HD mutation.

KI mice have been generated by two different mechanisms. The first mechanism was replacing the entire endogenous mouse exon 1 for a mutated human exon 1, thus creating a chimeric gene. Mouse models Q140 (257), and the spontaneously generated zQ175 mice (258) share this characteristic.

The other approach that has been used, is to introduce only an elongated CAG stretch conserving the mouse DNA sequence surrounding the mutation. Examples of these mice are the HdhQ92, HdhQ111 (259) and HdhQ150 mice (260).

In general, KI mice have a milder motor phenotype, and the age of onset (except for the zQ175 model) tends to be later when compared to transgenic mice. HdhQ92 and HdhQ111 mice start showing motor deficits around 20 months of age (259), while zQ175 mice show motor abnormalities as early as 4-8 weeks (258), suggesting an inverse correlation between length of the CAG repeat and the age of onset, similarly to human patients. The neuropathological findings follow a similar trend. HdhQ92 and HdhQ111 mice show no detectable brain atrophy even at 20 months of age (208), while zQ175 mice display progressive striatal and cortical atrophy, starting as early as 3 months of age (258).

One thing that does not seem to correlate with the length of CAG repeats, nor with the age of onset, is the presence of muHTT aggregates. HdhQ111 mice show large detectable nuclear and cytoplasmic muHTT aggregates as early as 1.5 months of age, while zQ175 mice have muHTT intranuclear cortical and striatal aggregation at 6 months of age, much later than the onset of the motor deficits (261). Moreover, only 25% of Q140 mice show muHTT aggregation at 1 month of age. Aggregates of muHTT in this model, become generalized at 4-6 months of age (257).

1.6.3. Cell models of HD

Cell models of HD have been, and still are, crucial for the understanding of the basic molecular and cellular mechanisms that underlay the pathogenesis of HD. The expression of full-length or N-terminal fragments of wtHTT and muHTT in neuronal and non-neuronal cell lines has allowed researchers to uncover HTT protein interactors, investigate the mechanism of aggregation, as well

as to explore the role of muHTT in various cellular processes. In general, cell lines are suitable models for the initial study of therapeutic approaches. Moreover, cell lines are very useful for high-throughput screening of potential small molecules in the context of drug discovery.

A commonly used cell model of HD was derived from embryonic striatal tissue of the HdhQ111 mouse (259). These cells, named STHdh Q111, were immortalized using a temperature-sensitive version of the large T antigen (TAg) of the simian vacuolating virus 40 (SV40). When cells are grown at 33°C, the TAg sequesters p53 protein, allowing cell division. Instead, when cells are cultured at 39°C, the TAg gets degraded, releasing p53 protein from sequestration, which in turns promotes apoptosis (262).

Additionally, cell repository banks (i.e. Coriell Institute) have collected human fibroblasts obtained from adult as well as juvenile-onset HD patients. These cells, being of human origin, offer many advantages in comparison to mouse cells. Not only they express the human full-length *HTT* gene, but also all possible HTT protein interactors are human as well. One obvious disadvantage is that fibroblasts are peripheral cells and do not share many of the characteristics of neuronal cell lines. However, by dedifferentiating human HD fibroblasts, a consortium of researchers has developed induced pluripotent stem cells (iPSCs) which can be differentiated into neuronal lineages (263). The development of HD iPSCs is a historical milestone that will most likely open the window to a new era of research in HD, from drug discovery (264) to cell-based therapy (265).

1.7. Therapeutic approaches

Despite intense research done all around the globe, there are no current therapies that effectively stop or slow down the progression of HD. (266). To date, only one drug has received approval

from the Federal Drug Administration (FDA) for the management of HD: tetrabenazine. Tetrabenazine is a reversible inhibitor of the vesicular monoamine transporter type 2 (VMAT2), causing dopamine depletion at the synaptic terminals in the striatum (267).

The TETRA-HD study, the first trial using tetrabenazine in HD patients, reported that 12 weeks of treatment reduced chorea severity (23.5% improvement), however did not slow or stop progression of HD, and it did not improve overall motor symptoms (268). Continuation of the TETRA-HD confirmed the safety of the drug after long-term usage (80 weeks) (269).

Given the poor results obtained with small molecules for the treatment of HD, researchers have turned into gene therapy as a possible mechanism to reduce the expression of muHTT, and perhaps, modify the progression of the disease. Using RNAi, Harper and collaborators (270) were able to decrease muHTT expression in HD cells. Moreover, when shRNA against HTT was delivered into the striatum of HD transgenic mice, it was able to reduce muHTT expression *in vivo* as well as muHTT aggregation, and also improved motor behaviour.

Based on the positive results obtained with gene therapy in animal models, Ionis Pharmaceuticals, in collaboration with Roche, are carrying out a clinical trial using intrathecal injections of antisense oligonucleotides (ASOs) directed against HTT (named IONIS-HTT_{RX}) in a total of 46 adult patients with HD. Last press release (dated April 24, 2018) informed that patients had a 40-60% reduction in muHTT found in CSF. Based on their predictions, they estimate that IONIS-HTT_{RX} treatment is causing a 55-85% reduction of muHTT expression in the cortex and a 20%-50% reduction of muHTT expression in caudate regions. Patients also showed significant improvement in two out of four motor tests after 13 weeks of treatment. So far, no serious adverse effects have been reported in any of the patients.

A new generation of ASOs directed specifically against the muHTT mRNA (allele-specific) is currently under development. Studies using allele-specific ASOs have been shown to reduce muHTT expression in brains of transgenic mice. Moreover, human HD fibroblasts treated with allele-specific ASOs showed reduced expression of muHTT, but the expression of wtHTT was relatively spared (271), which constitutes a desirable feature since it has been shown that deletion of *Htt* gene causes neurodegeneration in adult mice (98).

Previous work done in our laboratory has shown that levels of ganglioside GM1 are decreased in various cell and animal models of HD, and that exogenous supply of GM1 protects HD cells against apoptosis (272) and restores motor and non-motor behaviour across mouse models of HD (115,273). These behavioural effects of GM1 in HD mice are paralleled by a decrease in the amount of both, soluble muHTT and muHTT aggregates, indicating that supply of GM1 is a disease-modifying therapy in HD models (273). To date, GM1 usage for the treatment of HD remains at a pre-clinical stage, and further work would be required before its usage can be translated into clinical research. Further details about the role of GM1 in neurodegeneration, and more specifically in the context of HD, can be found in following chapters of this thesis.

1.8. General hypotheses and objectives of the thesis

During the course of my Ph.D. training, I worked on two different projects under the supervision of Dr. Simonetta Sipione, both of which will be summarized in the following chapters.

The first project was aimed to investigate whether cell and animal models of HD do show any defects in protein prenylation, due to a known dysfunction of the mevalonate pathway. Further literature review on the subject and experimental data regarding this project are found in Chapter 3 and Appendix I.

The second project was aimed to investigate the mechanisms underlying the therapeutic effects of GM1 in HD models. More specifically, I investigated whether the exogenous supply of ganglioside GM1 is able to decrease accumulation of protein aggregates in cell models of proteotoxic stress, such as muHTT expression and inhibition of the proteasome.

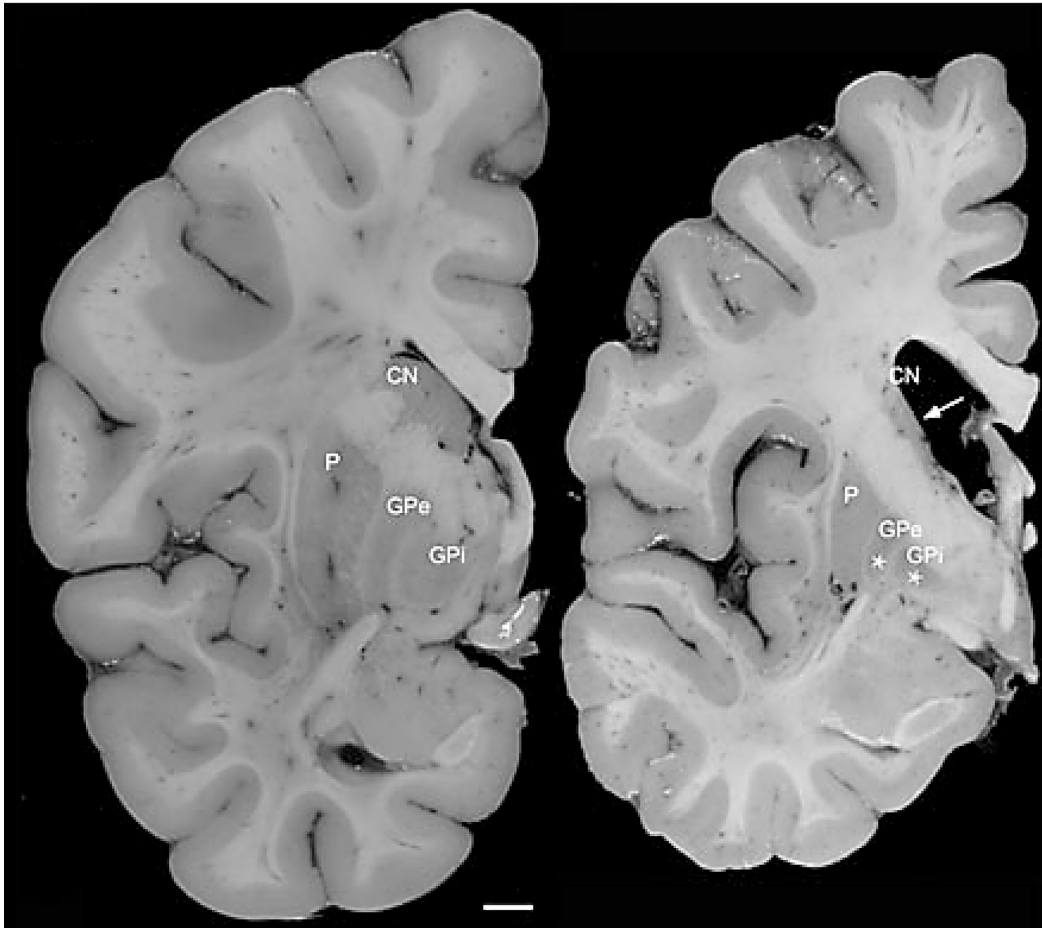
In chapter 4, I will show experimental data demonstrating that exogenous supply of GM1 can decrease the accumulation of protein aggregates in two established models of proteotoxic stress: expression of exon 1 of muHTT and pharmacological inhibition of the proteasome.

In chapter 5, I test the hypothesis that GM1 treatment increases cellular autophagic degradation of protein aggregates after expression of exon 1 of muHTT or pharmacological inhibition of the proteasome. I will show data suggesting that autophagy is not involved in the reduction of protein aggregates after GM1 treatment.

In chapter 6, I will address the question whether GM1 is able to increase the secretion of misfolded toxic proteins via extracellular vesicles. I will show data suggesting that GM1 treatment is able to increase the production of extracellular vesicles. Additionally, I will also show evidence suggesting that secretion of exon 1 of muHTT via extracellular vesicles is increased after GM1 treatment, suggesting that this could represent a neuroprotective mechanism activated by GM1 in HD models.

1.9. Figures

Figure 1.1 The Huntington's disease brain

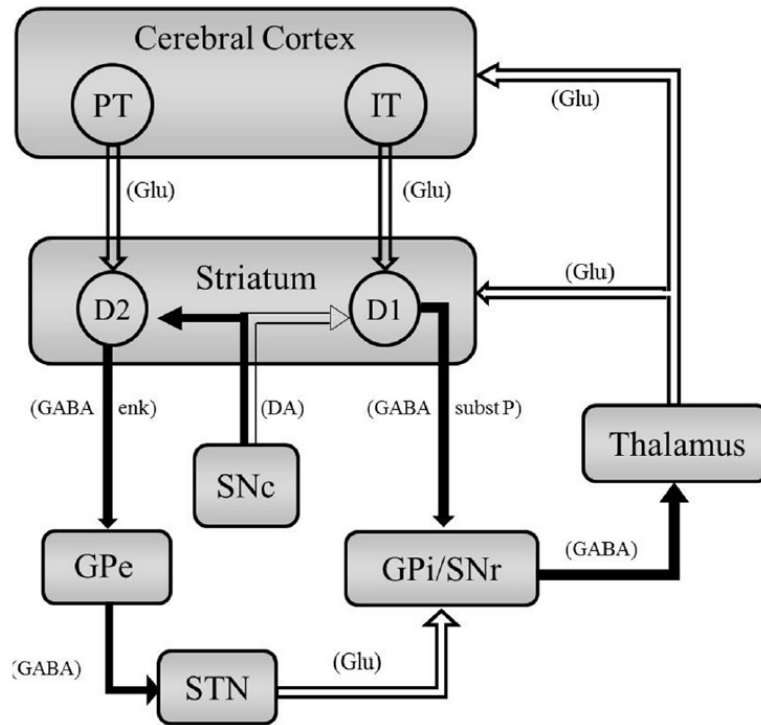


Coronal sections of a normal left brain hemisphere (left) and a left brain hemisphere of an HD patient, grade 3/4 (right).

CN = caudate nucleus, GPe = globus pallidus external segment, GPi = globus pallidus internal segment, P = putamen. Scale bar = 1 cm.

(Modified from (42): Waldvogel, H. J., et al. (2015). "The Neuropathology of Huntington's Disease." *Curr Top Behav Neurosci* 22: 33-80)

Figure 1.2. Simplified representation of the circuitry of the basal ganglia.



Schematic representation of basal ganglia circuits. Inhibitory connexions are shown as closed arrows and excitatory connections are shown as open arrows. Neurotransmitters are indicated in parenthesis. PT = Pyramidal tract, IT = intralencephalic projecting neurons, SNc/r = substantia nigra pars compacta/reticulata, GPe/i = globus pallidus external/internal segment, STN = subthalamic nucleus, Glu = glutamate, enk = enkephalin, subst P = Substance P.

(Reproduced from (274): Bunner, K. D. and G. V. Rebec (2016). "Corticostriatal Dysfunction in Huntington's Disease: The Basics." Front Hum Neurosci 10: 317)

Chapter 2: Materials and methods

This chapter is my original work.

2.1. Chemicals and reagents

Ganglioside GM1 was obtained from Enzo Life Sciences (Farmingdale, NY, USA) or from TRB Chemedica (Vouvry, Switzerland). MG132 was purchased from Millipore (Burlington, MA, USA). Protease inhibitor cocktail Complete® and phosphatase inhibitor cocktail PhosStop® were purchased from Roche (Basel, Switzerland). Culture media and cell culture buffers, including Dulbecco's Modified Eagle Medium (DMEM)/high glucose, Minimal Essential Medium (MEM), Opti-MEM® and Hibernate A®, Neurobasal A®, B27 supplement®, Glutamax® supplement, HBSS buffer and cell culture grade PBS were purchased from Gibco®, a sub-division of Thermo Scientific (Waltham, MA, USA). Fetal bovine serum was obtained from Sigma (St. Louis, MO, USA). All other reagents, including salts, non-cell culture grade buffers and detergents were purchased from Sigma (St. Louis, MO, USA) unless otherwise stated in this text. All DNA primers were custom synthesized by Integrated DNA Technologies (Coralville, IA, USA).

2.2. Administration of GM1

GM1 was dissolved in cell-culture grade water to a concentration of 10 mM (stock solution) and stored at -20°C until use. GM1 stock solution was diluted directly in the cell culture media to a final concentration of 50-100 µM, as indicated. GM1 is an amphipathic molecule which forms micelles at concentrations above 29 µM in aqueous solutions (275), and is readily incorporated into cells (272). No toxicity of the compound was observed at the concentrations and conditions used in my studies.

2.3. Cell models

STHdh Q7/7 cells are neuronal progenitor cells derived from embryonic striatal tissue of a WT mouse. Instead, **STHdh Q7/111** and **STHdh Q111/111** are neuronal progenitor cells derived from

embryonic striatal tissue from heterozygous and homozygous knock-in mice containing an elongated stretch with 111 CAG repeats in the exon 1 of the *Htt* gene (259). Cells were immortalized by using the tsA58 SV40 large T antigen (262). STHdh Q7/7, Q7/111 and 111/111 cells were a kind gift from Dr. Marcy McDonald (Massachusetts General Hospital, Boston, MA, USA).

Immortalized **ST14A** cells were obtained from embryonic rat striatal tissue. These cells were immortalized using the same approach as for STHdh Q7/7 cells (276). ST14A cells were stably transfected with a pLXSP plasmid encoding the first 548 amino acids of human HTT, containing either 15 or 128 glutamines (127). These cells were kindly donated by Dr. Elena Cattaneo (University of Milan, Italy).

Mouse neuroblastoma **Neuro2a** cells (hereafter referred to as N2a) (277) were kindly provided by Dr. Satyabrata Kar (University of Alberta, Canada).

Mouse immortalized astrocytes were kindly donated by Dr. Holtzman (Washington University School of Medicine, USA) (278). These astrocytes were further modified in our laboratory by transfecting the cells with a pLXSP plasmid encoding the first 548 amino acids of human HTT, containing either 15 or 128 glutamines (127). The plasmid was kindly provided by Dr. Elena Cattaneo (University of Milan, Italy).

Human fibroblasts were purchased from the Coriell Institute Cell Repository. Fibroblasts from 4 HD patients were purchased (Catalog numbers: GM05539, GM04855, GM03621, GM) as well as three control fibroblasts samples (Catalog numbers: GM101869, AG08181, AG07573). Full characterization of the patients and controls who donated the samples is available through the Coriell Institute Cell Repository website.

Postnatal mouse/rat primary neurons

Preparation and maintenance of postnatal neurons were done as published before (279), with minor modifications. First, glass coverslips (12 mm diameter, Thermo Scientific, Waltham, MA, USA) were coated with poly-L-lysine following the standard operating procedure optimized in Sipione laboratory. Briefly, coverslips were acid-washed with a 5N HCl solution for 1 h in a glass Petri dish. Then, coverslips were washed 5 times with MilliQ water. Coverslips were autoclaved and placed into 24-well plates under sterile conditions. Poly-L-lysine coating was performed by covering the coverslips with 300 μ L of a 75 μ g/mL solution of high molecular weight poly-L-Lysine (MW>300,000 Da, Sigma, St. Louis, MO, USA) dissolved in borate buffer 0.1 M (3.1 g/L boric acid, 4.75 g/L sodium tetraborate, pH 8.5). Coverslips were incubated in poly-L-lysine solution for at least 2 h and then washed twice with sterile PBS. Up to 500 μ L of plating media per well were added to each well, and the plates were stored at 37°C in the cell culture incubator until further use.

Newborn rat/mouse pups (P0-1) were decapitated according to a procedure approved by the University of Alberta's Animal Use Committee and the Canadian Council on Animal Care (CCAC). Brains were dissected in dissection buffer (10 mM HEPES, 1 mM sodium pyruvate, 200 U/mL penicillin, 200 μ g/mL streptomycin, in HBSS Ca⁺⁺/Mg⁺⁺-free). Cortices or striata were transferred into a 50 mL polystyrene tube. Tissue was resuspended in freshly prepared papain solution (1 mg/mL papain, 200 μ M Glutamax®, in HBSS Ca⁺⁺/Mg⁺⁺-free) and incubated at 37°C for 10 min. DNase I was added to a final concentration of 0.5 mg/mL to the suspension, and incubation continued for 5 min. Digestion was stopped by adding heat-inactivated FBS to a final concentration of 10% v/v. Digested tissue was centrifuged at 200 x g for 1 min at RT, supernatant was discarded, and trituration was performed by resuspending the tissue in plating/trituration

media (10% v/v heat-inactivated FBS, 1 mM sodium pyruvate, 2 mM L-glutamine, 100 U/mL penicillin, 100 µg/mL streptomycin, in MEM medium) and passing the tissue 10 times through a fire-polished glass Pasteur pipette. The cell suspension was filtered through a 40 µm pore-sized nylon cell strainer (Thermo Scientific, Waltham, MA, USA) before being counted and plated at a density of 0.75×10^5 cells/cm². Upon cell attachment, usually after 1.5-2 h of plating, the plating/trituration media was replaced with growth media (200 µM Glutamax®, 100 U/mL penicillin, 100 µg/mL streptomycin, 1X B27® supplement, in Neurobasal A® medium). On DIV2, cells were treated with cytosine arabinoside (5 µM) for 24 h to avoid glia overgrowth. Experiment/treatments were performed at DIV10-13.

Embryonic rat cortical primary neurons

Preparation and maintenance of embryonic primary neurons were performed as previously described (280) with minor modifications. Briefly, plates and coverslips were prepared as described above for postnatal mouse/rat primary neurons. Pregnant dams (Sprague Dawley) were anesthetized with isoflurane gas and euthanized by decapitation at day 18 of pregnancy. All procedures were approved by the University of Alberta's Animal Use Committee and the Canadian Council on Animal Care (CCAC). A transversal laparotomy was performed to expose the uterus horns containing the embryos. Uterus horns were dissected and transferred to a Petri dish placed on ice. Embryos were isolated and decapitated in ice-cold dissection buffer. Brains were then isolated, and cortices were dissected under a stereo microscope.

Cortices were transferred to a 50 mL polystyrene tube, resuspended in 0.25% w/v trypsin-EDTA solution (Thermo Scientific, Waltham, MA, USA) and incubated at 37°C for 20 min. Digestion was stopped by centrifuging the tissue at 300 x g for 2 min, removing trypsin solution and replacing it with trituration/plating media. Trituration was performed by passing the tissue 10 times through

a fire-polished glass Pasteur pipette. The cell suspension was filtered through a 40 µm pore-sized nylon cell strainer (Thermo Scientific, Waltham, MA, USA), counted and plated at a density of 1.3×10^5 cells/cm². After cell attachment, usually after 1.5-2 h of plating, the plating/trituration medium was replaced with growth media (200 µM Glutamax®, 100 U/mL penicillin, 100 µg/mL streptomycin, 1X B27® supplement, in Neurobasal® medium). On DIV2, cells were treated with cytosine arabinoside (3 µM) for 48 h to avoid glia overgrowth. Experiment/treatments were performed at DIV15-16.

2.4. Animal models

YAC128 mice (FVB background) overexpressing the full-length human *HTT* gene containing 128 CAG repeats, including promoter and regulatory regions (179) were obtained from the Jackson Laboratory (Bar Harbor, ME, USA) and maintained in our animal facility at the University of Alberta. WT littermates were used as controls.

Q140 knock-in mice (C57BL/6 background) expressing a chimeric *HTT* gene that comprises exon 1 of the human *HTT* gene with 140 CAG repeats (257) were obtained from the Jackson Laboratory (Bar Harbor, ME, USA) and maintained in our animal facility at the University of Alberta.

2.5. Gene expression analysis

For analysis of gene expression, total RNA was purified from cells and tissue using the RNeasy® kit (Qiagen, Venlo, Netherlands) according to the manufacturer's instructions. Total RNA was quantified by spectrophotometry. Superscript II® Reverse Transcriptase (Thermo Scientific, Waltham, MA, USA) was used to prepare complementary DNA (cDNA) from 500-4000 ng of total RNA. Oligo dT (12-18) primers were used for the initiation of the reverse transcription. For cDNA amplification and quantitation, PowerUp SYBR Green Master Mix® (Thermo Scientific,

Waltham, MA, USA) was used, according to manufacturer's recommendations. All reactions were carried out on a StepOnePlus® Real-Time PCR System (Thermo Scientific, Waltham, MA, USA). Relative abundance of targets was calculated by extrapolating the Ct values of the targets against a standard curve, and then normalized over the expression of one or more housekeeping genes, as published before (281). The sequence of the primers used in this thesis can be found in **Table 1**.

2.6. Preparation of Lipoprotein-Deficient Serum (LPDS)

Preparation of LPDS was performed as described before (282) with minor modifications. Briefly, increasing amounts of potassium chloride (KCl) were diluted in 50 mL of FBS, until the density of the solution reached 1.215 g/mL. Then, FBS was transferred to 10.4 mL polycarbonate bottles and centrifuged for 24 h at 285,000 x g, 4°C, using an MLA-55 rotor in an Optima MAX® Tabletop Ultracentrifuge (Beckman Coulter, Brea, CA, USA). After centrifugation, the upper layer containing the lipoproteins was discarded. LPDS was then dialyzed for 24 h using a 12,000-14,000 MWCO dialysis membrane (Spectrum Laboratories, Rancho Dominguez, CA, USA). Dialysis buffer (5 mM Tris-HCl, pH 7.4, 150 mM NaCl, 1 mM EDTA) was replaced at least 4 times during the dialysis process. LPDS was then filter-sterilized through a 0.22 µm pore-sized PVDF filter (Millipore, Burlington, MA, USA). To confirm lipoprotein removal, cholesterol content was measured before and after delipidation by using the Amplex® Red Cholesterol Assay Kit (Thermo Scientific, Waltham, MA, USA), according to manufacturer's instructions. Typically, cholesterol content after delipidation was <10%, when compared to unprocessed FBS.

2.7. Immunoblotting

All steps were done on ice unless otherwise stated. Cells or tissues were lysed in NP-40 lysis buffer (20 mM Tris-HCl, pH 7.4, 1% NP-40 v/v, 1 mM EDTA, 1 mM EGTA, 50 µM MG132

supplemented with 1X protease/phosphatase inhibitor cocktail) or RIPA buffer (20 mM Tris-HCl, pH 7.4, 0.5% Sodium deoxycholate w/v, 0.1% SDS w/v, 1% Triton X100 v/v, 150 mM sodium chloride, 1 mM EDTA, 1 mM EGTA, 50 μ M MG132, supplemented with 1X protease/phosphatase inhibitors). Briefly, cells were washed once with PBS and then lysis buffer was added directly to the cell culture dish. Cells were scraped and transferred into a clean 1.5 mL centrifuge tube. For tissue, cerebral cortices or striata were dissected from HD and WT mice. Tissue homogenization was performed in NP-40 or RIPA buffer by using a motorized pestle homogenizer (Wheaton, Millville, NJ, USA). Lysates from cells and tissue were then passed 10 times through a 26-27G needle and sonicated twice for 10 seconds each time. Protein concentration was determined using BCA assay (Thermo Scientific, Waltham, MA, USA). Protein samples (10-50 μ g) were boiled in SDS loading Buffer (5X concentration: 213.5 mM Tris-HCl, pH 6.8, 10% SDS w/v, 50% Glycerol v/v, 25% β -mercaptoethanol v/v) and then loaded onto SDS-PAGE gels. Proteins were run in a Mini-PROTEAN® II (Bio-Rad, Hercules, CA, USA) electrophoresis chamber and then transferred to an FL-PVDF membrane (Millipore, Burlington, MA, USA) using a Mini Trans-Blot® apparatus (Bio-Rad, Hercules, CA, USA). For most proteins, transfer was performed in regular Towbin buffer (25 mM Tris-HCl, 192 mM Glycine, 20% Methanol v/v). For full-length HTT, transfer was performed in modified Towbin buffer (25 mM Tris-HCl, 192 mM Glycine, 16% Methanol v/v, 0.05% SDS w/v). Proteins with a high isoelectric point (e.g. LC3 and COXIV) were transferred using CAPS buffer (10 mM 3-(cyclohexylamino)-1-propanesulfonic acid, pH 10.5, 10% Methanol v/v). Membranes were blocked in blocking solution (5% BSA w/v in TBS) for 1 hour.

Primary antibodies were dissolved in 2.5-5% BSA w/v in TBS-T. The complete list of primary antibodies used in this work can be found in **Table 2**. For detection, secondary antibodies

conjugated with horseradish peroxidase (Bio-Rad, Hercules, CA, USA) or with IRDye fluorophores (LiCor Biosciences, Lincoln, NE, USA) were used. For chemiluminescent detection, ECL Prime® Western Blotting Detection Reagent (GE Healthcare, Little Chalfont, U.K.) and an AI600® imager (GE Healthcare, Little Chalfont, U.K.) were used. For the detection of fluorescent secondary antibodies, an Odyssey® near-infrared scanner was used (LiCor Biosciences, Lincoln, NE, USA). Quantification of the signal was made using either NIH ImageJ® or Odyssey® Application Software v3.0, respectively. Protein levels were normalized over Revert® total protein stain (LiCor Biosciences, Lincoln, NE, USA), or over the signal for a housekeeping protein (e.g. tubulin), as indicated.

2.8. Triton X114 fractionation

Fractionation of proteins using Triton X114 was performed as previously published (283) with the following minor modifications:

- **Pre-condensation of Triton X114:** 20 g of Triton X114 were mixed with 980 mL of condensation solution (10 mM Tris-HCl, pH 7.6, 150 mM NaCl and 16 mg of butylated hydroxytoluene previously dissolved in 200 µL of ethanol). Detergent was dispersed at 0°C (on ice) on a magnetic stirring plate. To precipitate the detergent, the solution was warmed at 30°C for 18h and the aqueous top layer was removed and discarded. This procedure was repeated two more times. The concentration of Triton X114 was then determined by spectroscopy, assuming a molar absorption of $1.46 \times 10^3 \text{ Lmol}^{-1}\text{cm}^{-1}$ when dissolved in 1% SDS w/v solution, at 275 nm. Typically, the concentration of Triton X144 pre-condensed solution is around 10%.

- **Fractionation:** Cells were washed once with PBS and then lysed in harvest solution (20 mM Tris-HCl, pH 7.5, 1% Triton X114 v/v, 150 mM NaCl, supplemented with 1X protease/phosphatase inhibitor cocktail). Lysates were sonicated twice for 10 s each time, incubated on ice for 30 min and then centrifuged at 21,000 x g at 4°C to pellet unbroken cells and debris. The supernatant was transferred to a clean tube and protein concentration was measured by BCA assay (Thermo Scientific, Waltham, MA, USA). Typically, 80-120 µg of total protein were diluted in a final volume of 80-120 µL of harvest buffer and then placed over 40-60 µL of cushion buffer (20 mM Tris-HCl, pH 7.5, 0.06% Triton X114 v/v, 150 mM NaCl, 6% sucrose w/v). Tubes were incubated at 37° C for 10 min to allow the micellization of the detergent. Tubes were then centrifuged at 16,000 x g for 5 minutes at RT. The aqueous phase (upper layer) was then transferred to a clean tube and the detergent phase (bottom layer) was diluted with harvest buffer until both phases had the same volume. Equal volumes of both phases were loaded side by side onto an SDS-PAGE gel and immunoblotting was performed. Proteins that are hydrophobic due to lipidation (e.g. prenylation, palmitoylation, etc.) or to the presence of transmembrane domains, would appear preferentially in the detergent phase, while non-lipidated hydrophilic proteins are distributed to the aqueous phase. HSP90 and COXIV or VDAC proteins were used as markers of aqueous and detergent phases, respectively. The full list of antibodies used in this work is found in **Table 2**.

2.9. Cell transfection

Throughout this work, various cell lines were transfected with plasmids encoding a WT or a mutant version of the exon 1 of the HTT protein, tagged with enhanced GFP (Ex1-25Q-HTT-eGFP and Ex1-72Q-HTT-eGFP) (284). Plasmids were a kind gift from Dr. Housman (Massachusetts Institute

of Technology, Cambridge, MA, USA). Transfection of cells was performed using two different methods.

- **Lipid-based transfection:** This protocol was used for the generation of cell lines (HeLa and N2a) stably expressing N-terminal HTT fragments, used for the study of extracellular vesicles, mentioned in chapter 6. Briefly, cells were plated in 6-well plates and let attach overnight. Next day, 7.5 μL of Lipofectamine 3000[®] reagent (Thermo Scientific, Waltham, MA, USA) were diluted in 125 μL of OptiMEM[®] (Thermo Scientific, Waltham, MA, USA). In a separate tube, 2.5 μg of plasmid DNA were mixed with 5 μL of P3000[®] reagent and 125 μL of OptiMEM[®]. Contents of both tubes were mixed and incubated for 15 min at RT. Media in the dishes was replaced with fresh media, and the mix of reagents was added directly to the cells. Expression of fluorescent protein was assessed after 16-18 h of transfection.
- **Electroporation:** All transfections via electroporation were performed using a 4D-Nucleofector[®] X Unit (Lonza, Basel, Switzerland) and done accordingly to the standard operating procedures published on the manufacturer's website. This protocol was used for the transient transfection of HeLa and N2a cells with N-terminal HTT fragments, used for the analysis of protein aggregation, autophagy and extracellular vesicle secretion, mentioned in chapters 4, 5 and 6. Briefly, cells were washed once with PBS and then trypsinized. A total of $2\text{-}2.5 \times 10^6$ cells were resuspended in Nucleofector[®] solution (Lonza, Basel, Switzerland) containing 4-5 μg of plasmidic DNA. Cell suspension was then transferred to a Nucleocuvette[®]. Nucleofection programs used were DS-137 and CN-144, for N2a and HeLa cells, respectively.

After nucleofection, cells were allowed to recover in the Nucleocuvette® at 37°C for 10 min and then were plated onto 100 mm cell culture dishes at a density of 2.5-5x10⁶ cells/dish.

2.10. Generation of stably-transfected cell lines

HeLa and N2a cells stably expressing wt or muHTT fragments, tagged with GFP, were generated as follows. First, a dose-response curve for Geneticin® (Thermo Scientific, Waltham, MA, USA) was made using HeLa and N2a cells, in order to determine the optimal dose for positive selection in these two cell lines. It was determined that the optimal dose of Geneticin® is 800 µg /mL of cell culture media. Then, HeLa and N2a cells were transfected with Ex1-25Q-HTT-eGFP and Ex1-72Q-HTT-eGFP plasmids using Lipofectamine 3000® as stated above. After fluorescence was confirmed, Geneticin® was added to the culture media. Dead cells and debris were removed by replacing the media every 24-48 h. Additionally, GFP-positive cells were selected by fluorescence activated cell sorting (FACS) using a FACSAria® III cell sorter (Becton Dickinson, Franklin Lakes, NJ, USA). Expression of HTT fragments in GFP-positive cells was confirmed by immunoblotting.

For the generation of clonal lines, GFP-positive cells were sorted into 96-well plates at a concentration of one cell per well using a FACSAria® III cell sorter (Becton Dickinson, Franklin Lakes, NJ, USA). Wells were periodically checked for cell growth. Up to 10 clones with high fluorescence and normal morphology were later checked for expression of HTT fragments by immunoblotting. Stably transfected clones were expanded and maintained in medium containing 400 µg /mL of Geneticin®.

2.11. Immunocytochemistry

Cells were grown on glass coverslips coated with poly-L-lysine as described above. After the indicated treatments, cells were washed twice with HBSS with $\text{Ca}^{++}/\text{Mg}^{++}$ and fixed in freshly prepared 4% paraformaldehyde w/v in PBS for 15 min at RT. After fixation, cells were washed twice with PBS and permeabilization was performed using a 0.1% Triton X100-PBS v/v solution for 5 min. Detergent was removed by washing three times with PBS.

Non-specific epitopes were blocked by incubating the coverslips with 250 μL of 4% donkey serum v/v (Sigma, St. Louis, MO, USA) diluted in PBS for 1h. Primary and secondary antibodies were diluted in blocking solution and incubated for one hour each. Both, primary anti-p62 antibody and fluorescently-labelled secondary antibody were used at 1:500 dilution. Nuclear staining was performed using a 4',6-diamidino-2-phenylindole (DAPI) solution (0.6-1.2 nM) dissolved in PBS, for 5 min. After removing the excess of DAPI stain, coverslips were mounted on microscope slides using ProLong® Gold antifade mounting media (Thermo Scientific, Waltham, MA, USA).

Images from stained cells were obtained either with an Axio Observer® Z1 inverted fluorescence microscope using an oil 63X objective (Carl Zeiss, Oberkochen, Germany) or with a Leica SP5® scanning confocal microscope using an oil 100X objective (Leica, Wetzlar, Germany).

2.12. Lysosome staining

Staining for lysosomes was performed using LysoTracker® Deep Red reagent (Thermo Scientific, Waltham, MA, USA) following the manufacturer's recommendations. Briefly, the LysoTracker® stock solution (1 mM in DMSO) was diluted 1:100 in growth medium to make a working solution (10 μM), under sterile conditions. LysoTracker® Deep Red working solution was then added directly to the cell culture plate to achieve a final concentration of 50 nM. Cells were incubated at

37°C in a cell culture incubator for 30 min. After incubation, LysoTracker®-containing media was withdrawn and excess of stain was removed by washing the cells with PBS twice. After lysosome staining, cells underwent immunostaining as described above.

2.13. Image analysis

Microscopy images were exported as TIFF files using AxioVision v4.6 (Carl Zeiss, Oberkochen, Germany) or Leica Application Suite (Leica, Wetzlar, Germany). For further analyses, the open-source NIH ImageJ® software was used.

For analysis of inclusion bodies of muHTT (Fig. 4.4) the following procedure was applied: Individual channels were separated and resulting images were transformed to 8-bit images. To count the nuclei, an automatic intensity threshold was applied prior to image binarization. The “watershed” function in ImageJ® was applied to correctly identify individual nuclei before using the “analyze particle” function with a size threshold of 50 pixels. To analyze the size of muHTT aggregates, the pixel intensity threshold was set at 50 (minimum value) and 255 (maximum value) for both control and GM1-treated cells, before binarization of the images. The “analyze particle” function was then run using a size threshold of 1 pixel. No background subtraction was used for any of the images.

Analysis of aggresomes (Fig. 4.6C) and lysosomes (5.6A-D) was performed as follows: Scale was set at 60.546 nm per pixel. A maximum z-projection was generated from 4 z-stack images obtained with a separation of 0.13 µm between each image. Projection images were transformed to 8-bit images. For background subtraction, “rolling ball” radius was set at 20 pixels for all channels in all images. Then, the outline of each cell was drawn manually, and the selection was saved as a region of interest (ROI). For the analysis of p62 immunostaining, the threshold of pixel intensity

was set to 50-255 (min-max) before binarization, and the “analyze particle” function was run using a size threshold of 6 pixels to obtain number and size of p62 aggresomes. For the analysis of Lysotracker® Deep Red-labelled lysosomes, the threshold of pixel intensity was set to 20-255 (min-max) before binarization, and the “analyze particle” function was run using a size threshold of 6 pixels.

2.14. Protein p62 soluble/insoluble fractionation

Cells were washed once with PBS, on ice, before adding Triton X100 lysis buffer (20 mM Tris-HCl, pH 7.4, 1% Triton X100 v/v, 1 mM EDTA, 1 mM EGTA, 2.5 μ M sodium pyruvate, supplemented with 1X protease/phosphatase inhibitor cocktail) directly to the cell culture plate. Cells were scraped, and the lysate was transferred to a clean 1.5 mL centrifuge tube to be sonicated twice, for 10 s each time. Proteins were quantified by BCA assay. For fractionation, 20 μ g of total protein were transferred to a new tube, and the volume was brought up to 30 μ L with Triton X100 lysis buffer. Samples were centrifuged at 21,000 x g for 10 min at 4°C. The supernatant (soluble fraction) was transferred to a new tube, while the pellet was washed with 50 μ L of Triton X100 lysis buffer before being centrifuged. The second supernatant was discarded, and the pellet was resuspended in 20 μ L of SDS/Urea solution (6 M urea, 2% SDS w/v) by incubating the sample at RT for 30 min, vortexing each 10 min. Samples were boiled at 100°C for 10 min in SDS loading buffer. Both fractions were then loaded onto SDS-PAGE gels, and detection of protein p62 in both fractions was done by immunoblotting.

2.15. Preparation of extracellular vesicle-depleted serum (EVDS)

All experiments involving purification of extracellular vesicles were performed in cells cultured in EVDS. For this, 10 mL of fetal bovine serum (FBS) were transferred into a 10.4 mL

polycarbonate bottle and centrifuged for >16 h at 100,000 x g at 4°C, using an MLA-55 rotor in an Optima MAX® Tabletop Ultracentrifuge (Beckman Coulter, Brea, CA, USA). After centrifugation, the supernatant was filter-sterilized through a 0.22 µm pore sized PVDF filter (Millipore, Burlington, MA, USA). EVDS was then used to supplement cell culture media.

2.16. Purification of extracellular vesicles from conditioned media

Before media conditioning, excess of GM1 was removed by washing the cells once with HBSS with Ca⁺⁺/Mg⁺⁺, followed by an additional wash with HBSS with Ca⁺⁺/Mg⁺⁺ + 0.2% fatty acid free-BSA w/v, and two more washes with HBSS with Ca⁺⁺/Mg⁺⁺, before EVDS-supplemented media was added to the cells. This procedure was done to remove any non-incorporated GM1 from the surface of the cells.

Conditioned media (24 h incubation with cells lines, 72 h for embryonic primary neurons) were collected in 15 mL polypropylene centrifuge tubes and centrifuged at 2,000 x g at 4°C for 10 min in order to pellet detached cells, debris and apoptotic bodies. The pellet was discarded, and the supernatant was transferred to a 10.4 mL polycarbonate bottle and centrifuged for 1.5 h hours at 100,000 x g at 4°C, using an MLA-55 rotor in an Optima MAX® Tabletop Ultracentrifuge (Beckman Coulter, Brea, CA, USA). The pellet was washed once with PBS and centrifugation was repeated as above. The washed pellet was then resuspended in NP-40 lysis buffer if samples were to be analyzed by immunoblotting, in PBS for fluorescence analysis or in sodium cacodylate solution (0.1 M, pH 7.5) for electron microscopy analysis.

Alternatively, when microvesicle-enriched and exosome-enriched fractions were prepared, centrifugation at 10,000 x g at 4°C for 30 min was performed after pelleting cell debris, for the

collection of microvesicles (pellet). Supernatant was then centrifuged at 100,000 x g as stated above for further precipitation of exosomes.

2.17. Fluorescent staining of extracellular vesicles

To obtain fluorescently-labelled extracellular vesicles (EVs), HeLa and N2a cells were incubated with the lipophilic fluorophore 1,1'-dioctadecyl-3,3,3',3'-tetramethylindocarbocyanine perchlorate (Vibrant® DiI, Thermo Scientific, Waltham, MA, USA) as per the manufacturer's instructions. Briefly, cells were trypsinized and resuspended in serum-free medium at a density of 1×10^6 cells/mL. Then, 5 μ L of DiI stock solution (1 mM) were added per mL of cell suspension. HeLa cells were incubated at 37°C for 8 min, while N2a cells were incubated for 15 min. Excess of stain was removed by pelleting cells at 200 x g, removing the supernatant and resuspending the cell pellet in stain-free serum-free media twice before plating. Stained cells produced DiI-positive EVs that were then purified by ultracentrifugation, as indicated above. Fluorescence in lysates and EVs was measured in a SpectraMax® i3x plate reader (Molecular Devices, San Jose, CA, USA) and secretion of EVs was calculated as the ratio of total DiI fluorescence in the EVs over total DiI fluorescence in the lysate of cells, expressed as a percentage.

2.18. Transmission electron microscopy of extracellular vesicles

Electron microscopy of EVs was performed as previously published (285), with minor modifications. Briefly, the pellet of EVs was resuspended in 100 μ L of sodium cacodylate solution (0.1 M, pH 7.5) containing 2% paraformaldehyde w/v and 2% glutaraldehyde v/v. EVs were then resuspended and captured on carbon/formvar-coated 400 or 200 copper grids (Ted Pella Inc., Redding, CA, USA) following glow discharge. Grids were dipped once in MilliQ water, blotted dry onto tissue paper and transferred immediately on top of a drop of 2% uranyl acetate (UA) w/v

for 5-10 min. The grids were then blotted dry onto a tissue paper to remove the excess of UA, dipped in water once more and air dried. Images were captured using a Mega View III Soft imaging system (EMSIS, Muenster, Germany) using a digital camera mounted on a Philips 410 transmission electron microscope (Amsterdam, The Netherlands).

2.19. Detection and quantification of ganglioside GM1 in lysates and extracellular vesicles

Before preparing cell lysates or collecting EVs, cells were washed once with HBSS with $\text{Ca}^{++}/\text{Mg}^{++}$, followed by an additional wash with HBSS with $\text{Ca}^{++}/\text{Mg}^{++}$ + 0.2% fatty acid free-BSA w/v, and two more washes with HBSS with $\text{Ca}^{++}/\text{Mg}^{++}$. This to remove all non-incorporated GM1 from the surface of the cells. Cells were then lysed in NP-40 lysis buffer as stated before. Total proteins were quantified by BCA assay (Thermo Scientific, Waltham, MA, USA) and a dot blot was run using a 96-well Bio-Dot® apparatus (Bio-Rad, Hercules, CA, USA). A total of 500-1000 ng of protein (lysates) per well (in triplicates) were immobilized on a 0.45 μm pore size nitrocellulose membrane (Millipore, Burlington, MA, USA). For EVs, the total preparation was loaded into three wells of the 96-well Bio-Dot® apparatus (Bio-Rad, Hercules, CA, USA). Membrane was then blocked in Odyssey® blocking buffer (LiCor Biosciences, Lincoln, NE, USA) for 1 h. For the detection of GM1, membrane was incubated with cholera toxin subunit B conjugated with biotin (Thermo Scientific, Waltham, MA, USA) diluted in Odyssey® blocking buffer at a concentration of 0.2 $\mu\text{g}/\text{mL}$ for 1 h at RT. After washing the membrane with TBS-T, membrane was incubated with streptavidin conjugated with IRDye800® (LiCor Biosciences, Lincoln, NE, USA) diluted in Odyssey® blocking buffer at 1:5,000 dilution. Membrane was washed with TBS-T before being scanned in an Odyssey® near-infrared scanner. The signal was quantified using the Odyssey® Application Software v3.0.

2.20. Filter trap assay

Filter trap assay was performed as previously reported (286), with minor modifications. Cells or tissues were lysed in NP-40 lysis buffer as described above, and total protein content was quantified by BCA assay (Thermo Scientific, Waltham, MA, USA). A total of 50-100 μg of proteins were denatured by boiling the lysate at 100 °C for 5 min in a solution containing 2% SDS w/v and 100 mM DTT. Using a Bio-Dot® apparatus (Bio-Rad, Hercules, CA, USA), denatured lysate was filtered through a 200 nm-pore sized cellulose acetate membrane (Sterlitech, Kent, WA, USA). The membrane was then air dried for 30 min and washed twice with 0.1% SDS w/v in PBS. Excess of SDS on the membrane was removed by washing it three times in PBS. Regular immunodetection protocol was followed using anti-GFP antibodies, diluted 1:1,000 in 2.5% BSA w/v in TBS-T (Full list of antibodies is shown in **Table 2**). Secondary antibodies conjugated to IRDye fluorophores and an Odyssey® near-infrared scanner (LiCor Biosciences, Lincoln, NE, USA) were used for detection and imaging. Quantification of the signal was made using the Odyssey® Application Software v3.0.

2.21. Statistical analysis

All comparisons between two groups, unless stated otherwise, were performed by using unpaired two-tailed Student's t-test, with a significance cut-off (α) of 0.05. For comparisons between three or more groups, one-way ANOVA, followed by Tukey-Kramer post-hoc correction was used. Significance cut-off (α) was also set at 0.05 for multiple comparisons. Statistical analysis of the data presented in Fig 4.4B was performed using two-sample Kolmogorov–Smirnov test. GraphPad Prism v.6.01 software was used to perform all statistical analyses.

Chapter 3: The role of the mevalonate pathway in Huntington's disease

Data shown in this chapter were generated with Dr. Amany Mohamed and Dr. Elena Posse de Chaves (Department of Pharmacology, University of Alberta).

3.1. Introduction

Previous studies have shown that the mevalonate pathway, which is responsible for the synthesis of cholesterol and isoprenoids required for protein prenylation, is impaired in HD (214,287-292). However, whether this dysfunction could lead to impaired prenylation of proteins, crucial for normal cellular homeostasis and for neuronal functions, was not known and has been investigated in this chapter.

3.1.1. The mevalonate pathway: the biosynthesis of cholesterol, isoprenoids and more

Cholesterol is a fundamental lipid that is present in all cellular membranes throughout the body. Cholesterol has many functions. It contributes to the fluidity at the plasma membrane, thus modulating the mobility and function of membrane proteins (293). It is also an important component of membrane microdomains, sometimes referred as to “lipid rafts”, that are enriched in sphingolipids and cholesterol. These membrane microdomains act as signalling platforms for a variety of receptors within the plasma membrane. Changes in the levels of cholesterol in these membrane microdomains can result in activation or inactivation of raft-associated proteins, including death receptors, kinases and ion channels (294-296).

Neurons particularly, have high requirements of cholesterol due to the large extension of their plasma membrane surface that includes the dendrites, axons and synapses, where high cholesterol content has been detected (297-299). In fact, treatment of cultured hippocampal neurons with lovastatin, an inhibitor of cholesterol synthesis, is able to decrease neurite growth and synapse formation. These defects are prevented if neurons are co-treated with cholesterol-containing glial-derived lipoproteins (GLp) (300). Lovastatin was also shown to cause defects in synaptic vesicle release. Although GLp only partially rescued this phenotype, co-treatment with mevalonate, an

intermediate metabolite downstream of the enzyme inhibited by lovastatin, was able to fully rescue the defects in synaptic vesicle release caused by lovastatin (300).

Cholesterol also serves as a precursor for the synthesis of neurosteroids, molecules that exert important modulatory roles in the brain (301). As an example, allopregnanolone, a natural neurosteroid derived from cholesterol, has anti-apoptotic effects in cultured neurons due to an allosteric modulation of the GABA_A receptors, increasing chlorine conductance and promoting neuronal hyperpolarization after NMDA treatment (302,303). Moreover, 3- α -ol-5- β -pregnan-20-one hemisuccinate (ABHS), a synthetic homologue of pregnenolone, has inhibitory effects on NMDA receptors, reducing the calcium inward currents and protecting cultured neurons from NMDA-induced excitotoxicity. Administration of ABHS also reduced infarct size in a rat model of acute ischemia (304). Furthermore, neurosteroids have been associated with neurite growth, myelination and neural progenitor proliferation (301).

One of the least known functions of cholesterol is that it serves as a molecule used for post-translational modification of proteins. This is the case for the Hedgehog (Hh) family of secreted signalling proteins, which are covalently attached to a molecule of cholesterol during protein maturation. The Hh family of proteins is involved in development and morphogenesis by coordinating cell proliferation and preventing apoptosis, or by inducing specific cellular fates (305,306).

Evidence of the importance of cholesterol for the normal function of the brain is the fact that defects in the production of cholesterol can lead to severe developmental defects of the central nervous system, as it is seen in the Smith-Lemli-Opitz Syndrome (SLOS), a monogenic recessive disease caused by a loss-of-function mutation of the 7-dehydrocholesterol reductase (*DHCR7*) gene. SLOS is characterized by prenatal and postnatal growth retardation, microcephaly and severe

intellectual disability (307,308). Moreover, various neurodegenerative diseases, including Niemann-Pick C (NPC), AD and PD, have been linked to alterations in the homeostasis of cholesterol (309).

Cells obtain their cholesterol from two different sources, either from the diet or from *de novo* synthesis (310). While this statement is true for most of the cells in the body, cells in the central nervous system (CNS) depend entirely on *de novo* synthesis of cholesterol. This is due to the fact that the blood-brain barrier (BBB) prevents cholesterol from the systemic circulation to enter the brain (310,311). Interestingly, although neurons are cells with high requirement of cholesterol, it is generally accepted that these cells do not synthesize significant amounts of cholesterol on their own, but they rather rely on the astrocytes for cholesterol synthesis and delivery (310,311).

Even though the brain, which accounts for 2% of the total human body mass, does not significantly import cholesterol, it contains up to 25% of the whole body's cholesterol (312). Majority of the cholesterol in the brain is unesterified (free cholesterol), and most of it (70-80%) is incorporated into the myelin sheets formed by the oligodendrocytes. The remaining 20-30% is located in the membrane of the neurons, astrocytes, and other cells located within the CNS (313).

The pathway for the synthesis of cholesterol is called the mevalonate pathway (Fig. 3.1), a high-energy consuming sequence of reactions that initiates with the conjugation of two molecules of acetyl-CoA to form acetoacetyl-CoA, which is then conjugated to a third acetyl-CoA to form 3-hydroxy-3-methylglutaryl CoA (HMGCoA). These two reactions are carried out by two different enzymes: Acetoacetyl-CoA thiolase and HMGCoA synthase, respectively. The conversion from HMGCoA to mevalonate is carried out by the enzyme HMGCoA reductase (HMGCR), which is the rate-limiting and irreversible reaction in the mevalonate pathway. From here, a series of phosphorylations and one decarboxylation reaction convert the mevalonate molecule into

isopentenyl diphosphate (IPP), a 5-carbon molecule that is the building block of all the products derived from the mevalonate pathway. IPP is the simplest isoprenoid (314).

Conjugation of 3 molecules of IPP leads to the formation of farnesyl-diphosphate (FPP), a 15-carbon isoprenoid, and conjugation of 2 FPP molecules gives rise to squalene and later to lanosterol. From here, 19 more enzymatic reactions are required, until the molecule of cholesterol is finally synthesized (310,311).

Although cholesterol is the most known product of the mevalonate pathway, it is just one of many. In fact, FPP is a branching point in the mevalonate pathway (Fig. 3.1). FPP can be modified into other molecules, such as the 20-carbon isoprenoid geranylgeranyl-diphosphate (GGPP) (315). Isoprenoids, more specifically GGPP, is also the precursor for the synthesis of coenzyme Q (ubiquinone) (316) and dolichol (317), and therefore, the mevalonate pathway and particularly isoprenoids, are also involved in mitochondrial energy metabolism and protein glycosylation. FPP is the precursor of the heme A group, an essential component of hemoproteins such as myoglobin and hemoglobin, both involved in oxygen storage and transport throughout the body (310).

Short chain isoprenoids, such as FPP and GGPP, are used for protein prenylation (Fig. 3.2), a post-translational modification by which FPP or GGPP molecules are covalently attached to proteins, thus regulating protein localization and further activation, and consequently, a variety of cell processes from vesicle trafficking to neurotransmission, cell signaling and cell motility (318).

Regulation of the activity of the mevalonate pathway is controlled by the sterol response element binding protein 2 (SREBP2), a master transcription factor for most of the genes involved in the mevalonate pathway. This transcription factor binds to the canonical sequence of the sterol

response element (SRE) located in the promoter region of most, if not all, the enzymes of the mevalonate pathway, promoting their transcription (319,320).

SREBP2 is synthesized in the ER as an inactive full-length pro-protein. When the concentration of sterols is decreased in the ER, the full-length SREBP2 is translocated to the Golgi with the help of the SREBP cleavage-activating protein (SCAP). SREBP2 and SCAP reach the Golgi via COPII-coated vesicles (321) where SREBP2 is sequentially cleaved by the enzymes site-1 protease (S1P) (322) and site-2 protease (S2P) (323), releasing the mature form of SREBP2 (mSREBP2), which is later delivered to the nucleus by a direct interaction with importin β (324,325). Once in the nucleus, it promotes the transcription of enzymes of the mevalonate pathway, increasing the production of cholesterol, together with all the other products of this biosynthetic pathway (326).

When cholesterol concentration in the ER is high, cholesterol binds to SCAP at its sterol-sensing domain (327), promoting a conformational change in SCAP that facilitates the interaction with insulin-induced gene 1 & 2 (INSIG) proteins, which retain the SCAP-SREBP2 complex in the ER (328,329) preventing its further processing. Oxysterols also exert inhibitory actions on SREBP2 processing by binding directly to INSIG(s), increasing their affinity for SCAP (330).

Defects in SREBP2 processing and subsequent impairment of the mevalonate pathway have been reported in the context of Alzheimer's disease (AD). Mohamed and collaborators (331) demonstrated that neurons treated with oligomeric A β 42 show impaired processing of SREBP2 and decreased activity of the mevalonate pathway. This led to decreased synthesis of isoprenoids and to decreased prenylation of proteins. Because of impaired prenylation of proteins involved in vesicular traffic, neurons treated with oligomeric A β 42 showed cholesterol sequestration within organelles such as multivesicular bodies/late endosomes (MVB/LE) without changes the total

cellular content of cholesterol. Supply of exogenous GGPP reverted the defects in protein prenylation, as well as the cholesterol sequestration phenotype.

As detailed below, impaired SREBP2 activation was also shown in HD models (287), and aberrant cholesterol metabolism has been described in HD patients (332-334) and HD mouse models (288-290). However, to my knowledge, the role of isoprenoids has not been studied in the context of HD, and therefore their possible contribution to neuronal dysfunction is currently unknown.

3.1.2. The mevalonate pathway and Huntington's disease

Several studies carried out in cell and animal models of HD, have shown that the cholesterol biosynthetic pathway is impaired by muHTT (Fig. 3.1). Sipione and collaborators (214) found decreased transcription of genes involved in cholesterol synthesis in striatal cells expressing an N-terminal fragment of muHTT under control of a doxycycline-inducible promoter. Downregulation of cholesterologenic genes was observed after only 48 hours from the induction of the transgene expression, in the absence of evident muHTT aggregation and prior to neuronal apoptosis, suggesting that these transcriptional changes may reflect an early transcriptional dysfunction, potentially involved in the pathophysiology of HD.

Impairments in the biosynthetic pathway of cholesterol are also present in murine models of HD. Valenza and collaborators (288) showed that YAC128 mice have decreased amounts of total sterols in the striatum, but not in the cortex nor the cerebellum (two brain regions less affected in HD), at 10 months of age. Intermediate molecules in the synthesis of cholesterol, such as lathosterol and lanosterol, are decreased in brains of young (2 months old) YAC128 mice without affecting the total levels of cholesterol. These defects become more evident at an older age (10

months old) when the levels of cholesterol also show a mild, but significant decrease. Analysis of lipid contents in plasma from YAC128 mice revealed a similar decrease in sterol levels.

These findings were partially replicated in a second mouse model of HD, the R6/2 mice. Transcription of genes encoding HMGCR, sterol 14 α -demethylase and DHCR7 was reduced in the striatum of R6/2 mice and in post-mortem striatal tissue from human HD patients (287). These mice also showed a progressive decrease in the levels of lanosterol and lathosterol in the striatum and cortex, starting at 6 weeks of age, which correlated with a reduced activity of the enzyme HMGCR in brains, starting at 4 weeks of age. One interesting finding was that, despite the reduced activity of the mevalonate pathway, the total mass of cholesterol in these brains was conserved, even after 12 weeks of age (289).

Moreover, in line with the hypothesis of reduced activity of the mevalonate pathway in HD, two studies have shown neuroprotection and improvement of neuronal functions by exogenous supply of cholesterol. Primary neurons expressing an N-terminal fragment of muHTT were shown to be protected from cell death by addition of cholesterol in a dose-dependent manner (287). Additionally, systemic administration of cholesterol *in vivo* via polymeric nanoparticles, improved synaptic connectivity, reduced cognitive dysfunction and improved some parameters of the motor dysfunction observed in the R6/2 mice (335).

It is interesting how intermediate metabolites and precursors (i.e. lanosterol and lathosterol) in the mevalonate pathway are decreased at early disease stages in at least two different mouse models of HD, but brain cholesterol levels are either unaffected, or become affected only at very late stages of the disease (288-290). It has been hypothesized that this phenomenon could be due to a compensatory mechanism that limits cholesterol excretion. Elimination of cholesterol from the brain occurs via hydroxylation of cholesterol at the carbon 24, catalyzed by cholesterol 24-

hydroxylase, an enzyme that is expressed almost exclusively in neurons. The 24-hydroxycholesterol (24-OH-Chol) molecule can cross the BBB and exit the CNS to the systemic circulation, from where it is cleared by the liver and kidneys (336). Human plasma from early and late HD patients contains less 24-OH-Chol compared to control subjects (332,334). Moreover, the amount of 24-OH-Chol in the brain is decreased across various mouse models of HD, including transgenic and KI mice (290).

The cholesterol-related defects are not limited to neurons in HD, since decreased transcription of genes of the mevalonate pathway such as *Hmgcr*, *Cyp51a1*, *7dhcr*, and genes involved in cholesterol metabolism such as *Abca1* and *ApoE*, occurs also in primary astrocytes from two HD mouse models (YAC128 and R6/2 mice). In addition, HD astrocytes secrete less ApoE-containing HDL-like particles compared to wild-type astrocytes *in vitro* (290). Since the bulk of cholesterol is provided to neurons by astrocytes in normal conditions (337-340), these observations suggest that provision of cholesterol from HD astrocytes to neurons might be decreased compared to normal brains.

In spite of the evidence that clearly shows impairment of the mevalonate pathway and cholesterol synthesis in HD, whether cholesterol levels are decreased and to which extent, is still controversial. For instance, Carroll and collaborators (341), by using liquid chromatography/mass spectrometry (LC-MS) techniques, have shown that the striatum of HdhQ111 mice contains significantly more esterified cholesterol and triglycerides than the striatum of WT mice. Researchers interpreted the results as a possible impairment in the catabolism of these two species of lipids, most likely due to defects in selective autophagy, which have been documented in HD mice (152), rather than to an overproduction of cholesterol.

Additionally, muHTT-expressing striatal progenitor neurons have a higher content of ordered domains at the plasma membrane enriched in cholesterol and NMDA receptors (342). Cells treated with simvastatin, an HMGCR inhibitor, or with β -cyclodextrin, a compound used to deplete membranes from cholesterol, were less prone to cell death after treatment with NMDA, suggesting that the excess of cholesterol, specifically localized at these membrane domains, may contribute to cell degeneration in an excitotoxic-dependent manner (342).

Accumulation of unesterified cholesterol was also shown in mouse striatal primary neurons and brains from HdhQ111 mice, as well as in PC12 cells expressing muHTT (342,343), leading the authors to suggest that abnormal cholesterol accumulation, rather than a decrease of it, contributes to neuronal dysfunction and cell death observed in the context of HD. Nevertheless, these observations were made using filipin staining, a naturally fluorescent antibiotic that binds specifically to free cholesterol but not to esterified sterols. However, filipin staining is not a quantitative assay but instead, it detects free cholesterol accumulation in cellular compartments. In fact, in Niemann-Pick type C (NPC) disease, neurons show an intense reactivity to filipin within the lysosomes, but no difference is observed in the total cell or brain amount of cholesterol when measured by other methods (344,345), suggesting that intracellular accumulation of cholesterol does not necessarily mean higher total levels, but misdistribution of it instead.

A similar phenomenon also occurs in cell models of AD, where primary cortical neurons exposed to A β 42 peptide accumulate intracellular free cholesterol, which is detectable with filipin staining. However, the total mass of cholesterol in these cells remains unchanged after treatment with A β 42 (331), suggesting that local accumulation of cholesterol could be misinterpreted as an increase in total mass of cholesterol, if analyzed only by filipin staining.

The cause and mechanisms of downregulation of the mevalonate pathway in HD are under investigation in our laboratory. Initial studies by Valenza showed decreased levels of the mature active form of SREBP2 (mSREBP2) in the nucleus of HD cells (287), although the underlying reasons were not investigated.

Work in our laboratory suggests that, although total levels of mSREBP2 are unchanged in brains of YAC128 mice, muHTT affects nuclear localization of mSREBP2 by sequestering it in the cytoplasm in a complex with importin β (Di Pardo, Morales et al. in preparation). I contributed to further show that, while in basal culture conditions, HD cells express wild-type levels of the major cholesterologenic genes, in lipid-deficient medium, they fail to upregulate *HMGCR* transcription. These results are shown and discussed in more details in Appendix I.

All the studies published so far have focused on cholesterol and its metabolism, but to our knowledge, the non-cholesterologenic branch of the mevalonate pathway, including the production of isoprenoid for protein prenylation, has not been explored in the context of HD.

3.1.3. Small GTPases and HD

Small GTPases belong to a superfamily of proteins that have numerous and diverse functions, including cell cycle, microtubule organization, vesicular transport, autophagy, among many others (346). All members of the small GTPase superfamily of proteins share the characteristic GDP/GTP exchange mechanism of activation, where the GDP-bound form is inactive, while the GTP-bound form is active, and has various effects on downstream targets. All the members of the superfamily are regulated by GEF (guanine exchange factor) proteins which accelerate the transition from GDP-bound to GTP-bound, promoting the activation of the small GTPase protein. On the other

hand, the GTPase activity of small GTPases is turned off by GAPs (GTPase activating proteins), which promote the hydrolysis of GTP into GDP (346).

Classification of the small GTPases family of proteins is not straightforward due to the numerous members of this superfamily, as well as to the variety of, and sometimes overlapping, functions of these proteins. Nevertheless, researchers have attempted to classify small GTPases in subfamilies: The RAS GTPase subfamily, with 36 members, is mainly involved in cell growth, differentiation and survival (347). The RHO GTPase subfamily, with 22 members, has been linked to cellular processes such as morphogenesis, polarity, cell movement and cell division (348). The RAB GTPase subfamily, with at least 60 members, and the ARF subfamily, with 5 members have been classically associated with vesicular and organelle trafficking (349,350). RAN GTPase is the exception to the rule. Is a lonely member of its own family and it is mainly involved in the machinery responsible for the nuclear protein import cycle (351). Contrary to the other members of the superfamily, RAN GTPase lacks the consensus sequences required for prenylation (352).

Not all, but the vast majority of the Small GTPases proteins undergo prenylation. This post-translational modification is crucial for the membrane localization of these proteins, where most of them accomplish their functions. The multistep mechanism by which an isoprenoid molecule is attached to a cysteine residue at the C-terminal region the protein is mainly performed by one of three enzymatic complexes (Fig. 3.2) (353,354).

1) Farnesyl Transferase (FTase): The complex is formed by the proteins encoded by the *FNTA* and *FNTB* genes. This enzyme attaches an FPP molecule to the C-terminus of the protein at the consensus CAAX motif, where C is the cysteine where the FPP molecule is attached, A represents any aliphatic amino acid, and X represents any amino acid. Members of the RAS subfamily are usually, but not exclusively, prenylated by FTase.

2) Geranylgeranyl Transferase I (GGTase I): This enzymatic complex is formed by the proteins encoded by the *FNTA* gene, which is shared with the FTase complex, and *PGGT1* gene. It recognizes the same CAAX motif (as FTase), but it uses preferentially a GGPP molecule instead of FPP. Their substrates are usually the members of the RHO subfamily. Whether a small GTPase is farnesylated or geranylgeranylated by FTase or GGTase I, respectively, depends on the last amino acid in the CAAX motif. If X corresponds to the amino acids methionine or glutamine, the protein is farnesylated. Instead, if X is a leucine or a phenylalanine, the protein undergoes geranylgeranylation (355). However, there are certain exceptions to this rule, since some members of the RAS subfamily (i.e. KRAS4A, KRAS4B and NRAS) can be farnesylated or geranylgeranylated (354).

After FPP or GGPP has been added to the cysteine of the CAAX motif by either FTase or GGTase I, the last three amino acids are cleaved by RAS converting CAAX endopeptidase 1 (RCE1) (Fig. 3.2A).

3) Geranylgeranyl Transferase II (GGTase II): This complex is formed by the products of *RABGGTA* and *RABGGTB* genes, and despite having a similar function as GGTase I, structurally speaking, these two prenylation complexes are very different from each other. The unprenylated RAB is presented to GGTase II complex by the RAB escorting protein 1 (REP1). Then, GGTase II attaches two GGPP molecules to the C-terminus of the RAB subfamily of proteins at the CXC or CC motif, where C are the cysteine residues where the GGPP molecules are attached, and X represents any amino acid. REP1 also possess a prenyl-binding site, that maintains the prenylated RAB soluble until delivered to the distinct cellular membranes (353,354) (Fig. 3.2B).

I hypothesized that a decreased activity of the mevalonate pathway in HD could lead to a decreased availability of isoprenoids for protein prenylation, as it was observed in cell models of AD (331).

Among the complement of proteins that undergo protein prenylation, a few have been associated with the pathogenesis of HD or with cellular mechanisms known to be affected in HD, in particular, RAS, RAB11 and RAB7.

RAS protein was first identified as an oncogene that promotes cell survival and division and inhibits apoptosis. In fact, gain of function of RAS protein is one of the most commonly found mutations in cancer cells (347). The ERK signalling pathway, which lays downstream of RAS protein, has been found to be impaired in HD models. For instance, muHTT impairs the transcription of BDNF and alters glutamate uptake from the synaptic cleft, all functions dependent on ERK signalling. In addition, pharmacological activation of ERK pathway is beneficial in some models of HD (356-358).

RAB11 protein function is also affected in HD. Membrane fractions prepared from striatum of Q140 mice contained higher total levels of RAB11. However, these HD striatal membranes were deficient in stimulating RAB11 GDP/GTP exchange in an *in vitro* assay, suggesting that activity of RAB11 is reduced in HD striatal neurons, despite its increased abundance (359). Additionally, dendritic muHTT aggregates are associated with an impaired function of the recycling endosome and with loss of dendritic spines. Overexpression of RAB11, a GTPase associated with the recycling endosome, reduces the loss of dendritic spines associated to the expression of muHTT (360). Impairment of the recycling endosome also causes a deficient expression of the cysteine/glutamate interchanger at the level of the plasma membrane, compromising the uptake of cysteine and consequently, the production of glutathione, essential for the proper management of reactive oxygen species (ROS) (361).

RAB7 is one of the main components of the late endosomes (362). It also has a role in vesicle transport (363,364), and autophagy (365), all functions affected in HD (152,366,367). Moreover,

in the context of AD, A β 42 peptide treatment affects the mevalonate pathway through an impairment of SREBP2 maturation, therefore causing a reduction in prenylation of RAB7 that was corrected by the exogenous supply of GGPP. Additionally, A β 42 treatment caused an accumulation of cholesterol within the cells, presumably due to an impairment in vesicular transport caused by a deficient prenylation of RAB7 (331). Similar phenotypes have been observed in a few models of HD, but no connection with RAB7 or with protein prenylation was ever proposed (342,343).

Cell models of AD have shown impaired protein prenylation due to an inhibition in SREBP2 processing, and consequently, a reduction in the activity of the mevalonate pathway (331). Moreover, previous work in our laboratory has shown that muHTT impairs nuclear transport of mSREBP2 (see Appendix I), possibly explaining the decreased expression of cholesterologenic genes in cell and mouse models of HD (214,287).

I hypothesized that a decreased activity of the mevalonate pathway in HD models may lead to a decreased production of isoprenoids, perhaps affecting protein prenylation, similarly to observations in cell models of AD (331). Thus, I decided to test whether the prenylation status of a subset of small GTPases involved in cell processes known to be affected in HD (RAS, RAB7 and RAB11), would be altered in HD cells.

In the following section, I will show data suggesting that, contrary from what occurs in AD models (331), in HD, surrogate measures of RAS, RAB7 and RAB11 prenylation are not affected, although I found total levels of RAB7 to be decreased across cell and animal models of HD. Additional data regarding impairment of nuclear transport of mSREBP2 and regulation of transcription of cholesterologenic genes in HD models will be presented in Appendix I.

3.2. Results

3.2.1. Triton X114 fractionation of RAS and RAB7 is not affected in immortalized HD striatal cells

Triton X114 fractionation was used as a surrogate measure of the prenylation status of RAS and RAB7 in striatal cells expressing full-length muHTT (STHdh Q111/111), as well as in WT striatal cells (STHdh Q7/7). In this assay, lipidated proteins are retained in the detergent (D) phase, while the more hydrophilic non-lipidated proteins partition into the aqueous phase (Aq) (283). In addition to regular culture conditions (media supplemented with 10% of fetal bovine serum), cells were also cultured in lipoprotein-deficient media (LPDM) for 48 h.

Contrary to my expectations, HD immortalized cells showed a similar distribution of RAS and RAB7 proteins into detergent and aqueous phases when compared to WT cells (Fig. 3.3). Furthermore, culture in LPDM did not change the distribution of these proteins, neither in WT nor HD cells (Fig. 3.3). To test whether this assay was able to detect changes in the prenylation status, WT and HD cells were treated with a combination of FTase inhibitor (80 μ M FTI-277) and GGTase I inhibitor (5 μ M GGTI-2133) for 48 h. It is important to clarify that, while this treatment is expected to block RAS prenylation, none of the inhibitors would affect the prenylation of RAB7, since GGTase II, a very distinct enzyme from GGTase I, is the enzyme responsible for the prenylation of the RAB family of proteins (368-372). As expected, the combination of FTI-277 + GGTI-2133 caused a shift in the distribution of RAS but not RAB7, in both, WT and HD cells towards the aqueous phase (Fig.3.3).

These results were further confirmed by electrophoretic mobility shift assay (EMSA). In this assay, proteins are run in an SDS-PAGE gel to compare patterns of migration. Prenylated proteins

migrate faster compared to non-prenylated proteins. Thus, the proportion of prenylated and non-prenylated proteins can be assessed by analyzing the intensities of the bands after immunoblotting.

For this assay, equivalent amounts of proteins were run from both STHdh Q7/7 and Q111/111 cells, cultured in RM and LPDM for 48 h. I also run proteins from cells treated with FTI-277 + GGTI-2133 combination as a positive control for the assay. Additionally, the ubiquitin-proteasome system (UPS) inhibitor MG132 (10 μ M) was added to the culture media during the last 3 h of incubation in order to prolong the half-life of proteins, increasing the possibility of detection.

Consistent with the results obtained in the Triton X114 fractionation suggesting that prenylated RAB7 is the predominant form (>95%) (Fig. 3.3C) and that FTI-277 + GGTI-2133 does not affect its prenylation, a single band for RAB7 was detected across genotypes and treatments. In contrast, RAS showed a discrete band of a higher molecular weight, corresponding to an approximate 25% of the total intensity. This band corresponding to the non-prenylated RAS, was of comparable intensity between WT and HD cells, whether cultured in RM or LPDM (Fig. 3.4). As expected, addition of protein prenylation inhibitors caused an increase in non-prenylated RAS (Fig. 3.4).

3.2.2. Triton X114 fractionation of RAS and RAB7 is not affected in HD neurons nor astrocytes

Next, I investigated whether differences in Triton X114 distribution of selected proteins would be observed in primary neurons, a more precise model of HD compared to immortalized cells. For this, Triton X114 fractionation was performed in postnatal primary cultures of neurons from YAC128 mice and WT littermates at DIV 10-13. Similar to immortalized knock-in cells, lysates of primary cortical (Fig. 3.5A, left) and striatal (Fig. 3.5A, right) YAC128 neurons showed phase distributions of RAS and RAB7 comparable to WT neurons.

It is known that in the adult CNS, astrocytes synthesize most of the cholesterol required by the neurons (340,373). Moreover, Valenza and collaborators (290) have shown that HD astrocytes have a decreased transcription of enzymes related to cholesterol biosynthesis and efflux, as well as an impaired secretion of ApoE-containing particles. Therefore, next I assessed whether HD astrocytes would show changes in the distribution of selected proteins in Triton X114 fractionation.

HD immortalized astrocytes had similar Triton X114 phase distributions of RAS and RAB7 proteins whether cultured in RM or LPDM, in comparison to WT astrocytes (Fig. 3.5B, left panel). Once again, I tested the validity of my assay by treating both, WT and HD immortalized astrocytes with the HMGCR inhibitor simvastatin (25 μ M, 24 h) to block the synthesis of cholesterol and isoprenoids. As expected, the distribution of RAS and RAB7 was dramatically changed towards the aqueous phase in both treated WT and HD astrocytes (Fig. 3.5B, right panel), suggesting that by using Triton X114 fractionation, I could possibly detect changes in the status of prenylation of small GTPases, in conditions of low availability of isoprenoids. Importantly, the experiments performed in primary neurons and astrocytes were performed only once, and further replication will be required before reaching any definitive conclusion.

3.2.3. Triton X114 fractionation of RAS, RAB7 and RAB11 is not affected in brains of HD mice

Next, I performed Triton X114 fractionation of lysates prepared from the whole cortex (Fig. 3.6A) and striatum (Fig. 3.6B) obtained from six 10-12-month-old YAC128 mice and six age-matched WT littermates, as a surrogate measure of the prenylation status of selected small GTPases in the brains of WT and symptomatic HD mice.

The phase distribution of RAS, RAB7 and RAB11 proteins in cortical (Fig. 3.6A) and striatal tissue from HD mice (Fig. 3.6B) was indistinguishable from WT tissue, suggesting that the prenylation status of these three proteins is not affected in the brains of YAC128 mice.

The evidence presented so far suggests that, even though the mevalonate pathway is impaired in multiple HD models (214,287-290), the prenylation status of proteins is not affected in HD, at least for what concerns the specific subset of proteins with relevance to the HD pathogenesis investigated in this study.

3.2.4. Total levels of RAB7 are decreased across models of HD

In the process of investigating the Triton X114 distribution of RAB7 in HD cells and brains, I found that total levels of RAB7 protein were decreased in the striatum of 10-12-month-old YAC128 mice, when compared to WT littermates (Fig. 3.7A). To investigate whether this decrease was due to downregulation of *Rab7* gene expression, I quantified its mRNA levels in the striatum of 10-12-month-old WT and YAC128 mice by quantitative real-time PCR (qRT-PCR). There was no significant difference in *Rab7* gene expression between WT and HD striata (Fig. 3.7B), suggesting that the difference in protein abundance is not secondary to a change in expression, but rather to a difference in RAB7 turnover.

These findings were replicated in three samples of primary cultures of cortical neurons isolated from P0 YAC128 pups (Fig. 3.7C). Once again, there was no difference in *Rab7* mRNA levels between WT and HD primary cortical neurons (Fig. 3.7D). Decreased levels of RAB7 were also observed in the striatal tissue of homozygous Q140/140 mice, but not in heterozygous Q7/140 mice (Fig. 3.8A). Surprisingly, however, in the cortex of Q140/140 mice, levels of RAB7 were

significantly increased when compared to Q7/7 littermates (Fig. 3.8B), a phenomenon that was not replicated in the cortices of YAC128 mice (data not shown).

Additionally, in four human fibroblasts cell lines from HD patients, there was a trend towards a decrease of RAB7 levels, compared to three cell lines of WT fibroblasts, but the difference did not reach statistical significance ($p = 0.055$). Of note, the two HD fibroblast lines expressing more than 60 CAG repeats also had the lowest levels of RAB7 (Fig. 3.8C). It remains to be demonstrated whether levels of RAB7 are consistently decreased in human samples with larger CAG repeat expansions.

3.3. Discussion

I hypothesized that the impairment of the mevalonate pathway in brains of HD mice, and particularly in YAC128 striatum, would affect the production of isoprenoids such as FPP and GGPP, thus reducing, at least partially, the prenylation of proteins.

I used Triton X144 fractionation as a surrogate measure of the prenylation status of three small GTPases involved in cellular processes known to be affected in HD (RAS, RAB11 and RAB7). Contrary to my expectations, I could not detect any difference in the Triton X114 fractionation of these small GTPases in brain tissue from HD mice, nor in HD cell models.

One possible explanation for my findings is that cells may prioritize the usage of isoprenoids for protein prenylation (and/or synthesis of dolichol and ubiquinone) rather than for the synthesis of cholesterol. This goes in line with early studies done by Brown and Goldstein with the HMGCR inhibitor compactin. The dose of 1 μM of compactin was sufficient to inhibit 90-95% of HMGCR enzymatic activity. However, despite the profound inhibition of the production of mevalonate, cells were able to thrive and grow under these conditions, suggesting that cells have mechanisms

in place to preferentially shuttle the common substrate FPP towards the synthesis of non-cholesterogenic products, in the case of mevalonate shortage (374). Metabolic studies using [³H] mevalonate in human fibroblasts demonstrated that labelled mevalonate is incorporated 2-3 times faster into ubiquinone than into cholesterol, supporting the preferential usage of isoprenoids for non-sterol products (316).

The results of these early metabolic studies are explained by the differential affinity of the enzymes that utilize FPP as a substrate, at the branching point of the mevalonate pathway. The Michaelis-Menten constants (K_m) reported for FTase, GGTase I and GGTase II and their isoprenoid substrates are 2.8 nM, 0.8 nM and 8 nM, respectively (375-377), while the K_m reported for squalene synthase (of yeast origin) was between 40 nM and 440 nM depending on the availability of NADPH (378,379). Thus, in the event of a mild shortage of isoprenoids, it is likely that the cells would use available isoprenoids for the synthesis of ubiquinone, dolichol and protein prenylation, rather than for cholesterol.

In future studies, it would be important to know the total amount and the species of isoprenoids synthesized by WT and HD cells or tissues. Hoof and collaborators reported on a quantitative method based on derivatization of isoprenoids using dansyl-labelled pentapeptides. After derivatization, isoprenoids in a sample can be measured by high-performance liquid chromatography (HPLC)–fluorescence detection (FLD) methods, or by ultra-high-performance liquid chromatography (UHPLC)/tandem mass spectrometry (MS/MS) (380,381). Using these techniques, authors showed that samples of grey and white matter from human AD brains contained higher amounts of FPP and GGPP, without changes in the total mass of cholesterol, when compared to age-matched control samples (382).

In this study, I used Triton X114 fractionation as a surrogate measure of the prenylation status of selected small GTPases. However, a limitation of my studies is that only the Triton X114 fractionation of three representative proteins was measured in HD models, as an indication of the global prenylation process in the brain and cells expressing muHTT. Therefore, I cannot exclude that other small GTPases would potentially be under-prenylated in HD. In fact, Köhnke and collaborators (383) reported that not all the proteins of the RAB subfamily are prenylated at the same rate. Instead, due to the fact that non-prenylated RABs compete amongst them for the prenylation machinery, there is a hierarchy of prenylation. The two RAB proteins analyzed in this study, RAB7 and RAB11, have a “higher position” in this hierarchy, meaning that under a limited supply of isoprenoids, these RAB proteins would be preferentially prenylated. Instead, proteins such as RAB38, RAB27A and RAB27B are at a lower position in this hierarchical system. Thus, compared to RAB7 and RAB11, these proteins would have a higher probability of remaining in a non-prenylated state, in the event of a mild shortage of isoprenoids.

In the future, we plan to determine the prenylation status of RAB38 and RAB27, and to perform analysis of global protein prenylation by supplying cells in culture with modified versions of FPP and GGPP suitable for use with click chemistry tools. For instance, DeGraw and collaborators (384) were able to study global protein prenylation in HeLa cells by click chemistry after supplying cells with exogenous alkyne-modified isoprenoids. Analysis of total protein prenylation would allow us to determine whether muHTT alters the pattern of protein prenylation on a broader scale, instead of just relying on the prenylation status of a few selected proteins.

While investigating the Triton X114 fractionation of small GTPases, I was able to detect a decrease in RAB7 protein in the striatum, as well as in primary cortical neurons isolated from YAC128 mice. The amount of *Rab7* mRNA was similar between WT and HD samples, suggesting that the

changes in RAB7 protein levels are not due to transcriptional downregulation, but rather to protein stability. Total RAB7 protein was also reduced in the striatum of homozygous Q140/140 mice, but not in the heterozygous Q7/140 littermates, indicating that, at least in this mouse model, a dosage effect may be important for the reduction of RAB7 protein. The amount of RAB7 protein was also measured in 4 different primary lines of fibroblasts obtained from HD patients. When compared to 3 primary lines of fibroblasts obtained from controls, all HD cells had reduced quantities of RAB7 protein, but the difference did not reach statistical significance ($p=0.055$). However, In this particular set of primary fibroblasts, I observed that the two HD fibroblasts lines that had larger CAG expansions (more than 60 CAG repeats), had also a more pronounced reduction of RAB7 levels compared to HD fibroblasts with less than 60 CAG repeats. This very preliminary finding requires further confirmation in a larger number of HD primary fibroblast lines before reaching any conclusion.

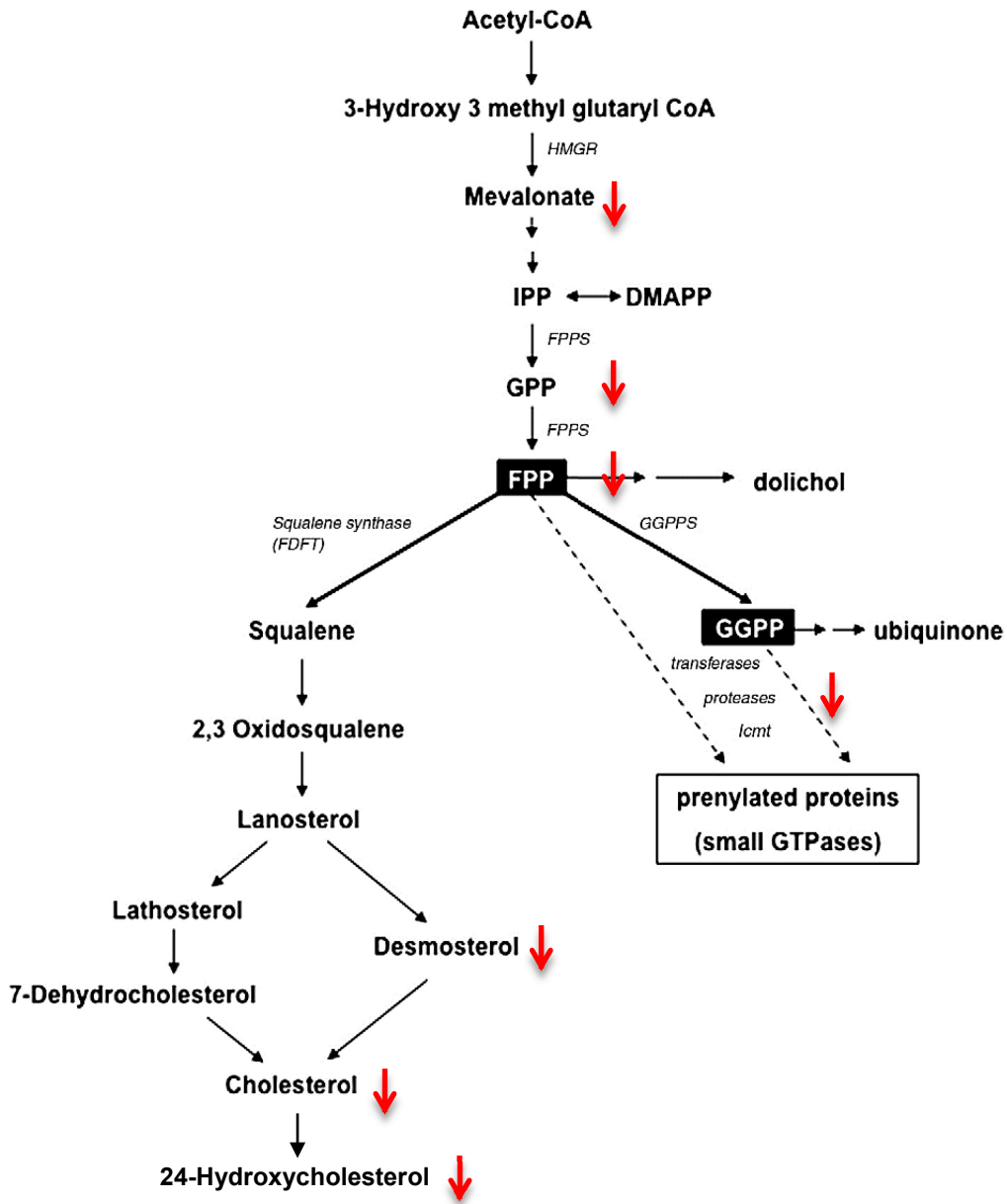
Both, gain- and loss-of-function mutations in RAB7 have been linked to a hereditary peripheral neuropathy, the Charcot-Marie-Tooth type 2B disease, characterized by severe loss of sensation in hands and feet, followed by muscle weakness and atrophy that usually starts in the second or third decade of life (385-389). However, this is the first time an alteration of RAB7 is associated to HD.

RAB7 is essential for the maturation of autophagosomes and endosomes (362,390). In fact, the fusion between autophagosomes and lysosomes has been shown to be dependent on RAB7 (391). RAB7 is also critical for the retrograde axonal transport of vesicles containing trophic factors and/or receptors (363,392). Interestingly, both autophagy and vesicular transport are affected in HD (152,366,367,393). More specifically, recently published papers have linked the activity of RAB7 to lipophagy (394) and mitophagy (395,396), two forms of selective autophagy that have

been reported to be impaired by muHTT (393). Further research will be required to determine whether restoring normal levels of RAB7 would improve selective autophagy and vesicle transport in HD models.

3.4. Figures

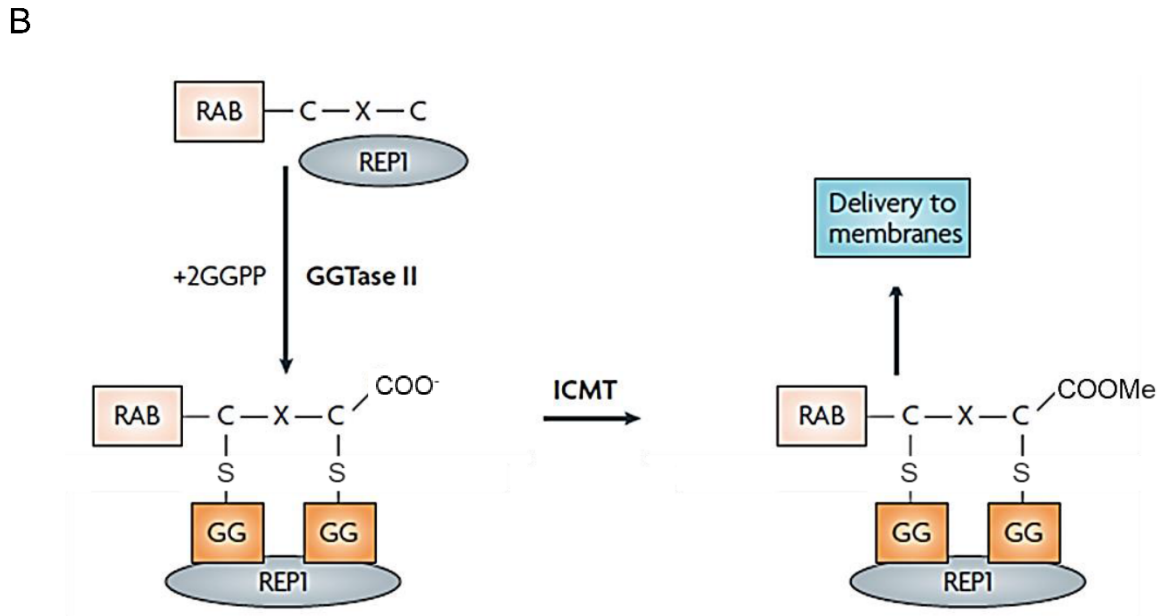
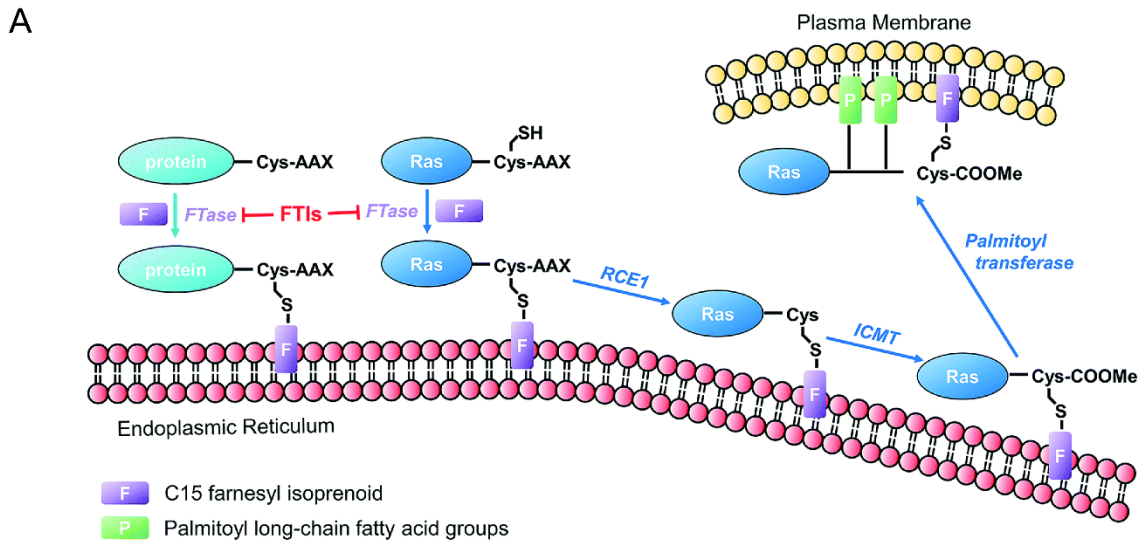
Figure 3.1. The mevalonate pathway and Huntington's disease



Scheme of the mevalonate pathway. Red arrows indicate the enzymes whose expression is downregulated in cell and animal models of HD.

(Modified from (318): "Isoprenoids, small GTPases and Alzheimer's disease". Hooff GP, et al. Biochim Biophys Acta. 2010 Aug;1801(8):896-905)

Figure 3.2. Prenylation reactions of small GTPases



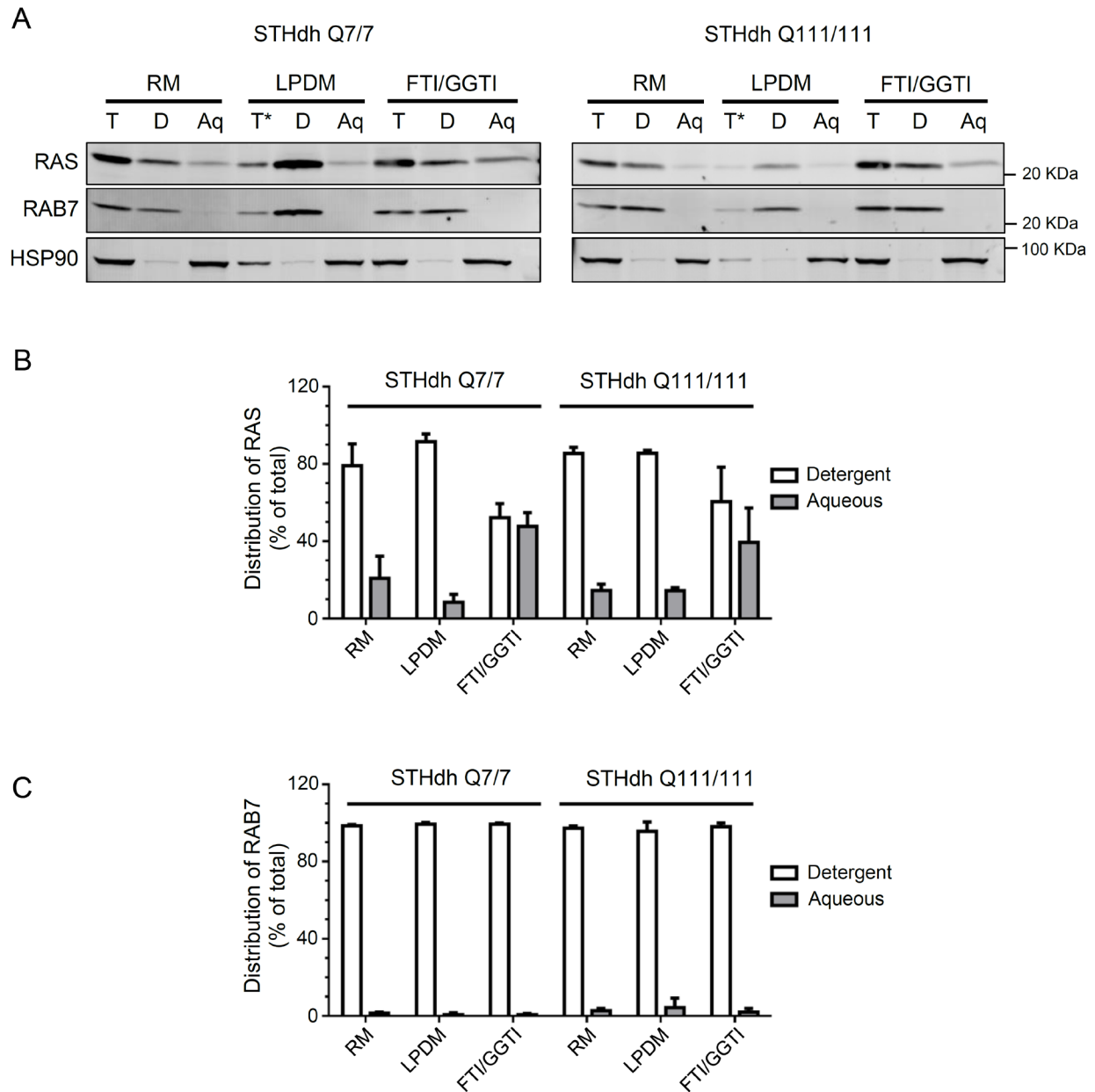
A) Small GTPases (except for RAB proteins) are prenylated by FTase or GGTase I complexes. FPP or GGPP are covalently attached to the cysteine at the CAAX motif. After prenylation RAS converting CAAX endopeptidase 1 (RCE1) cleaves the last three amino acids of the protein. Carboxymethylation is performed by the enzyme isoprenylcysteine carboxymethyltransferase (ICMT). Additionally, a subset of small GTPases can be further palmitoylated.

(Modified from (397): Wang, J., et al. (2017). "New tricks for human farnesyltransferase inhibitor: cancer and beyond." *Med Chem Commun* 8:841-854)

B) Members of the RAB subfamily of proteins are prenylated by GGTase II. RAB Escorting Protein I (REP1) presents the unprenylated RAB to GGTase II, which attaches two GGPP molecules to the cysteines of the CXC or CC motif of the RAB protein.

(Modified from (354): Konstantinopoulos, P. A., et al. (2007). "Post-translational modifications and regulation of the RAS superfamily of GTPases as anticancer targets." *Nat Rev Drug Discov* 6(7): 541-555)

Figure 3.3. Triton X114 fractionation of RAS and RAB7 is not affected in immortalized HD striatal cells



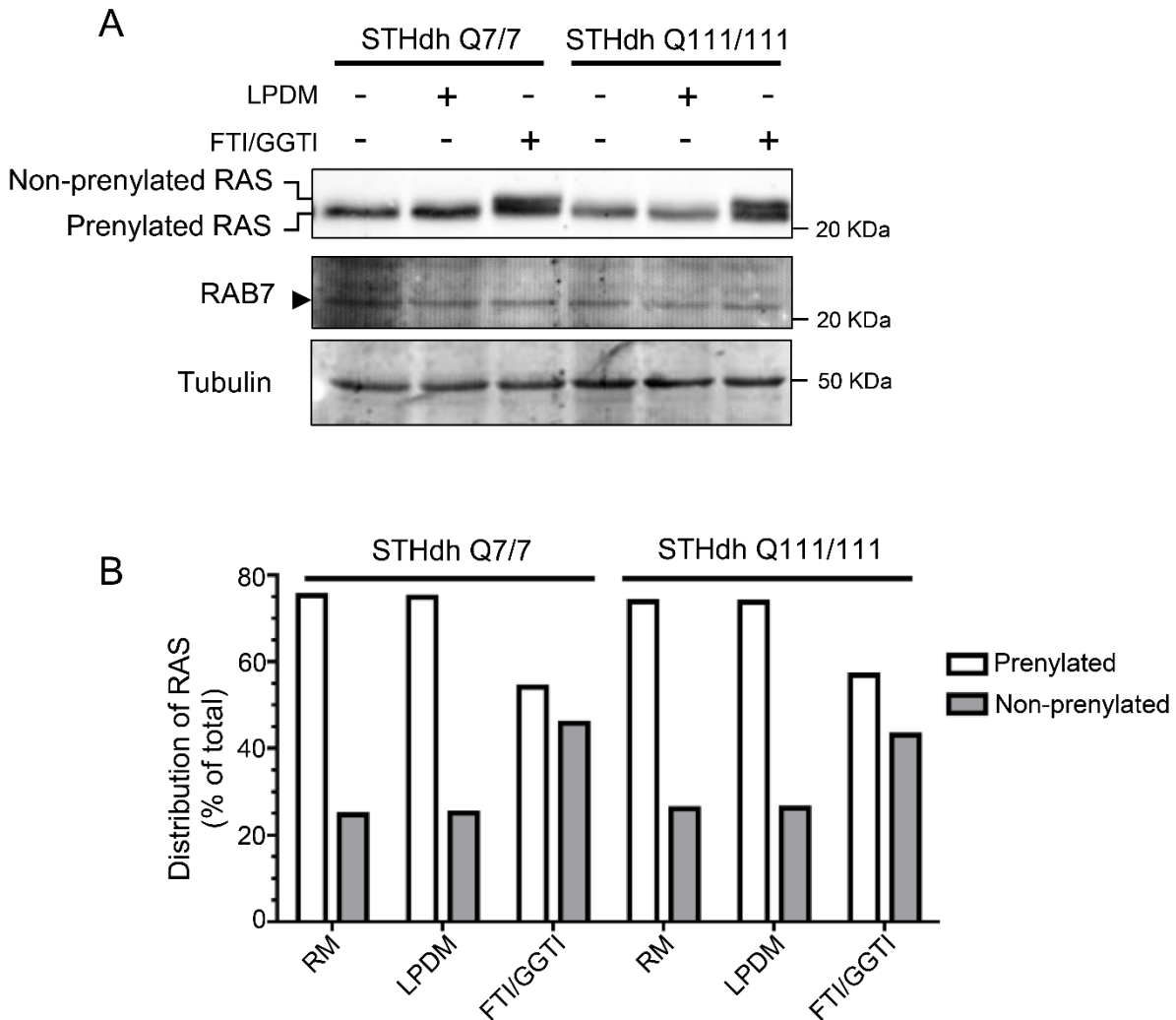
A) Representative immunoblots of Total (T), detergent (D), and aqueous (Aq) fractions prepared in Triton X114 lysis buffer from immortalized mouse knock-in striatal cells (STHdh) expressing full length HTT with 7 (Q7/7), or 111 CAG repeats (Q111/111) and grown in regular medium (RM) or lipoprotein-deficient medium (LPDM) for 48 h. Prenylated proteins partition into the detergent fraction. Treatment of cells with FTI/GGTI combination (80 μ M FTI-277 + 5 μ M

GGTI-2133) was used to confirm that the technique is able to detect changes in protein prenylation. Equivalent volumes of each fraction were loaded. HSP90 protein was used as a marker of aqueous fractions (* = less sample loaded due to technical problems).

B) Quantification of the distribution of RAS protein in the detergent and aqueous phases in lysates from STHdh Q7/7 and Q111 cells. Bars show mean values \pm SD of 2 independent experiments.

C) Quantification of the distribution of RAB7 protein in the detergent and aqueous phases in lysates from STHdh Q7/7 and Q111 cells. n=2. Bars show mean values \pm SD of 2 independent experiments.

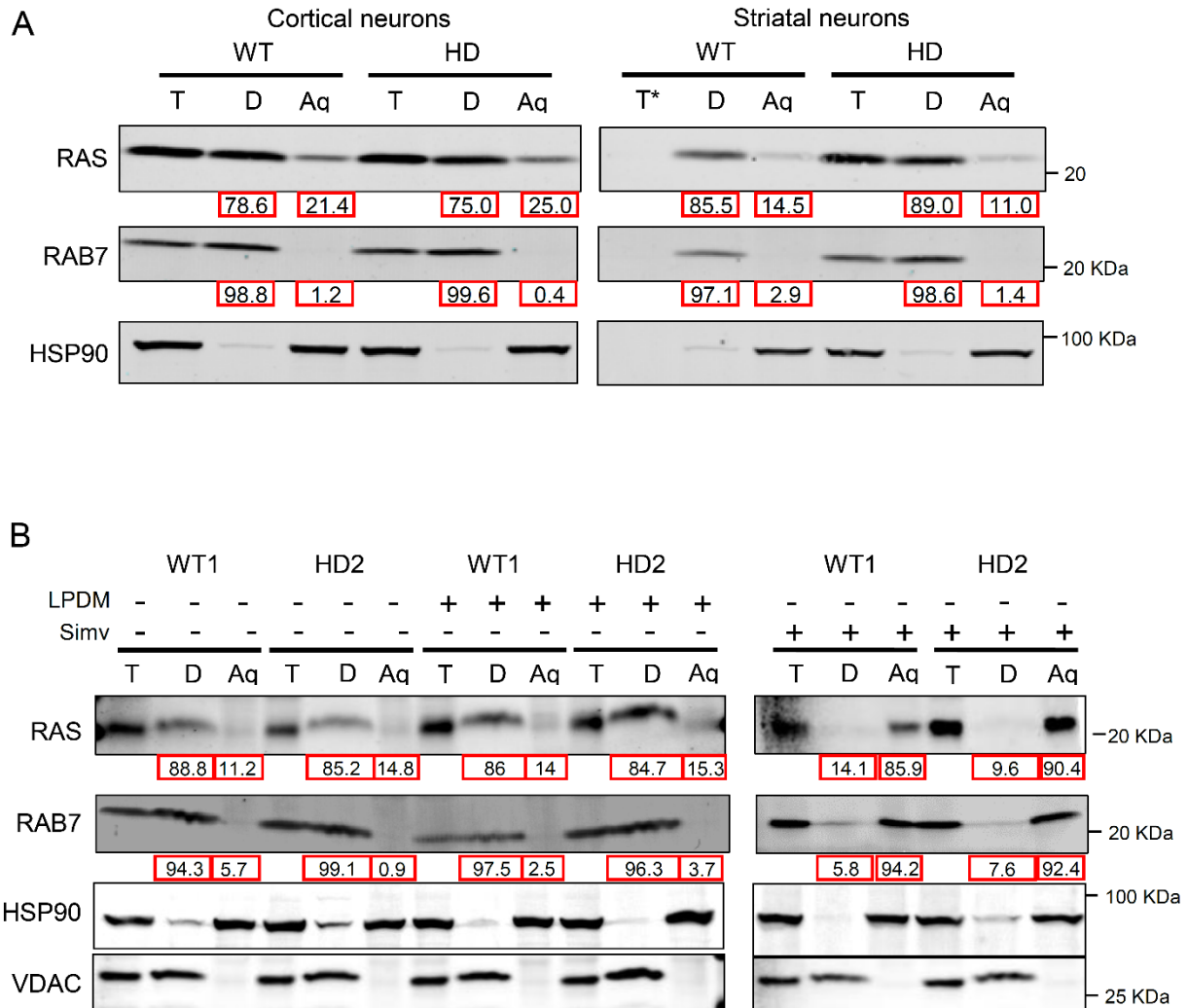
Figure 3.4. Electrophoretic mobility shift assay confirms that prenylation of RAS and RAB7 is normal in HD cells



A) Immortalized knock-in striatal cells (STHdh) expressing full-length HTT with 7 (Q7/7) or 111 CAG repeats (Q111/111) were cultured in regular medium (RM) or lipoprotein-deficient medium (LPDM) for 48 h. FTI/GGTI combination (80 μ M FTI-277 + 5 μ M GGTI-2133) was used to inhibit prenylation of RAS, to generate a positive control for the presence of unpreylated proteins. Proteins were loaded in a 12% SDS-PAGE gel to observe changes in electrophoretic mobility. Majority of RAB7 was prenylated in both cell lines.

B) Quantification of prenylated and unpreylated RAS in the immunoblot in (A), represented as a percentage of the total. This experiment was performed only once.

Figure 3.5. Triton X114 fractionation of RAS and RAB7 is not affected in HD neurons nor astrocytes



A) Immunoblot of Total (T), detergent (D), and aqueous (Aq) fractions prepared from cortical (left) and striatal (right) postnatal primary neurons from WT and YAC128 mice, upon lysis in Triton X114 buffer. Equivalent volumes of each fraction were loaded. Prenylated proteins partition into the detergent fraction. This experiment was performed only once (* = denotes loss of sample).

B) Immunoblot of Total (T), detergent (D), and aqueous (Aq) fractions prepared from immortalized mouse astrocytes stably expressing N548-HTT fragment with 15 CAG repeats

(WT), or 128 CAG repeats (HD), after being cultured in RM or LPDM for 48h. Treatment of cells with simvastatin (25 μ M, 24 h) was used to confirm that the technique is able to detect changes in protein prenylation. Equivalent volumes of each fraction were loaded. This experiment was performed only once.

Numbers under blots indicate the percentage of protein partitioning into each fraction. VDAC and HSP90 were used as proteins markers for detergent and aqueous fractions, respectively.

Figure 3.6. Triton X114 fractionation of RAS, RAB7 and RAB11 is not affected in brains of HD mice

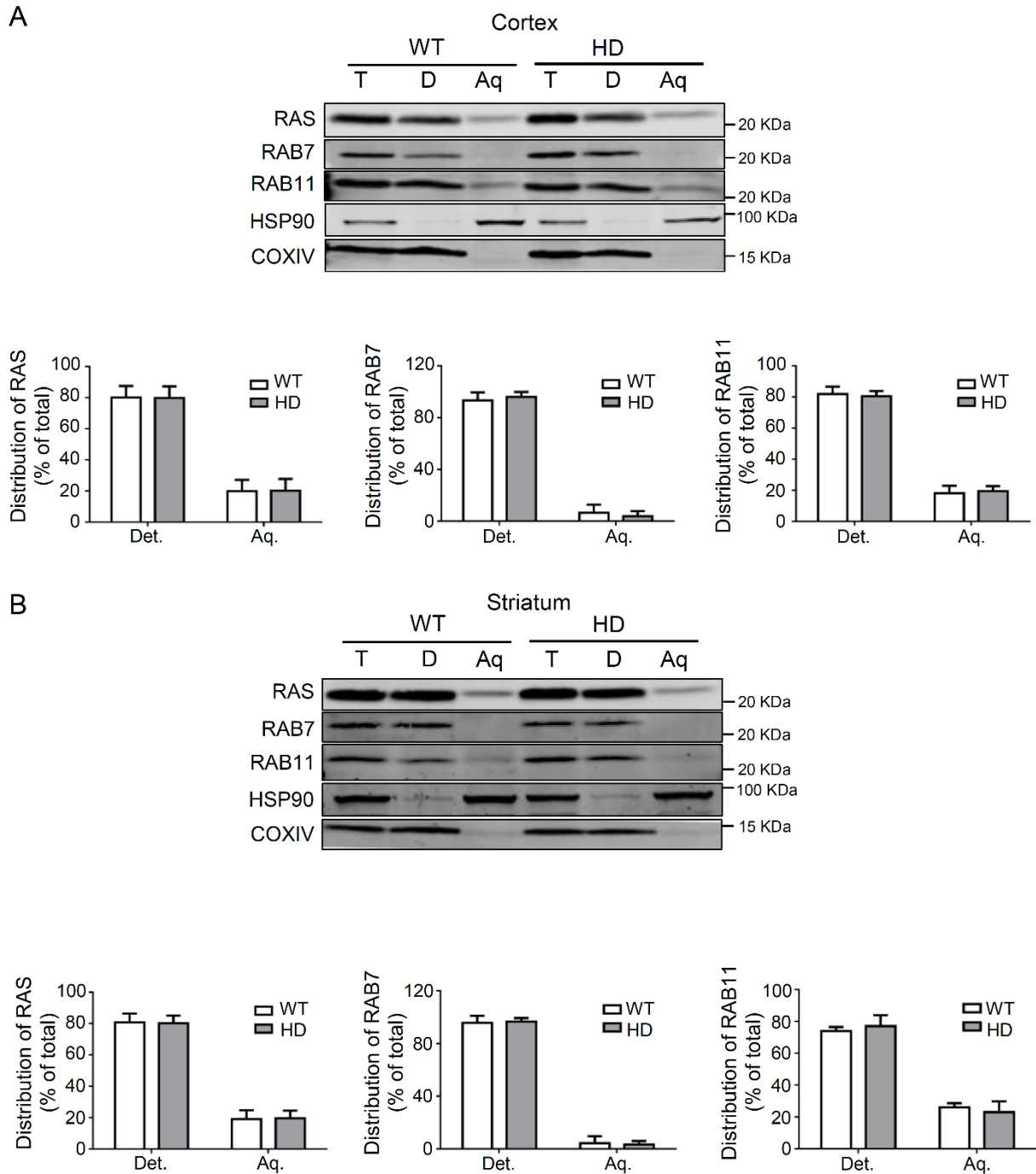


Figure 3.6. Triton X114 fractionation of RAS, RAB7 and RAB11 is not affected in brains of HD mice

A) Representative immunoblots and densitometric analysis of RAS, RAB7 and RAB11 distribution in Total (T), detergent (D), and aqueous (Aq) fractions prepared from brain cortical tissue of 10-12-month-old WT and YAC128 mice, upon lysis in Triton X114 buffer. Equivalent volumes of each fraction were loaded. Prenylated proteins partition into the detergent fraction, as expected, both in WT and HD samples. COXIV and HSP90 proteins were used as markers of detergent and aqueous fractions, respectively. WT N=6; HD N=6. Bars show mean values \pm SD.

B) Representative immunoblots and densitometric analysis of RAS, RAB7 and RAB11 distribution in Total (T), detergent (D), and aqueous (Aq) fractions prepared from brain striatal tissue of 10-12-month-old WT and YAC128 mice. WT N=6; HD N=6. Bars show mean values \pm SD.

Figure 3.7. Total levels of RAB7 are decreased in brain tissue and primary neurons from HD mice

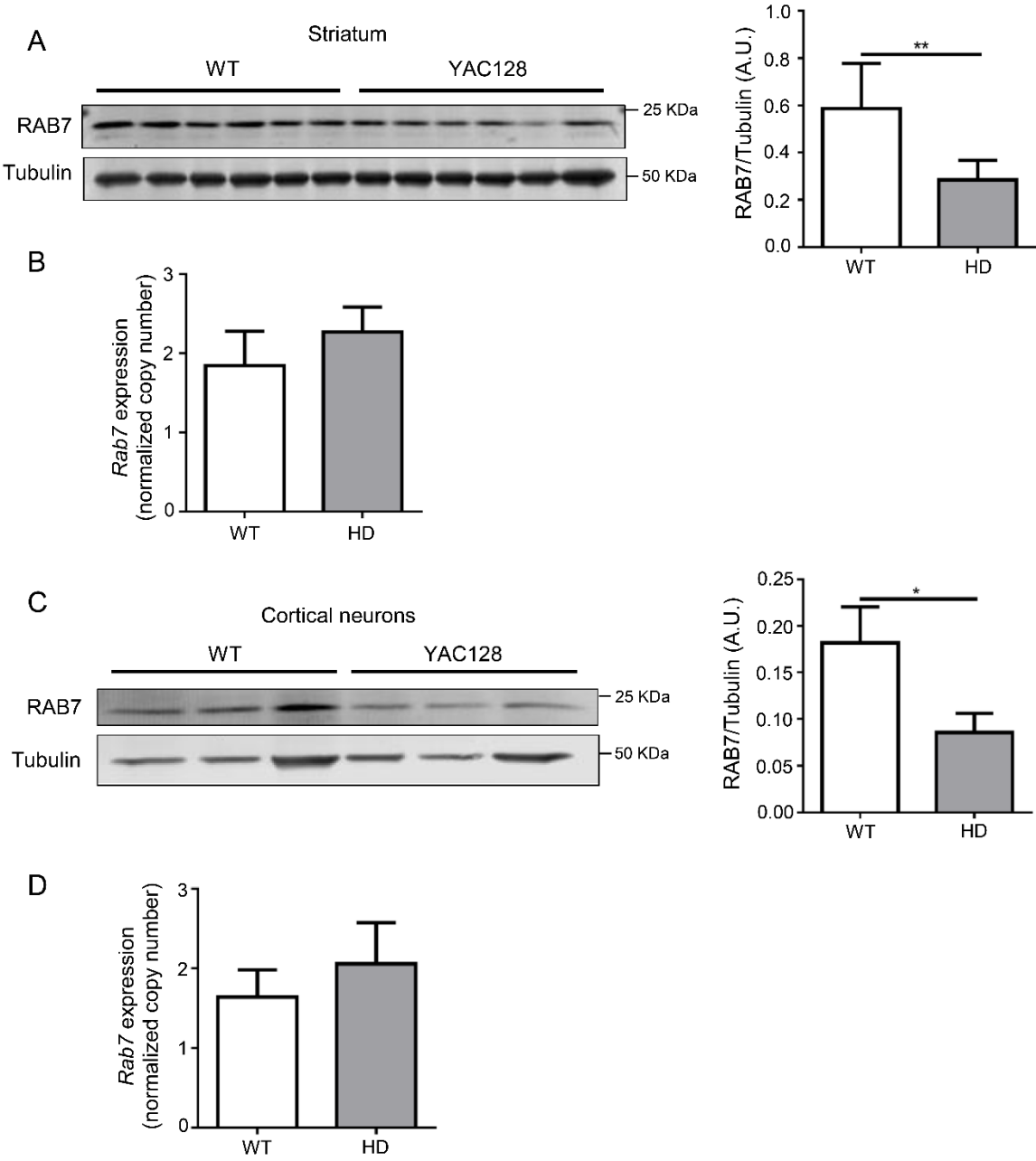
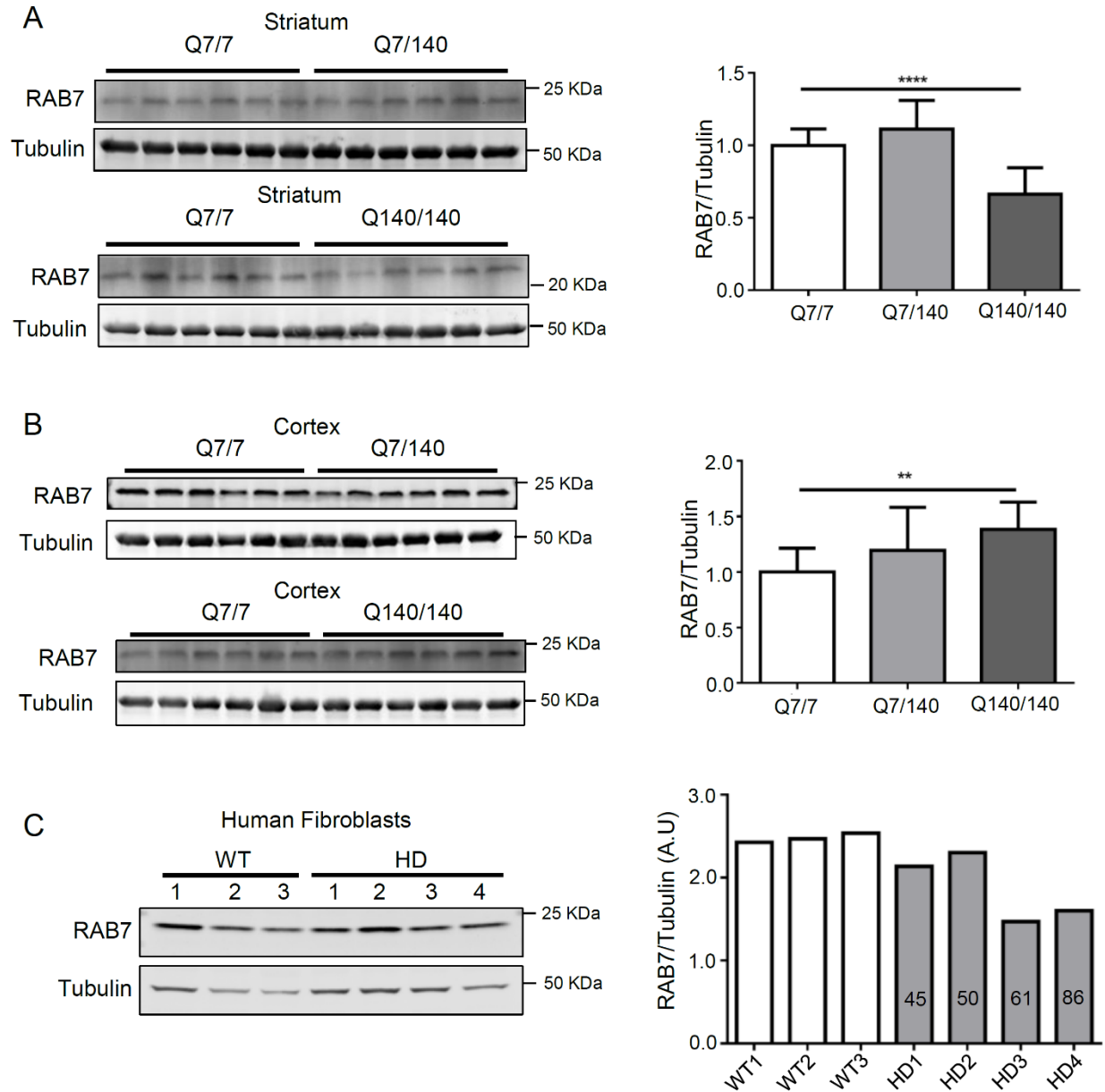


Figure 3.7. Total levels of RAB7 are decreased in brain tissue and primary neurons from HD mice

- A) Immunoblot and densitometric analysis of RAB7 in striatum from 6 YAC128 mice (10-12-month-old) and 6 age-matched WT littermates. Bars show mean values \pm SD. Two-tailed Student's t-test. $**p < 0.01$.
- B) *Rab7* mRNA levels quantified by qRT-PCR in striata from 7 YAC128 mice (10-12-month-old) and 4 age-matched WT littermates. Bars show mean values \pm SD.
- C) Immunoblot and densitometric analysis of RAB7 protein in lysates from postnatal cortical primary neurons from 3 YAC128 pups and 3 WT littermates (DIV10-13). Bars show mean values \pm SD. Two-tailed Student's t-test. $*p < 0.05$.
- D) *Rab7* mRNA levels quantified by qRT-PCR in postnatal cortical primary neurons from 5 YAC128 pups and 3 WT littermates (DIV10-13). Bars show mean values \pm SD.

Figure 3.8. Total levels of RAB7 are decreased across models of HD



A) Representative immunoblots and densitometric analysis of RAB7 in striatal lysates from 12 Q7/7 mice, 12 Q7/140 mice and 11 Q140/140 mice (8-10-month-old). Bars show mean values \pm SD for. One-way ANOVA with Tukey-Kramer post-hoc correction. **** p <0.0001.

B) Representative immunoblots and densitometric analysis of RAB7 in cortical lysates from 12 Q7/7 mice, 12 Q7/140 mice and 11 Q140/140 mice (8-10-month-old). Bars show mean values \pm SD for. One-way ANOVA with Tukey-Kramer post-hoc correction. $**p < 0.01$.

C) Immunoblot and densitometric analysis for RAB7 in lysates of 3 human fibroblasts obtained from healthy controls, and 4 fibroblasts obtained from HD patients. Numbers inside bars indicate the number of CAG repeats each patient contained in its *HTT* gene.

**Chapter 4: GM1 reduces protein aggregation in two models
of proteotoxic stress**

This chapter is my original work.

4.1. Introduction

Analyses of human samples obtained from patients suffering from HD, as well as from mouse models of HD, have shown that mutation of the HTT protein promotes the formation of intracellular muHTT aggregates (169-174). Furthermore, various studies have suggested that aggregation of muHTT may play a role in the striatal neuronal cell death observed in HD (85,174,177,178,398) that eventually leads to the development of the signs and symptoms that are characteristic of the disease. Our laboratory has focused on the research of potential therapeutic approaches for the treatment of HD, and in recent years, we found that intracerebroventricular (ICV) infusion of ganglioside GM1 in mouse models of HD decreases the amount of soluble and aggregated muHTT, concomitantly improving motor and non-motor behaviour in treated HD mice, suggesting that GM1 is a disease-modifying therapy in HD models (273). The mechanisms by which GM1 decreases the amount of soluble and aggregated muHTT protein, are still unknown.

In this chapter, I used two distinct cell models of proteotoxic stress to demonstrate that exogenous supply of ganglioside GM1 decreases the accumulation of protein aggregates *in vitro*, in a cell-autonomous manner (i.e. in homogenous cell populations and in the absence of potential confounding effects from glia cells). The models developed in this chapter will also be used in Chapters 5 and 6 to investigate the cellular mechanisms underlying the beneficial effects of GM1 treatment in HD.

4.1.1. Ganglioside GM1: Synthesis and functions within the CNS

4.1.1.1. Synthesis

Glycosphingolipids are complex lipids, composed of a ceramide moiety and a sugar head group. The ceramide moiety is composed by a long chain aminoalcohol, most commonly C:18 or C:20 (in the brain), with a double bond between carbons C4-C5 (sphingosine base), bound to a long chain fatty acid (C:16 or longer). Mono or polysaccharide chains can be attached to the primary alcohol group of the ceramide moiety. When a monosaccharide (e.g. glucose or galactose) is attached to ceramide, the resulting molecules are termed **cerebrosides**. If the sugar group is a sulphated mono or di-saccharide, the glycolipids are called **sulphatides**. **Complex glycosphingolipids** contain a linear or branched polysaccharide chain, and if at least one of those saccharide units is a sialic acid, the molecule is classified as a **ganglioside** (Fig. 4.1A) (399,400).

The synthesis of glycosphingolipids, gangliosides included, takes place in two membrane organelles: the ER and the Golgi apparatus. In the ER, the ceramide moiety is synthesized in a multistep process that involves the condensation of an activated fatty acid, either palmitoyl-CoA or stearoyl-CoA to a serine molecule, generating 3-keto-dihydrosphingosine. This reaction is catalyzed by serine-palmitoyl transferase. 3-keto-dihydrosphingosine is further reduced, resulting in hydroxy-dihydrosphingosine. Another acylation reaction, usually with a C:18 or a C:20 fatty acid, results in the formation of dihydroceramide. At last, carbons C4-5 are desaturated to give rise to ceramide (400). Ceramide can also be obtained from the re-acylation of the sphingosine molecule resulting from the catabolism of ceramide carried out by the enzyme ceramidase (401).

Once ceramide is synthesized, it must be transported to the Golgi for further glycosylation. However, ceramide has a very limited solubility in water, therefore it depends on two mechanisms

of transport for its delivery to the Golgi. The first one is mediated by the ceramide transfer protein (CERT), a cytosolic protein that is able to bind ceramide via its ceramide-binding domain, keeping the ceramide in a soluble state. The second possibility is the transfer of ceramide via coatamer protein (COP)-dependent vesicle transport (402).

Once in the Golgi, ceramide can be used for the synthesis of sphingomyelin, or be glycosylated into one of the multiple (and abundant) species of glycosphingolipids. In this document, I will briefly review the enzymatic steps that lead to the synthesis of gangliosides, and more specifically of GM1 (Fig. 4.1B).

Ceramide is first glycosylated in a reaction catalyzed by the enzyme UDP-glucose ceramide glucosyltransferase (UGCG) to form glucosylceramide (GluCer) (400,402). Lactosylceramide (LacCer) is then formed by the addition of a galactose unit, in a reaction catalyzed by the enzyme lactosylceramide synthase (403,404). LacCer is then sialosylated to give rise to the simplest ganglioside, GM3, by the enzyme sialyl-transferase I, (SAT I, encoded by the gene *ST3GAL5*). GM3 can be sequentially sialosylated to GD3 and GT3 by the addition of one or two more sialic acid units, respectively. These reactions are catalyzed by the enzymes SAT II and SAT III (encoded by the genes *ST8SIA1* and *ST8SIA3*, respectively) (405). GM3, GD3 and GT3 are the first gangliosides in the series a, b, and c, respectively. Sequential glycosylation reactions give rise to numerous gangliosides in each of the series. The details in the reactions and enzymes that lead to the synthesis of all gangliosides belonging to all respective series, are out of the scope of this document, but can be reviewed elsewhere (400,405).

Ganglioside GM1 (Fig. 4.1A) belongs to the a-series, and is the result of two sequential glycosylation reactions after GM3 synthesis. GM3 is transformed into GM2 by attaching an N-acetylgalactosamine in a reaction catalyzed by the enzyme β -1,4-N-acetyl-

galactosaminyltransferase 1 (encoded by *B4GALNT1*), followed by the transfer of a galactose unit by the enzyme β -1,3-galactosyltransferase 4 (encoded by *B3GALNT4*) (400,405). Once synthesized, GM1, together with other gangliosides, is transported from the Golgi to the plasma membrane, presumably via budding vesicles. In support of this hypothesis, it is known that the sugar headgroups of glycolipids face the lumen of the Golgi during synthesis, but in the plasma membrane, they face the extracellular side (400,405).

It is important to mention that, although I focused on reviewing the synthesis of ganglioside GM1, other gangliosides such as GD1a, GD1b and GT1b are also highly enriched in the brain (406).

4.1.1.2. Functions of ganglioside GM1

Ganglioside GM1 is highly enriched in the brain. It is mostly found in the plasma membrane as part of the lipid rafts but also localizes to recycling and late endosomes, lysosomes, Golgi and ER (406). Due to its localization in the membrane, and by interacting with many protein partners, GM1 modulates a plethora of cellular functions, including cell growth, differentiation, apoptosis, and more (406).

For instance, Wu and collaborators (407,408) determined that increasing the concentration of GM1 at the plasma membrane, either by exogenous supply of it or by treatment with sialidases of bacterial origin, promoted the generation of dendrites and an increased influx of calcium in neuroblastoma cells. Years later, the same research group reported that the induction of the neurite outgrowth was due to an interaction of GM1 with $\alpha 5\beta 1$ integrin that, through a signaling cascade dependent on phospholipase $C\gamma$, promoted the opening of the transient receptor potential cation channel C5 (TRPC5), permitting the influx of calcium and stimulating the neurite outgrowth (409).

Furthermore, axotomy increases the expression of neuraminidase 3 (NEU3) at the site of the lesion. This increase in NEU3 expression causes an increase in the ratio of GM1 to other gangliosides. Inhibition of NEU3 impairs axonal regeneration while exogenously supplied sialidase promotes it, suggesting that the presence of GM1 at the level of the plasma membrane, and localized at the site of lesion, is important for axonal regeneration (410).

GM1 also interacts with the receptors of neurotrophins/growth factors, altering their properties. Example of this phenomenon is the work of Mutoh and collaborators (411) reporting that GM1 binds directly to the TrkA receptor. This interaction potentiates the effects of nerve growth factor (NGF), the natural ligand of TrkA. In the presence of GM1, the level of autophosphorylation of TrkA, a measure of its activity, is more than 3-fold when compared to non-treated cells, thus promoting NGF effects such as neurite outgrowth and neurofilament expression in PC12 cells. Likewise, treatment with phorbol-12-myristate-13-acetate (PMA) decreases the association of GM1 to TrkB receptor. Under these conditions, brain-derived neurotrophic factor (BDNF) treatment is unable to promote the phosphorylation of TrkB, suggesting that GM1 has a role in the proper activation of neurotrophin receptors by their natural ligands (412).

But not all growth factor receptors are potentiated by GM1. In fact, Swiss 3T3 fibroblasts overexpressing enzymes involved in the synthesis of GM1 show less proliferation after stimulation with platelet-derived growth factor (PDGF). This reduced growth correlates with a reduced phosphorylation of the PDGF receptor, as well as with less activation of mitogen-activated protein (MAP) kinases downstream. Researchers also found less PDGF receptor in purified glycolipid-enriched microdomains in cells overexpressing GM1 in comparison to control cells, suggesting that excess of GM1 displaces the PDGF receptor out of the glycolipid-enriched microdomains, impairing its proper function (413).

Ganglioside GM1 may also have a function in the axon-myelin interaction. Mice lacking GM1 and GD1a, another ganglioside of the a-series, show defects in the adhesion of paranodal loops to the axonal membrane. Contactin associated protein 1 (CASPR) and neurofascin 155 (NF155), two proteins involved in the organization and assembly of the Ranvier node, are decreased in these mutant mice. Electrophysiological studies revealed slower nerve conduction and reduced nodal sodium currents in these mice, indicating the importance of gangliosides, particularly GM1 and GD1a, in the interaction of neuron-glia at the level of paranodes (414).

4.1.2. Ganglioside GM1 and neurodegeneration

GM1, or alterations in its metabolism, have been associated with the pathophysiology of various neurodegenerative diseases, including AD, PD and HD (406).

One of the most accepted hypotheses regarding AD pathogenesis is the amyloid hypothesis. In summary, it states that the deposition of amyloid β ($A\beta$) peptide within the neuropil, product of the cleavage of the amyloid precursor protein (APP), is the main driver of the pathology observed in AD. Other events, such as the neurofibrillary tangles and neurodegeneration, are secondary to the $A\beta$ deposition (415).

Yanagisawa and collaborators (416,417) reported on a new species of $A\beta$, the GM1-bound $A\beta$, that characteristically interacts with membranes and has different physical properties than unbound $A\beta$. Further studies demonstrated that GM1-bound $A\beta$ was able to act as a seed, accelerating the kinetics of aggregation of $A\beta$ species *in vitro*. Furthermore, aggregates that were formed in the presence of GM1 were shown to be toxic to cultured primary neurons (418). GM1-bound $A\beta$ is also present in human tissue specimens from AD patients (418).

The interaction between A β and GM1 could explain some of the electrophysiological phenomena observed in AD. For instance, A β oligomers injected into the brain interstitial fluid are rapidly depleted from the liquid phase and can then be recovered from membranes as GM1-bound A β . Oligomers of A β inhibit long-term potentiation (LTP), an electrophysiological property that is interpreted as an indication of synapse strength and is considered by many to be the cellular basis of memory. If hippocampal slices are pre-treated with cholera toxin, blocking the access to GM1 in the membranes, A β oligomers are unable to inhibit LTP (419). GM1 may also promote the biogenesis of A β peptides without changing the levels of full-length APP protein. These data suggest that GM1 may alter the pattern of cleavage of APP, promoting the generation of pro-aggregating peptides (420).

PD is a neurodegenerative disease characterized by a selective dopaminergic neuronal loss in the substantia nigra pars compacta, due to unknown causes. Clinically, it is characterized by hypokinesia and resting tremor, and although its cause is still under research, one pathological hallmark found in almost all patients is the aggregation of protein α -synuclein (α syn) in inclusion bodies called Lewy bodies, not only in the dopaminergic neurons of the substantia nigra, but also in other regions of the brain, and even in the enteric nervous system (421).

Early studies done in neurotoxic models of PD, such as the treatment of cultured mesencephalic neurons with 2,4,5-trihydroxyphenylalanine (TOPA), showed that ganglioside GM1 had neuroprotective properties against apoptosis induced by TOPA (422). GM1 has also been found to interact directly with α syn, promoting an α -helix conformation and thus, inhibiting the α syn fibril formation. Importantly, mutations in α syn associated to familial PD showed to have no association with GM1 (423).

GM1 also showed some beneficial effects in a rat model of PD induced by injection of 6-hydroxydopamine (6-OHDA) into the mesencephalon. Administration of intraperitoneal GM1 in 6-OHDA-injected rats decreased the amount of glutamate in the striatum, cerebral cortex and hippocampus, while the expression of pro-apoptotic proteins, such as B-cell lymphoma 2 (BCL-2) was significantly decreased in the substantia nigra and striatum of GM1-treated rats. GM1 was also able to partially improve motor behaviour in the rats injected with 6-OHDA (424). A second research group using the same model of PD, was able to reproduce the GM1-beneficial effects on motor behaviour. Authors also demonstrated that expression of pro-inflammatory cytokines, such as interleukin β , was reduced upon treatment with GM1 (425).

Importantly, mice with partial deficiency of GM1 and GD1a gangliosides due to a heterozygous mutation in *B4galnt1* gene, show symptomatology compatible with PD and a selective loss of tyrosine hydroxylase-positive (TH⁺) neurons in the subthalamic nucleus, similar to human patients with PD. These symptoms were alleviated by treatment with levo-DOPA, an analog of dopamine, or with LIGA20, a membrane-permeable analog of GM1. Moreover, the levels of GM1 are decreased in nigral dopaminergic neurons of PD patients, compared to age-matched controls (426).

4.1.3. Ganglioside GM1 and HD

Previous work in Dr. Sipione's laboratory has shown that GM1 levels are reduced in human HD fibroblasts, as well as in two striatal cells lines expressing either the full-length or an N-terminal fragment of muHTT (272). GM1 deficiency was also observed in the cortex and striatum of YAC128 mice. The reduced levels of ganglioside GM1 in HD cells and brains of YAC128 mice were correlated with a decreased expression of enzymes of the ganglioside synthetic pathway. Moreover, restoring levels of GM1 by exogenous supply, protected HD striatal cell from apoptosis (272).

Our laboratory also showed that intracerebroventricular (ICV) infusion of GM1 into YAC128 mice restored motor behaviour and increased the expression and activation of DARPP32, a specific marker of medium spiny neurons that is downregulated in HD (115). Cognitive and psychiatric-like dysfunctions were also corrected in Q140 mice after GM1 treatment (273). In R6/2 mice, a model with accelerated disease progression (166), treatment with GM1 decreased neurodegeneration and weight loss (273).

Importantly, GM1 ICV infusion reduced the amount of SDS-insoluble muHTT aggregates in the cortex of R6/2 mice, and both soluble muHTT and SDS-insoluble muHTT levels in the striata of Q140/140 mice (Fig. 4.2). Expression of the *Htt* gene was unaltered in treated mice, suggesting that changes in transcription are not responsible for the reduction of muHTT aggregates observed with GM1 treatment. Reduction of muHTT in its soluble and insoluble form might be an important mechanism that could explain neuroprotection and behavioural improvement in HD mice treated with GM1 (273).

4.1.4. The aggresome: A general response to misfolded proteins and proteotoxic stress

Upon proteotoxic stress caused by the accumulation of misfolded or toxic proteins, cells usually respond by promoting the generation of large perinuclear aggregates, named **aggresomes**. These aggregates not only contain the misfolded/toxic protein, but they also immunoreact with anti-ubiquitin antibodies, and contain protein p62, an autophagy adaptor protein. For this reason, these structures are also referred to as p62-aggresomes or p62-bodies (427-430).

The formation of aggresomes is a common cellular mechanism to cope with potentially toxic proteins, and it has been observed in multiple neurodegenerative diseases including prion disease

(431,432), AD (433,434), amyotrophic lateral sclerosis (ALS) (435,436), PD (437-440) and HD (232,441-443), all of which are characterized by the accumulation of a misfolded toxic protein.

Characteristically, aggresomes are found as a distinct population of p62-positive particles. Under regular conditions, when cells are not under proteotoxic stress, cells do contain p62-positive particles that are small and distributed across the cell body, measuring under 0.2 μm in diameter. Instead, aggresomes are bigger, ranging in size from **0.5-2.0 μm in diameter**, and are localized in proximity of the nucleus, at the microtubule organizing centre (MTOC) as evidenced by their colocalization with γ -tubulin, a specific marker of the MTOC. The aggresomes may vary among different cell types, and depending on the protein that is inducing the formation of the aggresome, among other factors (427,443,444). Besides size and localization, the morphology of aggresomes is also distinctive with respect to other p62 particles. Since p62 is preferentially localized in the periphery of the aggresome, when cells are labelled by immunostaining with anti-p62 antibodies, aggresomes appear to have an **empty core**, surrounded by p62 signal (443). Characteristically, the intermediate filament vimentin is also localized in the periphery of the aggresomes (427).

Aggresomes are enriched in components of protein quality control systems, such as the 20S subunit of the proteasome, proteasome activators PA700 and PA28, ubiquitin, and molecular chaperones such as HSP70, HSP90 and TCP1-chaperonin. This suggests that aggresomes are not passive structures formed only by the toxic proteins, but rather a dynamic structure in which degradation or unfolding of toxic proteins may occur (427,444-446).

In the specific context of HD, expression of the exon1 of HTT containing an expanded polyQ stretch promotes the formation of aggresomes in cultured cells. These aggresomes are immunoreactive for the transgene, but also for ubiquitin, the 20S and 19S components of the proteasome, as well as molecular chaperones including HSP70 and HSP40 (232). Importantly,

muHTT fragments co-immunoprecipitate with p62 while WT fragments do not, suggesting that p62 binds to an ubiquitinated form of muHTT within the aggresomes (442). Aggresomes formed by N-terminal fragments of muHTT are usually decorated with p62, which localizes almost exclusively at the edges of the aggresome (Fig 4.3). This “shell” formed by p62 colocalizes with LC3, a known marker of autophagosomes, and protein p62 has been found inside of autophagosomes, suggesting that at least partially, these structures are degraded via autophagy (443). Furthermore, treatment of cells expressing N-terminal fragments of muHTT with rapamycin, an inducer of autophagic activity, causes a slight decrease in p62 content, whereas treatment with bafilomycin A, an inhibitor of autophagic flux, causes further accumulation of p62 (443). It is important to mention that muHTT aggregates also colocalize with ubiquitin and p62 in tissue sections from R6/2 mice, suggesting that muHTT also induces the formation of aggresomes *in vivo*, in mouse models of HD (442).

Protein aggregates formed by muHTT can be analyzed by filter trap assay (also known as filter retardation assay) due to their insolubility in SDS (286,441). The intensity of the signal generated by insoluble muHTT trapped on top of the filter in this assay correlates with the number of cells containing aggresomes, when analyzed by microscopy (232). SDS-insoluble aggregates of muHTT are detected in brain lysates from R6/2 mice as well (447), suggesting that such aggregates are also formed *in vivo*.

The formation of aggresomes does not only occur after expression of mutant misfolded proteins, but it can also be induced by pharmacological inhibition of the ubiquitin-proteasome system (UPS). In fact, early studies done before the coinage of the term “aggresome” reported that the proteasome inhibitor N-benzyloxycarbonyl-Ile-Glu(O-t-butyl)-Ala-leucinal (proteasome inhibitor I, PSI), causes the formation of perinuclear structures that were enriched in proteasome

components and ubiquitin, that were also detectable with amido black staining, a stain for general proteins, in various cell lines. Interestingly, co-treatment with cycloheximide or nocodazole impedes the formation of such aggregates, indicating the importance of protein synthesis and the microtubule network in the formation of such structures (445,448).

Years later, Wójcik and collaborators (449) demonstrated that treatment of HeLa cells with MG132, a known inhibitor of the proteolytic activity of the UPS, causes a significant increase in the total cellular content of poly-ubiquitinated proteins and the formation of aggresomes, confirmed by the presence of ubiquitin, 26S proteasome, and pericentrin (a known marker of the MTOC). Likewise, Salemi and collaborators (450) showed that HeLa and HEK293 cells treated with MG132 contain aggresomes after 16 hours of treatment. Therefore, general inhibition of the UPS recapitulates, at least in part, cell responses and features induced by expression of muHTT and other pathogenic proteins involved in protein misfolding diseases.

In this chapter, I investigated the effects of GM1 administration in cell models of protein aggregation. Cell lines expressing full-length muHTT **do not form muHTT aggregates** under normal conditions (262) a phenomenon that is not well understood yet. To circumvent this issue, I used cells transfected with the exon1 of the mutant *HTT* gene, which codes for an N-terminal fragment of muHTT that is prone to aggregation and has increased toxicity when expressed in animal models (166). This model is very relevant to the human disease, since exon 1-derived HTT fragments are produced by aberrant splicing in human HD patients (165,167).

In addition, to determine whether the effects of GM1 administration on protein aggregates is HD-specific or more general, I used cells where aggresomes were generated by treatment with the UPS inhibitor MG132.

4.2. Results

4.2.1. Treatment with ganglioside GM1 reduces the amount of muHTT aggregates in cell models of HD

Striatal cells (STHdh Q7/7) expressing a plasmid encoding the exon 1 of the *HTT* gene with an expanded polyglutamine stretch (72Q) and tagged with eGFP (Ex1-72Q-HTT-eGFP) developed perinuclear aggregates containing the chimeric muHTT fragment and decorated by p62 (Fig 4.3).

To determine the effect of GM1 on muHTT aggregates, striatal cells (ST14A) were transfected with Ex1-72Q-HTT-eGFP (Fig. 4.4A). After transfection, cells were treated with GM1 (50 μ M) or with vehicle for 24 h, then fixed and analyzed by fluorescence microscopy. The mean number of aggregates per cell was not significantly different between treated and untreated cells (data not shown). However, the cumulative relative frequency distribution of the size of muHTT aggregates was shifted to the left in cells treated with GM1 (Fig. 4.4B), suggesting an overall decrease in muHTT aggregate size. In fact, the mean area of muHTT aggregates was $22.8\% \pm 3.98$ lower in GM1-treated cells compared to untreated (Fig. 4.4C). These results suggest that GM1 might decrease or slow down aggregate formation, or may facilitate its degradation. Unfortunately, the low transfection efficiency ($\sim 1\%$) in this model prevented any further biochemical analysis. In order to increase transfection efficiency, and to specifically analyze the effects of GM1 on muHTT insoluble aggregates, I turned to a second neuronal model represented by neuroblastoma N2a cells (277) transiently transfected with GFP alone, Ex1-25Q-HTT-eGFP or Ex1-72Q-HTT-eGFP. After transfection, cells were treated with GM1 (50 μ M) for 24 h, and HTT SDS-insoluble aggregates were analyzed by filter-trap assay, using an antibody against GFP. GFP- or Ex1-25Q-HTT-eGFP-transfected cells did not show any SDS-insoluble aggregates, as expected (Fig. 4.4D). Instead,

Ex1-72Q-HTT-eGFP-transfected cells did form SDS-insoluble aggregates, and the amount of these was decreased after GM1 treatment by ~66% when compared to untreated cells (Fig. 4.4D). This reduction in SDS-insoluble muHTT aggregates after GM1 treatment was replicated in HeLa cells stably expressing Ex1-72Q-HTT-eGFP, although in this model the reduction in GM1-treated cells was only ~14% compared to untreated (Fig. 4.4E).

4.2.2. Treatment with ganglioside GM1 reduces protein aggregation in striatal cells after inhibition of the proteasome

Next, I assessed the effects of GM1 on a muHTT-independent model of proteotoxic stress: inhibition of the ubiquitin-proteasome system (UPS). Similar to cells expressing muHTT, pharmacological inhibition of the UPS by MG132 causes accumulation of polyubiquitinated proteins and formation aggresomes, which are characteristically localized perinuclearly and decorated by p62 (387, 401, 440). This suggests that, although aggresomes in both cases are originated as a response to totally different stimuli, the formation of aggresomes after expression of muHTT or after UPS inhibition may share molecular and cellular mechanisms.

STHdh Q7/7 cells were incubated with vehicle or with MG132 (0.5 μ M) alone or in combination with GM1 (50 μ M) for 1 h, 2.5 h or 5 h. As expected in the presence of MG132, cells accumulated polyubiquitinated proteins, as detected with a pan-ubiquitin antibody, or with a specific K63-linked ubiquitin antibody in a time-dependent manner. In a short time-course, GM1 did not prevent accumulation of polyubiquitinated proteins (Fig.4.5A). However, after 24 h, GM1 co-administration resulted in reduced accumulation of pan-ubiquitinated (Fig. 4.5B) as well as K63-linked polyubiquitinated proteins (Fig. 4.5C) in STHdh Q7/7 cells, when compared to MG132 treatment alone. GM1 alone did not affect the levels of pan- or K63-linked polyubiquitinated proteins, when compared to vehicle. These data suggest a potential effect of the ganglioside on

proteostatic mechanisms responsible for the elimination of misfolded and/or ubiquitinated proteins (e.g. autophagy and/or protein elimination through extracellular vesicles).

Proteasome inhibition and proteotoxic stress cause accumulation of ubiquitinated proteins into aggresomes (p62-bodies) (449,450), identified by microscopy as large p62-positive intracellular inclusions with an empty core (427,428,450,451). About 37% of STHdh Q7/7 cells treated with MG132 alone developed aggresomes. Surprisingly, this proportion dropped to 17% when cells were co-treated with GM1 (Fig. 4.6A, B). Moreover, preliminary confocal analysis suggests that the mean size of p62-positive aggresomes was smaller in cells treated with a combination of MG132 and GM1, compared to MG132 alone (Fig. 4.6C). Cells treated with GM1 alone were indistinguishable from untreated controls (Fig. 4.6A-C).

Next, I sought to confirm my microscopy findings with a biochemical approach. Under proteotoxic stress conditions, aggresomes become detergent-resistant and can be precipitated by centrifugation of lysates prepared in mild detergents such as Triton X100. Moreover, it has been shown that the amount of Triton X100-insoluble p62 (hereafter referred to as insoluble p62) correlates with the number or the size of aggresomes in cell models of proteotoxic stress (393,452). Therefore, I analyzed the levels of insoluble p62 in cells treated with MG132 in the presence or absence of GM1.

In line with my previous findings, GM1 had no effect on insoluble p62 levels compared to MG132 alone at early time points (≤ 5 h.). However, GM1 significantly decreased the amount of insoluble p62 at 24 h of treatment (Figs. 4.7A-B), in line with the effects of the ganglioside on the accumulation of polyubiquitinated proteins (Figs. 4.5A-C). GM1 however, had no effect on the amount of soluble p62 in any of the models that were studied in my thesis, suggesting that GM1 may have effects only on aggresome (insoluble) p62.

Observations done in immortalized striatal cells were replicated in rat cortical primary neurons treated with MG132 (0.5 μ M, 24 h) and two different doses of GM1 (50 μ M and 100 μ M, 24 h) (Fig. 4.7C).

4.3. Discussion

My results suggest that administration of GM1 results in a decrease in the accumulation of aggresomes and insoluble muHTT in HD cells, as well as decreased accumulation of polyubiquitinated proteins and insoluble p62 in a general model of proteotoxic stress, based on pharmacological inhibition of the proteasome.

The formation of aggresomes appears to be a mechanism to cope with the toxicity of misfolded and noxious proteins. It is common to multiple neurodegenerative diseases, including AD, PD, ALS and HD, and even to pharmacological models of proteotoxic stress (inhibition of the UPS), suggesting that the proteins and signalling pathways involved in the formation of aggresomes are shared amongst various diseases, independently of the toxic protein/s that is/are sequestered (427,430,445,448-450).

HTT misfolding and aggregation is central to HD pathogenesis. Thus, interventions that target this process, or that promote the degradation of such aggregates are of great therapeutic interest.

Previous work in the Sipione laboratory showed that administration of GM1 to HD mouse models reduced the amount of SDS-insoluble muHTT aggregates and resulted in a dramatic improvement of both motor and non-motor signs of the disease (273). As transcription of the *Htt* gene is not affected by GM1 (273) I hypothesized that GM1 might trigger proteostatic mechanisms that prevent the accumulation of toxic muHTT, and that might mediate, at least in part, the therapeutic and neuroprotective effects of GM1 in HD models.

To determine whether GM1 decreases accumulation of misfolded proteins in a cultured cells, and to investigate the underlying mechanisms, I used two well-established cell models of proteotoxic stress: i) expression of N-terminal fragments of muHTT; and ii) pharmacological inhibition of the UPS using MG132.

Transfection of Ex1-72Q-HTT-eGFP into a striatal cell line resulted in evident perinuclear aggregation of the chimeric protein, as previously reported (232,441,442). Treatment with ganglioside GM1 was able to reduce the size of these perinuclear aggregates in a preliminary analysis. In line with these observations, N2a and HeLa cells expressing Ex1-72Q-HTT-eGFP did show significant reduction of muHTT SDS-insoluble aggregates after treatment with GM1. These results confirmed that GM1 treatment can reduce the amount of muHTT aggregates in cultured cells.

Interestingly, the effects of GM1 were more profound in N2a than in HeLa cells, even though the dose of GM1 and the time course of treatment were similar. This could be due to a number of different factors. First, it is possible that GM1 may not be equally incorporated into the two cell lines, affecting muHTT aggregates to different extents. Second, while the N2a cells used in these experiments were transiently transfected with Ex1-72Q-HTT-eGFP, HeLa cells were stably expressing the transgene. Consequently, the levels of cellular stress potentially affecting experimental results might be quite different between the two models. Finally, cells of neuronal origin, such as N2a cells, may have more efficient proteostatic mechanisms in place, compared to HeLa, due to their higher vulnerability to proteotoxic stress. Thus, GM1 may be more effective at enhancing such mechanisms in N2a than in HeLa cells.

GM1 was shown to trigger the phosphorylation of muHTT at Ser13 and Ser16 residues (115), a post-translational modification that can target muHTT for degradation via proteasome and

lysosome (112). While HTT phosphorylation might contribute to the reduction of muHTT aggregates induced by GM1, it is unlikely to be the only mechanism, since GM1 was able to decrease levels of polyubiquitinated proteins and insoluble p62 in a different and HTT-independent paradigm of proteotoxic stress. In line with the reduction in insoluble p62, GM1 was also able to decrease the proportion of cells containing visible aggresomes detected by p62 immunolabeling in this general model of protein aggregation.

The effects of GM1 on the accumulation of polyubiquitinated proteins during proteotoxic stress were modest compared to the reduction of aggresomes and insoluble p62. This might be due to the fact that ubiquitination of proteins, including K63-linked ubiquitination, is a post-translational modification that does not occur exclusively for the targeting of proteins to the aggresome. Instead, K63-linked ubiquitination also plays several roles in DNA repair (453), vesicular trafficking (454), and incorporation of cargo proteins into EVs (455-457).

Although in my studies I did not measure transgene expression upon administration of GM1, it is unlikely that GM1 would have affected expression of the transgene (Ex1-72Q-HTT-eGFP) in our cell models, since the latter was driven by a cytomegalovirus (CMV) promoter, which is known for its high efficiency and strength, and is generally not regulated by intracellular signaling events. Furthermore, our previous studies in HD animal models showed no changes in *Htt* gene expression upon treatment with GM1 (273).

One potential explanation for the effects of GM1 on protein aggregates is that GM1 would slow down aggregate formation, rather than promoting clearance. Although this hypothesis cannot be excluded and will require further specific testing, two lines of evidence suggest that GM1 might affect clearance of muHTT: 1) levels of soluble muHTT were decreased by GM1 treatment in vivo (273), or not significantly changed in cell models (Chapter 6). If GM1 had an effect exclusively

on the aggregation process, one could have expected levels of soluble HTT to proportionally increase; 2) GM1 decreased insoluble p62 levels at late, but not early time points, suggesting activation of degradative pathways once aggresomes are formed.

Although I never observed any toxicity of GM1 in my experiments, the effects of the ganglioside on cell viability were not directly assessed in this thesis, since previous studies in our laboratory extensively demonstrated anti-apoptotic and neuroprotective activity of GM1 in cell (272) and animal models (273).

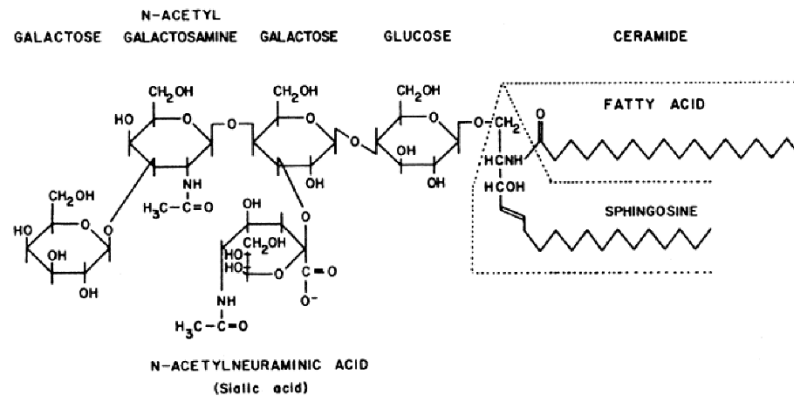
Autophagy is a cellular process involved in the elimination of misfolded and aggregated proteins in various proteotoxic conditions, including expression of muHTT (458,459) and inhibition of the proteasome (218,460). Therefore, I hypothesized that GM1 might activate autophagy to promote the degradation of muHTT in HD models, or polyubiquitinated proteins and aggresomes when UPS is blocked.

In the next chapter, I will describe a series of experiments aimed to investigate whether treatment with exogenous GM1 is able to engage or increase autophagic protein degradation during proteotoxic stress caused by UPS inhibition, as well as after the expression of muHTT.

4.4. Figures

Figure 4.1. Ganglioside GM1: Structure and synthesis

A



B

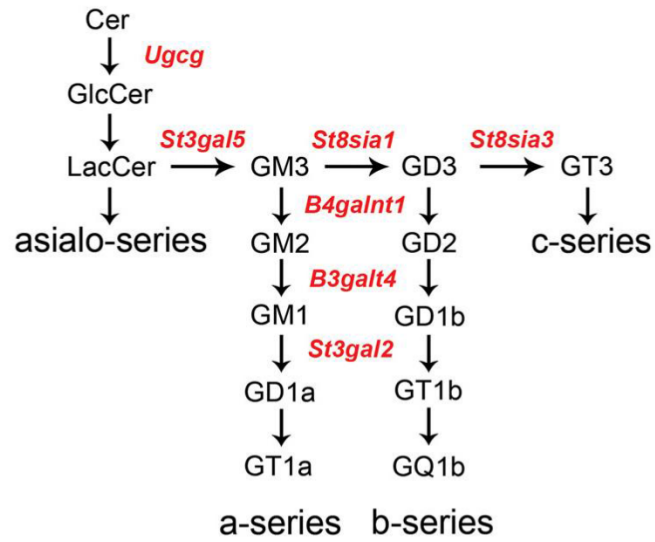


Figure 4.1. Ganglioside GM1: Structure and synthesis

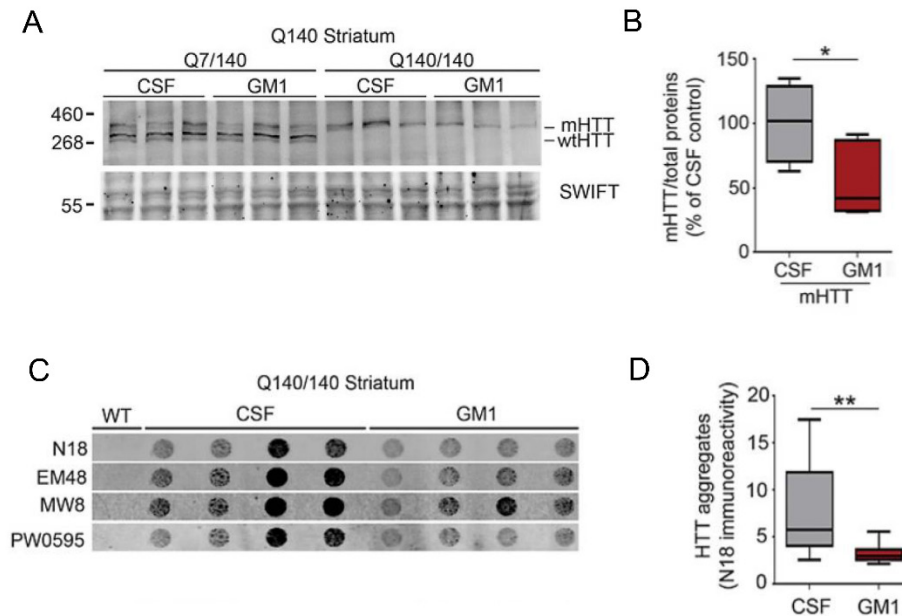
A) Schematic representation of the GM1 molecule.

(Reproduced from (461): Orthaber, D. and O. Glatter (1998). "Time and temperature dependent aggregation behaviour of the ganglioside GM1 in aqueous solution." *Chem Phys Lipids* 92(1): 53-62)

B) Simplified diagram of the synthesis of GM1. Enzymes are indicated in red (Cer = Ceramide. GlcCer = Glucosylceramide. LacCer = Lactosylceramide).

(Reproduced from (272): Maglione, V., et al. (2010). "Impaired ganglioside metabolism in Huntington's disease and neuroprotective role of GM1." *J Neurosci* 30(11): 4072-4080)

Figure 4.2. Ganglioside GM1 administration reduces the amount of muHTT in the brains of Q140/140 mice



A) Representative immunoblot against full-length HTT in striatum lysates from Q7/140 and Q140/140 mice, injected intracerebroventricularly with artificial cerebrospinal fluid (CSF) or GM1 solution, for 42 days. SWIFT® total protein staining was used as loading control.

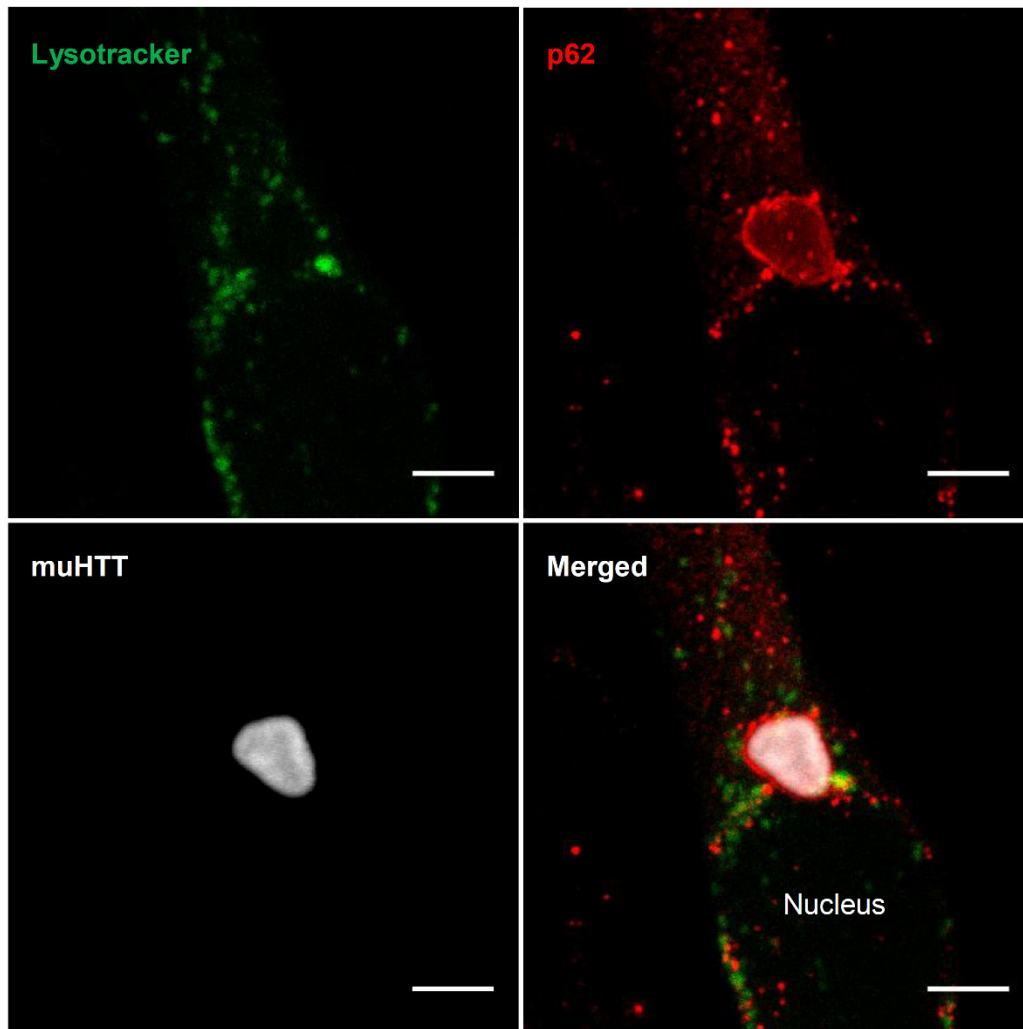
B) Densitometric analysis of muHTT (A, top band). muHTT abundance values from Q7/140 and Q140/140 mice were pooled together. CSF N=9; GM1 N=7. Bars show median values \pm range. Two-tailed Student's t-test. * $p < 0.05$.

C) SDS-insoluble muHTT aggregates detected by filter trap assay in striatum lysates of Q140/140 mice treated with artificial cerebrospinal fluid (CSF) or GM1. N18, EM48, MW8 and PW0595 are antibodies directed against different portions of the HTT protein. Brain lysate from WT mice was used as negative control.

D) Densitometric analysis of the N18-positive signal from (C). CSF N=12; GM1 N=11. Bars show median values \pm range. Mann-Whitney test. ** $p < 0.01$.

(Modified from (273): Alpaugh, M., et al. (2017). "Disease-modifying effects of ganglioside GM1 in Huntington's disease models." EMBO Mol Med 9(11): 1537-1557)

Figure 4.3. Aggregates formed by muHTT are decorated by p62



Representative confocal microscopy image of an STHdh Q7/7 cell transiently transfected with Ex1-72Q-HTT-eGFP (muHTT, white), immunolabeled with p62 (red) and stained with LysoTracker® (green). Observe how p62 decorates the perinuclear aggresome formed by muHTT (Scale bar = 5 μ m).

Figure 4.4. Ganglioside GM1 treatment reduces the amount of muHTT aggregates in cell models

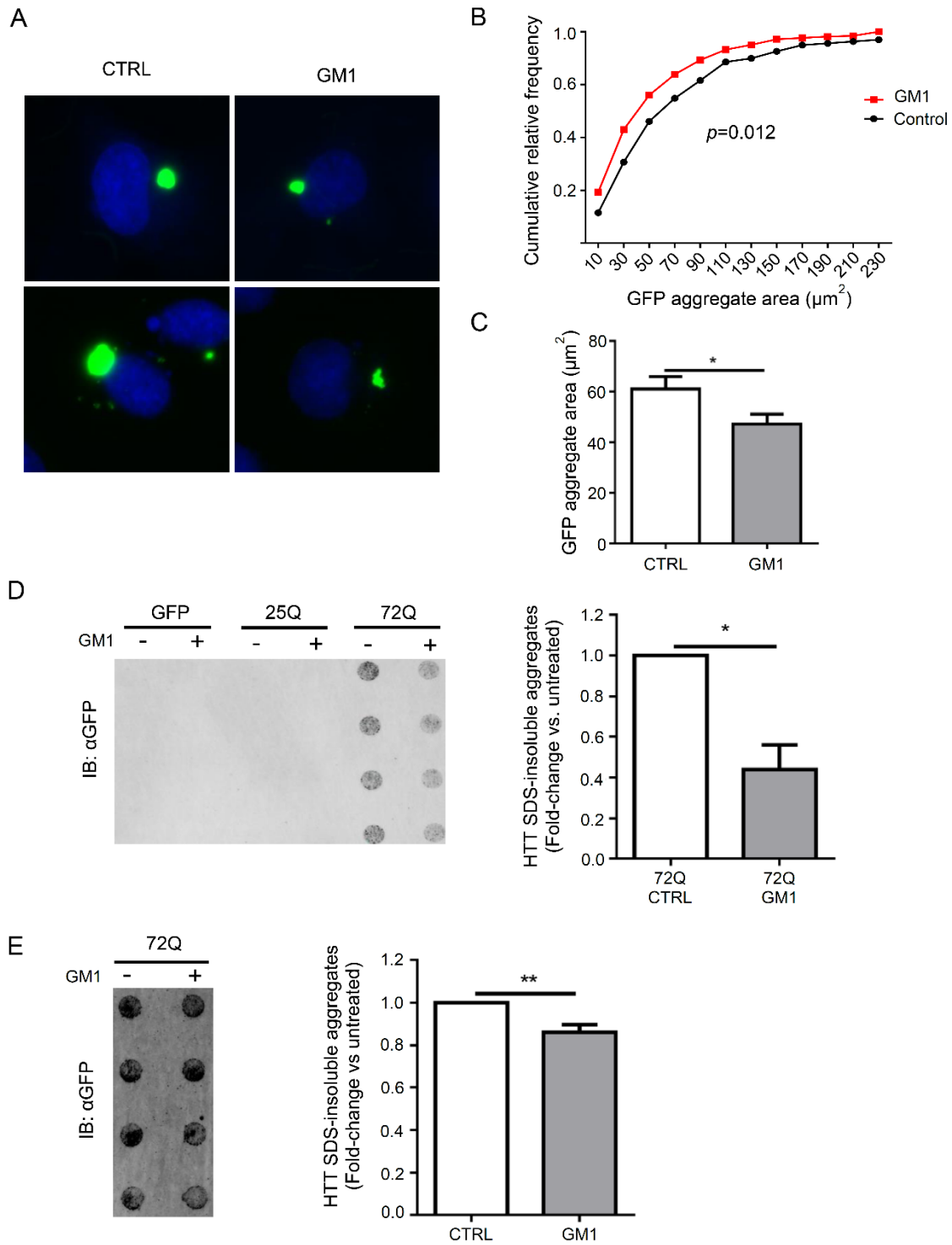


Figure 4.4. Ganglioside GM1 treatment reduces the amount of muHTT aggregates in cell models

- A) Representative pictures of ST14A cells transiently transfected with Ex1-72Q-HTT-eGFP (muHTT, green), treated with vehicle or GM1. Nuclei were stained with DAPI (blue).
- B) Cumulative relative frequency distribution of the area of muHTT aggregates in transfected cells. Treatment with GM1 shifts the curve to the left. Kolmogorov-Smirnov test. $p=0.012$. $N=1$.
- C) Mean muHTT aggregate area in cells treated with vehicle or GM1. A total of 230 and 328 cells were included in the analysis, respectively. Bars show mean values \pm SEM. Two-tailed Student's t-test. $*p<0.05$. This experiment was performed only once.
- D) Representative filter trap and densitometric analysis of lysates of N2a cells transiently transfected with GFP, Ex1-25Q-HTT-eGFP or Ex1-72Q-HTT-eGFP and treated with vehicle or GM1 for 24 h. Bars show mean values \pm SD of 3 independent experiments. Two-tailed Student's t-test. $*p<0.05$.
- E) Representative filter trap and densitometric analysis of lysates of HeLa cells stably expressing Ex1-72Q-HTT-eGFP, treated with vehicle or GM1 for 24 h. Bars show mean values \pm SD of 3 independent experiments. Two-tailed Student's t-test. $**p<0.01$.

Figure 4.5. Ganglioside GM1 treatment reduces accumulation of polyubiquitinated proteins in STHdh Q7/7 cells undergoing proteotoxic stress

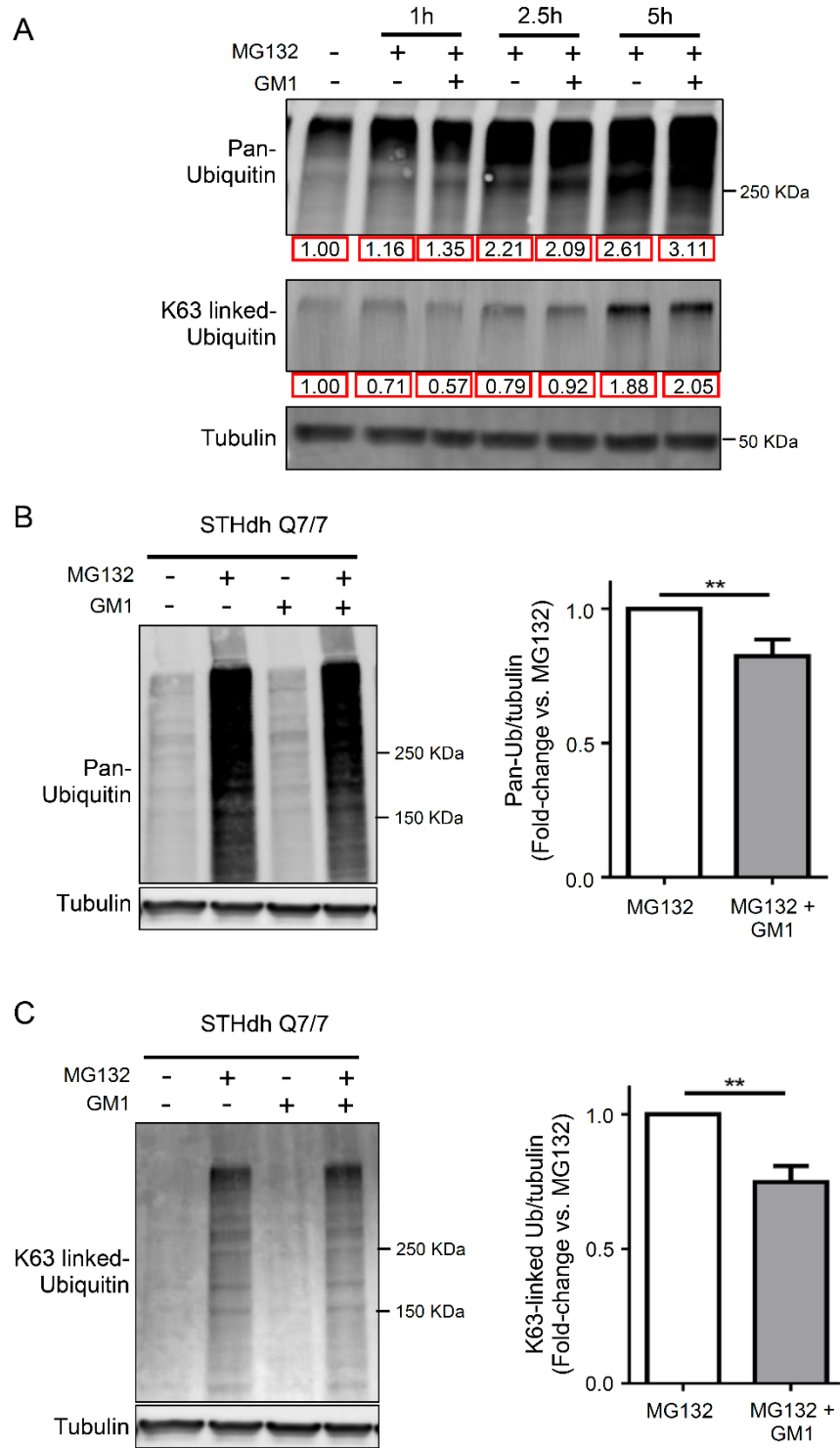


Figure 4.5. Ganglioside GM1 treatment reduces accumulation of polyubiquitinated proteins in STHdh Q7/7 cells undergoing proteotoxic stress

- A) Immunoblot against pan-ubiquitin and K63-linked ubiquitin in STHdh Q7/7 cells treated with MG132 alone (0.5 μ M) or in combination with GM1 (50 μ M) for 1, 2.5 and 5 hours. Numbers below blot represent fold-change vs untreated. Tubulin was used as loading control. This experiment was performed only once.
- B) Representative immunoblot and densitometric analysis of pan-ubiquitin in STHdh Q7/7 cells treated with MG132 (0.5 μ M), GM1 (50 μ M) or combination of both, for 24 h. The graph shows the mean \pm SD of 3 independent experiments comparing values of MG132/GM1 treated cells vs. MG132 alone. Two-tailed Student's t-test. **** p <0.01.**
- C) Representative immunoblot and densitometric analysis of K63-linked ubiquitin in STHdh Q7/7 cells treated with MG132 (0.5 μ M), GM1 (50 μ M) or combination of both, for 24 h. The graph shows the mean \pm SD of 3 independent experiments comparing values of MG132/GM1 treated cells vs. MG132 alone. Two-tailed Student's t-test. **** p <0.01.**

Figure 4.6. GM1 treatment reduces the number and size of aggresomes in STHdh Q7/7 cells undergoing proteotoxic stress

A) Representative images of STHdh Q7/7 cells treated with MG132 (0.5 μ M), GM1 (50 μ M) or combination of both, for 24 h, immunolabeled with anti-p62 antibodies (red). Nuclei were stained with DAPI (blue) (Scale bar = 5 μ m). Boxed areas are magnified on the right of each image to show details of the aggresomes (Scale bar = 2 μ m).

B) Quantification of cells containing aggresomes after treatment with MG132, GM1 or combination, in 3 independent experiments. Bars show mean values \pm SD. One-way ANOVA with Tukey-Kramer post-hoc correction. * p <0.05, ** p <0.01.

C) Area of p62-positive aggregates. Confocal microscopy images were obtained from slides shown in (A). Bars show mean values \pm SEM, One-way ANOVA with Tukey-Kramer post-hoc correction. **** p <0.0001. This analysis was performed in 49-53 cells in only one experiment.

Figure 4.7. Ganglioside GM1 treatment reduces the amount of Triton X100-insoluble p62 in neuronal cells undergoing proteotoxic stress

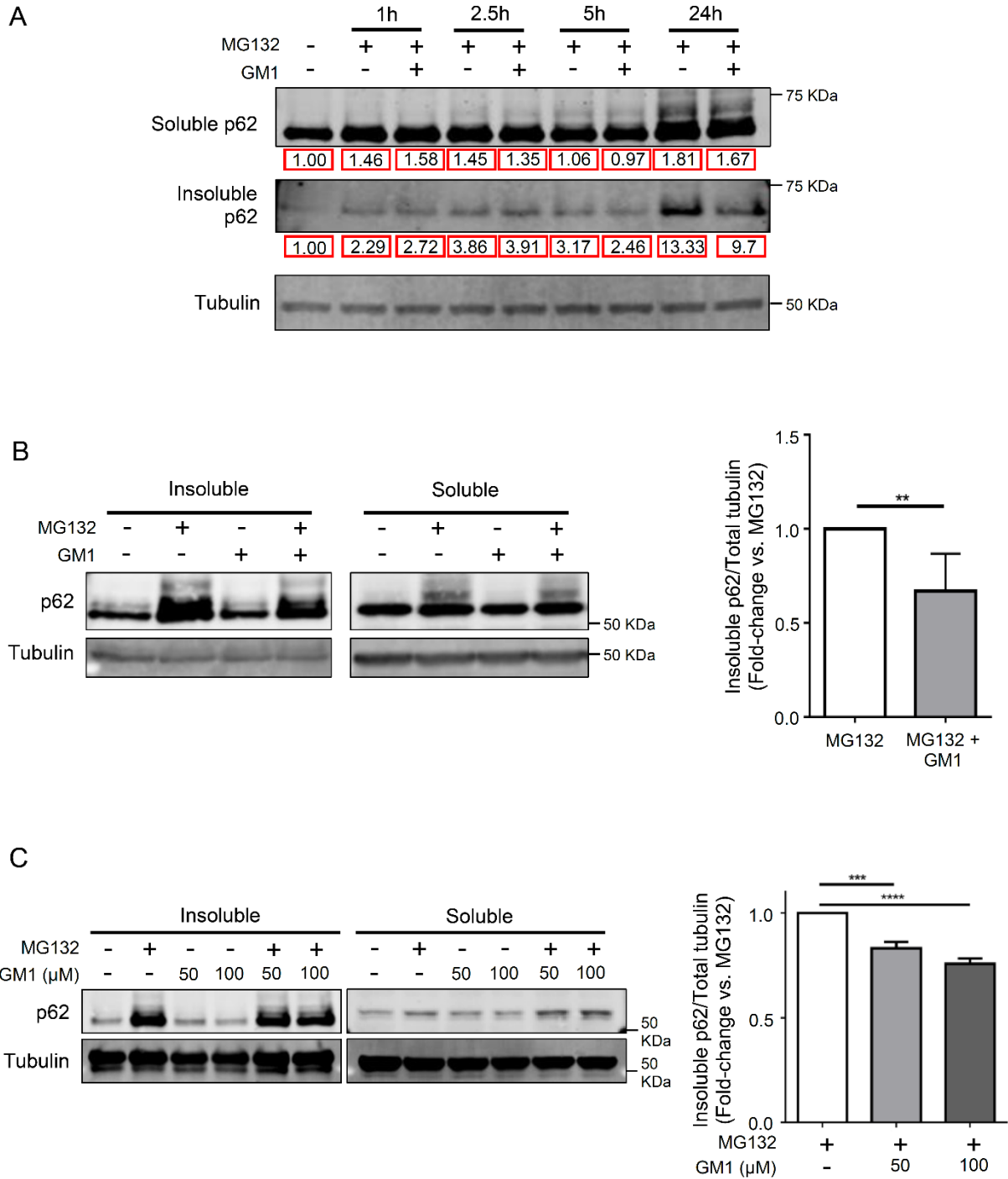


Figure 4.7. Ganglioside GM1 treatment reduces the amount of Triton X100-insoluble p62 in neuronal cells undergoing proteotoxic stress

- A) Immunoblot for soluble and insoluble p62 in STHdh Q7/7 cells treated with MG132 alone (0.5 μ M) or in combination with GM1 (50 μ M) for 1, 2.5, 5 and 24 h. Numbers below blot represent fold-change vs untreated. Tubulin was used as loading control. This experiment was performed only once.
- B) Representative immunoblot for p62 in Triton X100-soluble and insoluble fractions from lysates of STHdh Q7/7 cells treated with MG132 (0.5 μ M), GM1 (50 μ M) or combination of both for 24 h. Densitometric analysis of insoluble p62 shows the mean \pm SD of 5 independent experiments. Two-tailed Student's t-test. $**p < 0.01$.
- C) Representative immunoblot for p62 in Triton X100-soluble and insoluble fractions from lysates of primary cortical rat neurons treated with MG132 (0.5 μ M), GM1 (50 μ M or 100 μ M) or combination of both for 24 h. Densitometric analysis of insoluble p62 shows the mean \pm SD of 3 independent experiments. One-way ANOVA with Tukey-Kramer post-hoc correction. $***p < 0.001$, $****p < 0.0001$.

Chapter 5: Autophagy is not involved in the reduction of protein aggregates after GM1 treatment

This chapter is my original work.

5.1. Introduction

In the previous chapter, I presented evidence that treatment with ganglioside GM1 reduces the accumulation of misfolded/toxic proteins in two different paradigms of proteotoxic stress: i) expression of muHTT N-terminal fragments and ii) pharmacological inhibition of the UPS. Moreover, GM1 did not prevent the accumulation of polyubiquitinated proteins nor the formation of insoluble p62 mediated by MG132 in a shorter time-course (<5h), but rather decreased the accumulation of both after 24 h of treatment. This suggests that GM1 promotes the clearance of already misfolded and aggregated proteins, instead of preventing their aggregation.

It has been shown that protein aggregates, including muHTT aggregates, are preferentially degraded by autophagy (458,459,462,463). Thus, I explored whether GM1 promotes degradative pathways such as autophagy in an attempt to explain how GM1 treatment reduces accumulation of protein aggregates in cell models (Chapter 4) and in animal models of HD (273).

5.1.1. Autophagy: Molecular basis

Macroautophagy (commonly known as autophagy) is one of the various processes of intracellular degradation that cells use to eliminate defective proteins, organelles and even infectious agents. It is mainly characterized by the formation of **autophagosomes**: organelles composed of a double-membrane that engulf targets that have been “tagged” for degradation (245,464). The autophagosomes, at the very end of the autophagic process, fuse with the lysosomes in order to degrade and recycle the building blocks of the materials being digested. Macroautophagy takes place in basal conditions to ensure homeostasis of proteins and cellular components, but it can also be induced and enhanced under certain conditions such as nutrient deprivation or proteotoxic stress

(245). Autophagy plays a role in various cellular processes such as ageing (465), apoptosis (466), protection against oxidation (467), neurodegeneration (468) and many more.

Autophagy has been typically classified in two different, but related categories: **bulk autophagy** and **selective autophagy**. Bulk autophagy is the process by which cells non-selectively degrade cellular components or organelles in an attempt to correct a nutritional deficiency. It is triggered by the lack of nutrients, more specifically amino acids, and the lack of growth factors (245). Selective autophagy instead, mediates the degradation of aggregated/toxic proteins or damaged organelles, among other elements. It depends on adaptor proteins and/or “eat me” signals that allow the autophagosome to recognize specifically (hence, the name) the material to be degraded. Selective autophagy can be further divided into subcategories depending on the cellular components that are degraded (e.g. mitophagy, lipophagy, aggrephagy, etc.). Selective autophagy can also be triggered in conditions of proteotoxic stress caused by inhibition of the proteasome, and although the mechanisms of cross-talk between these two degradative pathways are still under investigation, proteins such as p53 (469), parkin (470) and pathways such as JNK and the unfolded protein response (UPR) (471), have been identified to have roles in the cross-talk between UPS inhibition and autophagy.

Although it is known that different subcategories of selective autophagy depend on different systems of cargo recognition (472,473), it is believed that the mechanism of formation of autophagosomes, herein referred to as the “core machinery of autophagy”, is similar across the different subcategories of selective autophagy.

5.1.2. The core machinery of autophagy

Autophagosome formation comprises the synthesis or the elongation of pre-existing membranes in order to form vesicles capable of containing the material to be degraded. The origin of the cellular membranes which will make part of the autophagosomes is still under investigation (474), but some of the proteins or protein complexes involved in the process have been already elucidated.

In general, the ultimate function of the core machinery is the creation of the autophagosomes. Although the formation of autophagosomes is a continuous process, it can be divided into three (overlapping) steps: i) initiation of autophagy, ii) formation of the nascent autophagosome and iii) elongation of autophagosome membranes.

Initiation of autophagy is mediated by the unc-51-like (ULK) complex, led by ULK1 serine/threonine kinase (also known as ATG1). ULK complex is the starting point and the key link between autophagy and cellular metabolic status (475). ULK complex is regulated by the mammalian target of rapamycin complex 1 (mTORC1) complex via inhibitory phosphorylation. Under nutrient-rich conditions, ULK is sequestered and inhibited by mTORC1, but during starvation, mTORC1 dissociates from the aforementioned complex, releasing ULK and promoting its activation, as well as the activation of proteins downstream of ULK (476). In addition, the mammalian homolog of ATG13 (mATG13) is dephosphorylated upon inactivation and dissociation of mTORC1, favouring its interaction with the ULK proteins. Interaction of mATG13 with ULK complex promotes the initiation of autophagy (476,477).

Once autophagy has initiated, the formation of the nascent autophagosome takes place and involves the class III PI3K complex that includes hVSP34, beclin 1 (the ortholog of ATG6), p150, BARKOR and UVRAG (478-480). Upon starvation, BARKOR localizes to ATG16L- and LC3-

positive structures (phagophore and autophagosome, respectively). Depletion of BARKOR impairs the formation of autophagosomes (481) and overexpression of this protein induces the phosphatidylinositol kinase activity of hVSP34, essential for the recruitment of other ATG proteins. A possible role for BARKOR is to direct the class III PI3K complex to the nascent phagophore and to collaborate in the recruitment of other autophagy-related proteins (478,482). UVRAG (together with BIF-1) is proposed to play a role as a membrane-bending element in the formation of the nascent autophagosome (483).

Finally, the membranes of the nascent autophagosome are expanded and elongated with the help of ubiquitin-like proteins and conjugation systems. To date, two ubiquitin-like proteins and their respective conjugation systems have been identified: ATG12 and LC3. ATG5 is conjugated with ATG12 in a concerted action of ATG7 (E1-like enzyme) and ATG10 (E2-like enzyme). The ATG5-ATG12 conjugate interacts with ATG16L favouring its oligomerization to form the “ATG16L complex” (484). Concomitantly, LC3 is cleaved by ATG4 to generate LC3-I, that will be later modified with a molecule of phosphatidylethanolamine in a reaction dependent on ATG3 and ATG7. The lipidated form of LC3 is known as LC3-II and it attaches to both sides of the membrane of the phagophore, but is later removed from the external side of the phagophore/autophagosome (484).

5.1.2.1. Cargo recognition

Selectivity in autophagy is conferred by adaptor proteins which are able to bring together cargo and autophagosome membranes. These proteins contain protein-protein interacting domains, allowing the adaptor proteins to bind the cargo to be degraded and, on a different domain - the LC3-interacting region, or LIR domain (473) – LC3-II on the membrane of the autophagosome,

acting as a bridge between the cargo and the nascent autophagosome (472,473). Members of the family of adaptor proteins are p62 (485), nuclear domain 10 protein 52 (NDP52) (486), neighbor of BRCA1 gene 1 (NBR1) (487), optineurin (OPTN) (488) and NIP3-like protein X (NIX) (489).

Protein p62, one of the best-studied adaptor proteins, interacts with ubiquitinated substrates via its ubiquitin-binding associated (UBA) domain. In basal conditions, its affinity for ubiquitinated proteins is not very high, in part due to the homodimerization of the protein. The affinity of p62 for ubiquitin increases dramatically after its phosphorylation at two different residues located within the UBA: Ser409, by ULK1, and Ser403 by casein kinase 2 (CK2) and/or ULK1. These phosphorylations promote a conformational change that disrupts the homodimers and increases dramatically the p62 affinity for ubiquitin (490,491). During selective autophagy, p62 oligomerizes to promote the interaction of ubiquitinated cargo with the LC3 protein within the autophagosomes, thus promoting the bending of the autophagosome membrane around the cargo (492). Importantly, p62 does not bind all polyubiquitin chains with equal affinity. In fact, it has more affinity for linear K63-linked polyubiquitin chains than any other type of polyubiquitination (492-494).

The p62-aggresomes are classically thought to be a preliminary stage in the degradation of protein aggregates by selective autophagy (aggrephagy). As previously reviewed in chapter 4, these structures are highly enriched in K63-linked polyubiquitinated proteins, as well as p62 (438,495,496). Moreover, components of the autophagosome, such as LC3 colocalize with p62 at the surface of the aggresome (497), and treatments that inhibit the fusion of the autophagosome with the lysosome, such as bafilomycin A, or inhibit the formation of autophagosomes, such as 3-methyladenine (3-MA), increase the size and/or number of aggresomes in various cell types (497,498).

5.1.2.2. Fusion with the lysosome

After the autophagosome has completed the cargo recognition process and the cargo is engulfed by the membranes of the autophagosome, the next step is the fusion with the lysosome. This process will start the degradation of the cargo by using a set of enzymes, including cathepsins and lipases, among others, that reside within the lysosome. The product of the fusion between these two compartments is named “autolysosome” (499). The regulation of this fusion process is still under investigation, but some of the key players have been already identified.

It is known that the microtubule network is essential for the fusion between autophagosomes and lysosomes. Treatment with agents that inhibit the polymerization of microtubules interfere with the formation of the autolysosome (500). Proteins located at the membrane of the lysosome may also play a role in the fusion since depletion of lysosomal associated proteins 1 and 2 (LAMP1 and LAMP2) impairs the fusion between autophagosomes and lysosomes (501).

Small GTPases, more specifically RAB7, also has a role in this process. RAB7 is normally associated with the membrane of the autophagosomes in basal conditions and after induction of autophagy. Dominant negative RAB7 (DN-RAB7) only partially associates with autophagosomes during autophagy and DN-RAB7-transfected cells contain more and larger autophagosomes during induction of autophagy, suggesting that their fusion with the lysosome, and therefore, their degradation is impaired by DN-RAB7 (391). Moreover, depletion of RAB7 or expression of DN-RAB7 interferes with the maturation of late endosomes/lysosomal vesicles (502).

Since lysosomes are essential for the degradation of cargo during autophagy, their genesis is activated during proteotoxic stress and selective autophagy (503).

5.1.3. Transcriptional regulation of autophagy

The transcription of the multiple genes involved in autophagy is controlled mainly by two proteins/protein complexes: mTORC1 and transcription factor EB (TFEB). In basal conditions, mTORC1 phosphorylates TFEB protein at residue Ser211, promoting its sequestration in the cytosol by a direct interaction with 14-3-3 proteins. Upon starvation or pharmacological inhibition of mTORC1, TFEB is rapidly de-phosphorylated, destabilizing its interaction with 14-3-3 proteins and promoting its translocation to the nucleus, where it works as a transcription factor of multiple genes involved in the autophagy, lysosomal biogenesis, as well as some of the enzymes present in the lysosome (i.e. cathepsins) (504-506).

Lysosomal calcium release is an important player in the regulation of TFEB activity. Microdomains of calcium released from the lysosome through the transient receptor potential channel mucolipin 1 (TRPML1) are able to activate calcineurin, a phosphatase that de-phosphorylates TFEB, promoting its translocation to the nucleus (507).

In recent years, it was discovered that the protein zinc finger with KRAB and SCAN domains 3 (ZKSCAN3) acts as a negative regulator of autophagy and lysosomal biogenesis. Depletion of ZKSCAN3 induced autophagy and promoted lysosome biogenesis, while overexpression of ZKSCAN3 reduced the formation of autophagosomes. ZKSCAN3 represses the transcription of over 60 genes related to autophagy. Interestingly, starvation induces the nuclear export and cytoplasmic accumulation of ZKSCAN3, suggesting that TFEB and ZKSCAN3 localization and activity are regulated in opposite manner (508).

5.1.4. Autophagy in neurodegeneration and in HD

Many of the neurodegenerative diseases are characterized by the intracellular accumulation of a misfolded protein that is prone to aggregation. As described before, aggregated proteins are, at least partially, cleared by autophagy. It has been suggested that impairment of aggregate clearance might contribute to the pathogenesis of diseases such as AD, PD, ALS and HD (509).

Aggresomes, a common finding in models of neurodegenerative diseases, are thought to be degraded, at least in part, by autophagy. Aggresomes are highly enriched in protein p62, an autophagy adaptor protein. LC3 colocalizes with p62 at the edges of the aggresome, suggesting that autophagosomes are present in the proximities of the aggresomes (443). Furthermore, K63-linked polyubiquitinated proteins, which have been shown to be enriched within the aggresome (496,510,511) are classic targets for autophagic degradation (495,496,512).

In the specific context of Alzheimer disease, it is known that pathological forms of A β aggregates are degraded through autophagy. For instance, increasing autophagic activity via pharmacological inhibition of mTORC1 prevents cognitive impairment and reduces brain levels of A β in a transgenic mouse model of AD (513). Results have been reproduced by using activators of AMP-activated protein kinase (AMPK) in cell models of AD. AMPK can indirectly activate autophagy by inhibition of mTORC1, and derivatives of resveratrol activate AMPK, promoting autophagic degradation of A β in cell lines overexpressing either WT or mutated APP (K595N/M596L, SwAPP) (514). Conversely, pharmacological inhibition of autophagy promotes the accumulation of A β , and depletion of genes involved in autophagy such as ATG5, ULK1 and beclin 1 causes similar effects in mouse primary neurons isolated from AD mice (515). Furthermore, beclin 1, a protein essential for the initiation of autophagy, has been shown to be decreased in brains of early AD patients (516).

In the context of Parkinson's disease, the products of genes involved in early-onset familial PD, including PTEN induced putative kinase 1 (*PINK1*) and *Parkin* (517-519) play a crucial role in the autophagic degradation of damaged or depolarized mitochondria via mitophagy (205,207,509,520).

Loss of *Parkin* (521) or *PINK1* (522) cause a reduced lifespan, defects in locomotion, male infertility, muscular degeneration and altered mitochondrial morphology in *Drosophila*. *Parkin*-deficient mice do not show loss of dopaminergic neurons in the substantia nigra, but they have behavioural impairments in motor tests that are sensitive to nigrostriatal dysfunctions (522). Proteomic studies revealed alterations compatible with mitochondrial dysfunctions and oxidative damage in these mice (523). *PINK1*-deficient mice have progressive weight loss and reduced motor activity at old age, as well as reduced amounts of dopamine in the nigrostriatal axonal projections (524). Altogether, these studies corroborate the crucial role of autophagy and mitophagy in PD.

Autophagy is impaired in HD (152) and its stimulation has been shown to be beneficial in various models of HD (459,525,526). Moreover, wtHTT has been shown to participate in selective autophagy since depletion of *Htt* gene in *Drosophila* disrupts autophagy (527). Analysis of the sequence of the *Drosophila* C-terminal domain of HTT revealed that it has high similarity with the yeast protein Atg11. Also, the C-terminal domain of HTT co-immunoprecipitates with various proteins involved in autophagy, including Atg1 (Ortholog of ULK1) and Atg8 (Ortholog of LC3C). Moreover, *in silico* analysis of the C-terminal sequence of HTT determined the presence of multiple LIR motifs and mutation of a specific LIR motif located at a.a. 3037, disrupted the interaction between HTT and Atg8 (527).

Further studies done in mammalian cells confirmed the role of HTT as an autophagy “scaffold”. Rui and collaborators (393,528) showed that the C-terminal HTT region interacts with protein p62, thus facilitating the association between p62 and K63-linked ubiquitinated substrates. Moreover, researchers were able to show that during selective autophagy activation (by using UPS inhibitors), ULK1 is dissociated from the mTORC1 complex and binds to HTT in a different domain than bound by p62. Thus, HTT protein brings together the cargo recognition process mediated by p62, and the core machinery of autophagy by its interaction with both ULK1 and p62 (393,528).

In HD, cargo recognition is impaired. Autophagosomes are found in normal or even increased numbers in HD cells, however, they appear to be empty when observed under the electron microscope. In fact, autophagosomes are degraded at normal rates. As a consequence of this failure in cargo recognition, HD cells had a significantly higher number of damaged mitochondria (impaired mitophagy) as well as an increased number of lipid droplets (impaired lipophagy) (152). Moreover, in isolated autophagosomes from Q111 mice livers, p62 interacts more strongly with muHTT than with wtHTT. It is hypothesized that this aberrantly increased interaction between muHTT and p62 may impair the ability of the autophagosomes to recognize and engulf the cargo (152). There is also evidence suggesting that muHTT affects autophagy initiation through an aberrant interaction with RHES, a striatal-enriched small GTPase (529). RHES promotes autophagosome formation via interaction with beclin 1. In HD, muHTT sequesters RHES impairing autophagy activation. Since RHES is almost exclusively expressed in the striatum, its sequestration by muHTT might explain the selective striatal neuronal death observed in HD (529). Finally, alterations of axonal retrograde transport of autophagosome may also contribute to the overall autophagy impairment observed in HD (530).

In spite of all, pharmacological induction of autophagy was shown to be still beneficial in HD models, reducing the accumulation of muHTT in cell, *Drosophila* and transgenic mouse models of HD (459,525,526). Activation of autophagy is also beneficial in models of AD (513,514), suggesting that increased autophagic degradation is an important common pathway for the elimination of misfolded proteins and a therapeutic target.

5.1.5. Autophagy and GM1

The role of gangliosides in autophagy is still unclear and controversial. For instance, exogenous supply of a mixture of gangliosides, including GM1, enhances autophagy in cultured astrocytes (531). Moreover, pharmacological inhibition of ganglioside synthesis using D-threo-1-phenyl-2-decanoylamino-3-morpholino-1-propanol (PDMP), an inhibitor of glucosylceramide synthase, causes lysosomal membrane permeabilization and cytotoxicity. Treatment of cells with PDMP also promotes the accumulation of α -synuclein in a cell model of synucleinopathy. Not surprisingly, the exogenous supply of gangliosides is able to reverse lysosomal defects, restores autophagy and decreases the accumulation of α -synuclein in this particular model (532,533).

Recently, GM1 was shown to induce autophagy in cell and animal models of AD. WT mice were injected with A β oligomers directly into the hippocampus as a model of AD. A subset of these mice was treated with GM1 intraperitoneally prior to the injection of A β oligomers, and after the procedure for up to 7 days. Mice that were treated with GM1 showed less spatial cognitive defects, as well as an increase in levels of autophagy markers (LC3-II and beclin 1) in the hippocampus (534). GM1 was also cytoprotective in PC12 cells treated with A β oligomers by increasing autophagic flux. Instead, GM1 protection was halted by the addition of autophagy inhibitors such as 3-methyladenine (3MA), an inhibitor of the formation of autophagosomes (534).

Contrary to the studies mentioned above, others have shown inhibitory, rather than stimulatory effects of GM1 on autophagy. GM1 is protective in a rat model of acute stroke, reducing autophagy activation. Moreover, TAT-beclin 1 (a peptide derived from a region of beclin 1, attached to the HIV-1 Tat protein transduction domain), a potent inducer of autophagy, reverts all GM1 protecting effects. These results suggest that GM1 decreases autophagic activity after stroke, protecting the cells located in the penumbra zone against apoptosis (535).

Our studies in HD mice (273) and my data in cell models (Chapter 4) suggest that administration of GM1 promotes degradation/elimination of HTT aggregates, as well as clearance of ubiquitinated proteins that accumulate in conditions of proteotoxic stress. Because of the role played by autophagy in these processes, and because of the potential effects of gangliosides on autophagy (532,533), in this chapter, I tested the hypothesis that the effects of GM1 on muHTT aggregates are mediated by stimulation of autophagy.

5.2. Results

5.2.1. Ganglioside GM1 does not affect autophagy markers in cells transfected with wtHTT or muHTT

To test whether GM1 may facilitate autophagy in cells transfected with fragments of HTT, HeLa cells were transfected with Ex1-25Q-HTT-eGFP, Ex1-72Q-HTT-eGFP or GFP alone, and then treated with vehicle or GM1 for 24 h. This time point was chosen because in previous experiments, insoluble p62 levels were found to be decreased after 24h of incubation with GM1 but not at earlier timepoints (Fig. 4.7). Furthermore, in preliminary experiments, the earliest time I could detect increased levels of LC3-II was 18h after induction of proteotoxic stress (data not shown). In my experiments, neither transfection of any of the HTT transgenes, nor the treatment with GM1

changed the levels of LC3-II, a major marker of autophagy, compared to cells expressing GFP alone (Fig. 5.1A). Additionally, levels of pS403-p62, a marker of the activation of selective autophagy, were barely detected across conditions (Fig. 5.1B). Moreover, levels of total p62 were not changed by the expression of HTT, nor by treatment with GM1 (Fig. 5.1B). As a positive control for induction of autophagy, a lysate from STHdh Q7/7 cells treated with MG132 (0.5 μ M, 24 h) was used (Fig. 5.1B).

To determine whether GM1 could increase autophagy in a neuronal model, a similar experiment was carried out in N2a cells transfected with Ex1-25Q-HTT-eGFP or Ex1-72Q-HTT-eGFP. Transfection itself appeared to increase the levels of LC3-II compared to non-transfected (N.T.) cells (Fig. 5.1C). However, treatment with GM1 did not change LC3-II levels in either of the transfected or non-transfected cells (Fig. 5.1C). Similar to results obtained in HeLa cells, levels of total and pS403-p62 were unchanged by transfection of HTT fragments, or treatment with GM1. (Fig. 5.1D). As a positive control for selective autophagy induction, a lysate from N2a cells treated with MG132 (1 μ M, 20 h) was used (Fig. 5.1D).

5.2.2. GM1 does not affect LC3-II levels in a model of proteotoxic stress induced by MG132

It was previously reported that proteotoxic stress caused by pharmacological inhibition of the UPS results in the induction of selective autophagy in cell models (460,471). Since GM1 was able to decrease the accumulation of p62 and ubiquitinated proteins (Chapter 4), I investigated whether this was due to increased autophagy. As expected, MG132 treatment (0.5 μ M, 24 h) caused an increase in the levels of LC3-II in STHdh Q7/7 cells (Fig. 5.2A). However, combined treatment of MG132 and GM1 (50 μ M, 24 h) showed similar levels of LC3-II in comparison to MG132 alone (Fig. 5.2A).

These results were confirmed in rat cortical primary neurons treated with MG132 (0.5 μ M, 24 h) and with two different doses of GM1 (50 and 100 μ M, 24 h) (Fig. 5.2B). Importantly, GM1 treatment alone did not have any effect on the levels of LC3-II in any of the two models. Altogether, these results suggest that GM1 may not have a significant effect on the number of autophagosomes formed in response to proteotoxic stress in any of the two cell models tested.

5.2.3. GM1 does not affect MG132-induced phosphorylation of p62

During the initiation of autophagy and formation of the autophagosome, ULK1 kinase protein complex plays a crucial role by phosphorylating and activating multiple substrates such as beclin 1, ATG13, ATG9 and p62. (464,490,491,536,537). Of particular interest to me, is the phosphorylation of p62 by ULK1 (pSer403), since it has been shown to cause a conformational change in the p62 ubiquitin-binding domain, allowing the recognition of poly-ubiquitinated proteins. This phosphorylation occurs preferentially during proteotoxic stress, such as UPS inhibition, but not under nutrient starvation conditions (490,491).

To test whether ULK1 activity was modified by GM1 in conditions of proteotoxic stress (UPS inhibition), STHdh Q7/7 cells were treated with MG132 (0.5 μ M, 24 h), GM1 (50 μ M, 24 h) or combination of the two drugs, and phosphorylation of p62 at residue serine 403 (pS403-p62) was measured by immunoblotting. As expected, MG132 caused an increase in pS403-p62 (Fig. 5.3). However, the combination of GM1 and MG132 did not change the levels of pS403-p62 nor the ratio pS403-p62/total p62 with respect to MG132 alone (Fig. 5.3). Levels of total p62 were also unaffected by GM1 (Fig. 5.3). GM1 alone did not change the levels of pS403-p62 nor total p62, when compared to untreated controls.

5.2.4. GM1 treatment does not decrease p62 protein half-life in STHdh Q7/7 cells

Differences in the rate of autophagic target degradation might result from changes in autophagic steps downstream of autophagy initiation or autophagosome formation, such as the fusion of autophagosomes with lysosomes and/or lysosomal degradation of the targets. Therefore, I investigated whether GM1 affects the degradation rate of a known autophagy target, protein p62 (538). To test whether GM1 accelerates degradation of p62 during proteotoxic stress induced by MG132, STHdh Q7/7 cells were treated with cycloheximide (CHX, 5 μ g/mL) in order to stop whole-cell protein synthesis and specifically look at the rate of protein degradation. The decline in the signal for total p62 protein was measured by Western blot (Fig. 5.4A). The slope of p62 signal decay was remarkably similar across treatments (Fig. 5.4B), suggesting that degradation of p62 is not modified by the addition of GM1 in conditions of proteotoxic stress. It is important to mention that I did not observe any decay in tubulin protein in my experiments, likely due to its long half-life that has been calculated to be ~50 h in certain cell models (539,540). This experiment was performed in two additional striatal cell clones, with nearly identical results (data not shown).

5.2.5. GM1 treatment prevents upregulation of lysosomal genes and lysosome biogenesis in proteotoxic stress conditions, but not in basal conditions

Finally, and to further confirm that GM1 does not affect autophagic protein degradation, I measured the amounts of lysosomes and lysosomal gene expression. Lysosomes are essential organelles for the degradation of cellular components via autophagy. Thus, lysosome function is tightly related to autophagy regulation. In fact, transcription factor EB (TFEB) is considered to be the master regulator of the transcription of genes associated with both autophagy and lysosome biogenesis (504-506).

The lysosomal genes *Lamp1* (Lysosome-associated membrane glycoprotein 1), *Atp6v1h* (V-type proton ATPase subunit H) and *Ctsd* (Cathepsin D) are targets of TFEB and were used as a surrogate measure of lysosomal biogenesis. As expected, concomitantly with the activation of selective autophagy, MG132 treatment caused upregulation of the expression of these three lysosomal genes (Fig. 5.5). Interestingly, the addition of GM1 prevented the MG132-dependent upregulation of lysosomal genes, although it did not affect their expression in basal conditions (Fig. 5.5). Similar experiments were conducted in two additional striatal cell clones, with nearly identical results (data not shown).

In order to explore the effects of GM1 in lysosome content during proteotoxic stress, cells were labelled with Lysotracker® Deep Red and analyzed by confocal microscopy to visualize and count lysosomes (Fig. 5.6A). In line with the expression of lysosomal genes, the number of Lysotracker®-positive particles per cell as well as total Lysotracker® intensity and percentage of cell area stained with Lysotracker® increased much more in cells treated with MG132 alone, compared to cells that received the combination of MG132 and GM1 (Figs. 5.6B-D). In basal conditions (no MG132), GM1 alone did not reduce any Lysotracker® staining parameters, compared to untreated control, suggesting that GM1 prevented lysosome biogenesis induced by MG132, rather than affecting lysosomes in basal conditions.

In conclusion, I could not find any evidence of autophagy being enhanced by GM1, at least in the autophagy markers and/or steps evaluated in my models of proteotoxicity, suggesting that GM1 may not stimulate autophagy in these cell models.

5.3. Discussion

Autophagy is a major pathway for the degradation of misfolded and aggregated proteins (462,463,541). Thus, my initial hypothesis was that GM1 administration increases autophagic degradation of muHTT, as well as components of the aggresomes. This hypothesis was supported by studies suggesting that, at least in some models, exogenous supply of gangliosides stimulate autophagy (532-534).

Following pharmacological inhibition of the UPS using MG132, I observed increased amounts of LC3-II in both, STHdh Q7/7 and rat cortical primary neurons, suggesting that MG132 treatment promotes the formation of autophagosomes. These results are in line with previous studies that reported that inhibition of the UPS activity causes accumulation of polyubiquitinated proteins, formation of aggresomes, as well as the activation of the autophagic machinery in various cell models (451,471,498). Contrary to my expectations, co-treatment with GM1 did not increase the levels of LC3-II when compared to MG132 alone, neither in STHdh Q7/7 cells nor in rat cortical primary neurons. Only steady-state levels of LC3-II were measured in my experiments, which could be affected by both rate of autophagosome formation, as well as rate of autophagy flux (i.e. the rate at which the autophagosomes fuse with lysosomes and autophagic cargo is degraded). To more specifically determine whether GM1 could have an effect on each or both of these autophagy steps, LC3-II levels should be measured in the presence of inhibitors of autophagosome-lysosome fusion or inhibitors of lysosomal activity (bafilomycin A1 or ammonium chloride). However, cell treatment with such inhibitors for the duration of the experiments (24 h) caused a dramatic increase in LC3-II levels (data not shown), even in the absence of MG132, thus profoundly confounding data interpretation. Nevertheless, the conclusion that GM1 does not enhance autophagic degradation of proteins is also supported by the fact that phosphorylation of p62 at residue Ser403,

a specific marker of selective autophagy initiation (490,491) was not affected by GM1. Moreover, treatment with GM1 did not reduce the half-life of total p62 protein after UPS inhibition, suggesting that autophagic degradation of proteins is also not affected by GM1. Furthermore, although my results do not indicate that transfection of HTT fragments triggers selective autophagy in either of the two cell lines analyzed, the fact that GM1 treatment did not cause any change in autophagy markers when compared to untreated cells, is also in support of the idea that GM1 does not increase autophagic degradation of misfolded proteins.

Since lysosomes are crucial for the autophagic degradation of protein aggregates and are the final stage of autophagy, I assessed whether GM1 might be increasing lysosomal biogenesis during proteotoxic stress. As expected, MG132 treatment increased the transcription of lysosomal genes such as *Lamp1*, *Atp6v1h* and *Ctsd*, as well as overall lysosome number. But surprisingly, co-treatment with GM1 completely abrogated these transcriptional effects, and also prevented lysosome biogenesis as determined by Lysotracker® staining. This phenomenon is, of course, not compatible with an increase in autophagic degradation of protein aggregates.

Thus, altogether, my data do not support the hypothesis that GM1 enhances autophagic degradation of aggregated proteins.

My studies are in line with data generated by a former student of our laboratory, Mrs. Sabine Schmelz, who found that levels of autophagy markers, including LC3-II and p62, were not affected in the brain of HD mice treated with GM1. Furthermore, while I focussed on studying selective autophagy because of its relevance in the context of protein aggregate degradation, Mrs. Schmelz showed that GM1 does not affect bulk autophagy in HD cells exposed to starvation.

The effect of GM1 on lysosomal biogenesis during proteotoxic stress caused by UPS inhibition was surprising. The genes analyzed in my experiments are targets of TFEB, considered to be the master regulator of the transcription of genes associated with autophagy and lysosomal biogenesis. The function of TFEB is mainly regulated in two ways: 1. TFEB is inhibited by the mTORC1 complex via phosphorylation. Upon starvation, phosphorylation of TFEB decreases, which promotes its translocation to the nucleus (504-506). 2. Lysosomal release of calcium activates calcineurin, which in turns de-phosphorylates TFEB, favouring its nuclear localization (507). Although there is no reference in literature regarding a direct action of GM1 on TFEB regulation, some hypotheses could be formulated, that could potentially be tested in the future.

The protein complex mTORC1 not only regulates the phosphorylation of TFEB, but is also, in concert with ULK1, a regulator of initiation of autophagy through the phosphorylation of multiple targets, including p62. Thus, based on my results that show that GM1 did not affect the initiation of autophagy, it is unlikely that GM1 may have an effect on mTORC1-dependent regulation of TFEB.

Instead, GM1 has been linked to the control of intracellular concentrations of calcium (542). For instance, GM1 stimulates neurite outgrowth during development by promoting the influx of calcium through TRPC5 channels (408,409). However, it has also been shown that GM1 may reduce cytosolic concentration of calcium by potentiating the sodium-calcium exchanger at the level of the nuclear envelope (543).

Lysosomal calcium release, responsible for activation of TFEB, is controlled by two families of lysosomal channels: i) two-pore channels 1 and 2 (TPC1-2) and ii) transient receptor potential mucolipin 1 channels 1-3 (TRPML1-3) (544). To the best of my knowledge, there are no previous reports of an association between exogenous supply of GM1 and activity of any of these channels.

However, it has been shown that TRPML1 activity, and consequently lysosomal calcium release, is decreased by lysosomal lipid accumulation (545). Moreover, cell models of Niemann-Pick type C (NPC) disease, characterized by the accumulation of cholesterol and ganglioside GM1 in the lysosomes (546) showed decreased activity of TRPML1 channel and an impaired lysosomal calcium release (547). One possibility is that exogenous GM1 would accumulate in the lysosome, decreasing TRPML1-dependant calcium release, thus decreasing TFEB activation (507).

However, in the context of NPC disease, pathological accumulation of cholesterol and gangliosides in the lysosomes is associated with cell dysfunction and death. In our studies, administration of GM1 was never linked to cell toxicity, but rather to neuroprotection (272,273). Furthermore, in my studies, administration of GM1 did not affect lysosomal markers in basal conditions. Importantly, even though lysosomal biogenesis was decreased by GM1 during proteotoxic stress induced by MG132, autophagic protein degradation did not appear to be disrupted, since I did not observe any accumulation of autophagosomes, nor changes in the half-life and degradation of p62. So, the question remains as to how GM1 increases clearance of protein aggregates in our models of proteotoxic stress.

Unconventional secretion pathways, independent of the Golgi and COPII-coated vesicles (548), represent an alternative for cells to deal with misfolded proteins and other cargos. It has been shown that autophagosomes, instead of fusing with the lysosome for the degradation of the cargo, can fuse with the plasma membrane, thus releasing the cargo towards the extracellular space (548). This mechanism is important for the secretion of cytokines such as IL-1 β and IL-18 (549), but also for proteins that have been linked to neurodegenerative diseases, such as α -synuclein (550) and A β peptide (551). Stimulation of unconventional secretion pathways by GM1 would be compatible with my findings in the model of proteotoxic stress induced by UPS inhibition, and it would

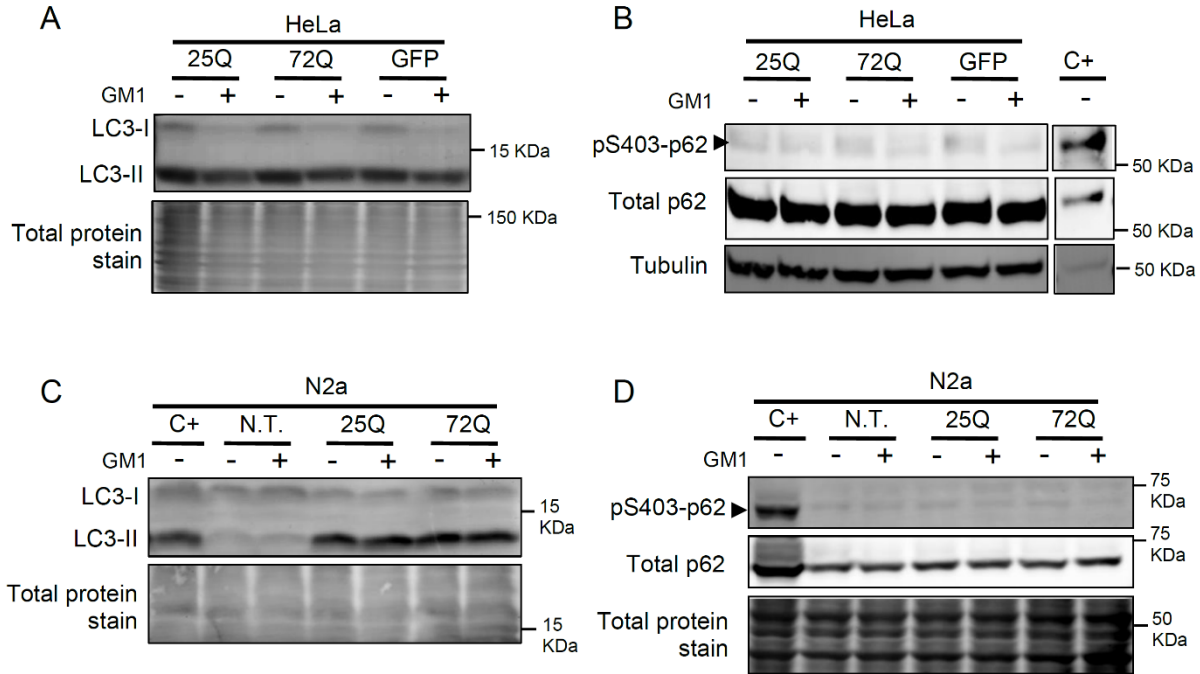
explain the apparent paradox that, in spite of unchanged levels of autophagosomes (as measured by LC3-II levels) and a rate of p62 degradation, the number of lysosomes was greatly reduced in cells treated with GM1 during proteotoxic stress. Future studies will address this hypothesis.

A second form of unconventional secretion is the production of extracellular vesicles (EVs). These vesicles are derived from the fusion of multivesicular bodies/late endosomes (MVB/LE) with the plasma membrane, or by direct budding of the plasma membrane (552). It has been shown that EVs may play a role in the elimination of toxic/misfolded proteins from diseased neurons. For instance, toxic TDP-43, a protein linked to neurodegenerative diseases such as ALS and FTD, can be secreted via EVs. Pharmacological and genetic inhibition of EV secretion causes an exacerbation of the disease in transgenic mice expressing a mutant form of human TDP-43 (553). A few studies have also reported the presence of muHTT fragments in EVs derived from various cell models (554,555). Interestingly, lysosome and/or autophagy inhibition can increase secretion of EVs in various cell models of PD and AD (556). Therefore it is possible that GM1, by affecting lysosomal biogenesis in the context of proteotoxic stress, may promote the secretion of EVs, as an alternative proteostatic mechanism (557).

In the next chapter, I will describe the experiments aimed to investigate whether GM1 promotes the secretion of toxic/misfolded proteins via EVs.

5.4. Figures

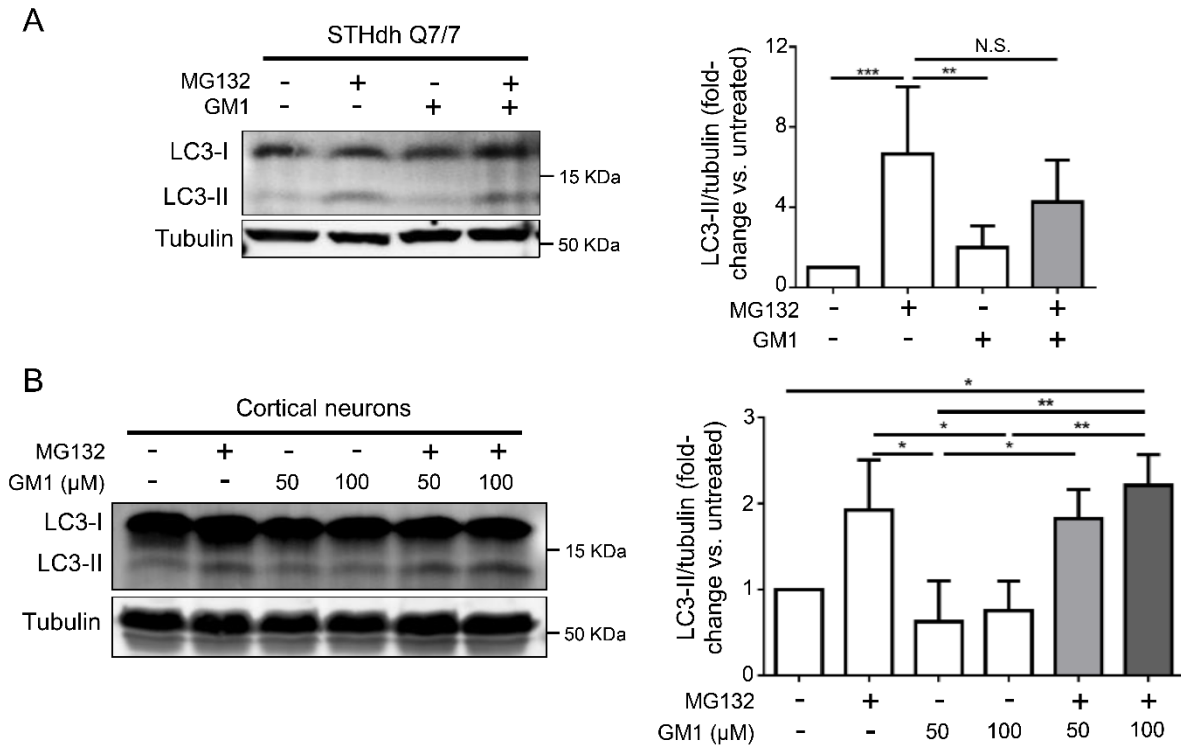
Figure 5.1. GM1 does not affect autophagy markers in cells transfected with WT or muHTT



A and B) HeLa cells were transiently transfected with Ex1-25Q-HTT-eGFP (25Q), Ex1-72Q-HTT-eGFP (72Q) or GFP alone, and then treated with vehicle or GM1 for 24 h. A) Immunoblot for LC3. Total protein stain was used as loading control. B) Immunoblot for pS403-p62 and total p62. Tubulin was used as a loading control. Positive control (C+) for pS403-p62 signal is a lysate from STHdh Q7/7 cells treated with MG132 (0.5 μ M, 24 h) to induce selective autophagy. This experiment was performed only once.

C and D) N2a cells were transiently transfected with Ex1-25Q-HTT-eGFP (25Q), Ex1-72Q-HTT-eGFP (72Q) or left non-transfected (N.T.) before being treated with vehicle or GM1 for 24 h. C) Immunoblot for LC3. Total protein stain was used as loading control D) Immunoblot for pS403-p62 and total p62. Total protein stain was used as a loading control. Positive control (C+) for pS403-p62 signal is a lysate from N2a cells treated with MG132 (1 μ M, 20 h) to induce selective autophagy. This experiment was performed only once.

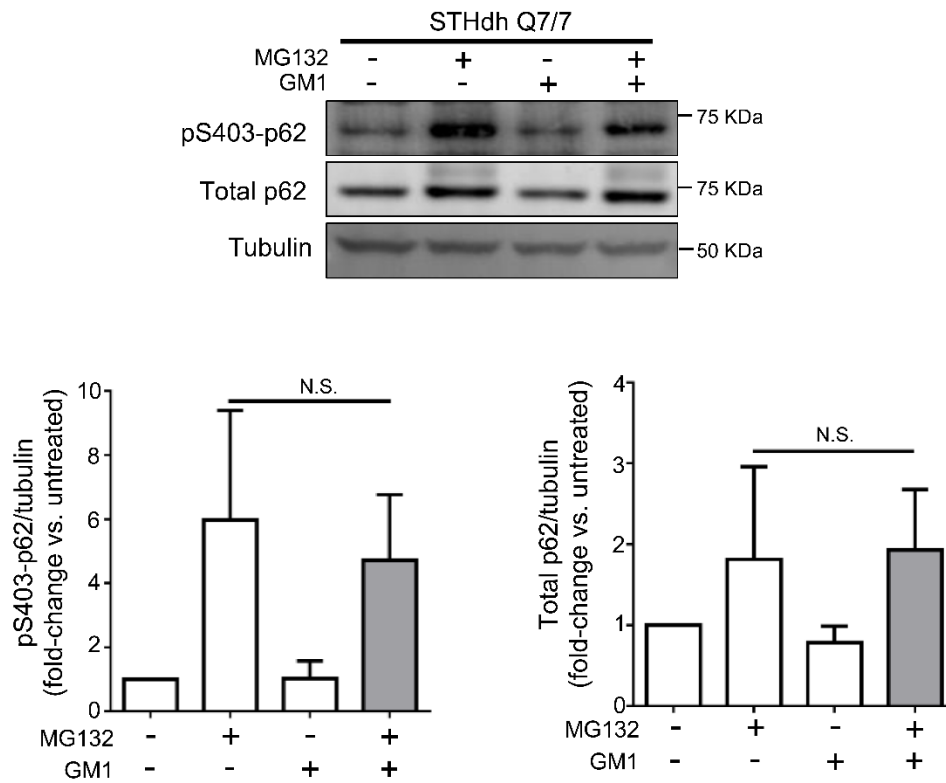
Figure 5.2. MG132 increases LC3-II levels in neuronal cells. Addition of GM1 does not modify the response to MG132



A) Representative immunoblot and densitometric analysis of LC3-II levels in STHdh Q7/7 cells treated with MG132 (0.5 μM), GM1 (50 μM) or combination of both, for 24 h. Tubulin was used as loading control. Bars show the mean ± SD of 5-7 independent experiments. One-way ANOVA with Tukey-Kramer post-hoc correction. ** $p < 0.01$, *** $p < 0.001$.

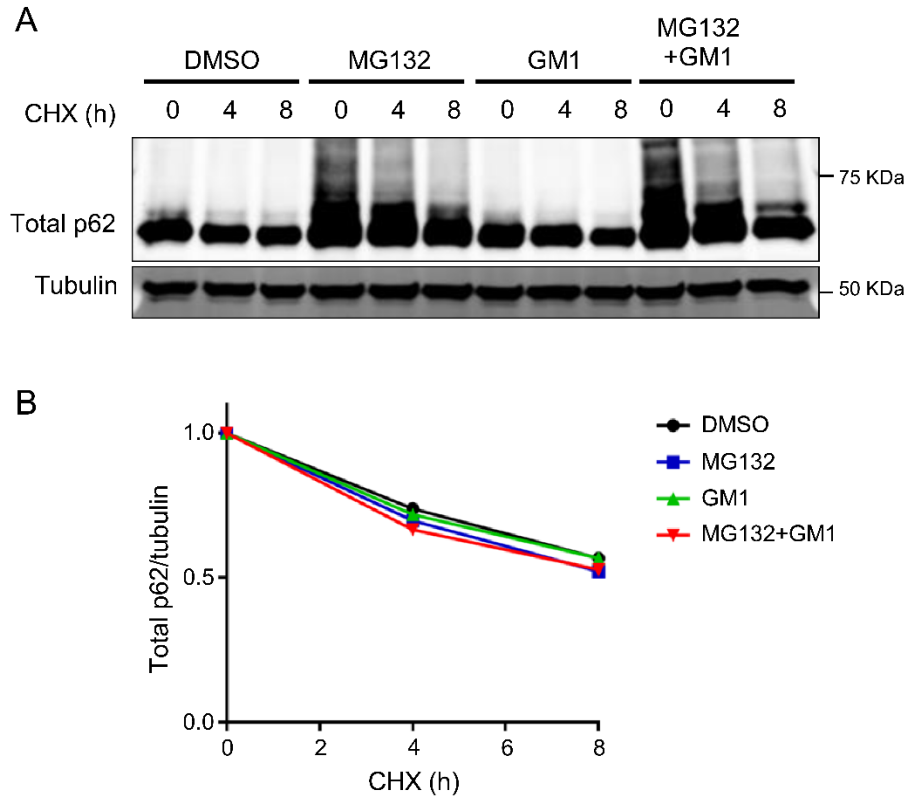
B) Representative immunoblot and densitometric analysis of LC3-II levels in rat primary cortical neurons treated with MG132 (0.5 μM), GM1 (50 μM or 100 μM) or combination of both, for 24 h. Bars show the mean ± SD of 3 independent experiments. One-way ANOVA with Tukey-Kramer post-hoc correction. * $p < 0.05$, ** $p < 0.01$.

Figure 5.3. GM1 does not affect MG132-induced phosphorylation of p62 at Ser403



Representative immunoblot and densitometric analysis of pSer403-p62 and total p62 in STHdh Q7/7 cells treated with MG132 (0.5 μ M), GM1 (50 μ M) or combination of both, for 24 h. Tubulin was used as loading control. The ratio pS403-p62/total p62 was not affected by GM1 (data not shown). Bars show the mean values \pm SD of 3 independent experiments.

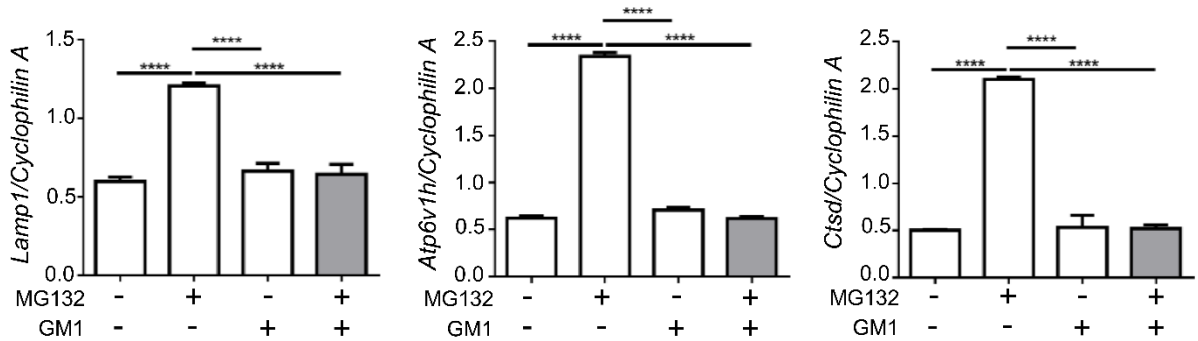
Figure 5.4. GM1 treatment does not affect p62 protein half-life in STHdh Q7/7 cells



A) Immunoblot showing the time-course of p62 degradation in STHdh Q7/7 cells. Cells were pre-incubated with MG132 (0.5 μ M), GM1 (50 μ M) or combination of both for 12 h, and then treated with cycloheximide (5 μ g/mL) for 0, 4 or 8 h.

B) The decline in p62 signal from the beginning of cycloheximide treatment (t=0 h) was calculated for each treatment as a fraction relative to t=0 h. Tubulin was used as loading control. This experiment was performed only once, in three different cell clones with nearly identical results.

Figure 5.5. GM1 treatment prevents upregulation of lysosomal genes in proteotoxic stress conditions



Expression of lysosomal-associated membrane protein 1 (*Lamp1*), ATPase H⁺ transporting V1 subunit H (*Atp6v1h*) and cathepsin D (*CtSD*) genes was measured in STHdh Q7/7 cells treated with MG132 (0.5 μM), GM1 (50 μM) or combination of both for 24 h. Cyclophilin A was used as housekeeping gene. Bars show the mean ± SD of technical replicates. One-way ANOVA with Tukey-Kramer post-hoc correction. **** $p < 0.0001$. This experiment was performed only once, in three different cell clones with nearly identical results.

Figure 5.6. Ganglioside GM1 decreases the number of LysoTracker®-positive puncta during proteotoxic stress

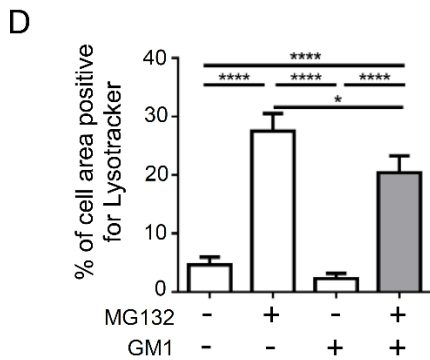
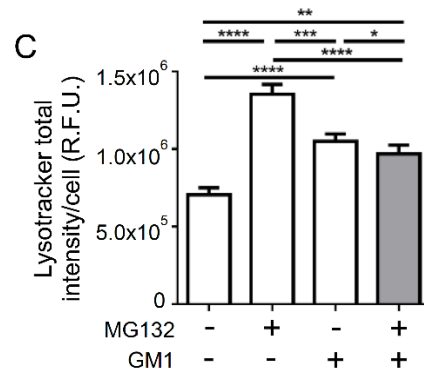
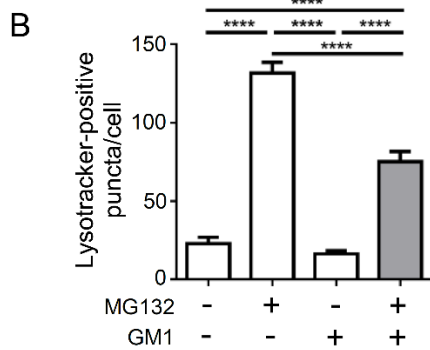
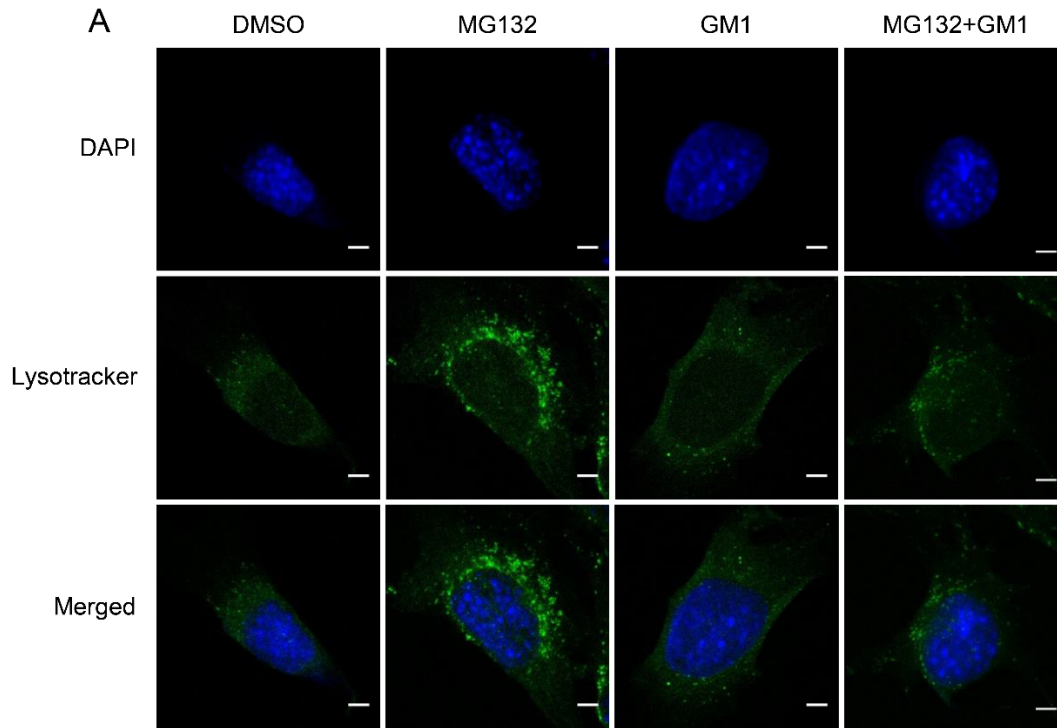


Figure 5.6. Ganglioside GM1 decreases the number of Lysotracker®-positive puncta during proteotoxic stress

- A) Representative confocal microscopy images of STHdh Q7/7 cells treated with MG132 (0.5 μ M), GM1 (50 μ M) or combination of both for 24 h, and then labelled with Lysotracker® Deep Red (green). Nuclei were stained with DAPI (blue). Scale bar = 5 μ m.
- B) Quantification of Lysotracker®-positive puncta per cell. Mean number of particles in each treatment were plotted.
- C) Total intensity of Lysotracker® staining per cell.
- D) Percentage of cellular area positive for Lysotracker® staining. One-way ANOVA with Tukey-Kramer post-hoc correction. * $p < 0.05$, ** $p < 0.01$, *** $p < 0.001$, **** $p < 0.0001$. Analyses were performed in 49-53 cells from one single experiment.

Chapter 6: GM1 increases the secretion of misfolded proteins via extracellular vesicles

Data of this chapter have been generated in collaboration with Ms. Vaibhavi Kadam (NMHI, University of Alberta) and Dr. Nasser Tahbaz (Department of Cell Biology, University of Alberta).

6.1. Introduction

In chapter 4, I presented evidence that exogenous supply of GM1 was able to decrease the accumulation of aggregates after expression of muHTT, as well as polyubiquitinated proteins and insoluble p62 after pharmacological inhibition of the UPS. In chapter 5, I showed that enhancement of autophagy is not the mechanism by which GM1 promotes clearance of protein aggregates. In this chapter, I investigate an alternative proteostatic mechanism that involves the elimination of toxic/misfolded proteins via extracellular vesicles.

Secretion of misfolded proteins has been shown to be an important pathway for the maintenance of proteostasis in models of neurodegenerative diseases (553,558). Moreover, the presence of muHTT fragments and/or ubiquitinated proteins in extracellular vesicles has been described in the literature (554,555,559,560). In fact, it has been shown that pharmacological inhibition of autophagy initiation promotes the production and release of EVs enriched in proteins such as p62 and LC3, suggesting that EV secretion may be triggered as a compensatory proteostatic mechanism to reduce the burden of aggregated proteins in vulnerable cells (559).

Therefore, I hypothesized that GM1 treatment promotes the secretion of misfolded proteins via extracellular vesicles, contributing, at least partially, to the decreased accumulation of protein aggregates observed in cell models of proteotoxic stress (shown in chapter 4) and animal models of HD after treatment with GM1 (273).

6.1.1. Extracellular vesicles: general concepts

In a general sense, the term “extracellular vesicle” (EV) refers to any kind of secreted particle that is composed by a lipid bilayer membrane, found in the extracellular space. EVs contain a portion of the cytosol of the secreting cell and their contents may include proteins, carbohydrates, genetic

material (especially RNAs of different nature) and/or lipids (552). EVs are found in almost any bodily fluid, such as urine, blood, cerebrospinal fluid, among others. EVs can also be found in the conditioned medium of cultured cells (285).

6.1.2. A brief review of the history of EVs

Presence of vesicles found outside of the cell limits or in bodily fluids (presumably EVs) has been reported for many years. Earlier reports include the presence of such vesicles in cartilage and blood (561,562). Isolated cells were also found to produce such vesicles, especially tumour cells and platelets (563,564), but very little was known about the mechanisms of production or release of these vesicles. Years later, two separate groups, while studying the maturation of sheep reticulocytes into erythrocytes, observed that internalized labelled transferrin receptor (TfR) was incorporated into small (~50nm) bodies present within the multivesicular bodies/late endosomes (MVB/LE). The same authors also discovered that the fusion of MVB/LE with the plasma membrane released such small bodies, still containing TfR, into the extracellular space (565,566). A few years later, Johnstone and collaborators (567) isolated these vesicles after ultracentrifugation of the conditioned media of reticulocytes in culture. The vesicles were enriched in sphingolipids and TfR, among other reticulocyte-related markers. Authors concluded that the vesicles were formed and secreted by reticulocytes as part of the process of maturation, and coined the term “exosomes” to describe such vesicles.

6.1.3. Classification of EVs

Classification and nomenclature of the different EVs has been, and still is a huge challenge in the absence of universally accepted rules. In the past, classification of EVs was based on size (microvesicles or nanovesicles), origin (prostasomes, when isolated from prostatic tissue, or

oncosomes, when the origin is a tumour) or function (calcifying matrix vesicles in the cartilage, argosomes during *Drosophila* morphogenesis) (568). This lack of consensus is still present today, however, most researchers now agree to classify EVs in three groups only:

- **Apoptotic bodies** are the biggest EVs, with sizes that range between 1-5 μm . These vesicles are generated during apoptosis as membrane protrusions, that eventually, as the apoptotic process continues, detach from the cell (569).
- **Microvesicles**, previously known as ectosomes, shedding vesicle or microparticles, are generally between 150-1,000 nm in diameter, although their size is still under debate. These EVs are generated by direct budding of the plasma membrane (552) (Fig. 6.1A).
- **Exosomes** are typically smaller, between 30-100 nm. Exosomes are of endosomal origin, produced by inwardly budding of the membranes into MVB, and are released upon fusion of MVB/LE with the plasma membrane (552) (Figs. 6.1A, B).

It is likely that every cell in the body secretes a combination of all kinds of EVs. To date, in spite of extensive research, clear discrimination between exosomes and microvesicles remains a challenge (552,568,570,571).

6.1.4. Mechanisms of formation and secretion of EVs

The mechanisms of EVs formation and release are still under investigation. Exosomes and microvesicles originate in distinct regions of the cells, therefore it is possible that the two kinds of EVs may have slight differences in the mechanism of formation. However, it has been shown that similar protein complexes may be involved in the generation of both, exosomes and microvesicles (552,568).

- **Exosomes**

The production of exosomes starts with the formation of the MVBs. This process is accomplished by selection of the cargo at the membrane of an endosome, followed by the invagination of the membrane, and finally, the detachment of vesicles towards the lumen of the forming MVB. More than 30 proteins, assembled into four multiprotein complexes named endosomal sorting complex responsible for transport (ESCRT)-0, -I, -II and -III, together with various accessory proteins (i.e. ALIX, VTA1, VPS4) are in charge of the formation of the intraluminal vesicles (ILVs) inside the MVBs, which eventually will become exosomes after the fusion of the MVBs with the plasma membrane (572).

The complex ESCRT-0 recognizes and sequesters ubiquitinated targets in the proximity of the endosomal membrane (572). Proteins that are either monoubiquitinated or K63-linked polyubiquitinated are preferentially bound by the ESCRT-0 complex (455). The complexes ESCRT-I and -II are responsible for the inward deformation of the membrane while “holding” the cargo and the ESCRT-0 proteins, and finally, the proteins of the ESCRT-III complex are responsible for the vesicle scission into the lumen of the MVBs (572).

Nevertheless, there is growing evidence for the existence of ESCRT-independent mechanisms for the formation of ILVs. Stuffers and collaborators (573) simultaneously inactivated four proteins of the four ESCRT complexes (HRS, TSG101, VPS22 and VPS24) in Hep2 cells. Researchers reported morphological alterations of the components of the endocytic pathway, however, the formation of MVBs still occurred (573). Another study did show that depletion of ESCRT-0 in HeLa cells did not block the formation of ILVs. Instead, protein CD63 was shown to be essential for the formation of ILVs when ESCRT-0 proteins are inactivated (574). Furthermore, two enzymes related to lipid metabolism are associated with the formation of ILVs, independent of the

ESCRT machinery: neutral sphingomyelinase (nSMase), which hydrolyzes sphingomyelin into ceramide and phosphocholine (575), and phospholipase D2, which catabolizes the hydrolysis of phosphatidylcholine into phosphatidic acid and choline (576). It is believed that the changes in the local lipid composition of the membrane may facilitate its budding, promoting the formation of vesicles (552,568). Pharmacological inhibition of nSMase with GW4869 reduces the secretion of exosomes from various cell lines (577-580). However, in human melanoma cells, treatment with GW4869 does not impair the formation of ILVs nor the secretion of EVs (581). These apparently contradictory results suggest that the mechanisms for the formation of ILVs, and therefore exosomes, might be cell-dependent, and may change depending on the specific conditions of the experiments (552,568).

Once the MVBs are formed, they can either be transported to the plasma membrane for the release of exosomes, or they can fuse with the lysosome for the degradation of their components. It is known that two distinct populations of MVBs, morphologically similar, co-exist within the cell. One population of MVBs is preferentially targeted to the lysosomes for their degradation, while the second pool of MVBs is directed towards the plasma membrane for exosomes secretion (582). Using biotinylated-perfringolysin O, a toxin that strongly binds cholesterol, Möbius and collaborators (582) showed that vesicles inside the MVBs located in the proximity of the plasma membrane, as well as exosomes at the cell surface, were strongly labeled by perfringolysin O, while the MVBs in proximity of the Golgi and other structures were negative for perfringolysin O, suggesting that the cholesterol content may contribute to the fate of the MVBs. Conversely, lyso-biphosphatidic acid has been detected in MVBs directed to the lysosomes (583), but is not present in the exosomes (584,585), suggesting that lipid composition of MVBs may determine their fate.

- **Microvesicles**

Less is known about the mechanism of microvesicle formation in comparison with exosomes (586). However, a few studies have shown some similarities between the two systems. For instance, microvesicles from T lymphocytes are secreted from distinct domains at the level of the plasma membrane that are enriched with proteins such as ALIX, TSG101 and VPS4, all components of the previously described ESCRT machinery (587), and activation of the ATP receptor P2X7 in cultured astrocytes promotes the activation of acid sphingomyelinase (aSMase), which in turn increases the secretion of microvesicles (588). Addition of recombinant aSMase to the culture media also increases the production of microvesicles, while pharmacological inhibition of aSMase by using imipramine, decreases the shedding of microvesicles (588).

- **Mechanisms of release of microvesicles and exosomes**

Other proteins that are not necessarily related to the genesis of microvesicle or exosomes may have a role in their secretion, for example proteins related to vesicular trafficking or interactors with the microtubule network. This is the case for some members of the RAB subfamily of proteins, which are associated with secretion of EVs. For instance, RAB11 has a role in EV secretion (589). Overexpression of WT RAB11 in K562 cells, a myeloid cell line, increases the secretion of EVs, while transfection with a dominant negative version of RAB11 inhibits EV release (589). Additionally, RAB11 promotes the tethering and docking of MVBs to the inner face of the plasma membrane, in a calcium-dependent manner. In cells treated with calcium chelator BAPTA-AM, MVBs approach the membrane but do not proceed with the fusion, suggesting that RAB11 participates in the docking of MVBs, but calcium promotes their fusion with the plasma membrane (590).

An RNAi screening in HeLa cells revealed that depletion of 5 RAB GTPases (RAB2b, RAB5a, RAB 9a, RAB 27a and RAB27b) decreased exosome secretion. Depletion of RAB27a and RAB27b impairs the docking of MVBs at the plasma membrane and silencing SLP4 and SLAC2B, two downstream effectors of RAB27, inhibited exosome secretion (591). A second screening done in Oli-neu cells, an oligodendrocyte cell line, showed that overexpression of known inactivators of RAB35, such as proteins of the TBC1D10 family (-A, -B and -C), as well as depletion of RAB35 or expression of a dominant negative RAB35, resulted in decreased EV secretion. Conversely, expression of constitutively active RAB35 promoted the secretion of EVs (592).

The soluble N-ethylmaleimide-sensitive factor attachment protein receptor (SNARE) family of proteins has been classically associated with the docking and fusion of multiple species of vesicles (i.e. synaptic vesicles, lysosomes), (593). Thus, VAMP7, a member of the SNARE family, participates in the fusion of the MVBs with the plasma membrane (594). Similarly, Gross and collaborators (595) have shown that WNT proteins are secreted on exosomes, in a process that is dependent on YKT6 protein, another member of the SNARE family.

6.1.5. Physiological and pathophysiological role of EVs

Production of EVs is considered to be a mechanism of communication between cells. EVs have been detected in almost every bodily fluid, including breast milk, saliva, synovial fluid, bile, amniotic fluid, semen and even feces (596). By using EVs, cells can interchange genetic material, proteins, second messengers, lipids and more. Thus, EVs could potentially be, and have been associated with numerous functions in multiple systems, including neural development, antigen presentation and/or neovascularization in the context of cancer. This subject is reviewed in detail elsewhere (596).

EVs were proposed to have important roles in neurodegenerative diseases caused by misfolded proteins (558). EVs can export, and even transfer from cell to cell, misfolded proteins involved in various diseases. However, whether EVs have a detrimental role in neurodegenerative diseases, or rather serve a proteostatic function in conditions of proteotoxic stress, is still controversial.

Some studies suggest that EVs contribute to the pathophysiology or the progression of neurodegenerative diseases. For instance, Fevrier and collaborators (597) showed that the prion protein PrP^{Sc} is packaged into exosomes and secreted from infected cells. Moreover, exosomes containing PrP^{Sc} are “infectious” to other cells, suggesting that EVs may constitute a vehicle for the spreading of the toxic protein to neighbouring neurons. Similarly, multiple groups have reported the presence of APP or A β in EVs, suggesting that EVs may also play a role in the development or progression of AD (598-600). CSF from patients suffering from AD or mild cognitive impairment has increased amounts of microglia-derived EVs. EVs purified from the CSF of AD patients can promote the generation of toxic A β species that are neurotoxic to cultured hippocampal neurons (601).

On the other hand, there are some reports suggesting that EVs may play a protective role in neurodegeneration. For instance, neuroblastoma-derived exosomes injected into the brains of AD mice are able to sequester A β , that is then promptly internalized and degraded by microglia. Chronic intracerebral injections of exosomes result in decreased A β levels, plaque formation and reduction in the synaptic dysfunction in AD mice (602). Furthermore, EV-mediated secretion of mutant TDP-43, a protein with neurotoxic roles in ALS and frontotemporal dementia (FTD), represents an important proteostatic mechanisms and is protective in cell and animal models of ALS/FTD (553).

In the context of HD, the role of EVs has just started to be explored, and whether EVs are beneficial or detrimental in the pathophysiology of HD, remains to be elucidated.

There is evidence of muHTT fragments being incorporated into EVs. Diaz-Hidalgo and collaborators (554) showed that muHTT is recruited into exosomes in a complex with transglutaminase 2 (TG2), ALIX, TSG101 and BAG3, a co-chaperone that is involved in the clearance of muHTT. However, whether exosomes containing muHTT can transfer the toxic protein to normal cells, is still unclear (555).

The first indication that muHTT could be transported and transmitted via EVs came from histopathological studies done in HD patients who received neural allografts from control individuals. Examination of the pathology specimens revealed muHTT aggregation inside of the grafts, which did not express the muHTT gene, suggesting that the mutant protein can spread into non-HD tissue (603). To further explore the mechanism of spread of muHTT protein, researchers implanted fibroblasts derived from HD patients, as well as HD induced pluripotent stem cells (iPSCs) into the ventricle of neonatal wild-type mice. Surprisingly, mice injected with HD fibroblasts or HD iPSCs developed motor and non-motor dysfunctions compatible with HD at later ages (>30 weeks). Furthermore, upon co-culture with HD fibroblast, wild-type iPSC-derived neurons were found to contain muHTT, and to undergo morphological changes compatible with neurodegeneration. Finally, injection of exosomes derived from HD fibroblasts into the ventricle of newborn wild-type pups was sufficient to induce an HD-compatible motor phenotype 8 weeks post-injection (560).

Prion-like spreading of muHTT protein/aggregates was also suggested in *Drosophila* models of the disease, where neuronal muHTT aggregates phagocytosed by microglia can act as intracellular seeds that promote the aggregation of wtHTT (604). The findings of this study suggest that

professional phagocytes, such as microglia, can participate in the spreading of the disease, although it was not determined whether spreading was mediated by extracellular vesicles. In another study in mouse models of AD (602), however, phagocytosis of A β -loaded EVs was shown to be beneficial. Thus, it will be important to determine whether EVs could play a beneficial role also in HD, potentially depending on EVs membrane/cargo composition, as well as their ability to shuttle the toxic cargo from susceptible cells (neurons) to professional phagocytes (microglia) for clearance.

In this chapter, I will show data suggesting that GM1 promotes the secretion of EVs in neuronal and non-neuronal cells, and with them, the elimination of misfolded proteins, possibly explaining, at least in part, the decrease in protein aggregates induced by GM1, and perhaps, the disease-modifying properties of GM1 in HD mice treated with this ganglioside (273).

6.2. Results

6.2.1. GM1 promotes the secretion of extracellular vesicles from neuronal cells

Ganglioside GM1 is present in EVs purified from neuronal cells (605), however, it is not known whether it has a specific function in these membrane-limited vesicles, or if it is rather “passively” incorporated into EVs. Additionally, to the best of my knowledge, the effects of exogenously supplied GM1 on the production and secretion of EVs, has never been studied.

In order to test whether GM1 could promote secretion of EVs, I incubated N2a cells with the lipophilic dye Vibrant® DiI to label cellular membranes (Fig. 6.2A) and then analyzed the release of DiI into the EV fraction purified by ultracentrifugation of the conditioned media. GM1 treatment (16-18h) caused an increase in the secretion of DiI-stained membranes (Fig. 6.2B), as well as an

increase in the secretion of ALIX, an established marker of EVs (571) (Fig. 6.2C). Together, these data suggest that GM1 treatment promotes secretion of EVs towards the extracellular medium.

Administration of GM1 (50 μ M) for 72 h had similar effects in cultures (DIV15) of embryonic primary neurons, as determined by immunoblotting for the EVs markers TSG101 and flotillin-1 (571). Treatment with GM1 did not significantly change the abundance of TSG101 or flotillin-1 in the lysates of primary neurons (Figs. 6.3A-C). However, GM1 treatment significantly increased the amount of both TSG101 and flotillin-1 in the EVs fraction (Figs. 6.3A-C). Purified EVs fractions were probed for the presence of calnexin, to exclude contamination with apoptotic bodies or cell debris.

6.2.2. Exogenously administered GM1 is internalized by cells and incorporated into extracellular vesicles

To check whether exogenously supplied GM1 was incorporated into cells and subsequently released in the EVs, N2a and HeLa cells were stained with Vibrant® DiI to label membranes, and then treated with GM1 (50 μ M) or vehicle overnight, prior to collection and purification of EVs from the media. Lysates from N2a cells treated with GM1 contained approximately 3 times more GM1 than untreated cells (Figs. 6.4A, B). In HeLa cells, the amount of GM1 increased by approximately 112-fold (Figs. 6.4A, B). The higher fold-increase in HeLa compared to N2a cells is due to the fact that the basal content of GM1 in HeLa cells is very small compared to N2a cells.

In EV fractions, the amount of GM1 increased \sim 10 times (N2a cells) and \sim 185 times (HeLa cells), compared to untreated cells (Fig. 6.4C). Interestingly, the ratio of the amount of GM1 over Vibrant® DiI fluorescence in EV fraction was higher in cells treated with GM1 (Fig. 6.4D). This suggests that not only cell treatment with GM1 increases the amount of EVs secreted (as

determined by DiI measurements in the conditioned medium), but it also results in EV particle-enrichment with the ganglioside. Since GM1 may be present in small amounts in the serum, unconditioned media was used for background subtraction in my experiments (Fig. 6.4A).

6.2.3. GM1 promotes the secretion of HTT via extracellular vesicles

Next, I investigated whether administration of GM1 could promote secretion of misfolded proteins, specifically muHTT into EVs. To answer this question, I transiently transfected HeLa cells with GFP alone, Ex1-25Q-HTT-eGFP or Ex1-72Q-HTT-eGFP and then treated the cells with GM1 (50 μ M) or vehicle for 24 h.

I confirmed the expression of GFP and both chimeric wtHTT and muHTT fragments in the lysates of transfected HeLa cells (Fig. 6.5A). GM1 treatment did not significantly change the amount of wtHTT nor muHTT fragments in the lysates (Fig. 6.5A). However, in the EVs, the amounts of GFP, wtHTT and muHTT were increased by GM1 treatment (Fig. 6.5B). Interestingly, despite the fact that the secretion of all transfected proteins was increased by GM1, the amount of flotillin-1 in EV fraction was increased by GM1 treatment, only in cells expressing the toxic muHTT fragment, but not in cells expressing wtHTT or GFP alone (Fig. 6.5B).

To assess whether GM1 treatment promotes the secretion of microvesicles or exosomes in a differential manner, after removing apoptotic bodies, microvesicle-enriched and exosome-enriched fractions were prepared by differential centrifugation of the conditioned media (285,606). GM1 caused an increase in the secretion of wtHTT and muHTT in both fractions (Fig. 6.6), suggesting that GM1 promotes the secretion of HTT in microvesicles, as well as in exosomes.

To confirm the effects of GM1 in a neuronal cell line, experiments were replicated in N2a cells transfected with Ex1-25Q-HTT-eGFP or Ex1-72Q-HTT-eGFP and then treated with GM1. In this

model, GM1 did not significantly change the amount of wtHTT within the cells. Instead, levels of muHTT showed a trend towards a decrease, which however did not reach statistical significance due to the very high variability among experiments (Fig. 6.7A).

As in HeLa cells, GM1 promoted the secretion of both wtHTT and muHTT (Fig. 6.7B). This increase in the secretion of HTT fragments was accompanied by an increase in the amount of the EV marker ALIX (Fig. 6.7B). Once again, absence of calnexin confirmed the purity of the EV preparation.

To avoid potential confounding effects due to the cellular stress induced by transient transfection and protein overexpression, I generated, with the help of another student, miss Vaibhavi Kadam, N2a and HeLa stable cell lines expressing Ex1-72Q-HTT-eGFP.

Treatment with GM1 (50 μ M, 16-18h) did not affect muHTT or flotillin-1 levels in lysates of muHTT-expressing N2a cells (Fig. 6.8A). However, the amount of muHTT and flotillin-1 detected in the EVs purified from GM1-treated cells was higher, when compared to untreated cells (Fig. 6.8B). Concomitantly, GM1 treatment increased the amount of total proteins secreted (Fig. 6.8B) as well as the amount of DiI-stained EV membranes (Fig. 6.8C).

These findings were replicated in HeLa cells stably expressing Ex1-72Q-HTT-eGFP (Figs. 6.9A, B), where GM1 treatment increased DiI-stained membrane secretion (Fig. 6.9C) and the abundance of muHTT and EV markers, such as flotillin-1 and TSG101, in the EV fraction (Fig. 6.9B).

Altogether, these data support the hypothesis that GM1 promotes EV secretion and through this, secretion of muHTT.

6.2.4. GM1 promotes the secretion of p62 via extracellular vesicles in cells undergoing proteotoxic stress

In chapter 4, I showed that GM1 promotes the clearance of p62 and ubiquitinated proteins in a second model of proteotoxic stress, induced by MG132. Thus, I sought to determine whether GM1 may also contribute to the secretion of other aggregated proteins, such as p62, that accumulate upon cell treatment with MG132.

STHdh Q7/7 cells were treated with MG132 (0.5 μ M, 24 h), GM1 (50 μ M and 100 μ M), or combination of both. MG132 treatment alone increased the amount of p62 detected in the EV fraction, compared to untreated cells. GM1 supplied in combination with MG132, but not when given alone, further increased the amount of p62 detected in the EV fraction (Fig. 6.10). Instead, the amount of ALIX detected in the EV fraction increased with both treatments, even when GM1 was provided in the absence of proteotoxic stress (Fig. 6.10). This experiment was performed only once, and further experimentation is required before reaching any conclusion.

6.3. Discussion

In previous chapters, I showed that GM1 is able to reduce the accumulation of misfolded aggregated proteins in two cell models of proteotoxic stress, and that such reduction is not achieved by a GM1-dependent enhancement of autophagic degradation.

Here I showed evidence that GM1 increases secretion of p62 and muHTT into the medium of cells of neuronal (N2a) and non-neuronal (HeLa) origin. Furthermore, GM1 increased overall secretion of EVs, as determined by an increase in both, EV protein markers and DiI fluorescence (a surrogate measure of membrane content) in isolated EV fractions. Of note, the ratio GM1 over DiI in the EV fraction was increased when cells were treated with GM1, suggesting that, not only GM1 increases

the secretion of EVs but also that these EVs are enriched with GM1, more than in basal conditions. It was previously shown that GM1 localizes to EVs membranes (605), thus it is not surprising that an increased availability of GM1 ganglioside, would result in more incorporation of GM1 into EVs.

My initial experiments were performed in transiently transfected cells, where transfection (electroporation) itself may cause cellular stress with unpredictable consequences and potentially confounding effects. For this reason, it was important to confirm my findings in stable cell lines expressing muHTT. Moreover, the effects of GM1 on EV secretion extended also to a model of proteotoxic stress induced by inhibition of the UPS, where treatment with GM1 increased the secretion of p62 in EVs. Although the presence of muHTT fragments and/or autophagy adaptors proteins such as p62 in EVs has been reported in the past (554,555,559,560), there are no previous reports of EV and protein secretion being enhanced by treatment with exogenous GM1.

My data are in line and further supported by preliminary gene ontology analysis of proteomics data performed by other members of our laboratory, showing an enrichment of proteins in the “extracellular vesicle” category among the proteins whose abundance was changed in HD mouse brains treated with GM1 (unpublished data).

The potential consequences of increasing EV formation bearing a toxic protein such as muHTT are currently unknown, and will be investigated in further studies. On one side, it is possible that an increased secretion of EVs may contribute to the spreading of the disease, as it was reported by previous studies in HD (560) and in other neurodegenerative diseases (607,608). Nevertheless, some other studies suggest that EVs may have a protective role against neurodegeneration. For instance, inhibition of EV secretion increased intraneuronal aggregation of mutant TDP-43, a protein associated with diseases such as FTD and ALS, and worsened the behavioral phenotype of

mice expressing mutant TDP-43 (553). In another study, sequestration of A β peptides by EVs and delivery to microglia for subsequent degradation was associated with decreased A β pathology and improved synaptic dysfunctions in AD mice (602). Based on the fact that administration of GM1 has profound therapeutic effects in HD, being able to improve motor and non-motor behaviour, as well as neuropathology across HD mouse models (115,273), it is unlikely that enhancement of EV secretion by GM1 treatment would promote the spreading of the disease. I speculate that a higher content of GM1 in EVs (as observed in my studies upon cell treatment with the ganglioside) might facilitate their phagocytosis and clearance by microglia, thus promoting EVs protective roles, rather than detrimental ones. This hypothesis will be tested in future studies.

One question that remains unanswered is whether GM1-dependent increase in muHTT secretion is sufficient and necessary for the reduction in intracellular protein aggregates. Future experiments could address this question, using pharmacological inhibitors of nSMase, or by genetic depletion of proteins of the ESCRT complexes or members of the RAB subfamily of GTPases, such as RAB27a and RAB27b (591) which are required for the secretion of EVs.

In my experiments, the increase in muHTT secretion after treatment with GM1 did not correspond to a statistically significant decrease in intracellular levels of soluble muHTT, contrary to what we observed in the brains of Q140 mice treated with GM1 (273). This may be due to various reasons. First, in our *in vivo* experiments, mice were treated for a total of 42 days, while in my studies, HTT-expressing cells were treated for a maximum of 24 h. A prolonged treatment may be necessary to detect a decrease in the total (SDS-soluble and -insoluble) levels of HTT protein. Second, expression of muHTT in the cell models used in my study was driven by a CMV promoter, which is known for its high efficiency and strength. Thus, it is possible that any reduction in soluble

muHTT caused by GM1 would be quickly masked by a steady supply of newly synthesized protein.

Both problems could be addressed in the future by using inducible cell models. Our laboratory has recently obtained PC12 cells stably expressing the first 171 a.a. of HTT with an expanded polyQ, under the control of an inducible promoter (kindly donated by Dr. Sue-Ann Mok, University of Alberta). In this cell model, the effects of GM1 could be tested after removal of the hormone that allows for the expression of the transgene, thus preventing confounding effects related to continuous transgene expression.

A potential caveat of my work is that I only used surrogate measures, such as DiI secretion or abundance of EV markers, to infer the amount of EVs produced by cells in culture. Although these techniques are widely accepted, a more in-depth analysis of the effects of GM1 on EV secretion will require the use of specific techniques such as nanoparticle tracking analysis (NTA), direct light scattering (DLS), and nano-FACS, to obtain information about exact size and number of particles secreted by the cells.

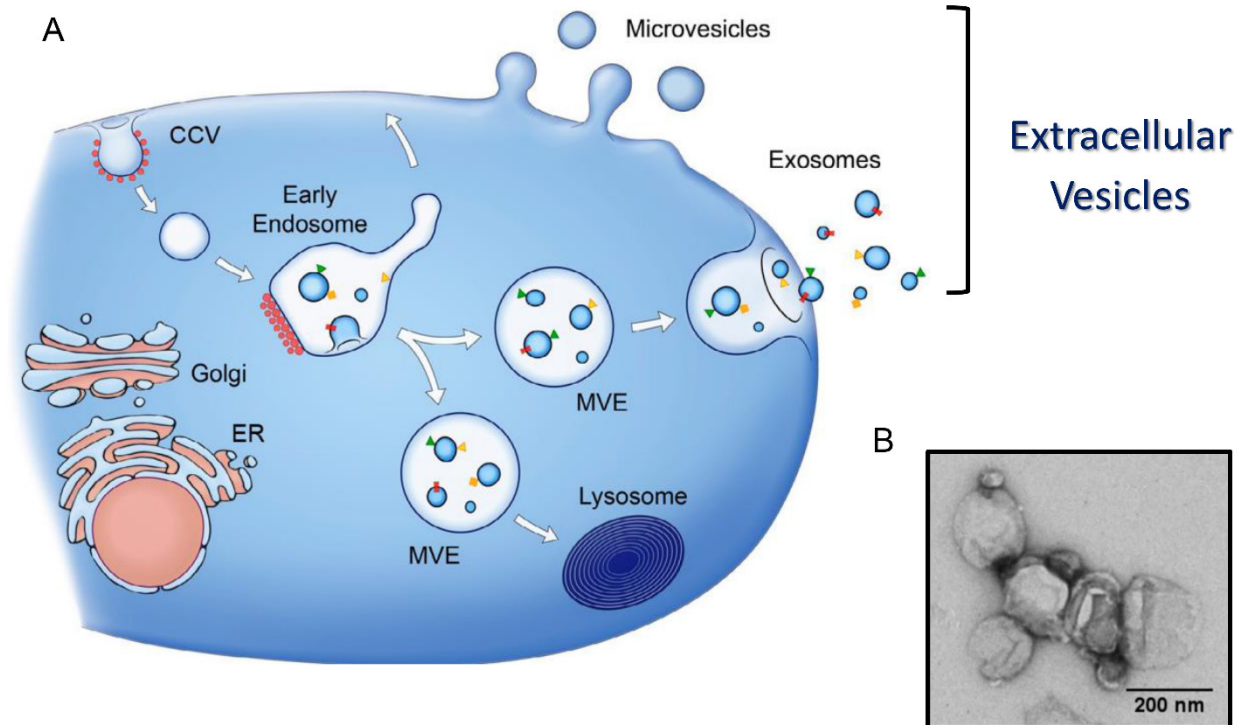
Different EV markers were used in my experiments depending on the cell model, in line with growing evidence that EV markers may differ among cells, tissues and samples of different origins (609-613).

Most of my experiments were done using GM1 at 50 μ M concentration. This dose was chosen based on previous studies performed in our laboratory, where it was determined that 50 μ M was the optimal GM1 dose to observe anti-apoptotic effects and no toxicity in cell models of HD, while higher concentrations affected cell adhesion (but not viability) if used in the absence of serum in the culture medium (272).

In my work, I have not explored the possibility that, in addition to promote muHTT secretion through EVs, GM1 treatment might also slow down the kinetics of muHTT aggregation. For instance, in a cell model of PD, GM1 does prevent α -synuclein aggregation by directly interacting with it (423). The two mechanisms (i.e. increased secretion and decreased aggregation) are not mutually exclusive, and could potentially act in concert to mediate the disease-modifying properties exerted by GM1 in HD models. Alternatively, GM1 could promote disaggregase activity (614,615), with the release of muHTT from aggregates followed by its elimination through the UPS or via EVs. GM1 is a very versatile molecule, playing roles at multiple levels (542). Most likely, the beneficial effects observed in animals and cells treated with exogenous GM1 may result from a combination of different protective mechanisms triggered upon administration of this ganglioside.

6.4. Figures

Figure 6.1. Extracellular vesicles: microvesicles and exosomes



A) Schematic representation of extracellular vesicles (exosomes and microvesicles). Exosomes derived from the fusion of multivesicular endosomes (MVE) with the plasma membrane, while microvesicles are originated by budding of the plasma membrane (CCV = Clathrin-coated vesicle; ER = Endoplasmic reticulum).

(Modified from (552): Raposo, G. and W. Stoorvogel (2013). "Extracellular vesicles: exosomes, microvesicles, and friends." *J Cell Biol* 200(4): 373-383)

B) Transmission electron microscopy (TEM) microphotograph of exosomes isolated from N2a cells, showing their typical cup-like shape.

Figure 6.2. GM1 promotes the secretion of extracellular vesicles from neuronal cells

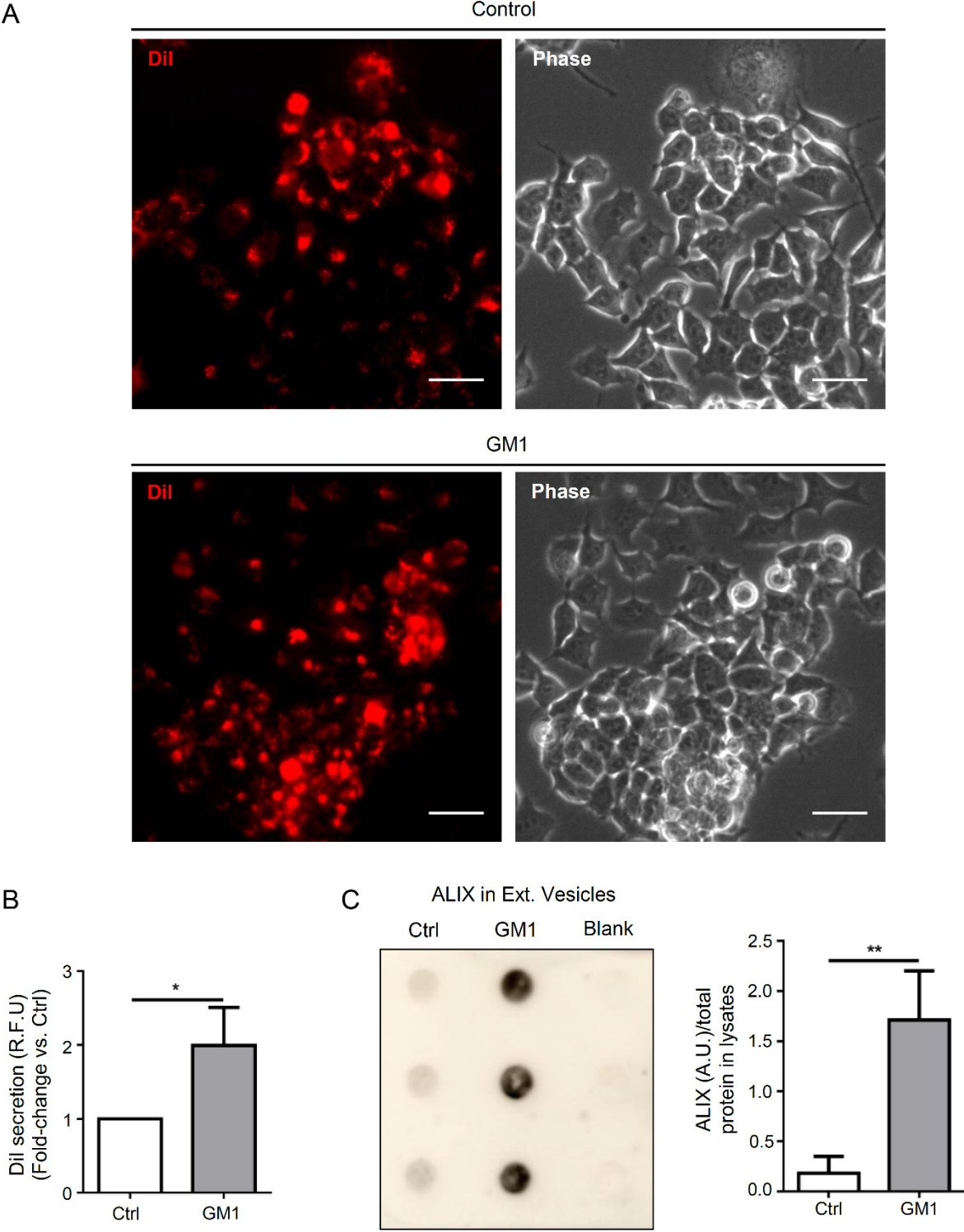


Figure 6.2. GM1 promotes the secretion of extracellular vesicles from neuronal cells

A) Representative images of N2a cells stained with DiI and then treated with vehicle or GM1. Scale bar = 40 μ m.

B) DiI fluorescence in EVs collected from medium conditioned by N2a cells treated with vehicle or GM1 was used as a surrogate measure of EV abundance, and normalized over total cellular DiI content. Bars show the mean values \pm SD of 3 independent experiments. Two-tailed Student's t-test $*p < 0.05$.

C) Dot blot and densitometric analysis of the EV marker ALIX in extracellular vesicles purified from N2a cells treated with vehicle or GM1, normalized over total cellular protein content. Unconditioned media (blank) was run as a control for ALIX protein content in the unconditioned culture media. Bars show mean values \pm SD of technical replicates of one experiment. Two-tailed Student's t-test. $**p < 0.01$.

Figure 6.3. GM1 promotes the secretion of extracellular vesicles from embryonic cortical primary neurons

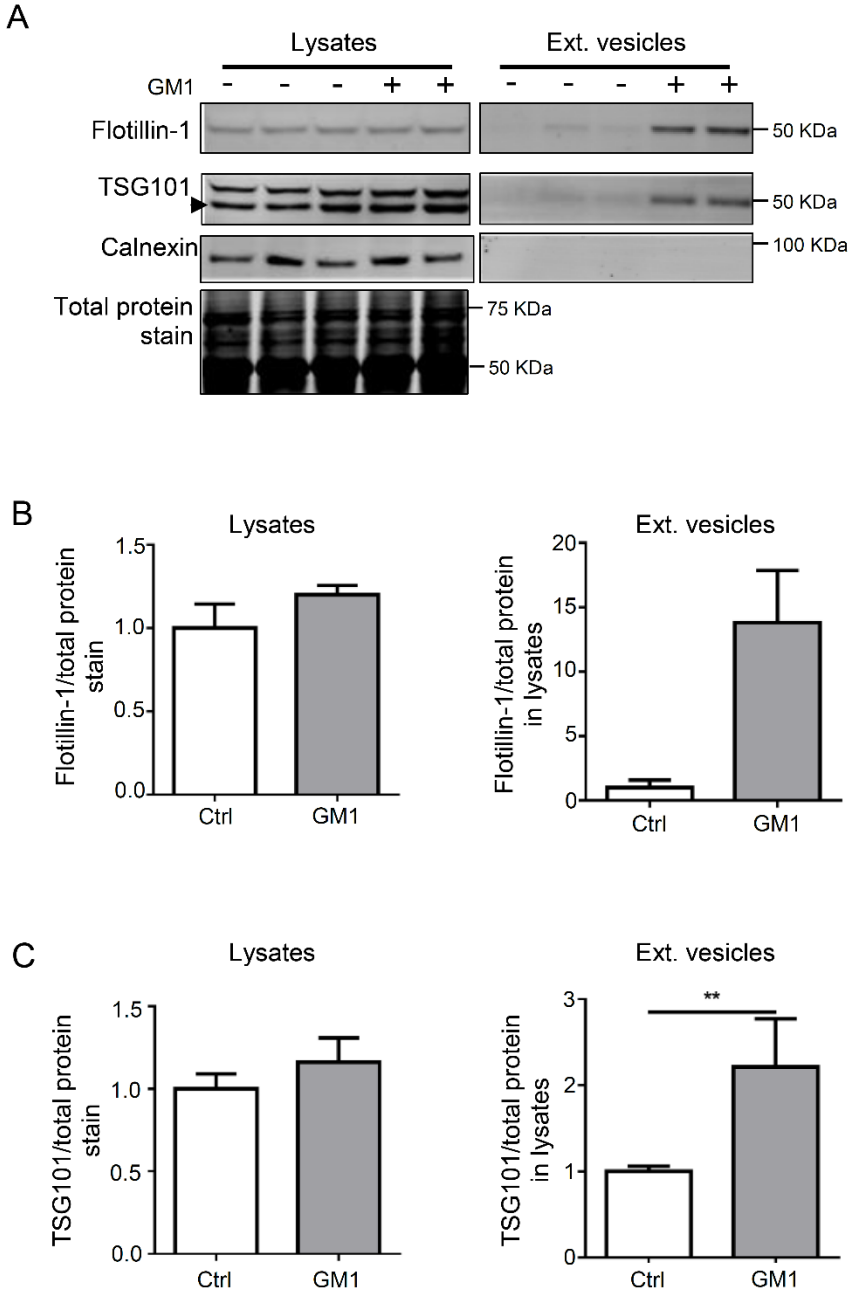


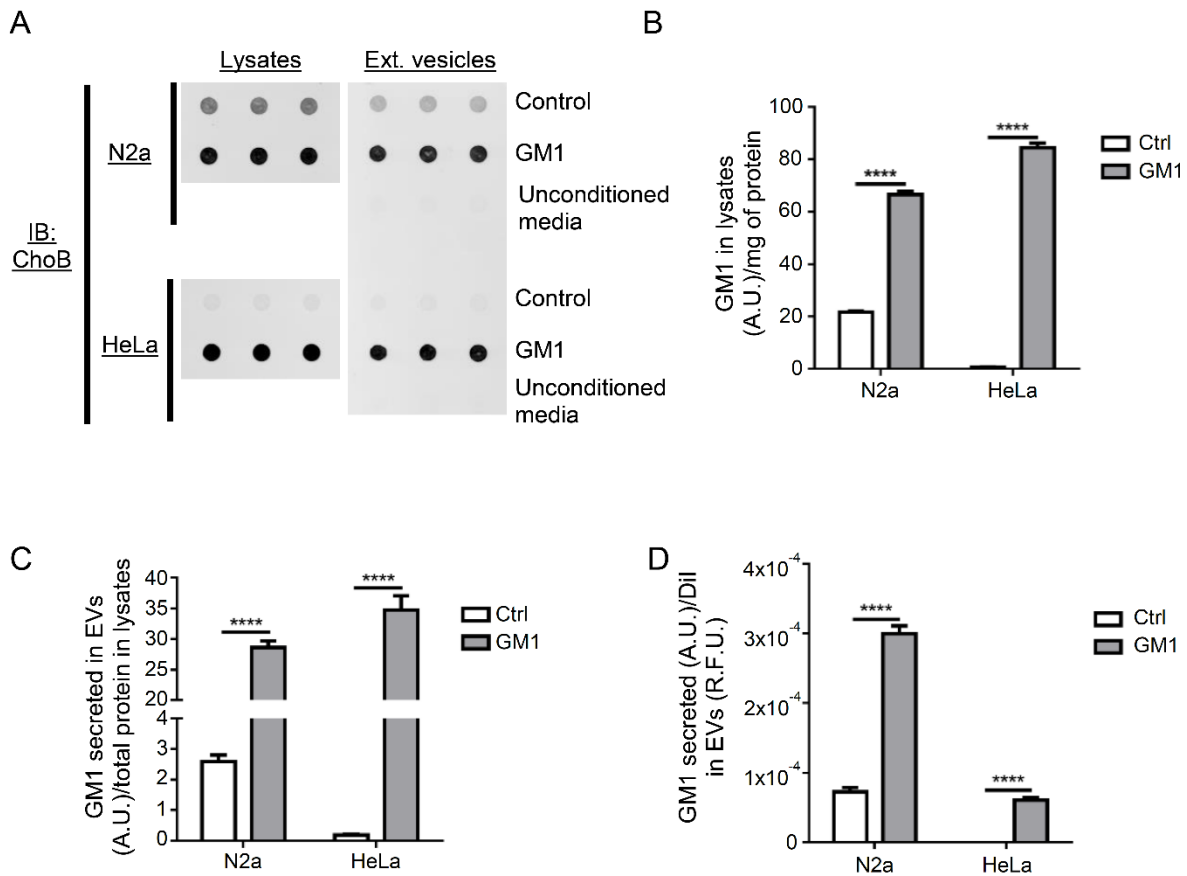
Figure 6.3. GM1 promotes the secretion of extracellular vesicles from embryonic cortical primary neurons

A) Representative immunoblot against extracellular vesicle markers flotillin-1 and TSG101 in lysates and extracellular vesicles purified from embryonic rat cortical primary neurons treated with vehicle or GM1 (50 μ M, 72 h). The absence of calnexin is used as a marker of purity of the extracellular vesicle preparation.

B) Densitometric analysis of flotillin-1 in cell lysates and EV fractions (N=2-3). Bars show mean values \pm SD.

C) Densitometric analysis of TSG101 in cell lysates and EV fractions (N=3-4). Bars show mean values \pm SD. Two-tailed Student's t-test. $**p < 0.01$.

Figure 6.4. Exogenously administered GM1 is internalized by cells and incorporated into extracellular vesicles



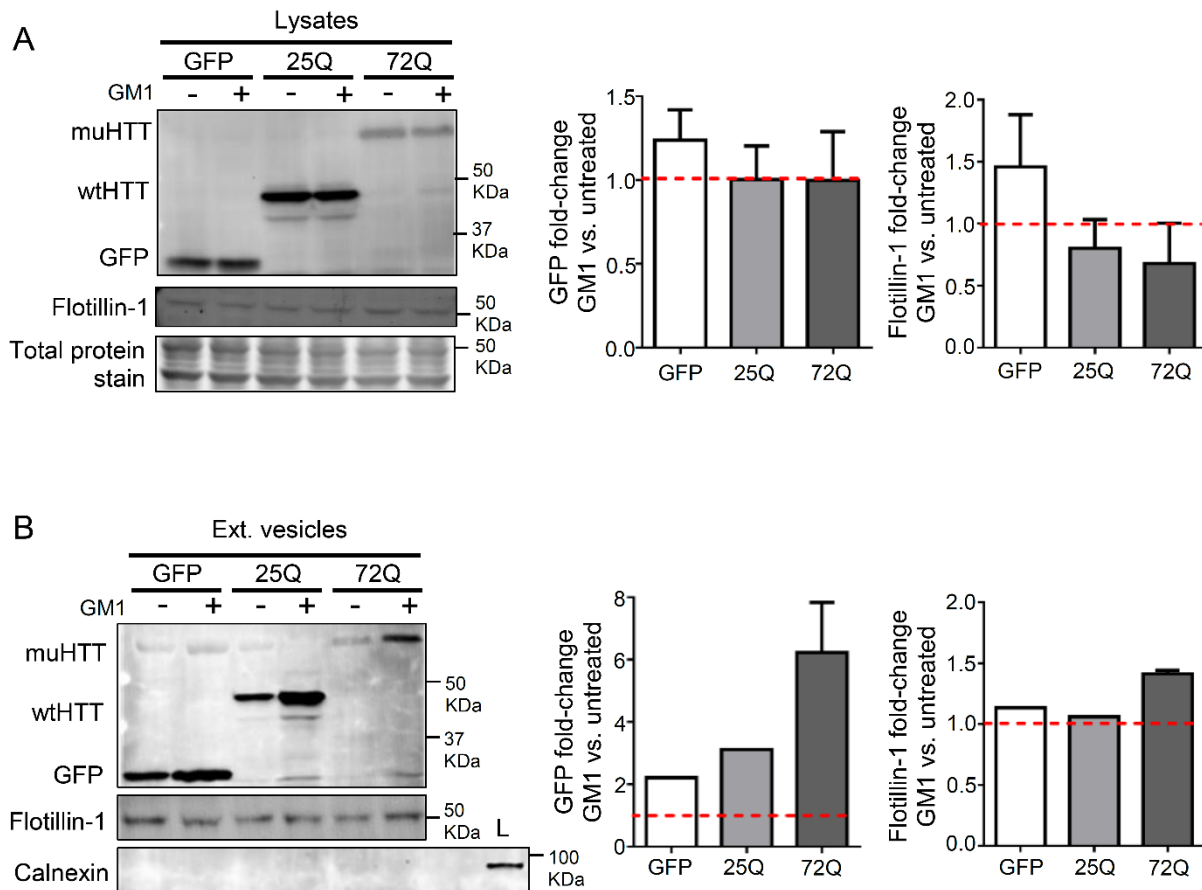
A) Dot blot of lysates and extracellular vesicles purified from N2a and HeLa cells after treatment with vehicle or GM1. Cholera toxin subunit B (ChoB) was used to detect GM1. Unconditioned media was loaded as negative control. This experiment was performed only once.

B) Densitometric analysis of GM1 levels in cell lysates, normalized over total proteins.

C) Densitometric analysis of GM1 levels in the extracellular vesicles, normalized over the total protein content in the lysates.

D) Ratio of GM1 levels in EVs, divided by DiI fluorescence in EVs. Bars show mean values \pm SD of technical replicates of one experiment. Two-tailed Student's t-test. **** $p < 0.0001$.

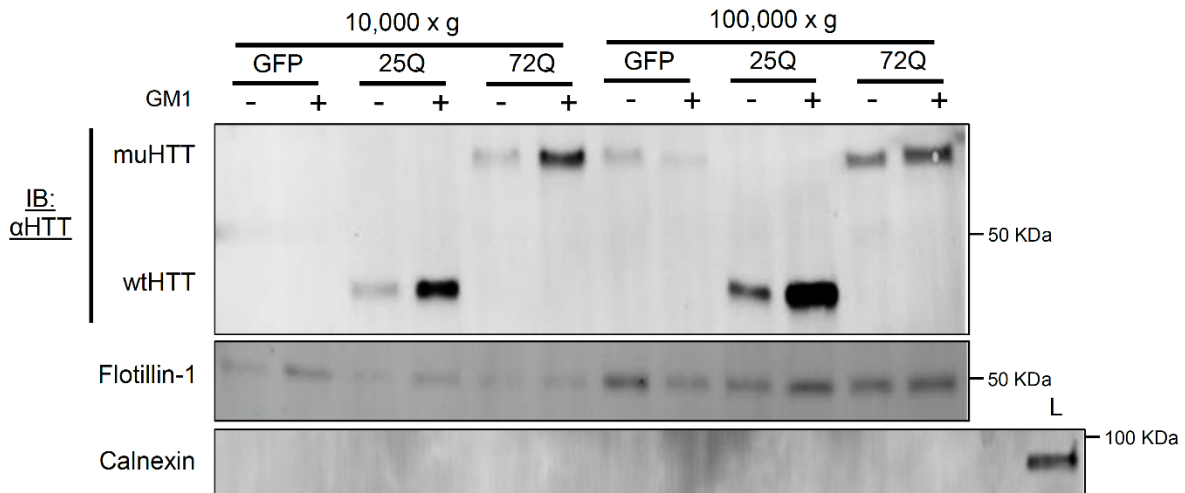
Figure 6.5. GM1 promotes the secretion of HTT via extracellular vesicles in transiently transfected HeLa cells



A) Representative immunoblot and densitometric analysis of GFP, SDS-soluble HTT-eGFP and flotillin-1 in lysates from HeLa cells transiently transfected with GFP, Ex1-25Q-HTT-eGFP (25Q) or Ex1-72Q-HTT-eGFP (72Q), treated with vehicle or GM1. Each bar represents the fold-change normalized over total protein content and over control (untreated) levels (indicated by the red dashed line). Bars show mean values \pm SD of 4 independent experiments.

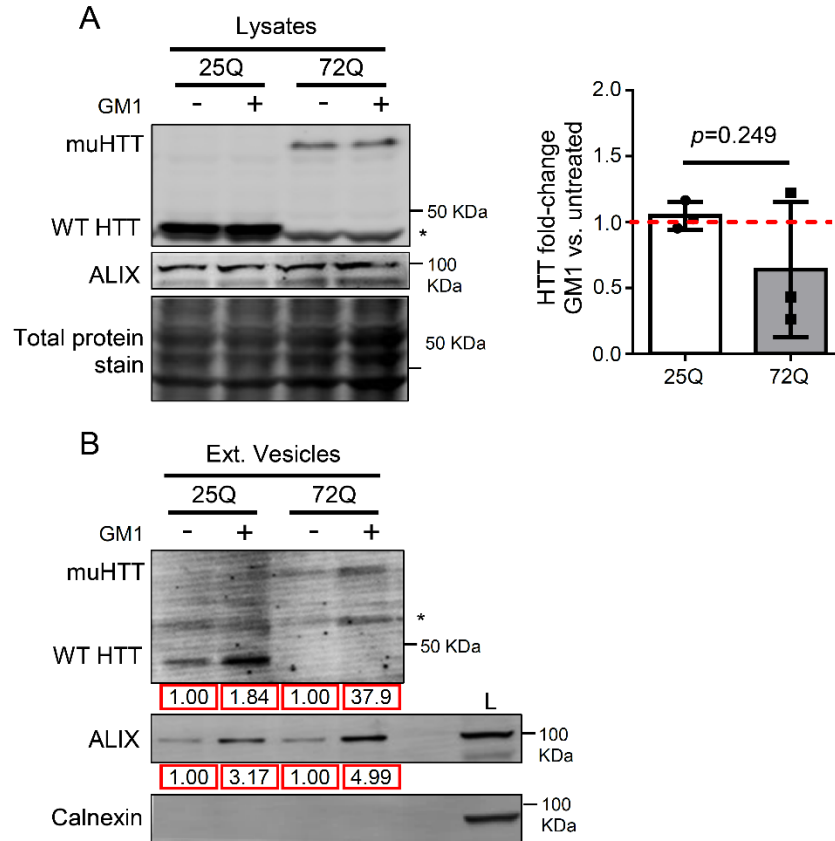
B) Immunoblot and densitometric analysis of GFP, HTT-eGFP and flotillin-1 in extracellular vesicles purified from HeLa cells transiently transfected with GFP, Ex1-25Q-HTT-eGFP (25Q) or Ex1-72Q-HTT-eGFP (72Q), treated with vehicle or GM1. L=Lysate. In the graph, each bar represents the fold-change normalized over total protein content in lysates and over control (untreated) levels (indicated by the red dashed line). N=1 for GFP and 25Q. N=2 for 72Q.

Figure 6.6. GM1 promotes the secretion of HTT in both, microvesicles and exosomes



Immunoblot against HTT and flotillin-1 in microvesicle-enriched (10,000 x g) and exosome-enriched (100,000 x g) fractions, purified from conditioned media of HeLa cells transiently transfected with GFP, Ex1-25Q-HTT-eGFP (25Q) or Ex1-72Q-HTT-eGFP (72Q) plasmids, treated with vehicle or GM1. L=Lysate. This experiment was only performed once.

Figure 6.7. GM1 promotes the secretion of HTT via extracellular vesicles in transiently transfected N2a cells

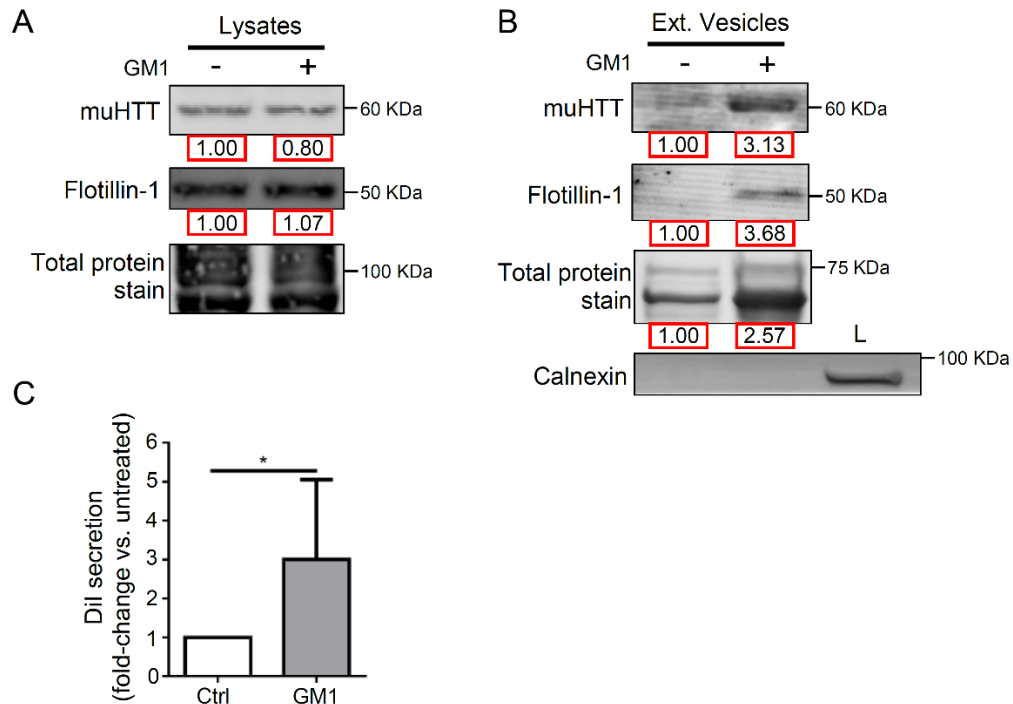


A) Immunoblot and densitometric analysis of SDS-soluble HTT and ALIX in lysates from N2a cells transiently transfected with Ex1-25Q-HTT-eGFP (25Q) or Ex1-72Q-HTT-eGFP (72Q) and treated with vehicle or GM1. The asterisk marks a non-specific band. GM1 did not change the amount of wtHTT (25Q) or muHTT (72Q) in the lysates in a statistically significant manner, compared to untreated. Each bar represents the fold-change normalized over total protein stain and over control (untreated) levels (indicated by the red dashed line). Bars show mean values \pm SD of 3 independent experiments. The immunoblot for ALIX was performed only once.

B) Immunoblot and densitometric analysis of HTT and ALIX in extracellular vesicles purified from N2a cells transiently transfected with Ex1-25Q-HTT-eGFP (25Q) or Ex1-72Q-HTT-eGFP (72Q) and treated with vehicle or GM1. The asterisk marks a non-specific band.

L=Lysate. Each number under the blot indicates fold-change vs. untreated. Data were normalized over total protein content in lysates. The analysis of extracellular vesicles was performed only once.

Figure 6.8. GM1 promotes the secretion of muHTT via extracellular vesicles in stably transfected N2a cells

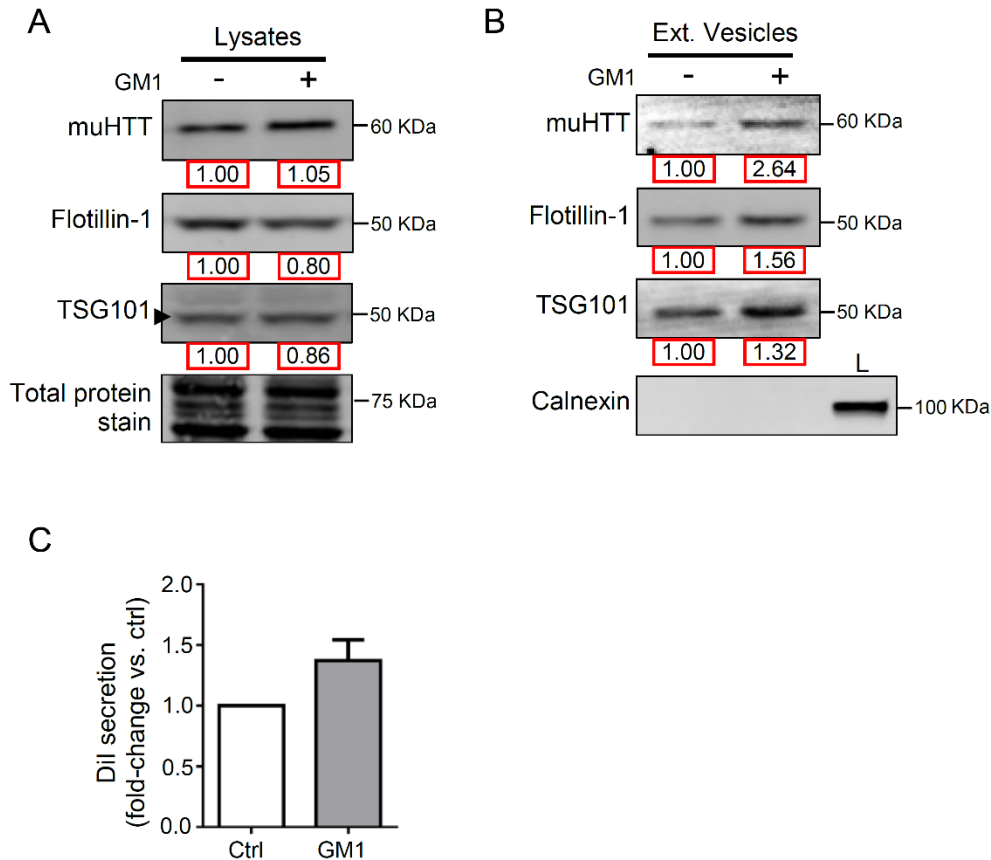


A) Immunoblot and densitometric analysis of SDS-soluble muHTT and flotillin-1 in lysates from N2a cells stably expressing Ex1-72Q-HTT-eGFP (muHTT), treated with vehicle or GM1. Each number under the blot indicates fold-change vs. untreated. GM1 did not significantly change the levels of muHTT (72Q) or flotillin-1 in the lysates. The experiment was repeated twice more with similar results

B) Immunoblot and densitometric analysis of muHTT, flotillin-1 and total protein stain in extracellular vesicles purified from N2a cells stably expressing Ex1-72Q-HTT-eGFP (muHTT), treated with vehicle or GM1. L=Lysate. Each number under the blot indicates fold-change vs. untreated. Data were normalized over total protein content in lysates. The experiment was repeated once more with nearly identical results.

C) DiI fluorescence in EVs collected from medium conditioned by N2a cells stably expressing Ex1-72Q-HTT-eGFP (muHTT), treated with vehicle or GM1, normalized over total cellular DiI content. Bars show the mean values \pm SD of 6 independent experiments. Two-tailed Student's t-test. * $p < 0.05$.

Figure 6.9. GM1 promotes the secretion of muHTT via extracellular vesicles in stably transfected HeLa cells

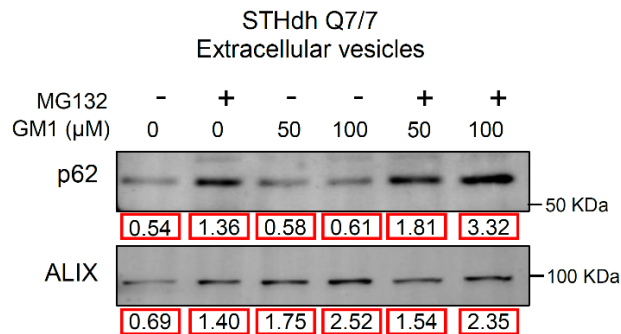


A) Immunoblot and densitometric analysis of SDS-soluble muHTT, flotillin-1 and TSG101 in lysates from HeLa cells stably expressing Ex1-72Q-HTT-eGFP (muHTT), treated with vehicle or GM1. Each number under the blot indicates fold-change vs. untreated. GM1 did not significantly change the levels of muHTT (72Q), flotillin-1 or TSG101 in the lysates. The experiment was repeated twice more with similar results.

B) Immunoblot and densitometric analysis of muHTT, flotillin-1 and TSG101 in extracellular vesicles purified from HeLa cells stably expressing Ex1-72Q-HTT-eGFP (muHTT), treated with vehicle or GM1. L=Lysate. Each number under the blot represents the fold-change vs. untreated. Data were normalized over total protein content in lysates. The experiment was repeated once more with nearly identical results.

C) DiI fluorescence in EVs collected from medium conditioned by HeLa cells stably expressing Ex1-72Q-HTT-eGFP (muHTT), treated with vehicle or GM1, normalized over total cellular DiI content. Bars show the mean values \pm SD of 2 independent experiments.

Figure 6.10. GM1 promotes the secretion of p62 via extracellular vesicles in cells undergoing proteotoxic stress



Western blot against and densitometric analysis of p62 and ALIX in extracellular vesicles purified from STHdh Q7/7 cells treated with MG132 (0.5 μ M), GM1 (50 μ M or 100 μ M) or combination, for 24 h. Each number under the blot represents the raw density value normalized over total protein content in lysates. This experiment was performed only once.

Chapter 7: General discussion and conclusions

This chapter is my original work

7.1. Summary of findings

7.1.1. The mevalonate pathway is impaired in HD models, but protein prenylation is not affected

Decreased activity of the mevalonate pathway and decreased synthesis of cholesterol have been implicated in the pathogenesis of HD (214,287-290), but whether production of isoprenoids - also products of the mevalonate pathway - and downstream protein prenylation could also be affected in HD, was not known. In this thesis, as a surrogate measure of global protein prenylation, the prenylation status of selected small GTPases was assessed in cell and animal models of HD. Contrary to my expectations, I could not detect any alteration in the prenylation status of these selected small GTPases in any of the models that were analyzed. Future studies will extend this investigation to the entire cell “prenylome” to determine whether my findings are applicable to all prenylated proteins or whether selected proteins that have been shown to be a “low priority” (383) for the prenylation machinery, might be under-prenylated in HD.

Interestingly, while analyzing the prenylation status of RAB7, I found that total levels of this protein were decreased across multiple cell and animal models of HD. RAB7 is a small GTPase that is involved in selective autophagy (394-396) and vesicular trafficking (363,392). Whether restoring RAB7 would improve selective autophagy and vesicle transport in HD models, remains to be investigated.

7.1.2. Exogenous supply of ganglioside GM1 reduces accumulation of aggregated proteins in an autophagy-independent manner, and increases misfolded protein secretion via extracellular vesicles

Previous work done in the Sipione laboratory has shown that levels of ganglioside GM1 are reduced in various cell models of HD (272) and that exogenous supply of GM1 protects HD striatal cells from apoptosis (272) and restores motor and non-motor behaviour to normal, in three different HD mouse models (115,273).

The mechanisms by which GM1 exerts these dramatic therapeutic effects in HD models are still under investigation. In recent work to which I collaborated, we observed decreased levels of soluble and insoluble muHTT in the brains of HD mice treated with GM1 (273). In this thesis, I investigated this phenomenon and the potential underlying mechanism/s in more detail.

I showed that exogenous supply of GM1 decreases SDS-insoluble muHTT aggregates in cells expressing a toxic N-terminal fragment of muHTT. Moreover, GM1 was also able to decrease the size and number of aggresomes, as well as the amount of insoluble p62, after pharmacological inhibition of the UPS, suggesting that the beneficial effects of GM1 might extend beyond HD, and to other protein misfolding disorders such as Parkinson's disease and Alzheimer's disease. The underlying mechanisms are still not completely clear, but I made progress by showing that autophagy - contrary to our initial expectations and to literature reports that suggest that gangliosides increase autophagy (531-534) - does not mediate the effects of GM1 in our models. Through an investigation of multiple autophagy steps, I was able to show that GM1 does not increase the levels of LC3-II, a surrogate measure of autophagosome abundance, nor induces the activation of selective autophagy, measured by phosphorylation of p62 after pharmacological inhibition of the UPS or expression of an N-terminal muHTT fragment, nor reduces the half-life

of p62, a known autophagy target. Moreover, GM1 decreases activation of lysosomal biogenesis during proteotoxic stress (inhibition of UPS).

My studies have revealed that GM1 treatment causes the activation of an alternative pathway for elimination of toxic cargo, i.e. the secretion of extracellular vesicles (EVs) containing muHTT. The protein p62, one of the main components of the aggresome, can also be secreted via EVs during inhibition of the UPS, and its secretion was further increased when cells were treated with GM1. However, the extent of the contribution of this proteostatic mechanism to the decrease of protein aggregates caused by GM1, remains to be determined.

7.2. Overall significance of findings and concluding remarks

HD is a devastating neurodegenerative disease for which there is no cure nor effective disease-modifying treatments (266). Thus, pharmacological treatments that modify the course of HD, are urgently needed.

Understanding the mechanisms by which muHTT leads to neurodegeneration is essential for the design of new therapies. Here I report that levels of RAB7, a protein that is essential for vesicular trafficking (363,392) and selective autophagy (394-396), is decreased across cell and mouse models of HD. Selective autophagy and vesicular trafficking are two of the many cellular functions that have been found to be affected in HD (152,366,367,393). Therefore, it is possible that restoring normal levels of RAB7 would improve these two dysfunctions in HD models.

In the second part of my thesis, I made significant progress towards understanding the molecular mechanisms underlying the neuroprotective activity of ganglioside GM1 in HD. A clear understanding of GM1 mechanism of action is crucial to move GM1 to clinical trials, as well as to elucidate the role of gangliosides in brain and cell physiology.

The discovery that GM1 promotes the secretion of muHTT through EVs, and away from vulnerable neurons, has important implications not only for HD, but also for other protein misfolding disorders of the nervous system.

7.3. Future directions

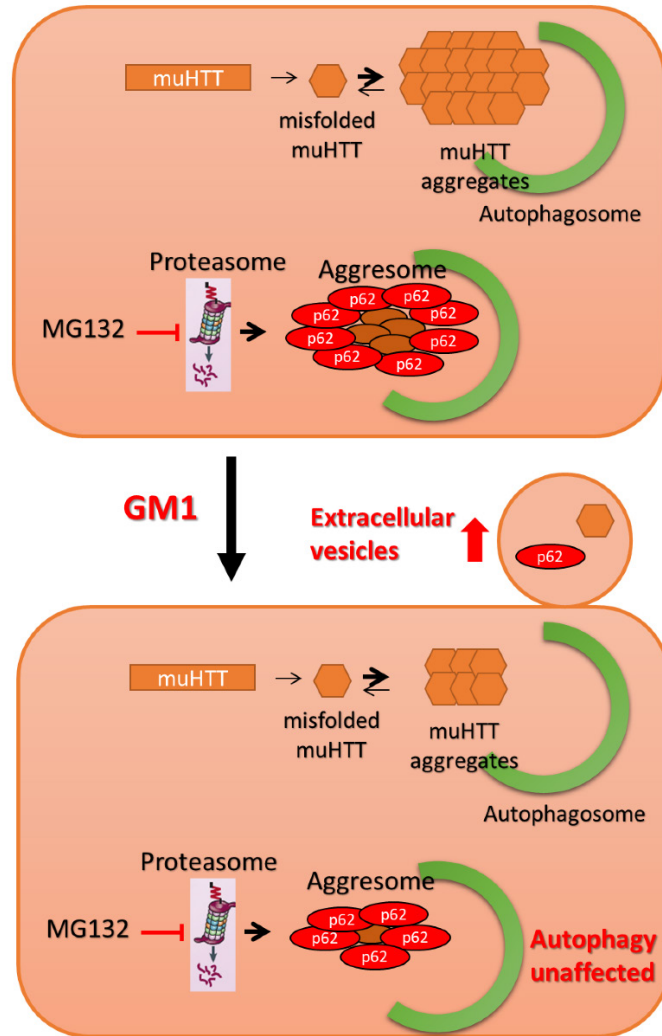
While answering, at least in part, important questions related to the impact of dysfunction of the mevalonate pathway in HD, and to the mechanism of action of GM1 as a disease-modifying therapy in HD, my studies have opened the door to new questions that will need to be investigated in future studies. What is the role of decreased levels of RAB7 in HD pathogenesis? And can it be corrected? Are there other prenylated proteins that might be impacted by dysfunction of the mevalonate pathway in HD more than the ones I selected in my studies?

My discovery that GM1 can affect protein aggregates and their elimination from neurons through EVs might promote the development of GM1 as a therapy for HD, and potentially also other protein misfolding diseases.

Systemic administration of GM1 has been already tested in humans as a potential treatment for PD. In 1995, Schneider and collaborators (616) recruited 10 PD patients who received GM1 intravenously once, followed by subcutaneous administration for up to 18 weeks. None of the patients suffered from severe adverse reactions. Follow-up trials confirmed the safety of systemic GM1 administration (617), even in patients who continued receiving GM1 for up to 5 years (618). These results suggest that systemic administration of GM1 is safe in humans, and could be tested in clinical trials in HD patients.

7.4. Figures

Figure 7.1. GM1 effects on the accumulation of protein aggregates: a working model



Cells treated with GM1 show decreased accumulation of misfolded proteins. I could not find any evidence of increased autophagic degradation upon GM1 treatment. However, cells treated with GM1 showed increased secretion of extracellular vesicle (EV) markers along with muHTT and p62, which suggests that GM1 might modulate misfolded protein secretion through EVs.

Bibliography

1. McColgan, P., and Tabrizi, S. J. (2018) Huntington's disease: a clinical review. *European journal of neurology* **25**, 24-34
2. Group, T. H. s. D. C. R. (1993) A novel gene containing a trinucleotide repeat that is expanded and unstable on Huntington's disease chromosomes. The Huntington's Disease Collaborative Research Group. *Cell* **72**, 971-983
3. Langbehn, D. R., Hayden, M. R., Paulsen, J. S., and and the, P.-H. D. I. o. t. H. S. G. (2010) CAG-repeat length and the age of onset in Huntington disease (HD): a review and validation study of statistical approaches. *American journal of medical genetics. Part B, Neuropsychiatric genetics : the official publication of the International Society of Psychiatric Genetics* **153B**, 397-408
4. Ranen, N. G., Stine, O. C., Abbott, M. H., Sherr, M., Codori, A. M., Franz, M. L., Chao, N. I., Chung, A. S., Pleasant, N., Callahan, C., Kasch, L. M., Ghaffari, M., Chase, G. A., Kazazian, H. H., Brandt, J., Folstein, S. E., and Ross, C. A. (1995) Anticipation and instability of IT-15 (CAG)_n repeats in parent-offspring pairs with Huntington disease. *American journal of human genetics* **57**, 593-602
5. Sharp, A. H., and Ross, C. A. (1996) Neurobiology of Huntington's disease. *Neurobiology of disease* **3**, 3-15
6. Rawlins, M. D., Wexler, N. S., Wexler, A. R., Tabrizi, S. J., Douglas, I., Evans, S. J., and Smeeth, L. (2016) The Prevalence of Huntington's Disease. *Neuroepidemiology* **46**, 144-153
7. Evans, S. J., Douglas, I., Rawlins, M. D., Wexler, N. S., Tabrizi, S. J., and Smeeth, L. (2013) Prevalence of adult Huntington's disease in the UK based on diagnoses recorded in

- general practice records. *Journal of neurology, neurosurgery, and psychiatry* **84**, 1156-1160
8. Lekoubou, A., Echouffo-Tcheugui, J. B., and Kengne, A. P. (2014) Epidemiology of neurodegenerative diseases in sub-Saharan Africa: a systematic review. *BMC public health* **14**, 653
 9. Folstein, S. E., Chase, G. A., Wahl, W. E., McDonnell, A. M., and Folstein, M. F. (1987) Huntington disease in Maryland: clinical aspects of racial variation. *American journal of human genetics* **41**, 168-179
 10. Alonso, M. E., Ochoa, A., Boll, M. C., Sosa, A. L., Yescas, P., Lopez, M., Macias, R., Familiar, I., and Rasmussen, A. (2009) Clinical and genetic characteristics of Mexican Huntington's disease patients. *Movement disorders : official journal of the Movement Disorder Society* **24**, 2012-2015
 11. Paradisi, I., Hernandez, A., and Arias, S. (2008) Huntington disease mutation in Venezuela: age of onset, haplotype analyses and geographic aggregation. *Journal of human genetics* **53**, 127-135
 12. Castilhos, R. M., Augustin, M. C., Santos, J. A., Perandones, C., Saraiva-Pereira, M. L., and Jardim, L. B. (2016) Genetic aspects of Huntington's disease in Latin America. A systematic review. *Clinical genetics* **89**, 295-303
 13. Shannon, K. M. (2011) Huntington's disease - clinical signs, symptoms, presymptomatic diagnosis, and diagnosis. *Handbook of clinical neurology* **100**, 3-13
 14. (1996) Unified Huntington's Disease Rating Scale: reliability and consistency. Huntington Study Group. *Movement disorders : official journal of the Movement Disorder Society* **11**, 136-142

15. Ross, C. A., Aylward, E. H., Wild, E. J., Langbehn, D. R., Long, J. D., Warner, J. H., Scahill, R. I., Leavitt, B. R., Stout, J. C., Paulsen, J. S., Reilmann, R., Unschuld, P. G., Wexler, A., Margolis, R. L., and Tabrizi, S. J. (2014) Huntington disease: natural history, biomarkers and prospects for therapeutics. *Nature reviews. Neurology* **10**, 204-216
16. Dorsey, E. R., Beck, C. A., Darwin, K., Nichols, P., Brocht, A. F., Biglan, K. M., Shoulson, I., and Huntington Study Group, C. I. (2013) Natural history of Huntington disease. *JAMA neurology* **70**, 1520-1530
17. Plotkin, J. L., and Surmeier, D. J. (2015) Corticostriatal synaptic adaptations in Huntington's disease. *Current opinion in neurobiology* **33**, 53-62
18. Louis, E. D., Lee, P., Quinn, L., and Marder, K. (1999) Dystonia in Huntington's disease: prevalence and clinical characteristics. *Movement disorders : official journal of the Movement Disorder Society* **14**, 95-101
19. Jankovic, J., and Ashizawa, T. (1995) Tourettism associated with Huntington's disease. *Movement disorders : official journal of the Movement Disorder Society* **10**, 103-105
20. Thompson, P. D., Bhatia, K. P., Brown, P., Davis, M. B., Pires, M., Quinn, N. P., Luthert, P., Honovar, M., O'Brien, M. D., Marsden, C. D., and Harding, A. E. (1994) Cortical myoclonus in Huntington's disease. *Movement disorders : official journal of the Movement Disorder Society* **9**, 633-641
21. Carella, F., Scaioli, V., Ciano, C., Binelli, S., Oliva, D., and Girotti, F. (1993) Adult onset myoclonic Huntington's disease. *Movement disorders : official journal of the Movement Disorder Society* **8**, 201-205

22. Gonzalez-Alegre, P., and Afifi, A. K. (2006) Clinical characteristics of childhood-onset (juvenile) Huntington disease: report of 12 patients and review of the literature. *Journal of child neurology* **21**, 223-229
23. Yoon, G., Kramer, J., Zanko, A., Guzijan, M., Lin, S., Foster-Barber, A., and Boxer, A. L. (2006) Speech and language delay are early manifestations of juvenile-onset Huntington disease. *Neurology* **67**, 1265-1267
24. Hansotia, P., Cleeland, C. S., and Chun, R. W. (1968) Juvenile Huntington's chorea. *Neurology* **18**, 217-224
25. Gambardella, A., Muglia, M., Labate, A., Magariello, A., Gabriele, A. L., Mazzei, R., Pirritano, D., Conforti, F. L., Patitucci, A., Valentino, P., Zappia, M., and Quattrone, A. (2001) Juvenile Huntington's disease presenting as progressive myoclonic epilepsy. *Neurology* **57**, 708-711
26. Paulsen, J. S., Miller, A. C., Hayes, T., and Shaw, E. (2017) Cognitive and behavioral changes in Huntington disease before diagnosis. *Handbook of clinical neurology* **144**, 69-91
27. Teixeira, A. L., de Souza, L. C., Rocha, N. P., Furr-Stimming, E., and Lauterbach, E. C. (2016) Revisiting the neuropsychiatry of Huntington's disease. *Dementia & neuropsychologia* **10**, 261-266
28. Stout, J. C., Jones, R., Labuschagne, I., O'Regan, A. M., Say, M. J., Dumas, E. M., Queller, S., Justo, D., Santos, R. D., Coleman, A., Hart, E. P., Durr, A., Leavitt, B. R., Roos, R. A., Langbehn, D. R., Tabrizi, S. J., and Frost, C. (2012) Evaluation of longitudinal 12 and 24 month cognitive outcomes in premanifest and early Huntington's disease. *Journal of neurology, neurosurgery, and psychiatry* **83**, 687-694

29. Stout, J. C., Paulsen, J. S., Queller, S., Solomon, A. C., Whitlock, K. B., Campbell, J. C., Carlozzi, N., Duff, K., Beglinger, L. J., Langbehn, D. R., Johnson, S. A., Biglan, K. M., and Aylward, E. H. (2011) Neurocognitive signs in prodromal Huntington disease. *Neuropsychology* **25**, 1-14
30. Peavy, G. M., Jacobson, M. W., Goldstein, J. L., Hamilton, J. M., Kane, A., Gamst, A. C., Lessig, S. L., Lee, J. C., and Corey-Bloom, J. (2010) Cognitive and functional decline in Huntington's disease: dementia criteria revisited. *Movement disorders : official journal of the Movement Disorder Society* **25**, 1163-1169
31. Snowden, J. S., Craufurd, D., Thompson, J., and Neary, D. (2002) Psychomotor, executive, and memory function in preclinical Huntington's disease. *Journal of clinical and experimental neuropsychology* **24**, 133-145
32. Solomon, A. C., Stout, J. C., Johnson, S. A., Langbehn, D. R., Aylward, E. H., Brandt, J., Ross, C. A., Beglinger, L., Hayden, M. R., Kieburtz, K., Kayson, E., Julian-Baros, E., Duff, K., Guttman, M., Nance, M., Oakes, D., Shoulson, I., Penziner, E., Paulsen, J. S., and Predict, H. D. i. o. t. H. S. G. (2007) Verbal episodic memory declines prior to diagnosis in Huntington's disease. *Neuropsychologia* **45**, 1767-1776
33. Tabrizi, S. J., Scahill, R. I., Durr, A., Roos, R. A., Leavitt, B. R., Jones, R., Landwehrmeyer, G. B., Fox, N. C., Johnson, H., Hicks, S. L., Kennard, C., Craufurd, D., Frost, C., Langbehn, D. R., Reilmann, R., and Stout, J. C. (2011) Biological and clinical changes in premanifest and early stage Huntington's disease in the TRACK-HD study: the 12-month longitudinal analysis. *Lancet neurology* **10**, 31-42
34. Tabrizi, S. J., Reilmann, R., Roos, R. A., Durr, A., Leavitt, B., Owen, G., Jones, R., Johnson, H., Craufurd, D., Hicks, S. L., Kennard, C., Landwehrmeyer, B., Stout, J. C.,

- Borowsky, B., Scahill, R. I., Frost, C., and Langbehn, D. R. (2012) Potential endpoints for clinical trials in premanifest and early Huntington's disease in the TRACK-HD study: analysis of 24 month observational data. *Lancet neurology* **11**, 42-53
35. Tabrizi, S. J., Scahill, R. I., Owen, G., Durr, A., Leavitt, B. R., Roos, R. A., Borowsky, B., Landwehrmeyer, B., Frost, C., Johnson, H., Craufurd, D., Reilmann, R., Stout, J. C., and Langbehn, D. R. (2013) Predictors of phenotypic progression and disease onset in premanifest and early-stage Huntington's disease in the TRACK-HD study: analysis of 36-month observational data. *Lancet neurology* **12**, 637-649
36. Ribai, P., Nguyen, K., Hahn-Barma, V., Gourfinkel-An, I., Vidailhet, M., Legout, A., Dode, C., Brice, A., and Durr, A. (2007) Psychiatric and cognitive difficulties as indicators of juvenile huntington disease onset in 29 patients. *Archives of neurology* **64**, 813-819
37. Thompson, J. C., Harris, J., Sollom, A. C., Stopford, C. L., Howard, E., Snowden, J. S., and Craufurd, D. (2012) Longitudinal evaluation of neuropsychiatric symptoms in Huntington's disease. *The Journal of neuropsychiatry and clinical neurosciences* **24**, 53-60
38. Fiedorowicz, J. G., Mills, J. A., Ruggle, A., Langbehn, D., Paulsen, J. S., and Group, P.-H. I. o. t. H. S. (2011) Suicidal behavior in prodromal Huntington disease. *Neurodegenerative diseases* **8**, 483-490
39. Tabrizi, S. J., Langbehn, D. R., Leavitt, B. R., Roos, R. A., Durr, A., Craufurd, D., Kennard, C., Hicks, S. L., Fox, N. C., Scahill, R. I., Borowsky, B., Tobin, A. J., Rosas, H. D., Johnson, H., Reilmann, R., Landwehrmeyer, B., and Stout, J. C. (2009) Biological and clinical manifestations of Huntington's disease in the longitudinal TRACK-HD study: cross-sectional analysis of baseline data. *Lancet neurology* **8**, 791-801

40. Carpenter, M. B., Nakano, K., and Kim, R. (1976) Nigrothalamic projections in the monkey demonstrated by autoradiographic technics. *The Journal of comparative neurology* **165**, 401-415
41. Smith, Y., Bevan, M. D., Shink, E., and Bolam, J. P. (1998) Microcircuitry of the direct and indirect pathways of the basal ganglia. *Neuroscience* **86**, 353-387
42. Waldvogel, H. J., Kim, E. H., Tippett, L. J., Vonsattel, J. P., and Faull, R. L. (2015) The Neuropathology of Huntington's Disease. *Current topics in behavioral neurosciences* **22**, 33-80
43. McGeorge, A. J., and Faull, R. L. (1989) The organization of the projection from the cerebral cortex to the striatum in the rat. *Neuroscience* **29**, 503-537
44. Yung, K. K., Smith, A. D., Levey, A. I., and Bolam, J. P. (1996) Synaptic connections between spiny neurons of the direct and indirect pathways in the neostriatum of the rat: evidence from dopamine receptor and neuropeptide immunostaining. *The European journal of neuroscience* **8**, 861-869
45. Graybiel, A. M. (1995) The basal ganglia. *Trends in neurosciences* **18**, 60-62
46. Kayahara, T., and Nakano, K. (1996) Pallido-thalamo-motor cortical connections: an electron microscopic study in the macaque monkey. *Brain research* **706**, 337-342
47. Rub, U., Seidel, K., Heinsen, H., Vonsattel, J. P., den Dunnen, W. F., and Korf, H. W. (2016) Huntington's disease (HD): the neuropathology of a multisystem neurodegenerative disorder of the human brain. *Brain pathology (Zurich, Switzerland)* **26**, 726-740
48. Vonsattel, J. P., and DiFiglia, M. (1998) Huntington disease. *Journal of neuropathology and experimental neurology* **57**, 369-384

49. Vonsattel, J. P., Keller, C., and Del Pilar Amaya, M. (2008) Neuropathology of Huntington's disease. *Handbook of clinical neurology* **89**, 599-618
50. de la Monte, S. M., Vonsattel, J. P., and Richardson, E. P., Jr. (1988) Morphometric demonstration of atrophic changes in the cerebral cortex, white matter, and neostriatum in Huntington's disease. *Journal of neuropathology and experimental neurology* **47**, 516-525
51. Vonsattel, J. P., Myers, R. H., Stevens, T. J., Ferrante, R. J., Bird, E. D., and Richardson, E. P., Jr. (1985) Neuropathological classification of Huntington's disease. *Journal of neuropathology and experimental neurology* **44**, 559-577
52. Roos, R. A., Pruyt, J. F., de Vries, J., and Bots, G. T. (1985) Neuronal distribution in the putamen in Huntington's disease. *Journal of neurology, neurosurgery, and psychiatry* **48**, 422-425
53. Braak, H., and Braak, E. (1992) Allocortical involvement in Huntington's disease. *Neuropathology and applied neurobiology* **18**, 539-547
54. Hedreen, J. C., Peyser, C. E., Folstein, S. E., and Ross, C. A. (1991) Neuronal loss in layers V and VI of cerebral cortex in Huntington's disease. *Neuroscience letters* **133**, 257-261
55. Sotrel, A., Paskevich, P. A., Kiely, D. K., Bird, E. D., Williams, R. S., and Myers, R. H. (1991) Morphometric analysis of the prefrontal cortex in Huntington's disease. *Neurology* **41**, 1117-1123
56. Cudkovicz, M., and Kowall, N. W. (1990) Degeneration of pyramidal projection neurons in Huntington's disease cortex. *Annals of neurology* **27**, 200-204
57. Markham, C. H., and Knox, J. W. (1965) Observations on Huntington's Chorea in Childhood. *The Journal of pediatrics* **67**, 46-57

58. Holt, D. J., Graybiel, A. M., and Saper, C. B. (1997) Neurochemical architecture of the human striatum. *The Journal of comparative neurology* **384**, 1-25
59. Deng, Y. P., Albin, R. L., Penney, J. B., Young, A. B., Anderson, K. D., and Reiner, A. (2004) Differential loss of striatal projection systems in Huntington's disease: a quantitative immunohistochemical study. *Journal of chemical neuroanatomy* **27**, 143-164
60. Seto-Ohshima, A., Emson, P. C., Lawson, E., Mountjoy, C. Q., and Carrasco, L. H. (1988) Loss of matrix calcium-binding protein-containing neurons in Huntington's disease. *Lancet* **1**, 1252-1255
61. Goto, S., Hirano, A., and Rojas-Corona, R. R. (1989) An immunohistochemical investigation of the human neostriatum in Huntington's disease. *Annals of neurology* **25**, 298-304
62. Guo, Z., Rudow, G., Pletnikova, O., Codispoti, K. E., Orr, B. A., Crain, B. J., Duan, W., Margolis, R. L., Rosenblatt, A., Ross, C. A., and Troncoso, J. C. (2012) Striatal neuronal loss correlates with clinical motor impairment in Huntington's disease. *Movement disorders : official journal of the Movement Disorder Society* **27**, 1379-1386
63. Reiner, A., Albin, R. L., Anderson, K. D., D'Amato, C. J., Penney, J. B., and Young, A. B. (1988) Differential loss of striatal projection neurons in Huntington disease. *Proceedings of the National Academy of Sciences of the United States of America* **85**, 5733-5737
64. Albin, R. L., Reiner, A., Anderson, K. D., Dure, L. S. t., Handelin, B., Balfour, R., Whetsell, W. O., Jr., Penney, J. B., and Young, A. B. (1992) Preferential loss of striato-external pallidal projection neurons in presymptomatic Huntington's disease. *Annals of neurology* **31**, 425-430

65. Reiner, A., and Deng, Y. P. (2018) Disrupted striatal neuron inputs and outputs in Huntington's disease. *CNS neuroscience & therapeutics* **24**, 250-280
66. Dowie, M. J., Bradshaw, H. B., Howard, M. L., Nicholson, L. F., Faull, R. L., Hannan, A. J., and Glass, M. (2009) Altered CB1 receptor and endocannabinoid levels precede motor symptom onset in a transgenic mouse model of Huntington's disease. *Neuroscience* **163**, 456-465
67. Allen, K. L., Waldvogel, H. J., Glass, M., and Faull, R. L. (2009) Cannabinoid (CB(1)), GABA(A) and GABA(B) receptor subunit changes in the globus pallidus in Huntington's disease. *Journal of chemical neuroanatomy* **37**, 266-281
68. Glass, M., Dragunow, M., and Faull, R. L. (2000) The pattern of neurodegeneration in Huntington's disease: a comparative study of cannabinoid, dopamine, adenosine and GABA(A) receptor alterations in the human basal ganglia in Huntington's disease. *Neuroscience* **97**, 505-519
69. Aylward, E. H., Anderson, N. B., Bylsma, F. W., Wagster, M. V., Barta, P. E., Sherr, M., Feeney, J., Davis, A., Rosenblatt, A., Pearlson, G. D., and Ross, C. A. (1998) Frontal lobe volume in patients with Huntington's disease. *Neurology* **50**, 252-258
70. Selemon, L. D., Rajkowska, G., and Goldman-Rakic, P. S. (2004) Evidence for progression in frontal cortical pathology in late-stage Huntington's disease. *The Journal of comparative neurology* **468**, 190-204
71. Sotrel, A., Williams, R. S., Kaufmann, W. E., and Myers, R. H. (1993) Evidence for neuronal degeneration and dendritic plasticity in cortical pyramidal neurons of Huntington's disease: a quantitative Golgi study. *Neurology* **43**, 2088-2096

72. Macdonald, V., and Halliday, G. (2002) Pyramidal cell loss in motor cortices in Huntington's disease. *Neurobiology of disease* **10**, 378-386
73. Mehrabi, N. F., Waldvogel, H. J., Tippett, L. J., Hogg, V. M., Synek, B. J., and Faull, R. L. (2016) Symptom heterogeneity in Huntington's disease correlates with neuronal degeneration in the cerebral cortex. *Neurobiology of disease* **96**, 67-74
74. Nana, A. L., Kim, E. H., Thu, D. C., Oorschot, D. E., Tippett, L. J., Hogg, V. M., Synek, B. J., Roxburgh, R., Waldvogel, H. J., and Faull, R. L. (2014) Widespread heterogeneous neuronal loss across the cerebral cortex in Huntington's disease. *Journal of Huntington's disease* **3**, 45-64
75. Hobbs, N. Z., Pedrick, A. V., Say, M. J., Frost, C., Dar Santos, R., Coleman, A., Sturrock, A., Craufurd, D., Stout, J. C., Leavitt, B. R., Barnes, J., Tabrizi, S. J., and Scahill, R. I. (2011) The structural involvement of the cingulate cortex in premanifest and early Huntington's disease. *Movement disorders : official journal of the Movement Disorder Society* **26**, 1684-1690
76. Thu, D. C., Oorschot, D. E., Tippett, L. J., Nana, A. L., Hogg, V. M., Synek, B. J., Luthi-Carter, R., Waldvogel, H. J., and Faull, R. L. (2010) Cell loss in the motor and cingulate cortex correlates with symptomatology in Huntington's disease. *Brain : a journal of neurology* **133**, 1094-1110
77. Myers, R. H., Vonsattel, J. P., Paskevich, P. A., Kiely, D. K., Stevens, T. J., Cupples, L. A., Richardson, E. P., Jr., and Bird, E. D. (1991) Decreased neuronal and increased oligodendroglial densities in Huntington's disease caudate nucleus. *Journal of neuropathology and experimental neurology* **50**, 729-742

78. Hedreen, J. C., and Folstein, S. E. (1995) Early loss of neostriatal striosome neurons in Huntington's disease. *Journal of neuropathology and experimental neurology* **54**, 105-120
79. Gomez-Tortosa, E., MacDonald, M. E., Friend, J. C., Taylor, S. A., Weiler, L. J., Cupples, L. A., Srinidhi, J., Gusella, J. F., Bird, E. D., Vonsattel, J. P., and Myers, R. H. (2001) Quantitative neuropathological changes in presymptomatic Huntington's disease. *Annals of neurology* **49**, 29-34
80. Sapp, E., Kegel, K. B., Aronin, N., Hashikawa, T., Uchiyama, Y., Tohyama, K., Bhide, P. G., Vonsattel, J. P., and DiFiglia, M. (2001) Early and progressive accumulation of reactive microglia in the Huntington disease brain. *Journal of neuropathology and experimental neurology* **60**, 161-172
81. Simmons, D. A., Casale, M., Alcon, B., Pham, N., Narayan, N., and Lynch, G. (2007) Ferritin accumulation in dystrophic microglia is an early event in the development of Huntington's disease. *Glia* **55**, 1074-1084
82. Pavese, N., Gerhard, A., Tai, Y. F., Ho, A. K., Turkheimer, F., Barker, R. A., Brooks, D. J., and Piccini, P. (2006) Microglial activation correlates with severity in Huntington disease: a clinical and PET study. *Neurology* **66**, 1638-1643
83. Tai, Y. F., Pavese, N., Gerhard, A., Tabrizi, S. J., Barker, R. A., Brooks, D. J., and Piccini, P. (2007) Imaging microglial activation in Huntington's disease. *Brain research bulletin* **72**, 148-151
84. Becher, M. W., Kotzuk, J. A., Sharp, A. H., Davies, S. W., Bates, G. P., Price, D. L., and Ross, C. A. (1998) Intranuclear neuronal inclusions in Huntington's disease and dentatorubral and pallidoluysian atrophy: correlation between the density of inclusions and IT15 CAG triplet repeat length. *Neurobiology of disease* **4**, 387-397

85. DiFiglia, M., Sapp, E., Chase, K. O., Davies, S. W., Bates, G. P., Vonsattel, J. P., and Aronin, N. (1997) Aggregation of huntingtin in neuronal intranuclear inclusions and dystrophic neurites in brain. *Science* **277**, 1990-1993
86. Scherzinger, E., Lurz, R., Turmaine, M., Mangiarini, L., Hollenbach, B., Hasenbank, R., Bates, G. P., Davies, S. W., Lehrach, H., and Wanker, E. E. (1997) Huntingtin-encoded polyglutamine expansions form amyloid-like protein aggregates in vitro and in vivo. *Cell* **90**, 549-558
87. Gutekunst, C. A., Li, S. H., Yi, H., Mulroy, J. S., Kuemmerle, S., Jones, R., Rye, D., Ferrante, R. J., Hersch, S. M., and Li, X. J. (1999) Nuclear and neuropil aggregates in Huntington's disease: relationship to neuropathology. *The Journal of neuroscience : the official journal of the Society for Neuroscience* **19**, 2522-2534
88. Trottier, Y., Lutz, Y., Stevanin, G., Imbert, G., Devys, D., Cancel, G., Saudou, F., Weber, C., David, G., Tora, L., Agid, Y., Brice, A., and Mandel, J. L. (1995) Polyglutamine expansion as a pathological epitope in Huntington's disease and four dominant cerebellar ataxias. *Nature* **378**, 403-406
89. Trottier, Y., Devys, D., Imbert, G., Saudou, F., An, I., Lutz, Y., Weber, C., Agid, Y., Hirsch, E. C., and Mandel, J. L. (1995) Cellular localization of the Huntington's disease protein and discrimination of the normal and mutated form. *Nature genetics* **10**, 104-110
90. Kuemmerle, S., Gutekunst, C. A., Klein, A. M., Li, X. J., Li, S. H., Beal, M. F., Hersch, S. M., and Ferrante, R. J. (1999) Huntington aggregates may not predict neuronal death in Huntington's disease. *Annals of neurology* **46**, 842-849
91. Ambrose, C. M., Duyao, M. P., Barnes, G., Bates, G. P., Lin, C. S., Srinidhi, J., Baxendale, S., Hummerich, H., Lehrach, H., Altherr, M., Wasmuth, J., Buckler, A., Church, D.,

- Housman, D., Berks, M., Micklem, G., Durbin, R., Dodge, A., Read, A., Gusella, J., and MacDonald, M. (1994) Structure and expression of the Huntington's disease gene: evidence against simple inactivation due to an expanded CAG repeat. *Somatic cell and molecular genetics* **20**, 27-38
92. Barnes, G. T., Duyao, M. P., Ambrose, C. M., McNeil, S., Persichetti, F., Srinidhi, J., Gusella, J. F., and MacDonald, M. E. (1994) Mouse Huntington's disease gene homolog (Hdh). *Somatic cell and molecular genetics* **20**, 87-97
93. Tartari, M., Gissi, C., Lo Sardo, V., Zuccato, C., Picardi, E., Pesole, G., and Cattaneo, E. (2008) Phylogenetic comparison of huntingtin homologues reveals the appearance of a primitive polyQ in sea urchin. *Molecular biology and evolution* **25**, 330-338
94. DiFiglia, M., Sapp, E., Chase, K., Schwarz, C., Meloni, A., Young, C., Martin, E., Vonsattel, J. P., Carraway, R., Reeves, S. A., Boyce, F. M., and Aronin, N. (1995) Huntingtin is a cytoplasmic protein associated with vesicles in human and rat brain neurons. *Neuron* **14**, 1075-1081
95. Landwehrmeyer, G. B., McNeil, S. M., Dure, L. S. t., Ge, P., Aizawa, H., Huang, Q., Ambrose, C. M., Duyao, M. P., Bird, E. D., Bonilla, E., Young, M., Avila-Gonzales, A. J., Wexler, N. S., Difiglia, M., Gusella, J., MacDonald, M., Penney, J., Young, A. B., and Vonsattel, J. P. (1995) Huntington's disease gene: regional and cellular expression in brain of normal and affected individuals. *Annals of neurology* **37**, 218-230
96. Duyao, M. P., Auerbach, A. B., Ryan, A., Persichetti, F., Barnes, G. T., McNeil, S. M., Ge, P., Vonsattel, J. P., Gusella, J. F., Joyner, A. L., and MacDonald, M. E. (1995) Inactivation of the mouse Huntington's disease gene homolog Hdh. *Science* **269**, 407-410

97. Nasir, J., Floresco, S. B., O'Kusky, J. R., Diewert, V. M., Richman, J. M., Zeisler, J., Borowski, A., Marth, J. D., Phillips, A. G., and Hayden, M. R. (1995) Targeted disruption of the Huntington's disease gene results in embryonic lethality and behavioral and morphological changes in heterozygotes. *Cell* **81**, 811-823
98. Dragatsis, I., Levine, M. S., and Zeitlin, S. (2000) Inactivation of Hdh in the brain and testis results in progressive neurodegeneration and sterility in mice. *Nature genetics* **26**, 300-306
99. Guo, Q., Bin, H., Cheng, J., Seefeldt, M., Engler, T., Pfeifer, G., Oeckl, P., Otto, M., Moser, F., Maurer, M., Pautsch, A., Baumeister, W., Fernandez-Busnadiego, R., and Kochanek, S. (2018) The cryo-electron microscopy structure of huntingtin. *Nature* **555**, 117-120
100. Andrade, M. A., and Bork, P. (1995) HEAT repeats in the Huntington's disease protein. *Nature genetics* **11**, 115-116
101. Yoshimura, S. H., and Hirano, T. (2016) HEAT repeats - versatile arrays of amphiphilic helices working in crowded environments? *Journal of cell science* **129**, 3963-3970
102. Desmond, C. R., Atwal, R. S., Xia, J., and Truant, R. (2012) Identification of a karyopherin beta1/beta2 proline-tyrosine nuclear localization signal in huntingtin protein. *The Journal of biological chemistry* **287**, 39626-39633
103. Xia, J., Lee, D. H., Taylor, J., Vandelft, M., and Truant, R. (2003) Huntingtin contains a highly conserved nuclear export signal. *Human molecular genetics* **12**, 1393-1403
104. Cornett, J., Cao, F., Wang, C. E., Ross, C. A., Bates, G. P., Li, S. H., and Li, X. J. (2005) Polyglutamine expansion of huntingtin impairs its nuclear export. *Nature genetics* **37**, 198-204

105. Davies, S. W., Turmaine, M., Cozens, B. A., DiFiglia, M., Sharp, A. H., Ross, C. A., Scherzinger, E., Wanker, E. E., Mangiarini, L., and Bates, G. P. (1997) Formation of neuronal intranuclear inclusions underlies the neurological dysfunction in mice transgenic for the HD mutation. *Cell* **90**, 537-548
106. Wang, Y., Lin, F., and Qin, Z. H. (2010) The role of post-translational modifications of huntingtin in the pathogenesis of Huntington's disease. *Neuroscience bulletin* **26**, 153-162
107. Steffan, J. S., Agrawal, N., Pallos, J., Rockabrand, E., Trotman, L. C., Slepko, N., Illes, K., Lukacsovich, T., Zhu, Y. Z., Cattaneo, E., Pandolfi, P. P., Thompson, L. M., and Marsh, J. L. (2004) SUMO modification of Huntingtin and Huntington's disease pathology. *Science* **304**, 100-104
108. Cariulo, C., Azzollini, L., Verani, M., Martufi, P., Boggio, R., Chiki, A., Deguire, S. M., Cherubini, M., Gines, S., Marsh, J. L., Conforti, P., Cattaneo, E., Santimone, I., Squitieri, F., Lashuel, H. A., Petricca, L., and Caricasole, A. (2017) Phosphorylation of huntingtin at residue T3 is decreased in Huntington's disease and modulates mutant huntingtin protein conformation. *Proceedings of the National Academy of Sciences of the United States of America* **114**, E10809-E10818
109. Chiki, A., DeGuire, S. M., Ruggeri, F. S., Sanfelice, D., Ansaloni, A., Wang, Z. M., Cendrowska, U., Burai, R., Vieweg, S., Pastore, A., Dietler, G., and Lashuel, H. A. (2017) Mutant Exon1 Huntingtin Aggregation is Regulated by T3 Phosphorylation-Induced Structural Changes and Crosstalk between T3 Phosphorylation and Acetylation at K6. *Angewandte Chemie* **56**, 5202-5207
110. Bustamante, M. B., Ansaloni, A., Pedersen, J. F., Azzollini, L., Cariulo, C., Wang, Z. M., Petricca, L., Verani, M., Puglisi, F., Park, H., Lashuel, H., and Caricasole, A. (2015)

- Detection of huntingtin exon 1 phosphorylation by Phos-Tag SDS-PAGE: Predominant phosphorylation on threonine 3 and regulation by IKKbeta. *Biochemical and biophysical research communications* **463**, 1317-1322
111. Aiken, C. T., Steffan, J. S., Guerrero, C. M., Khashwji, H., Lukacsovich, T., Simmons, D., Purcell, J. M., Menhaji, K., Zhu, Y. Z., Green, K., Laferla, F., Huang, L., Thompson, L. M., and Marsh, J. L. (2009) Phosphorylation of threonine 3: implications for Huntingtin aggregation and neurotoxicity. *The Journal of biological chemistry* **284**, 29427-29436
112. Thompson, L. M., Aiken, C. T., Kaltenbach, L. S., Agrawal, N., Illes, K., Khoshnan, A., Martinez-Vincente, M., Arrasate, M., O'Rourke, J. G., Khashwji, H., Lukacsovich, T., Zhu, Y. Z., Lau, A. L., Massey, A., Hayden, M. R., Zeitlin, S. O., Finkbeiner, S., Green, K. N., LaFerla, F. M., Bates, G., Huang, L., Patterson, P. H., Lo, D. C., Cuervo, A. M., Marsh, J. L., and Steffan, J. S. (2009) IKK phosphorylates Huntingtin and targets it for degradation by the proteasome and lysosome. *The Journal of cell biology* **187**, 1083-1099
113. Atwal, R. S., Desmond, C. R., Caron, N., Maiuri, T., Xia, J., Sipione, S., and Truant, R. (2011) Kinase inhibitors modulate huntingtin cell localization and toxicity. *Nature chemical biology* **7**, 453-460
114. Gu, X., Greiner, E. R., Mishra, R., Kodali, R., Osmand, A., Finkbeiner, S., Steffan, J. S., Thompson, L. M., Wetzel, R., and Yang, X. W. (2009) Serines 13 and 16 are critical determinants of full-length human mutant huntingtin induced disease pathogenesis in HD mice. *Neuron* **64**, 828-840
115. Di Pardo, A., Maglione, V., Alpaugh, M., Horkey, M., Atwal, R. S., Sassone, J., Ciammola, A., Steffan, J. S., Fouad, K., Truant, R., and Sipione, S. (2012) Ganglioside GM1 induces phosphorylation of mutant huntingtin and restores normal motor behavior in Huntington

- disease mice. *Proceedings of the National Academy of Sciences of the United States of America* **109**, 3528-3533
116. Humbert, S., Bryson, E. A., Cordelieres, F. P., Connors, N. C., Datta, S. R., Finkbeiner, S., Greenberg, M. E., and Saudou, F. (2002) The IGF-1/Akt pathway is neuroprotective in Huntington's disease and involves Huntingtin phosphorylation by Akt. *Developmental cell* **2**, 831-837
117. Luo, S., Vacher, C., Davies, J. E., and Rubinsztein, D. C. (2005) Cdk5 phosphorylation of huntingtin reduces its cleavage by caspases: implications for mutant huntingtin toxicity. *The Journal of cell biology* **169**, 647-656
118. Warby, S. C., Chan, E. Y., Metzler, M., Gan, L., Singaraja, R. R., Crocker, S. F., Robertson, H. A., and Hayden, M. R. (2005) Huntingtin phosphorylation on serine 421 is significantly reduced in the striatum and by polyglutamine expansion in vivo. *Human molecular genetics* **14**, 1569-1577
119. Schilling, B., Gafni, J., Torcassi, C., Cong, X., Row, R. H., LaFevre-Bernt, M. A., Cusack, M. P., Ratovitski, T., Hirschhorn, R., Ross, C. A., Gibson, B. W., and Ellerby, L. M. (2006) Huntingtin phosphorylation sites mapped by mass spectrometry. Modulation of cleavage and toxicity. *The Journal of biological chemistry* **281**, 23686-23697
120. Zala, D., Colin, E., Rangone, H., Liot, G., Humbert, S., and Saudou, F. (2008) Phosphorylation of mutant huntingtin at S421 restores anterograde and retrograde transport in neurons. *Human molecular genetics* **17**, 3837-3846
121. Metzler, M., Gan, L., Mazarei, G., Graham, R. K., Liu, L., Bissada, N., Lu, G., Leavitt, B. R., and Hayden, M. R. (2010) Phosphorylation of huntingtin at Ser421 in YAC128 neurons is associated with protection of YAC128 neurons from NMDA-mediated excitotoxicity

- and is modulated by PP1 and PP2A. *The Journal of neuroscience : the official journal of the Society for Neuroscience* **30**, 14318-14329
122. Watkin, E. E., Arbez, N., Waldron-Roby, E., O'Meally, R., Ratovitski, T., Cole, R. N., and Ross, C. A. (2014) Phosphorylation of mutant huntingtin at serine 116 modulates neuronal toxicity. *PLoS one* **9**, e88284
 123. Jeong, H., Then, F., Melia, T. J., Jr., Mazzulli, J. R., Cui, L., Savas, J. N., Voisine, C., Paganetti, P., Tanese, N., Hart, A. C., Yamamoto, A., and Krainc, D. (2009) Acetylation targets mutant huntingtin to autophagosomes for degradation. *Cell* **137**, 60-72
 124. Yanai, A., Huang, K., Kang, R., Singaraja, R. R., Arstikaitis, P., Gan, L., Orban, P. C., Mullard, A., Cowan, C. M., Raymond, L. A., Drisdell, R. C., Green, W. N., Ravikumar, B., Rubinsztein, D. C., El-Husseini, A., and Hayden, M. R. (2006) Palmitoylation of huntingtin by HIP14 is essential for its trafficking and function. *Nature neuroscience* **9**, 824-831
 125. Martin, D. D., Heit, R. J., Yap, M. C., Davidson, M. W., Hayden, M. R., and Berthiaume, L. G. (2014) Identification of a post-translationally myristoylated autophagy-inducing domain released by caspase cleavage of huntingtin. *Human molecular genetics* **23**, 3166-3179
 126. Zhang, Y., Li, M., Drozda, M., Chen, M., Ren, S., Mejia Sanchez, R. O., Leavitt, B. R., Cattaneo, E., Ferrante, R. J., Hayden, M. R., and Friedlander, R. M. (2003) Depletion of wild-type huntingtin in mouse models of neurologic diseases. *Journal of neurochemistry* **87**, 101-106
 127. Rigamonti, D., Bauer, J. H., De-Fraja, C., Conti, L., Sipione, S., Sciorati, C., Clementi, E., Hackam, A., Hayden, M. R., Li, Y., Cooper, J. K., Ross, C. A., Govoni, S., Vincenz, C., and Cattaneo, E. (2000) Wild-type huntingtin protects from apoptosis upstream of caspase-

3. *The Journal of neuroscience : the official journal of the Society for Neuroscience* **20**, 3705-3713
128. Rigamonti, D., Sipione, S., Goffredo, D., Zuccato, C., Fossale, E., and Cattaneo, E. (2001) Huntingtin's neuroprotective activity occurs via inhibition of procaspase-9 processing. *The Journal of biological chemistry* **276**, 14545-14548
129. Leavitt, B. R., van Raamsdonk, J. M., Shehadeh, J., Fernandes, H., Murphy, Z., Graham, R. K., Wellington, C. L., Raymond, L. A., and Hayden, M. R. (2006) Wild-type huntingtin protects neurons from excitotoxicity. *Journal of neurochemistry* **96**, 1121-1129
130. Gervais, F. G., Singaraja, R., Xanthoudakis, S., Gutekunst, C. A., Leavitt, B. R., Metzler, M., Hackam, A. S., Tam, J., Vaillancourt, J. P., Houtzager, V., Rasper, D. M., Roy, S., Hayden, M. R., and Nicholson, D. W. (2002) Recruitment and activation of caspase-8 by the Huntingtin-interacting protein Hip-1 and a novel partner Hippi. *Nature cell biology* **4**, 95-105
131. Majumder, P., Chattopadhyay, B., Mazumder, A., Das, P., and Bhattacharyya, N. P. (2006) Induction of apoptosis in cells expressing exogenous Hippi, a molecular partner of huntingtin-interacting protein Hip1. *Neurobiology of disease* **22**, 242-256
132. Bhattacharyya, N. P., Banerjee, M., and Majumder, P. (2008) Huntington's disease: roles of huntingtin-interacting protein 1 (HIP-1) and its molecular partner HIPPI in the regulation of apoptosis and transcription. *The FEBS journal* **275**, 4271-4279
133. Zuccato, C., and Cattaneo, E. (2009) Brain-derived neurotrophic factor in neurodegenerative diseases. *Nature reviews. Neurology* **5**, 311-322
134. Zuccato, C., Tartari, M., Crotti, A., Goffredo, D., Valenza, M., Conti, L., Cataudella, T., Leavitt, B. R., Hayden, M. R., Timmusk, T., Rigamonti, D., and Cattaneo, E. (2003)

- Huntingtin interacts with REST/NRSF to modulate the transcription of NRSE-controlled neuronal genes. *Nature genetics* **35**, 76-83
135. Buren, C., Wang, L., Smith-Dijak, A., and Raymond, L. A. (2014) Region-specific pro-survival signaling and global neuronal protection by wild-type Huntingtin. *Journal of Huntington's disease* **3**, 365-376
136. Caviston, J. P., and Holzbaur, E. L. (2009) Huntingtin as an essential integrator of intracellular vesicular trafficking. *Trends in cell biology* **19**, 147-155
137. Truant, R., Atwal, R., and Burtnik, A. (2006) Hypothesis: Huntingtin may function in membrane association and vesicular trafficking. *Biochemistry and cell biology = Biochimie et biologie cellulaire* **84**, 912-917
138. Atwal, R. S., Xia, J., Pinchev, D., Taylor, J., Epand, R. M., and Truant, R. (2007) Huntingtin has a membrane association signal that can modulate huntingtin aggregation, nuclear entry and toxicity. *Human molecular genetics* **16**, 2600-2615
139. Kegel, K. B., Sapp, E., Yoder, J., Cuiffo, B., Sobin, L., Kim, Y. J., Qin, Z. H., Hayden, M. R., Aronin, N., Scott, D. L., Isenberg, G., Goldmann, W. H., and DiFiglia, M. (2005) Huntingtin associates with acidic phospholipids at the plasma membrane. *The Journal of biological chemistry* **280**, 36464-36473
140. Colin, E., Zala, D., Liot, G., Rangone, H., Borrell-Pages, M., Li, X. J., Saudou, F., and Humbert, S. (2008) Huntingtin phosphorylation acts as a molecular switch for anterograde/retrograde transport in neurons. *The EMBO journal* **27**, 2124-2134
141. Caviston, J. P., Ross, J. L., Antony, S. M., Tokito, M., and Holzbaur, E. L. (2007) Huntingtin facilitates dynein/dynactin-mediated vesicle transport. *Proceedings of the National Academy of Sciences of the United States of America* **104**, 10045-10050

142. Rong, J., McGuire, J. R., Fang, Z. H., Sheng, G., Shin, J. Y., Li, S. H., and Li, X. J. (2006) Regulation of intracellular trafficking of huntingtin-associated protein-1 is critical for TrkA protein levels and neurite outgrowth. *The Journal of neuroscience : the official journal of the Society for Neuroscience* **26**, 6019-6030
143. Engelender, S., Sharp, A. H., Colomer, V., Tokito, M. K., Lanahan, A., Worley, P., Holzbaur, E. L., and Ross, C. A. (1997) Huntingtin-associated protein 1 (HAP1) interacts with the p150Glued subunit of dynactin. *Human molecular genetics* **6**, 2205-2212
144. Li, S. H., Gutekunst, C. A., Hersch, S. M., and Li, X. J. (1998) Interaction of huntingtin-associated protein with dynactin P150Glued. *The Journal of neuroscience : the official journal of the Society for Neuroscience* **18**, 1261-1269
145. Colomer, V., Engelender, S., Sharp, A. H., Duan, K., Cooper, J. K., Lanahan, A., Lyford, G., Worley, P., and Ross, C. A. (1997) Huntingtin-associated protein 1 (HAP1) binds to a Trio-like polypeptide, with a rac1 guanine nucleotide exchange factor domain. *Human molecular genetics* **6**, 1519-1525
146. Gauthier, L. R., Charrin, B. C., Borrell-Pages, M., Dompierre, J. P., Rangone, H., Cordelieres, F. P., De Mey, J., MacDonald, M. E., Lessmann, V., Humbert, S., and Saudou, F. (2004) Huntingtin controls neurotrophic support and survival of neurons by enhancing BDNF vesicular transport along microtubules. *Cell* **118**, 127-138
147. Her, L. S., and Goldstein, L. S. (2008) Enhanced sensitivity of striatal neurons to axonal transport defects induced by mutant huntingtin. *The Journal of neuroscience : the official journal of the Society for Neuroscience* **28**, 13662-13672
148. Smith, R., Brundin, P., and Li, J. Y. (2005) Synaptic dysfunction in Huntington's disease: a new perspective. *Cellular and molecular life sciences : CMLS* **62**, 1901-1912

149. Sun, Y., Savanenin, A., Reddy, P. H., and Liu, Y. F. (2001) Polyglutamine-expanded huntingtin promotes sensitization of N-methyl-D-aspartate receptors via post-synaptic density 95. *The Journal of biological chemistry* **276**, 24713-24718
150. Cattaneo, E., Rigamonti, D., Goffredo, D., Zuccato, C., Squitieri, F., and Sipione, S. (2001) Loss of normal huntingtin function: new developments in Huntington's disease research. *Trends in neurosciences* **24**, 182-188
151. Nucifora, F. C., Jr., Sasaki, M., Peters, M. F., Huang, H., Cooper, J. K., Yamada, M., Takahashi, H., Tsuji, S., Troncoso, J., Dawson, V. L., Dawson, T. M., and Ross, C. A. (2001) Interference by huntingtin and atrophin-1 with cbp-mediated transcription leading to cellular toxicity. *Science* **291**, 2423-2428
152. Martinez-Vicente, M., Talloczy, Z., Wong, E., Tang, G., Koga, H., Kaushik, S., de Vries, R., Arias, E., Harris, S., Sulzer, D., and Cuervo, A. M. (2010) Cargo recognition failure is responsible for inefficient autophagy in Huntington's disease. *Nature neuroscience* **13**, 567-576
153. Wellington, C. L., Ellerby, L. M., Hackam, A. S., Margolis, R. L., Trifiro, M. A., Singaraja, R., McCutcheon, K., Salvesen, G. S., Propp, S. S., Bromm, M., Rowland, K. J., Zhang, T., Rasper, D., Roy, S., Thornberry, N., Pinsky, L., Kakizuka, A., Ross, C. A., Nicholson, D. W., Bredesen, D. E., and Hayden, M. R. (1998) Caspase cleavage of gene products associated with triplet expansion disorders generates truncated fragments containing the polyglutamine tract. *The Journal of biological chemistry* **273**, 9158-9167
154. Wellington, C. L., Leavitt, B. R., and Hayden, M. R. (2000) Huntington disease: new insights on the role of huntingtin cleavage. *Journal of neural transmission. Supplementum*, 1-17

155. Wellington, C. L., Singaraja, R., Ellerby, L., Savill, J., Roy, S., Leavitt, B., Cattaneo, E., Hackam, A., Sharp, A., Thornberry, N., Nicholson, D. W., Bredesen, D. E., and Hayden, M. R. (2000) Inhibiting caspase cleavage of huntingtin reduces toxicity and aggregate formation in neuronal and nonneuronal cells. *The Journal of biological chemistry* **275**, 19831-19838
156. Kim, Y. J., Yi, Y., Sapp, E., Wang, Y., Cuiffo, B., Kegel, K. B., Qin, Z. H., Aronin, N., and DiFiglia, M. (2001) Caspase 3-cleaved N-terminal fragments of wild-type and mutant huntingtin are present in normal and Huntington's disease brains, associate with membranes, and undergo calpain-dependent proteolysis. *Proceedings of the National Academy of Sciences of the United States of America* **98**, 12784-12789
157. Wellington, C. L., Ellerby, L. M., Gutekunst, C. A., Rogers, D., Warby, S., Graham, R. K., Loubser, O., van Raamsdonk, J., Singaraja, R., Yang, Y. Z., Gafni, J., Bredesen, D., Hersch, S. M., Leavitt, B. R., Roy, S., Nicholson, D. W., and Hayden, M. R. (2002) Caspase cleavage of mutant huntingtin precedes neurodegeneration in Huntington's disease. *The Journal of neuroscience : the official journal of the Society for Neuroscience* **22**, 7862-7872
158. Gafni, J., Hermel, E., Young, J. E., Wellington, C. L., Hayden, M. R., and Ellerby, L. M. (2004) Inhibition of calpain cleavage of huntingtin reduces toxicity: accumulation of calpain/caspase fragments in the nucleus. *The Journal of biological chemistry* **279**, 20211-20220
159. Hermel, E., Gafni, J., Propp, S. S., Leavitt, B. R., Wellington, C. L., Young, J. E., Hackam, A. S., Logvinova, A. V., Peel, A. L., Chen, S. F., Hook, V., Singaraja, R., Krajewski, S., Goldsmith, P. C., Ellerby, H. M., Hayden, M. R., Bredesen, D. E., and Ellerby, L. M.

- (2004) Specific caspase interactions and amplification are involved in selective neuronal vulnerability in Huntington's disease. *Cell death and differentiation* **11**, 424-438
160. Graham, R. K., Deng, Y., Slow, E. J., Haigh, B., Bissada, N., Lu, G., Pearson, J., Shehadeh, J., Bertram, L., Murphy, Z., Warby, S. C., Doty, C. N., Roy, S., Wellington, C. L., Leavitt, B. R., Raymond, L. A., Nicholson, D. W., and Hayden, M. R. (2006) Cleavage at the caspase-6 site is required for neuronal dysfunction and degeneration due to mutant huntingtin. *Cell* **125**, 1179-1191
161. Landles, C., Sathasivam, K., Weiss, A., Woodman, B., Moffitt, H., Finkbeiner, S., Sun, B., Gafni, J., Ellerby, L. M., Trotter, Y., Richards, W. G., Osmand, A., Paganetti, P., and Bates, G. P. (2010) Proteolysis of mutant huntingtin produces an exon 1 fragment that accumulates as an aggregated protein in neuronal nuclei in Huntington disease. *The Journal of biological chemistry* **285**, 8808-8823
162. Schilling, G., Klevytska, A., Tebbenkamp, A. T., Juenemann, K., Cooper, J., Gonzales, V., Slunt, H., Poirer, M., Ross, C. A., and Borchelt, D. R. (2007) Characterization of huntingtin pathologic fragments in human Huntington disease, transgenic mice, and cell models. *Journal of neuropathology and experimental neurology* **66**, 313-320
163. El-Daher, M. T., Hangen, E., Bruyere, J., Poizat, G., Al-Ramahi, I., Pardo, R., Bourg, N., Souquere, S., Mayet, C., Pierron, G., Leveque-Fort, S., Botas, J., Humbert, S., and Saudou, F. (2015) Huntingtin proteolysis releases non-polyQ fragments that cause toxicity through dynamin 1 dysregulation. *The EMBO journal* **34**, 2255-2271
164. Gipson, T. A., Neueder, A., Wexler, N. S., Bates, G. P., and Housman, D. (2013) Aberrantly spliced HTT, a new player in Huntington's disease pathogenesis. *RNA biology* **10**, 1647-1652

165. Sathasivam, K., Neueder, A., Gipson, T. A., Landles, C., Benjamin, A. C., Bondulich, M. K., Smith, D. L., Faull, R. L., Roos, R. A., Howland, D., Detloff, P. J., Housman, D. E., and Bates, G. P. (2013) Aberrant splicing of HTT generates the pathogenic exon 1 protein in Huntington disease. *Proceedings of the National Academy of Sciences of the United States of America* **110**, 2366-2370
166. Mangiarini, L., Sathasivam, K., Seller, M., Cozens, B., Harper, A., Hetherington, C., Lawton, M., Trottier, Y., Lehrach, H., Davies, S. W., and Bates, G. P. (1996) Exon 1 of the HD gene with an expanded CAG repeat is sufficient to cause a progressive neurological phenotype in transgenic mice. *Cell* **87**, 493-506
167. Neueder, A., Landles, C., Ghosh, R., Howland, D., Myers, R. H., Faull, R. L. M., Tabrizi, S. J., and Bates, G. P. (2017) The pathogenic exon 1 HTT protein is produced by incomplete splicing in Huntington's disease patients. *Scientific reports* **7**, 1307
168. Wagner, A. S., Politi, A. Z., Ast, A., Bravo-Rodriguez, K., Baum, K., Buntru, A., Stempel, N. U., Brusendorf, L., Hanig, C., Boeddrich, A., Plassmann, S., Klockmeier, K., Ramirez-Anguita, J. M., Sanchez-Garcia, E., Wolf, J., and Wanker, E. E. (2018) Self-assembly of Mutant Huntingtin Exon-1 Fragments into Large Complex Fibrillar Structures Involves Nucleated Branching. *Journal of molecular biology*
169. Legleiter, J., Mitchell, E., Lotz, G. P., Sapp, E., Ng, C., DiFiglia, M., Thompson, L. M., and Muchowski, P. J. (2010) Mutant huntingtin fragments form oligomers in a polyglutamine length-dependent manner in vitro and in vivo. *The Journal of biological chemistry* **285**, 14777-14790
170. Martindale, D., Hackam, A., Wieczorek, A., Ellerby, L., Wellington, C., McCutcheon, K., Singaraja, R., Kazemi-Esfarjani, P., Devon, R., Kim, S. U., Bredesen, D. E., Tufaro, F.,

- and Hayden, M. R. (1998) Length of huntingtin and its polyglutamine tract influences localization and frequency of intracellular aggregates. *Nature genetics* **18**, 150-154
171. Sapp, E., Schwarz, C., Chase, K., Bhide, P. G., Young, A. B., Penney, J., Vonsattel, J. P., Aronin, N., and DiFiglia, M. (1997) Huntingtin localization in brains of normal and Huntington's disease patients. *Annals of neurology* **42**, 604-612
172. Sathasivam, K., Lane, A., Legleiter, J., Warley, A., Woodman, B., Finkbeiner, S., Paganetti, P., Muchowski, P. J., Wilson, S., and Bates, G. P. (2010) Identical oligomeric and fibrillar structures captured from the brains of R6/2 and knock-in mouse models of Huntington's disease. *Human molecular genetics* **19**, 65-78
173. Hackam, A. S., Singaraja, R., Wellington, C. L., Metzler, M., McCutcheon, K., Zhang, T., Kalchman, M., and Hayden, M. R. (1998) The influence of huntingtin protein size on nuclear localization and cellular toxicity. *The Journal of cell biology* **141**, 1097-1105
174. Li, S. H., and Li, X. J. (1998) Aggregation of N-terminal huntingtin is dependent on the length of its glutamine repeats. *Human molecular genetics* **7**, 777-782
175. Ross, C. A., and Poirier, M. A. (2005) Opinion: What is the role of protein aggregation in neurodegeneration? *Nature reviews. Molecular cell biology* **6**, 891-898
176. Branco-Santos, J., Herrera, F., Pocas, G. M., Pires-Afonso, Y., Giorgini, F., Domingos, P. M., and Outeiro, T. F. (2017) Protein phosphatase 1 regulates huntingtin exon 1 aggregation and toxicity. *Human molecular genetics* **26**, 3763-3775
177. Yamamoto, A., Lucas, J. J., and Hen, R. (2000) Reversal of neuropathology and motor dysfunction in a conditional model of Huntington's disease. *Cell* **101**, 57-66
178. Schilling, G., Becher, M. W., Sharp, A. H., Jinnah, H. A., Duan, K., Kotzuk, J. A., Slunt, H. H., Ratovitski, T., Cooper, J. K., Jenkins, N. A., Copeland, N. G., Price, D. L., Ross, C.

- A., and Borchelt, D. R. (1999) Intranuclear inclusions and neuritic aggregates in transgenic mice expressing a mutant N-terminal fragment of huntingtin. *Human molecular genetics* **8**, 397-407
179. Slow, E. J., van Raamsdonk, J., Rogers, D., Coleman, S. H., Graham, R. K., Deng, Y., Oh, R., Bissada, N., Hossain, S. M., Yang, Y. Z., Li, X. J., Simpson, E. M., Gutekunst, C. A., Leavitt, B. R., and Hayden, M. R. (2003) Selective striatal neuronal loss in a YAC128 mouse model of Huntington disease. *Human molecular genetics* **12**, 1555-1567
180. Gray, M., Shirasaki, D. I., Cepeda, C., Andre, V. M., Wilburn, B., Lu, X. H., Tao, J., Yamazaki, I., Li, S. H., Sun, Y. E., Li, X. J., Levine, M. S., and Yang, X. W. (2008) Full-length human mutant huntingtin with a stable polyglutamine repeat can elicit progressive and selective neuropathogenesis in BACHD mice. *The Journal of neuroscience : the official journal of the Society for Neuroscience* **28**, 6182-6195
181. Gong, B., Lim, M. C., Wanderer, J., Wytttenbach, A., and Morton, A. J. (2008) Time-lapse analysis of aggregate formation in an inducible PC12 cell model of Huntington's disease reveals time-dependent aggregate formation that transiently delays cell death. *Brain research bulletin* **75**, 146-157
182. Cajavec, B., Bernard, S., and Herzog, H. (2005) Aggregation in Huntington's disease: insights through modelling. *Genome informatics. International Conference on Genome Informatics* **16**, 262-271
183. Mukai, H., Isagawa, T., Goyama, E., Tanaka, S., Bence, N. F., Tamura, A., Ono, Y., and Kopito, R. R. (2005) Formation of morphologically similar globular aggregates from diverse aggregation-prone proteins in mammalian cells. *Proceedings of the National Academy of Sciences of the United States of America* **102**, 10887-10892

184. Sun, C. S., Lee, C. C., Li, Y. N., Yao-Chen Yang, S., Lin, C. H., Chang, Y. C., Liu, P. F., He, R. Y., Wang, C. H., Chen, W., Chern, Y., and Jen-Tse Huang, J. (2015) Conformational switch of polyglutamine-expanded huntingtin into benign aggregates leads to neuroprotective effect. *Scientific reports* **5**, 14992
185. Fontan-Lozano, A., Lopez-Lluch, G., Delgado-Garcia, J. M., Navas, P., and Carrion, A. M. (2008) Molecular bases of caloric restriction regulation of neuronal synaptic plasticity. *Molecular neurobiology* **38**, 167-177
186. Chan, D. C. (2006) Mitochondria: dynamic organelles in disease, aging, and development. *Cell* **125**, 1241-1252
187. Moran, M., Moreno-Lastres, D., Marin-Buera, L., Arenas, J., Martin, M. A., and Ugalde, C. (2012) Mitochondrial respiratory chain dysfunction: implications in neurodegeneration. *Free radical biology & medicine* **53**, 595-609
188. Martin, L. J. (2012) Biology of mitochondria in neurodegenerative diseases. *Progress in molecular biology and translational science* **107**, 355-415
189. Arduino, D. M., Esteves, A. R., and Cardoso, S. M. (2011) Mitochondrial fusion/fission, transport and autophagy in Parkinson's disease: when mitochondria get nasty. *Parkinson's disease* **2011**, 767230
190. Delettre, C., Lenaers, G., Griffoin, J. M., Gigarel, N., Lorenzo, C., Belenguer, P., Pelloquin, L., Grosgeorge, J., Turc-Carel, C., Perret, E., Astarie-Dequeker, C., Lasquelléc, L., Arnaud, B., Ducommun, B., Kaplan, J., and Hamel, C. P. (2000) Nuclear gene OPA1, encoding a mitochondrial dynamin-related protein, is mutated in dominant optic atrophy. *Nature genetics* **26**, 207-210

191. Zuchner, S., Mersiyanova, I. V., Muglia, M., Bissar-Tadmouri, N., Rochelle, J., Dadali, E. L., Zappia, M., Nelis, E., Patitucci, A., Senderek, J., Parman, Y., Evgrafov, O., Jonghe, P. D., Takahashi, Y., Tsuji, S., Pericak-Vance, M. A., Quattrone, A., Battaloglu, E., Polyakov, A. V., Timmerman, V., Schroder, J. M., and Vance, J. M. (2004) Mutations in the mitochondrial GTPase mitofusin 2 cause Charcot-Marie-Tooth neuropathy type 2A. *Nature genetics* **36**, 449-451
192. Wanker, E. E. (2002) Hip1 and Hipp1 participate in a novel cell death-signaling pathway. *Developmental cell* **2**, 126-128
193. Li, S. H., and Li, X. J. (2004) Huntingtin-protein interactions and the pathogenesis of Huntington's disease. *Trends in genetics : TIG* **20**, 146-154
194. Borrell-Pages, M., Zala, D., Humbert, S., and Saudou, F. (2006) Huntington's disease: from huntingtin function and dysfunction to therapeutic strategies. *Cellular and molecular life sciences : CMLS* **63**, 2642-2660
195. Kaltenbach, L. S., Romero, E., Becklin, R. R., Chettier, R., Bell, R., Phansalkar, A., Strand, A., Torcassi, C., Savage, J., Hurlburt, A., Cha, G. H., Ukani, L., Chepanoske, C. L., Zhen, Y., Sahasrabudhe, S., Olson, J., Kurschner, C., Ellerby, L. M., Peltier, J. M., Botas, J., and Hughes, R. E. (2007) Huntingtin interacting proteins are genetic modifiers of neurodegeneration. *PLoS genetics* **3**, e82
196. Kim, J., Moody, J. P., Edgerly, C. K., Bordiuk, O. L., Cormier, K., Smith, K., Beal, M. F., and Ferrante, R. J. (2010) Mitochondrial loss, dysfunction and altered dynamics in Huntington's disease. *Human molecular genetics* **19**, 3919-3935
197. Shirendeb, U., Reddy, A. P., Manczak, M., Calkins, M. J., Mao, P., Tagle, D. A., and Reddy, P. H. (2011) Abnormal mitochondrial dynamics, mitochondrial loss and mutant

- huntingtin oligomers in Huntington's disease: implications for selective neuronal damage. *Human molecular genetics* **20**, 1438-1455
198. Shirendeb, U. P., Calkins, M. J., Manczak, M., Anekonda, V., Dufour, B., McBride, J. L., Mao, P., and Reddy, P. H. (2012) Mutant huntingtin's interaction with mitochondrial protein Drp1 impairs mitochondrial biogenesis and causes defective axonal transport and synaptic degeneration in Huntington's disease. *Human molecular genetics* **21**, 406-420
199. Song, W., Chen, J., Petrilli, A., Liot, G., Klinglmayr, E., Zhou, Y., Poquiz, P., Tjong, J., Pouladi, M. A., Hayden, M. R., Masliah, E., Ellisman, M., Rouiller, I., Schwarzenbacher, R., Bossy, B., Perkins, G., and Bossy-Wetzler, E. (2011) Mutant huntingtin binds the mitochondrial fission GTPase dynamin-related protein-1 and increases its enzymatic activity. *Nature medicine* **17**, 377-382
200. Perez-Severiano, F., Rios, C., and Segovia, J. (2000) Striatal oxidative damage parallels the expression of a neurological phenotype in mice transgenic for the mutation of Huntington's disease. *Brain research* **862**, 234-237
201. Bogdanov, M. B., Andreassen, O. A., Dedeoglu, A., Ferrante, R. J., and Beal, M. F. (2001) Increased oxidative damage to DNA in a transgenic mouse model of Huntington's disease. *Journal of neurochemistry* **79**, 1246-1249
202. Polidori, M. C., Mecocci, P., Browne, S. E., Senin, U., and Beal, M. F. (1999) Oxidative damage to mitochondrial DNA in Huntington's disease parietal cortex. *Neuroscience letters* **272**, 53-56
203. Pickrell, A. M., and Youle, R. J. (2015) The roles of PINK1, parkin, and mitochondrial fidelity in Parkinson's disease. *Neuron* **85**, 257-273

204. Narendra, D. P., Jin, S. M., Tanaka, A., Suen, D. F., Gautier, C. A., Shen, J., Cookson, M. R., and Youle, R. J. (2010) PINK1 is selectively stabilized on impaired mitochondria to activate Parkin. *PLoS biology* **8**, e1000298
205. Geisler, S., Holmstrom, K. M., Skujat, D., Fiesel, F. C., Rothfuss, O. C., Kahle, P. J., and Springer, W. (2010) PINK1/Parkin-mediated mitophagy is dependent on VDAC1 and p62/SQSTM1. *Nature cell biology* **12**, 119-131
206. Narendra, D., Tanaka, A., Suen, D. F., and Youle, R. J. (2008) Parkin is recruited selectively to impaired mitochondria and promotes their autophagy. *The Journal of cell biology* **183**, 795-803
207. Vives-Bauza, C., Zhou, C., Huang, Y., Cui, M., de Vries, R. L., Kim, J., May, J., Tocilescu, M. A., Liu, W., Ko, H. S., Magrane, J., Moore, D. J., Dawson, V. L., Grailhe, R., Dawson, T. M., Li, C., Tieu, K., and Przedborski, S. (2010) PINK1-dependent recruitment of Parkin to mitochondria in mitophagy. *Proceedings of the National Academy of Sciences of the United States of America* **107**, 378-383
208. Zheng, Z., and Diamond, M. I. (2012) Huntington disease and the huntingtin protein. *Progress in molecular biology and translational science* **107**, 189-214
209. Dunah, A. W., Jeong, H., Griffin, A., Kim, Y. M., Standaert, D. G., Hersch, S. M., Mouradian, M. M., Young, A. B., Tanese, N., and Krainc, D. (2002) Sp1 and TAFII130 transcriptional activity disrupted in early Huntington's disease. *Science* **296**, 2238-2243
210. Steffan, J. S., Kazantsev, A., Spasic-Boskovic, O., Greenwald, M., Zhu, Y. Z., Gohler, H., Wanker, E. E., Bates, G. P., Housman, D. E., and Thompson, L. M. (2000) The Huntington's disease protein interacts with p53 and CREB-binding protein and represses

- transcription. *Proceedings of the National Academy of Sciences of the United States of America* **97**, 6763-6768
211. Okazawa, H., Rich, T., Chang, A., Lin, X., Waragai, M., Kajikawa, M., Enokido, Y., Komuro, A., Kato, S., Shibata, M., Hatanaka, H., Mouradian, M. M., Sudol, M., and Kanazawa, I. (2002) Interaction between mutant ataxin-1 and PQBP-1 affects transcription and cell death. *Neuron* **34**, 701-713
212. Zuccato, C., Belyaev, N., Conforti, P., Ooi, L., Tartari, M., Papadimou, E., MacDonald, M., Fossale, E., Zeitlin, S., Buckley, N., and Cattaneo, E. (2007) Widespread disruption of repressor element-1 silencing transcription factor/neuron-restrictive silencer factor occupancy at its target genes in Huntington's disease. *The Journal of neuroscience : the official journal of the Society for Neuroscience* **27**, 6972-6983
213. Cui, L., Jeong, H., Borovecki, F., Parkhurst, C. N., Tanese, N., and Krainc, D. (2006) Transcriptional repression of PGC-1alpha by mutant huntingtin leads to mitochondrial dysfunction and neurodegeneration. *Cell* **127**, 59-69
214. Sipione, S., Rigamonti, D., Valenza, M., Zuccato, C., Conti, L., Pritchard, J., Kooperberg, C., Olson, J. M., and Cattaneo, E. (2002) Early transcriptional profiles in huntingtin-inducible striatal cells by microarray analyses. *Human molecular genetics* **11**, 1953-1965
215. Dubnikov, T., Ben-Gedalya, T., and Cohen, E. (2017) Protein Quality Control in Health and Disease. *Cold Spring Harbor perspectives in biology* **9**
216. Yerbury, J. J., Ooi, L., Dillin, A., Saunders, D. N., Hatters, D. M., Beart, P. M., Cashman, N. R., Wilson, M. R., and Ecroyd, H. (2016) Walking the tightrope: proteostasis and neurodegenerative disease. *Journal of neurochemistry* **137**, 489-505

217. Harding, R. J., and Tong, Y. F. (2018) Proteostasis in Huntington's disease: disease mechanisms and therapeutic opportunities. *Acta pharmacologica Sinica*
218. Cohen-Kaplan, V., Livneh, I., Avni, N., Cohen-Rosenzweig, C., and Ciechanover, A. (2016) The ubiquitin-proteasome system and autophagy: Coordinated and independent activities. *The international journal of biochemistry & cell biology* **79**, 403-418
219. Hershko, A., and Ciechanover, A. (1998) The ubiquitin system. *Annual review of biochemistry* **67**, 425-479
220. Ikeda, F., and Dikic, I. (2008) Atypical ubiquitin chains: new molecular signals. 'Protein Modifications: Beyond the Usual Suspects' review series. *EMBO reports* **9**, 536-542
221. Thrower, J. S., Hoffman, L., Rechsteiner, M., and Pickart, C. M. (2000) Recognition of the polyubiquitin proteolytic signal. *The EMBO journal* **19**, 94-102
222. Hofmann, R. M., and Pickart, C. M. (2001) In vitro assembly and recognition of Lys-63 polyubiquitin chains. *The Journal of biological chemistry* **276**, 27936-27943
223. Saeki, Y., Kudo, T., Sone, T., Kikuchi, Y., Yokosawa, H., Toh-e, A., and Tanaka, K. (2009) Lysine 63-linked polyubiquitin chain may serve as a targeting signal for the 26S proteasome. *The EMBO journal* **28**, 359-371
224. Xu, P., Duong, D. M., Seyfried, N. T., Cheng, D., Xie, Y., Robert, J., Rush, J., Hochstrasser, M., Finley, D., and Peng, J. (2009) Quantitative proteomics reveals the function of unconventional ubiquitin chains in proteasomal degradation. *Cell* **137**, 133-145
225. Li, W., and Ye, Y. (2008) Polyubiquitin chains: functions, structures, and mechanisms. *Cellular and molecular life sciences : CMLS* **65**, 2397-2406

226. Husnjak, K., Elsasser, S., Zhang, N., Chen, X., Randles, L., Shi, Y., Hofmann, K., Walters, K. J., Finley, D., and Dikic, I. (2008) Proteasome subunit Rpn13 is a novel ubiquitin receptor. *Nature* **453**, 481-488
227. Paraskevopoulos, K., Kriegenburg, F., Tatham, M. H., Rosner, H. I., Medina, B., Larsen, I. B., Brandstrup, R., Hardwick, K. G., Hay, R. T., Kragelund, B. B., Hartmann-Petersen, R., and Gordon, C. (2014) Dss1 is a 26S proteasome ubiquitin receptor. *Molecular cell* **56**, 453-461
228. Shi, Y., Chen, X., Elsasser, S., Stocks, B. B., Tian, G., Lee, B. H., Shi, Y., Zhang, N., de Poot, S. A., Tuebing, F., Sun, S., Vannoy, J., Tarasov, S. G., Engen, J. R., Finley, D., and Walters, K. J. (2016) Rpn1 provides adjacent receptor sites for substrate binding and deubiquitination by the proteasome. *Science* **351**
229. Fu, H., Sadis, S., Rubin, D. M., Glickman, M., van Nocker, S., Finley, D., and Vierstra, R. D. (1998) Multiubiquitin chain binding and protein degradation are mediated by distinct domains within the 26 S proteasome subunit Mcb1. *The Journal of biological chemistry* **273**, 1970-1981
230. Livneh, I., Cohen-Kaplan, V., Cohen-Rosenzweig, C., Avni, N., and Ciechanover, A. (2016) The life cycle of the 26S proteasome: from birth, through regulation and function, and onto its death. *Cell research* **26**, 869-885
231. Gallastegui, N., and Groll, M. (2010) The 26S proteasome: assembly and function of a destructive machine. *Trends in biochemical sciences* **35**, 634-642
232. Waelter, S., Boeddrich, A., Lurz, R., Scherzinger, E., Lueder, G., Lehrach, H., and Wanker, E. E. (2001) Accumulation of mutant huntingtin fragments in aggresome-like inclusion bodies as a result of insufficient protein degradation. *Mol Biol Cell* **12**, 1393-1407

233. Wang, J., Wang, C. E., Orr, A., Tydlacka, S., Li, S. H., and Li, X. J. (2008) Impaired ubiquitin-proteasome system activity in the synapses of Huntington's disease mice. *The Journal of cell biology* **180**, 1177-1189
234. Bennett, E. J., Bence, N. F., Jayakumar, R., and Kopito, R. R. (2005) Global impairment of the ubiquitin-proteasome system by nuclear or cytoplasmic protein aggregates precedes inclusion body formation. *Molecular cell* **17**, 351-365
235. Holmberg, C. I., Staniszewski, K. E., Mensah, K. N., Matouschek, A., and Morimoto, R. I. (2004) Inefficient degradation of truncated polyglutamine proteins by the proteasome. *The EMBO journal* **23**, 4307-4318
236. Venkatraman, P., Wetzel, R., Tanaka, M., Nukina, N., and Goldberg, A. L. (2004) Eukaryotic proteasomes cannot digest polyglutamine sequences and release them during degradation of polyglutamine-containing proteins. *Molecular cell* **14**, 95-104
237. Juenemann, K., Schipper-Krom, S., Wiemhoefer, A., Kloss, A., Sanz Sanz, A., and Reits, E. A. (2013) Expanded polyglutamine-containing N-terminal huntingtin fragments are entirely degraded by mammalian proteasomes. *The Journal of biological chemistry* **288**, 27068-27084
238. Michalik, A., and Van Broeckhoven, C. (2004) Proteasome degrades soluble expanded polyglutamine completely and efficiently. *Neurobiology of disease* **16**, 202-211
239. Kaushik, S., Bandyopadhyay, U., Sridhar, S., Kiffin, R., Martinez-Vicente, M., Kon, M., Orenstein, S. J., Wong, E., and Cuervo, A. M. (2011) Chaperone-mediated autophagy at a glance. *Journal of cell science* **124**, 495-499
240. Dice, J. F. (1990) Peptide sequences that target cytosolic proteins for lysosomal proteolysis. *Trends in biochemical sciences* **15**, 305-309

241. Agarraberes, F. A., Terlecky, S. R., and Dice, J. F. (1997) An intralysosomal hsp70 is required for a selective pathway of lysosomal protein degradation. *The Journal of cell biology* **137**, 825-834
242. Qi, L., and Zhang, X. D. (2014) Role of chaperone-mediated autophagy in degrading Huntington's disease-associated huntingtin protein. *Acta biochimica et biophysica Sinica* **46**, 83-91
243. Koga, H., Martinez-Vicente, M., Arias, E., Kaushik, S., Sulzer, D., and Cuervo, A. M. (2011) Constitutive upregulation of chaperone-mediated autophagy in Huntington's disease. *The Journal of neuroscience : the official journal of the Society for Neuroscience* **31**, 18492-18505
244. Qi, L., Zhang, X. D., Wu, J. C., Lin, F., Wang, J., DiFiglia, M., and Qin, Z. H. (2012) The role of chaperone-mediated autophagy in huntingtin degradation. *PloS one* **7**, e46834
245. Ryter, S. W., Cloonan, S. M., and Choi, A. M. (2013) Autophagy: a critical regulator of cellular metabolism and homeostasis. *Molecules and cells* **36**, 7-16
246. Bingol, B. (2018) Autophagy and lysosomal pathways in nervous system disorders. *Molecular and cellular neurosciences*
247. DeMartino, G. N. (2018) Introduction to the Thematic Minireview Series: Autophagy. *The Journal of biological chemistry* **293**, 5384-5385
248. Fujikake, N., Shin, M., and Shimizu, S. (2018) Association Between Autophagy and Neurodegenerative Diseases. *Frontiers in neuroscience* **12**, 255
249. Thorburn, A. (2018) Autophagy and disease. *The Journal of biological chemistry* **293**, 5425-5430

250. Marsh, J. L., and Thompson, L. M. (2006) *Drosophila* in the study of neurodegenerative disease. *Neuron* **52**, 169-178
251. Miller, V. M., Nelson, R. F., Gouvion, C. M., Williams, A., Rodriguez-Lebron, E., Harper, S. Q., Davidson, B. L., Rebagliati, M. R., and Paulson, H. L. (2005) CHIP suppresses polyglutamine aggregation and toxicity in vitro and in vivo. *The Journal of neuroscience : the official journal of the Society for Neuroscience* **25**, 9152-9161
252. Gunawardena, S., Her, L. S., Bruschi, R. G., Laymon, R. A., Niesman, I. R., Gordesky-Gold, B., Sintasath, L., Bonini, N. M., and Goldstein, L. S. (2003) Disruption of axonal transport by loss of huntingtin or expression of pathogenic polyQ proteins in *Drosophila*. *Neuron* **40**, 25-40
253. Parker, J. A., Connolly, J. B., Wellington, C., Hayden, M., Dausset, J., and Neri, C. (2001) Expanded polyglutamines in *Caenorhabditis elegans* cause axonal abnormalities and severe dysfunction of PLM mechanosensory neurons without cell death. *Proceedings of the National Academy of Sciences of the United States of America* **98**, 13318-13323
254. Faber, P. W., Alter, J. R., MacDonald, M. E., and Hart, A. C. (1999) Polyglutamine-mediated dysfunction and apoptotic death of a *Caenorhabditis elegans* sensory neuron. *Proceedings of the National Academy of Sciences of the United States of America* **96**, 179-184
255. Brooks, S. P., and Dunnett, S. B. (2015) Mouse Models of Huntington's Disease. *Current topics in behavioral neurosciences* **22**, 101-133
256. Hodgson, J. G., Agopyan, N., Gutekunst, C. A., Leavitt, B. R., LePiane, F., Singaraja, R., Smith, D. J., Bissada, N., McCutcheon, K., Nasir, J., Jamot, L., Li, X. J., Stevens, M. E., Rosemond, E., Roder, J. C., Phillips, A. G., Rubin, E. M., Hersch, S. M., and Hayden, M.

- R. (1999) A YAC mouse model for Huntington's disease with full-length mutant huntingtin, cytoplasmic toxicity, and selective striatal neurodegeneration. *Neuron* **23**, 181-192
257. Menalled, L. B., Sison, J. D., Dragatsis, I., Zeitlin, S., and Chesselet, M. F. (2003) Time course of early motor and neuropathological anomalies in a knock-in mouse model of Huntington's disease with 140 CAG repeats. *The Journal of comparative neurology* **465**, 11-26
258. Menalled, L. B., Kudwa, A. E., Miller, S., Fitzpatrick, J., Watson-Johnson, J., Keating, N., Ruiz, M., Mushlin, R., Alosio, W., McConnell, K., Connor, D., Murphy, C., Oakeshott, S., Kwan, M., Beltran, J., Ghavami, A., Brunner, D., Park, L. C., Ramboz, S., and Howland, D. (2012) Comprehensive behavioral and molecular characterization of a new knock-in mouse model of Huntington's disease: zQ175. *PloS one* **7**, e49838
259. Wheeler, V. C., White, J. K., Gutekunst, C. A., Vrbanac, V., Weaver, M., Li, X. J., Li, S. H., Yi, H., Vonsattel, J. P., Gusella, J. F., Hersch, S., Auerbach, W., Joyner, A. L., and MacDonald, M. E. (2000) Long glutamine tracts cause nuclear localization of a novel form of huntingtin in medium spiny striatal neurons in HdhQ92 and HdhQ111 knock-in mice. *Human molecular genetics* **9**, 503-513
260. Lin, C. H., Tallaksen-Greene, S., Chien, W. M., Cearley, J. A., Jackson, W. S., Crouse, A. B., Ren, S., Li, X. J., Albin, R. L., and Detloff, P. J. (2001) Neurological abnormalities in a knock-in mouse model of Huntington's disease. *Human molecular genetics* **10**, 137-144
261. Peng, Q., Wu, B., Jiang, M., Jin, J., Hou, Z., Zheng, J., Zhang, J., and Duan, W. (2016) Characterization of Behavioral, Neuropathological, Brain Metabolic and Key Molecular

- Changes in zQ175 Knock-In Mouse Model of Huntington's Disease. *PloS one* **11**, e0148839
262. Trettel, F., Rigamonti, D., Hilditch-Maguire, P., Wheeler, V. C., Sharp, A. H., Persichetti, F., Cattaneo, E., and MacDonald, M. E. (2000) Dominant phenotypes produced by the HD mutation in STHdh(Q111) striatal cells. *Human molecular genetics* **9**, 2799-2809
263. Consortium, H. D. i. (2012) Induced pluripotent stem cells from patients with Huntington's disease show CAG-repeat-expansion-associated phenotypes. *Cell stem cell* **11**, 264-278
264. Zhang, N., Bailus, B. J., Ring, K. L., and Ellerby, L. M. (2015) iPSC-based drug screening for Huntingtons disease. *Brain research*
265. Chen, Y., Carter, R. L., Cho, I. K., and Chan, A. W. (2014) Cell-based therapies for Huntington's disease. *Drug discovery today* **19**, 980-984
266. Jimenez-Sanchez, M., Licitra, F., Underwood, B. R., and Rubinsztein, D. C. (2017) Huntington's Disease: Mechanisms of Pathogenesis and Therapeutic Strategies. *Cold Spring Harbor perspectives in medicine* **7**
267. Guay, D. R. (2010) Tetrabenazine, a monoamine-depleting drug used in the treatment of hyperkinetic movement disorders. *The American journal of geriatric pharmacotherapy* **8**, 331-373
268. Huntington Study, G. (2006) Tetrabenazine as antichorea therapy in Huntington disease: a randomized controlled trial. *Neurology* **66**, 366-372
269. Frank, S. (2009) Tetrabenazine as anti-chorea therapy in Huntington disease: an open-label continuation study. Huntington Study Group/TETRA-HD Investigators. *BMC neurology* **9**, 62

270. Harper, S. Q., Staber, P. D., He, X., Eliason, S. L., Martins, I. H., Mao, Q., Yang, L., Kotin, R. M., Paulson, H. L., and Davidson, B. L. (2005) RNA interference improves motor and neuropathological abnormalities in a Huntington's disease mouse model. *Proceedings of the National Academy of Sciences of the United States of America* **102**, 5820-5825
271. Carroll, J. B., Warby, S. C., Southwell, A. L., Doty, C. N., Greenlee, S., Skotte, N., Hung, G., Bennett, C. F., Freier, S. M., and Hayden, M. R. (2011) Potent and selective antisense oligonucleotides targeting single-nucleotide polymorphisms in the Huntington disease gene / allele-specific silencing of mutant huntingtin. *Molecular therapy : the journal of the American Society of Gene Therapy* **19**, 2178-2185
272. Maglione, V., Marchi, P., Di Pardo, A., Lingrell, S., Horkey, M., Tidmarsh, E., and Sipione, S. (2010) Impaired ganglioside metabolism in Huntington's disease and neuroprotective role of GM1. *The Journal of neuroscience : the official journal of the Society for Neuroscience* **30**, 4072-4080
273. Alpaugh, M., Galleguillos, D., Forero, J., Morales, L. C., Lackey, S. W., Kar, P., Di Pardo, A., Holt, A., Kerr, B. J., Todd, K. G., Baker, G. B., Fouad, K., and Sipione, S. (2017) Disease-modifying effects of ganglioside GM1 in Huntington's disease models. *EMBO molecular medicine* **9**, 1537-1557
274. Bunner, K. D., and Rebec, G. V. (2016) Corticostriatal Dysfunction in Huntington's Disease: The Basics. *Frontiers in human neuroscience* **10**, 317
275. Rauvala, H. (1979) Monomer-micelle transition of the ganglioside GM1 and the hydrolysis by *Clostridium perfringens* neuraminidase. *European journal of biochemistry* **97**, 555-564
276. Cattaneo, E., and Conti, L. (1998) Generation and characterization of embryonic striatal conditionally immortalized ST14A cells. *Journal of neuroscience research* **53**, 223-234

277. Olmsted, J. B., Carlson, K., Klebe, R., Ruddle, F., and Rosenbaum, J. (1970) Isolation of microtubule protein from cultured mouse neuroblastoma cells. *Proceedings of the National Academy of Sciences of the United States of America* **65**, 129-136
278. Morikawa, M., Fryer, J. D., Sullivan, P. M., Christopher, E. A., Wahrle, S. E., DeMattos, R. B., O'Dell, M. A., Fagan, A. M., Lashuel, H. A., Walz, T., Asai, K., and Holtzman, D. M. (2005) Production and characterization of astrocyte-derived human apolipoprotein E isoforms from immortalized astrocytes and their interactions with amyloid-beta. *Neurobiology of disease* **19**, 66-76
279. Beaudoin, G. M., 3rd, Lee, S. H., Singh, D., Yuan, Y., Ng, Y. G., Reichardt, L. F., and Arikath, J. (2012) Culturing pyramidal neurons from the early postnatal mouse hippocampus and cortex. *Nature protocols* **7**, 1741-1754
280. Brewer, G. J., Torricelli, J. R., Evege, E. K., and Price, P. J. (1993) Optimized survival of hippocampal neurons in B27-supplemented Neurobasal, a new serum-free medium combination. *Journal of neuroscience research* **35**, 567-576
281. Vandesompele, J., De Preter, K., Pattyn, F., Poppe, B., Van Roy, N., De Paepe, A., and Speleman, F. (2002) Accurate normalization of real-time quantitative RT-PCR data by geometric averaging of multiple internal control genes. *Genome biology* **3**, RESEARCH0034
282. Havel, R. J., Eder, H. A., and Bragdon, J. H. (1955) The distribution and chemical composition of ultracentrifugally separated lipoproteins in human serum. *The Journal of clinical investigation* **34**, 1345-1353
283. Bordier, C. (1981) Phase separation of integral membrane proteins in Triton X-114 solution. *The Journal of biological chemistry* **256**, 1604-1607

284. Kazantsev, A., Preisinger, E., Dranovsky, A., Goldgaber, D., and Housman, D. (1999) Insoluble detergent-resistant aggregates form between pathological and nonpathological lengths of polyglutamine in mammalian cells. *Proceedings of the National Academy of Sciences of the United States of America* **96**, 11404-11409
285. They, C., Amigorena, S., Raposo, G., and Clayton, A. (2006) Isolation and characterization of exosomes from cell culture supernatants and biological fluids. *Current protocols in cell biology* **Chapter 3**, Unit 3 22
286. Wanker, E. E., Scherzinger, E., Heiser, V., Sittler, A., Eickhoff, H., and Lehrach, H. (1999) Membrane filter assay for detection of amyloid-like polyglutamine-containing protein aggregates. *Methods in enzymology* **309**, 375-386
287. Valenza, M., Rigamonti, D., Goffredo, D., Zuccato, C., Fenu, S., Jamot, L., Strand, A., Tarditi, A., Woodman, B., Racchi, M., Mariotti, C., Di Donato, S., Corsini, A., Bates, G., Pruss, R., Olson, J. M., Sipione, S., Tartari, M., and Cattaneo, E. (2005) Dysfunction of the cholesterol biosynthetic pathway in Huntington's disease. *The Journal of neuroscience : the official journal of the Society for Neuroscience* **25**, 9932-9939
288. Valenza, M., Carroll, J. B., Leoni, V., Bertram, L. N., Bjorkhem, I., Singaraja, R. R., Di Donato, S., Lutjohann, D., Hayden, M. R., and Cattaneo, E. (2007) Cholesterol biosynthesis pathway is disturbed in YAC128 mice and is modulated by huntingtin mutation. *Human molecular genetics* **16**, 2187-2198
289. Valenza, M., Leoni, V., Tarditi, A., Mariotti, C., Bjorkhem, I., Di Donato, S., and Cattaneo, E. (2007) Progressive dysfunction of the cholesterol biosynthesis pathway in the R6/2 mouse model of Huntington's disease. *Neurobiology of disease* **28**, 133-142

290. Valenza, M., Leoni, V., Karasinska, J. M., Petricca, L., Fan, J., Carroll, J., Pouladi, M. A., Fossale, E., Nguyen, H. P., Riess, O., MacDonald, M., Wellington, C., DiDonato, S., Hayden, M., and Cattaneo, E. (2010) Cholesterol defect is marked across multiple rodent models of Huntington's disease and is manifest in astrocytes. *The Journal of neuroscience : the official journal of the Society for Neuroscience* **30**, 10844-10850
291. Valenza, M., Marullo, M., Di Paolo, E., Cesana, E., Zuccato, C., Biella, G., and Cattaneo, E. (2014) Disruption of astrocyte-neuron cholesterol cross talk affects neuronal function in Huntington's disease. *Cell death and differentiation*
292. Leoni, V., and Caccia, C. (2015) The impairment of cholesterol metabolism in Huntington disease. *Biochimica et biophysica acta* **1851**, 1095-1105
293. Borochoy, H., Abbott, R. E., Schachter, D., and Shinitzky, M. (1979) Modulation of erythrocyte membrane proteins by membrane cholesterol and lipid fluidity. *Biochemistry* **18**, 251-255
294. George, K. S., and Wu, S. (2012) Lipid raft: A floating island of death or survival. *Toxicology and applied pharmacology* **259**, 311-319
295. Sonnino, S., and Prinetti, A. (2016) The role of sphingolipids in neuronal plasticity of the brain. *Journal of neurochemistry* **137**, 485-488
296. Sonnino, S., Aureli, M., Mauri, L., Ciampa, M. G., and Prinetti, A. (2015) Membrane lipid domains in the nervous system. *Frontiers in bioscience (Landmark edition)* **20**, 280-302
297. Pfenninger, K. H. (2009) Plasma membrane expansion: a neuron's Herculean task. *Nature reviews. Neuroscience* **10**, 251-261
298. Takamori, S., Holt, M., Stenius, K., Lemke, E. A., Gronborg, M., Riedel, D., Urlaub, H., Schenck, S., Brugger, B., Ringler, P., Muller, S. A., Rammner, B., Grater, F., Hub, J. S.,

- De Groot, B. L., Mieskes, G., Moriyama, Y., Klingauf, J., Grubmuller, H., Heuser, J., Wieland, F., and Jahn, R. (2006) Molecular anatomy of a trafficking organelle. *Cell* **127**, 831-846
299. Goritz, C., Mauch, D. H., and Pfrieder, F. W. (2005) Multiple mechanisms mediate cholesterol-induced synaptogenesis in a CNS neuron. *Molecular and cellular neurosciences* **29**, 190-201
300. Mailman, T., Hariharan, M., and Karten, B. (2011) Inhibition of neuronal cholesterol biosynthesis with lovastatin leads to impaired synaptic vesicle release even in the presence of lipoproteins or geranylgeraniol. *Journal of neurochemistry* **119**, 1002-1015
301. Charalampopoulos, I., Remboutsika, E., Margioris, A. N., and Gravanis, A. (2008) Neurosteroids as modulators of neurogenesis and neuronal survival. *Trends in endocrinology and metabolism: TEM* **19**, 300-307
302. Puia, G., Santi, M. R., Vicini, S., Pritchett, D. B., Purdy, R. H., Paul, S. M., Seeburg, P. H., and Costa, E. (1990) Neurosteroids act on recombinant human GABAA receptors. *Neuron* **4**, 759-765
303. Xilouri, M., and Papazafiri, P. (2006) Anti-apoptotic effects of allopregnanolone on P19 neurons. *The European journal of neuroscience* **23**, 43-54
304. Weaver, C. E., Jr., Marek, P., Park-Chung, M., Tam, S. W., and Farb, D. H. (1997) Neuroprotective activity of a new class of steroidal inhibitors of the N-methyl-D-aspartate receptor. *Proceedings of the National Academy of Sciences of the United States of America* **94**, 10450-10454
305. Porter, J. A., Young, K. E., and Beachy, P. A. (1996) Cholesterol modification of hedgehog signaling proteins in animal development. *Science* **274**, 255-259

306. Jeong, J., and McMahon, A. P. (2002) Cholesterol modification of Hedgehog family proteins. *The Journal of clinical investigation* **110**, 591-596
307. Irons, M., Elias, E. R., Salen, G., Tint, G. S., and Batta, A. K. (1993) Defective cholesterol biosynthesis in Smith-Lemli-Opitz syndrome. *Lancet* **341**, 1414
308. Nowaczyk, M. J. M. (1993) Smith-Lemli-Opitz Syndrome. in *GeneReviews((R))* (Adam, M. P., Ardinger, H. H., Pagon, R. A., Wallace, S. E., Bean, L. J. H., Stephens, K., and Amemiya, A. eds.), Seattle (WA). pp
309. Klein, A. D., Alvarez, A., and Zanolungo, S. (2014) The unique case of the Niemann-Pick type C cholesterol storage disorder. *Pediatric endocrinology reviews : PER* **12 Suppl 1**, 166-175
310. Goldstein, J. L., and Brown, M. S. (1990) Regulation of the mevalonate pathway. *Nature* **343**, 425-430
311. Zhang, J., and Liu, Q. (2015) Cholesterol metabolism and homeostasis in the brain. *Protein & cell* **6**, 254-264
312. Bjorkhem, I., and Meaney, S. (2004) Brain cholesterol: long secret life behind a barrier. *Arteriosclerosis, thrombosis, and vascular biology* **24**, 806-815
313. Dietschy, J. M., and Turley, S. D. (2004) Thematic review series: brain Lipids. Cholesterol metabolism in the central nervous system during early development and in the mature animal. *Journal of lipid research* **45**, 1375-1397
314. Miziorko, H. M. (2011) Enzymes of the mevalonate pathway of isoprenoid biosynthesis. *Archives of biochemistry and biophysics* **505**, 131-143
315. Moutinho, M., Nunes, M. J., and Rodrigues, E. (2017) The mevalonate pathway in neurons: It's not just about cholesterol. *Experimental cell research* **360**, 55-60

316. Faust, J. R., Goldstein, J. L., and Brown, M. S. (1979) Synthesis of ubiquinone and cholesterol in human fibroblasts: regulation of a branched pathway. *Archives of biochemistry and biophysics* **192**, 86-99
317. Butterworth, P. H., Draper, H. H., Hemming, F. W., and Morton, R. A. (1966) In vivo incorporation of [2-14-C]-mevalonate into dolichol of rabbit and pig liver. *Archives of biochemistry and biophysics* **113**, 646-653
318. Hooff, G. P., Wood, W. G., Muller, W. E., and Eckert, G. P. (2010) Isoprenoids, small GTPases and Alzheimer's disease. *Biochimica et biophysica acta* **1801**, 896-905
319. Horton, J. D., Goldstein, J. L., and Brown, M. S. (2002) SREBPs: activators of the complete program of cholesterol and fatty acid synthesis in the liver. *The Journal of clinical investigation* **109**, 1125-1131
320. Horton, J. D., Shah, N. A., Warrington, J. A., Anderson, N. N., Park, S. W., Brown, M. S., and Goldstein, J. L. (2003) Combined analysis of oligonucleotide microarray data from transgenic and knockout mice identifies direct SREBP target genes. *Proceedings of the National Academy of Sciences of the United States of America* **100**, 12027-12032
321. Espenshade, P. J., Li, W. P., and Yabe, D. (2002) Sterols block binding of COPII proteins to SCAP, thereby controlling SCAP sorting in ER. *Proceedings of the National Academy of Sciences of the United States of America* **99**, 11694-11699
322. Nohturfft, A., DeBose-Boyd, R. A., Scheek, S., Goldstein, J. L., and Brown, M. S. (1999) Sterols regulate cycling of SREBP cleavage-activating protein (SCAP) between endoplasmic reticulum and Golgi. *Proceedings of the National Academy of Sciences of the United States of America* **96**, 11235-11240

323. Duncan, E. A., Dave, U. P., Sakai, J., Goldstein, J. L., and Brown, M. S. (1998) Second-site cleavage in sterol regulatory element-binding protein occurs at transmembrane junction as determined by cysteine panning. *The Journal of biological chemistry* **273**, 17801-17809
324. Nagoshi, E., Imamoto, N., Sato, R., and Yoneda, Y. (1999) Nuclear import of sterol regulatory element-binding protein-2, a basic helix-loop-helix-leucine zipper (bHLH-Zip)-containing transcription factor, occurs through the direct interaction of importin beta with HLH-Zip. *Mol Biol Cell* **10**, 2221-2233
325. Nagoshi, E., and Yoneda, Y. (2001) Dimerization of sterol regulatory element-binding protein 2 via the helix-loop-helix-leucine zipper domain is a prerequisite for its nuclear localization mediated by importin beta. *Molecular and cellular biology* **21**, 2779-2789
326. Brown, M. S., and Goldstein, J. L. (1997) The SREBP pathway: regulation of cholesterol metabolism by proteolysis of a membrane-bound transcription factor. *Cell* **89**, 331-340
327. Radhakrishnan, A., Sun, L. P., Kwon, H. J., Brown, M. S., and Goldstein, J. L. (2004) Direct binding of cholesterol to the purified membrane region of SCAP: mechanism for a sterol-sensing domain. *Molecular cell* **15**, 259-268
328. Yabe, D., Brown, M. S., and Goldstein, J. L. (2002) Insig-2, a second endoplasmic reticulum protein that binds SCAP and blocks export of sterol regulatory element-binding proteins. *Proceedings of the National Academy of Sciences of the United States of America* **99**, 12753-12758
329. Yang, T., Espenshade, P. J., Wright, M. E., Yabe, D., Gong, Y., Aebersold, R., Goldstein, J. L., and Brown, M. S. (2002) Crucial step in cholesterol homeostasis: sterols promote

- binding of SCAP to INSIG-1, a membrane protein that facilitates retention of SREBPs in ER. *Cell* **110**, 489-500
330. Radhakrishnan, A., Ikeda, Y., Kwon, H. J., Brown, M. S., and Goldstein, J. L. (2007) Sterol-regulated transport of SREBPs from endoplasmic reticulum to Golgi: oxysterols block transport by binding to Insig. *Proceedings of the National Academy of Sciences of the United States of America* **104**, 6511-6518
331. Mohamed, A., Saavedra, L., Di Pardo, A., Sipione, S., and Posse de Chaves, E. (2012) beta-amyloid inhibits protein prenylation and induces cholesterol sequestration by impairing SREBP-2 cleavage. *The Journal of neuroscience : the official journal of the Society for Neuroscience* **32**, 6490-6500
332. Leoni, V., Mariotti, C., Tabrizi, S. J., Valenza, M., Wild, E. J., Henley, S. M., Hobbs, N. Z., Mandelli, M. L., Grisoli, M., Bjorkhem, I., Cattaneo, E., and Di Donato, S. (2008) Plasma 24S-hydroxycholesterol and caudate MRI in pre-manifest and early Huntington's disease. *Brain : a journal of neurology* **131**, 2851-2859
333. Markianos, M., Panas, M., Kalfakis, N., and Vassilopoulos, D. (2008) Low plasma total cholesterol in patients with Huntington's disease and first-degree relatives. *Molecular genetics and metabolism* **93**, 341-346
334. Leoni, V., Mariotti, C., Nanetti, L., Salvatore, E., Squitieri, F., Bentivoglio, A. R., Bandettini di Poggio, M., Piacentini, S., Monza, D., Valenza, M., Cattaneo, E., and Di Donato, S. (2011) Whole body cholesterol metabolism is impaired in Huntington's disease. *Neuroscience letters* **494**, 245-249
335. Valenza, M., Chen, J. Y., Di Paolo, E., Ruozi, B., Belletti, D., Ferrari Bardile, C., Leoni, V., Caccia, C., Brillì, E., Di Donato, S., Boido, M. M., Vercelli, A., Vandelli, M. A., Forni,

- F., Cepeda, C., Levine, M. S., Tosi, G., and Cattaneo, E. (2015) Cholesterol-loaded nanoparticles ameliorate synaptic and cognitive function in Huntington's disease mice. *EMBO molecular medicine* **7**, 1547-1564
336. Lutjohann, D., Breuer, O., Ahlborg, G., Nennesmo, I., Siden, A., Diczfalusy, U., and Bjorkhem, I. (1996) Cholesterol homeostasis in human brain: evidence for an age-dependent flux of 24S-hydroxycholesterol from the brain into the circulation. *Proceedings of the National Academy of Sciences of the United States of America* **93**, 9799-9804
337. Lopes-Cardozo, M., Larsson, O. M., and Schousboe, A. (1986) Acetoacetate and glucose as lipid precursors and energy substrates in primary cultures of astrocytes and neurons from mouse cerebral cortex. *Journal of neurochemistry* **46**, 773-778
338. Poirier, J., Baccichet, A., Dea, D., and Gauthier, S. (1993) Cholesterol synthesis and lipoprotein reuptake during synaptic remodelling in hippocampus in adult rats. *Neuroscience* **55**, 81-90
339. Vance, J. E., Pan, D., Campenot, R. B., Bussiere, M., and Vance, D. E. (1994) Evidence that the major membrane lipids, except cholesterol, are made in axons of cultured rat sympathetic neurons. *Journal of neurochemistry* **62**, 329-337
340. Nieweg, K., Schaller, H., and Pfrieder, F. W. (2009) Marked differences in cholesterol synthesis between neurons and glial cells from postnatal rats. *Journal of neurochemistry* **109**, 125-134
341. Carroll, J. B., Deik, A., Fossale, E., Weston, R. M., Guide, J. R., Arjomand, J., Kwak, S., Clish, C. B., and MacDonald, M. E. (2015) HdhQ111 Mice Exhibit Tissue Specific Metabolite Profiles that Include Striatal Lipid Accumulation. *PloS one* **10**, e0134465

342. del Toro, D., Xifro, X., Pol, A., Humbert, S., Saudou, F., Canals, J. M., and Alberch, J. (2010) Altered cholesterol homeostasis contributes to enhanced excitotoxicity in Huntington's disease. *Journal of neurochemistry* **115**, 153-167
343. Trushina, E., Singh, R. D., Dyer, R. B., Cao, S., Shah, V. H., Parton, R. G., Pagano, R. E., and McMurray, C. T. (2006) Mutant huntingtin inhibits clathrin-independent endocytosis and causes accumulation of cholesterol in vitro and in vivo. *Human molecular genetics* **15**, 3578-3591
344. Vanier, M. T. (1999) Lipid changes in Niemann-Pick disease type C brain: personal experience and review of the literature. *Neurochemical research* **24**, 481-489
345. Elleder, M., Jirasek, A., Smid, F., Ledvinova, J., and Besley, G. T. (1985) Niemann-Pick disease type C. Study on the nature of the cerebral storage process. *Acta neuropathologica* **66**, 325-336
346. Cherfils, J., and Zeghouf, M. (2013) Regulation of small GTPases by GEFs, GAPs, and GDIs. *Physiological reviews* **93**, 269-309
347. Diez, D., Sanchez-Jimenez, F., and Ranea, J. A. (2011) Evolutionary expansion of the Ras switch regulatory module in eukaryotes. *Nucleic acids research* **39**, 5526-5537
348. Jaffe, A. B., and Hall, A. (2005) Rho GTPases: biochemistry and biology. *Annual review of cell and developmental biology* **21**, 247-269
349. D'Souza-Schorey, C., and Chavrier, P. (2006) ARF proteins: roles in membrane traffic and beyond. *Nature reviews. Molecular cell biology* **7**, 347-358
350. Hutagalung, A. H., and Novick, P. J. (2011) Role of Rab GTPases in membrane traffic and cell physiology. *Physiological reviews* **91**, 119-149

351. Stewart, M. (2007) Molecular mechanism of the nuclear protein import cycle. *Nature reviews. Molecular cell biology* **8**, 195-208
352. Lui, K., and Huang, Y. (2009) RanGTPase: A Key Regulator of Nucleocytoplasmic Trafficking. *Molecular and cellular pharmacology* **1**, 148-156
353. Berndt, N., Hamilton, A. D., and Sebt, S. M. (2011) Targeting protein prenylation for cancer therapy. *Nature reviews. Cancer* **11**, 775-791
354. Konstantinopoulos, P. A., Karamouzis, M. V., and Papavassiliou, A. G. (2007) Post-translational modifications and regulation of the RAS superfamily of GTPases as anticancer targets. *Nature reviews. Drug discovery* **6**, 541-555
355. Reid, T. S., Terry, K. L., Casey, P. J., and Beese, L. S. (2004) Crystallographic analysis of CaaX prenyltransferases complexed with substrates defines rules of protein substrate selectivity. *Journal of molecular biology* **343**, 417-433
356. Bodai, L., and Marsh, J. L. (2012) A novel target for Huntington's disease: ERK at the crossroads of signaling. The ERK signaling pathway is implicated in Huntington's disease and its upregulation ameliorates pathology. *BioEssays : news and reviews in molecular, cellular and developmental biology* **34**, 142-148
357. Maher, P., Dargusch, R., Bodai, L., Gerard, P. E., Purcell, J. M., and Marsh, J. L. (2011) ERK activation by the polyphenols fisetin and resveratrol provides neuroprotection in multiple models of Huntington's disease. *Human molecular genetics* **20**, 261-270
358. Apostol, B. L., Illes, K., Pallos, J., Bodai, L., Wu, J., Strand, A., Schweitzer, E. S., Olson, J. M., Kazantsev, A., Marsh, J. L., and Thompson, L. M. (2006) Mutant huntingtin alters MAPK signaling pathways in PC12 and striatal cells: ERK1/2 protects against mutant huntingtin-associated toxicity. *Human molecular genetics* **15**, 273-285

359. Li, X., Sapp, E., Chase, K., Comer-Tierney, L. A., Masso, N., Alexander, J., Reeves, P., Kegel, K. B., Valencia, A., Esteves, M., Aronin, N., and Difiglia, M. (2009) Disruption of Rab11 activity in a knock-in mouse model of Huntington's disease. *Neurobiology of disease* **36**, 374-383
360. Richards, P., Didszun, C., Campesan, S., Simpson, A., Horley, B., Young, K. W., Glynn, P., Cain, K., Kyriacou, C. P., Giorgini, F., and Nicotera, P. (2011) Dendritic spine loss and neurodegeneration is rescued by Rab11 in models of Huntington's disease. *Cell death and differentiation* **18**, 191-200
361. Li, X., Valencia, A., Sapp, E., Masso, N., Alexander, J., Reeves, P., Kegel, K. B., Aronin, N., and Difiglia, M. (2010) Aberrant Rab11-dependent trafficking of the neuronal glutamate transporter EAAC1 causes oxidative stress and cell death in Huntington's disease. *The Journal of neuroscience : the official journal of the Society for Neuroscience* **30**, 4552-4561
362. Lebrand, C., Corti, M., Goodson, H., Cosson, P., Cavalli, V., Mayran, N., Faure, J., and Gruenberg, J. (2002) Late endosome motility depends on lipids via the small GTPase Rab7. *The EMBO journal* **21**, 1289-1300
363. Deinhardt, K., Salinas, S., Verastegui, C., Watson, R., Worth, D., Hanrahan, S., Bucci, C., and Schiavo, G. (2006) Rab5 and Rab7 control endocytic sorting along the axonal retrograde transport pathway. *Neuron* **52**, 293-305
364. Feng, Y., Press, B., and Wandinger-Ness, A. (1995) Rab 7: an important regulator of late endocytic membrane traffic. *The Journal of cell biology* **131**, 1435-1452

365. Hyttinen, J. M., Niittykoski, M., Salminen, A., and Kaarniranta, K. (2013) Maturation of autophagosomes and endosomes: a key role for Rab7. *Biochimica et biophysica acta* **1833**, 503-510
366. Smith, R., Bacos, K., Fedele, V., Soulet, D., Walz, H. A., Obermuller, S., Lindqvist, A., Bjorkqvist, M., Klein, P., Onnerfjord, P., Brundin, P., Mulder, H., and Li, J. Y. (2009) Mutant huntingtin interacts with β -tubulin and disrupts vesicular transport and insulin secretion. *Human molecular genetics* **18**, 3942-3954
367. Sinadinos, C., Burbidge-King, T., Soh, D., Thompson, L. M., Marsh, J. L., Wyttenbach, A., and Mudher, A. K. (2009) Live axonal transport disruption by mutant huntingtin fragments in Drosophila motor neuron axons. *Neurobiology of disease* **34**, 389-395
368. Nurenberg, G., and Volmer, D. A. (2012) The analytical determination of isoprenoid intermediates from the mevalonate pathway. *Analytical and bioanalytical chemistry* **402**, 671-685
369. Deraeve, C., Guo, Z., Bon, R. S., Blankenfeldt, W., DiLucrezia, R., Wolf, A., Menninger, S., Stigter, E. A., Wetzels, S., Choidas, A., Alexandrov, K., Waldmann, H., Goody, R. S., and Wu, Y. W. (2012) Psoromic acid is a selective and covalent Rab-prenylation inhibitor targeting autoinhibited RabGGTase. *Journal of the American Chemical Society* **134**, 7384-7391
370. Gutkowska, M., and Swiezewska, E. (2012) Structure, regulation and cellular functions of Rab geranylgeranyl transferase and its cellular partner Rab Escort Protein. *Molecular membrane biology* **29**, 243-256
371. Shinde, S. R., and Maddika, S. (2017) Post translational modifications of Rab GTPases. *Small GTPases*, 1-8

372. Srikanth, S., Woo, J. S., and Gwack, Y. (2017) A large Rab GTPase family in a small GTPase world. *Small GTPases* **8**, 43-48
373. Pfrieger, F. W. (2003) Outsourcing in the brain: do neurons depend on cholesterol delivery by astrocytes? *BioEssays : news and reviews in molecular, cellular and developmental biology* **25**, 72-78
374. Brown, M. S., and Goldstein, J. L. (1980) Multivalent feedback regulation of HMG CoA reductase, a control mechanism coordinating isoprenoid synthesis and cell growth. *Journal of lipid research* **21**, 505-517
375. Hartman, H. L., Bowers, K. E., and Fierke, C. A. (2004) Lysine beta311 of protein geranylgeranyltransferase type I partially replaces magnesium. *The Journal of biological chemistry* **279**, 30546-30553
376. Thoma, N. H., Iakovenko, A., Owen, D., Scheidig, A. S., Waldmann, H., Goody, R. S., and Alexandrov, K. (2000) Phosphoisoprenoid binding specificity of geranylgeranyltransferase type II. *Biochemistry* **39**, 12043-12052
377. Furfine, E. S., Leban, J. J., Landavazo, A., Moomaw, J. F., and Casey, P. J. (1995) Protein farnesyltransferase: kinetics of farnesyl pyrophosphate binding and product release. *Biochemistry* **34**, 6857-6862
378. Mookhtiar, K. A., Kalinowski, S. S., Zhang, D., and Poulter, C. D. (1994) Yeast squalene synthase. A mechanism for addition of substrates and activation by NADPH. *The Journal of biological chemistry* **269**, 11201-11207
379. Zhang, D., Jennings, S. M., Robinson, G. W., and Poulter, C. D. (1993) Yeast squalene synthase: expression, purification, and characterization of soluble recombinant enzyme. *Archives of biochemistry and biophysics* **304**, 133-143

380. Hooff, G. P., Volmer, D. A., Wood, W. G., Muller, W. E., and Eckert, G. P. (2008) Isoprenoid quantitation in human brain tissue: a validated HPLC-fluorescence detection method for endogenous farnesyl- (FPP) and geranylgeranylpyrophosphate (GGPP). *Analytical and bioanalytical chemistry* **392**, 673-680
381. Hooff, G. P., Patel, N., Wood, W. G., Muller, W. E., Eckert, G. P., and Volmer, D. A. (2010) A rapid and sensitive assay for determining human brain levels of farnesyl-(FPP) and geranylgeranylpyrophosphate (GGPP) and transferase activities using UHPLC-MS/MS. *Analytical and bioanalytical chemistry* **398**, 1801-1808
382. Eckert, G. P., Hooff, G. P., Strandjord, D. M., Igbavboa, U., Volmer, D. A., Muller, W. E., and Wood, W. G. (2009) Regulation of the brain isoprenoids farnesyl- and geranylgeranylpyrophosphate is altered in male Alzheimer patients. *Neurobiology of disease* **35**, 251-257
383. Kohnke, M., Delon, C., Hastie, M. L., Nguyen, U. T., Wu, Y. W., Waldmann, H., Goody, R. S., Gorman, J. J., and Alexandrov, K. (2013) Rab GTPase prenylation hierarchy and its potential role in choroideremia disease. *PloS one* **8**, e81758
384. DeGraw, A. J., Palsuledesai, C., Ochocki, J. D., Dozier, J. K., Lenevich, S., Rashidian, M., and Distefano, M. D. (2010) Evaluation of alkyne-modified isoprenoids as chemical reporters of protein prenylation. *Chemical biology & drug design* **76**, 460-471
385. Cogli, L., Progida, C., Lecci, R., Bramato, R., Kruttgen, A., and Bucci, C. (2010) CMT2B-associated Rab7 mutants inhibit neurite outgrowth. *Acta neuropathologica* **120**, 491-501
386. BasuRay, S., Mukherjee, S., Romero, E., Wilson, M. C., and Wandinger-Ness, A. (2010) Rab7 mutants associated with Charcot-Marie-Tooth disease exhibit enhanced NGF-stimulated signaling. *PloS one* **5**, e15351

387. Cogli, L., Piro, F., and Bucci, C. (2009) Rab7 and the CMT2B disease. *Biochemical Society transactions* **37**, 1027-1031
388. Spinosa, M. R., Progidia, C., De Luca, A., Colucci, A. M., Alifano, P., and Bucci, C. (2008) Functional characterization of Rab7 mutant proteins associated with Charcot-Marie-Tooth type 2B disease. *The Journal of neuroscience : the official journal of the Society for Neuroscience* **28**, 1640-1648
389. Cherry, S., Jin, E. J., Ozel, M. N., Lu, Z., Agi, E., Wang, D., Jung, W. H., Epstein, D., Meinertzhagen, I. A., Chan, C. C., and Hiesinger, P. R. (2013) Charcot-Marie-Tooth 2B mutations in *rab7* cause dosage-dependent neurodegeneration due to partial loss of function. *eLife* **2**, e01064
390. Lin, M. G., and Zhong, Q. (2011) Interaction between small GTPase Rab7 and PI3KC3 links autophagy and endocytosis: A new Rab7 effector protein sheds light on membrane trafficking pathways. *Small GTPases* **2**, 85-88
391. Gutierrez, M. G., Munafo, D. B., Beron, W., and Colombo, M. I. (2004) Rab7 is required for the normal progression of the autophagic pathway in mammalian cells. *Journal of cell science* **117**, 2687-2697
392. Zhang, K., Fishel Ben Kenan, R., Osakada, Y., Xu, W., Sinit, R. S., Chen, L., Zhao, X., Chen, J. Y., Cui, B., and Wu, C. (2013) Defective axonal transport of Rab7 GTPase results in dysregulated trophic signaling. *The Journal of neuroscience : the official journal of the Society for Neuroscience* **33**, 7451-7462
393. Rui, Y. N., Xu, Z., Patel, B., Chen, Z., Chen, D., Tito, A., David, G., Sun, Y., Stimming, E. F., Bellen, H. J., Cuervo, A. M., and Zhang, S. (2015) Huntingtin functions as a scaffold for selective macroautophagy. *Nature cell biology* **17**, 262-275

394. Schroeder, B., Schulze, R. J., Weller, S. G., Sletten, A. C., Casey, C. A., and McNiven, M. A. (2015) The small GTPase Rab7 as a central regulator of hepatocellular lipophagy. *Hepatology (Baltimore, Md.)* **61**, 1896-1907
395. Yamano, K., Wang, C., Sarraf, S. A., Munch, C., Kikuchi, R., Noda, N. N., Hizukuri, Y., Kanemaki, M. T., Harper, W., Tanaka, K., Matsuda, N., and Youle, R. J. (2018) Endosomal Rab cycles regulate Parkin-mediated mitophagy. *eLife* **7**
396. Jimenez-Orgaz, A., Kvainickas, A., Nagele, H., Denner, J., Eimer, S., Dengjel, J., and Steinberg, F. (2018) Control of RAB7 activity and localization through the retromer-TBC1D5 complex enables RAB7-dependent mitophagy. *The EMBO journal* **37**, 235-254
397. Wang, J., Yao, X., and Huang, J. (2017) New tricks for human farnesyltransferase inhibitor: cancer and beyond. *MedChemComm* **8**, 841-854
398. Bates, G. (2003) Huntingtin aggregation and toxicity in Huntington's disease. *Lancet* **361**, 1642-1644
399. Tadano-Aritomi, K., Kubo, H., Ireland, P., Hikita, T., and Ishizuka, I. (1998) Isolation and characterization of a unique sulfated ganglioside, sulfated GM1a, from rat kidney. *Glycobiology* **8**, 341-350
400. Tettamanti, G. (2004) Ganglioside/glycosphingolipid turnover: new concepts. *Glycoconjugate journal* **20**, 301-317
401. Gatt, S. (1966) Enzymatic hydrolysis of sphingolipids. I. Hydrolysis and synthesis of ceramides by an enzyme from rat brain. *The Journal of biological chemistry* **241**, 3724-3730

402. Gault, C. R., Obeid, L. M., and Hannun, Y. A. (2010) An overview of sphingolipid metabolism: from synthesis to breakdown. *Advances in experimental medicine and biology* **688**, 1-23
403. Basu, S., Kaufman, B., and Roseman, S. (1968) Enzymatic synthesis of ceramide-glucose and ceramide-lactose by glycosyltransferases from embryonic chicken brain. *The Journal of biological chemistry* **243**, 5802-5804
404. Nomura, T., Takizawa, M., Aoki, J., Arai, H., Inoue, K., Wakisaka, E., Yoshizuka, N., Imokawa, G., Dohmae, N., Takio, K., Hattori, M., and Matsuo, N. (1998) Purification, cDNA cloning, and expression of UDP-Gal: glucosylceramide beta-1,4-galactosyltransferase from rat brain. *The Journal of biological chemistry* **273**, 13570-13577
405. Huwiler, A., Kolter, T., Pfeilschifter, J., and Sandhoff, K. (2000) Physiology and pathophysiology of sphingolipid metabolism and signaling. *Biochimica et biophysica acta* **1485**, 63-99
406. Posse de Chaves, E., and Sipione, S. (2010) Sphingolipids and gangliosides of the nervous system in membrane function and dysfunction. *FEBS letters* **584**, 1748-1759
407. Wu, G., Fang, Y., Lu, Z. H., and Ledeen, R. W. (1998) Induction of axon-like and dendrite-like processes in neuroblastoma cells. *Journal of neurocytology* **27**, 1-14
408. Wu, G., and Ledeen, R. W. (1991) Stimulation of neurite outgrowth in neuroblastoma cells by neuraminidase: putative role of GM1 ganglioside in differentiation. *Journal of neurochemistry* **56**, 95-104
409. Wu, G., Lu, Z. H., Obukhov, A. G., Nowycky, M. C., and Ledeen, R. W. (2007) Induction of calcium influx through TRPC5 channels by cross-linking of GM1 ganglioside associated

- with alpha5beta1 integrin initiates neurite outgrowth. *The Journal of neuroscience : the official journal of the Society for Neuroscience* **27**, 7447-7458
410. Kappagantula, S., Andrews, M. R., Cheah, M., Abad-Rodriguez, J., Dotti, C. G., and Fawcett, J. W. (2014) Neu3 sialidase-mediated ganglioside conversion is necessary for axon regeneration and is blocked in CNS axons. *The Journal of neuroscience : the official journal of the Society for Neuroscience* **34**, 2477-2492
411. Mutoh, T., Tokuda, A., Miyadai, T., Hamaguchi, M., and Fujiki, N. (1995) Ganglioside GM1 binds to the Trk protein and regulates receptor function. *Proceedings of the National Academy of Sciences of the United States of America* **92**, 5087-5091
412. Pitto, M., Mutoh, T., Kuriyama, M., Ferraretto, A., Palestini, P., and Masserini, M. (1998) Influence of endogenous GM1 ganglioside on TrkB activity, in cultured neurons. *FEBS letters* **439**, 93-96
413. Mitsuda, T., Furukawa, K., Fukumoto, S., Miyazaki, H., Urano, T., and Furukawa, K. (2002) Overexpression of ganglioside GM1 results in the dispersion of platelet-derived growth factor receptor from glycolipid-enriched microdomains and in the suppression of cell growth signals. *The Journal of biological chemistry* **277**, 11239-11246
414. Susuki, K., Baba, H., Tohyama, K., Kanai, K., Kuwabara, S., Hirata, K., Furukawa, K., Furukawa, K., Rasband, M. N., and Yuki, N. (2007) Gangliosides contribute to stability of paranodal junctions and ion channel clusters in myelinated nerve fibers. *Glia* **55**, 746-757
415. Hardy, J., and Selkoe, D. J. (2002) The amyloid hypothesis of Alzheimer's disease: progress and problems on the road to therapeutics. *Science* **297**, 353-356

416. Yanagisawa, K., Odaka, A., Suzuki, N., and Ihara, Y. (1995) GM1 ganglioside-bound amyloid beta-protein (A beta): a possible form of preamyloid in Alzheimer's disease. *Nature medicine* **1**, 1062-1066
417. Yanagisawa, K., and Ihara, Y. (1998) GM1 ganglioside-bound amyloid beta-protein in Alzheimer's disease brain. *Neurobiology of aging* **19**, S65-67
418. Hayashi, H., Kimura, N., Yamaguchi, H., Hasegawa, K., Yokoseki, T., Shibata, M., Yamamoto, N., Michikawa, M., Yoshikawa, Y., Terao, K., Matsuzaki, K., Lemere, C. A., Selkoe, D. J., Naiki, H., and Yanagisawa, K. (2004) A seed for Alzheimer amyloid in the brain. *The Journal of neuroscience : the official journal of the Society for Neuroscience* **24**, 4894-4902
419. Hong, S., Ostaszewski, B. L., Yang, T., O'Malley, T. T., Jin, M., Yanagisawa, K., Li, S., Bartels, T., and Selkoe, D. J. (2014) Soluble Abeta oligomers are rapidly sequestered from brain ISF in vivo and bind GM1 ganglioside on cellular membranes. *Neuron* **82**, 308-319
420. Zha, Q., Ruan, Y., Hartmann, T., Beyreuther, K., and Zhang, D. (2004) GM1 ganglioside regulates the proteolysis of amyloid precursor protein. *Molecular psychiatry* **9**, 946-952
421. Del Tredici, K., and Braak, H. (2016) Review: Sporadic Parkinson's disease: development and distribution of alpha-synuclein pathology. *Neuropathology and applied neurobiology* **42**, 33-50
422. Skaper, S. D., Facci, L., Schiavo, N., Vantini, G., Moroni, F., Dal Toso, R., and Leon, A. (1992) Characterization of 2,4,5-trihydroxyphenylalanine neurotoxicity in vitro and protective effects of ganglioside GM1: implications for Parkinson's disease. *The Journal of pharmacology and experimental therapeutics* **263**, 1440-1446

423. Martinez, Z., Zhu, M., Han, S., and Fink, A. L. (2007) GM1 specifically interacts with alpha-synuclein and inhibits fibrillation. *Biochemistry* **46**, 1868-1877
424. Xu, R., Zhou, Y., Fang, X., Lu, Y., Li, J., Zhang, J., Deng, X., and Li, S. (2014) The possible mechanism of Parkinson's disease progressive damage and the preventive effect of GM1 in the rat model induced by 6-hydroxydopamine. *Brain research* **1592**, 73-81
425. Ba, X. H. (2016) Therapeutic effects of GM1 on Parkinson's disease in rats and its mechanism. *The International journal of neuroscience* **126**, 163-167
426. Wu, G., Lu, Z. H., Kulkarni, N., and Ledeen, R. W. (2012) Deficiency of ganglioside GM1 correlates with Parkinson's disease in mice and humans. *Journal of neuroscience research* **90**, 1997-2008
427. Johnston, J. A., Ward, C. L., and Kopito, R. R. (1998) Aggresomes: a cellular response to misfolded proteins. *The Journal of cell biology* **143**, 1883-1898
428. Goldberg, A. L. (2003) Protein degradation and protection against misfolded or damaged proteins. *Nature* **426**, 895-899
429. Corboy, M. J., Thomas, P. J., and Wigley, W. C. (2005) Aggresome formation. *Methods Mol Biol* **301**, 305-327
430. Paine, M. G., Babu, J. R., Seibenhener, M. L., and Wooten, M. W. (2005) Evidence for p62 aggregate formation: role in cell survival. *FEBS letters* **579**, 5029-5034
431. Mishra, R. S., Bose, S., Gu, Y., Li, R., and Singh, N. (2003) Aggresome formation by mutant prion proteins: the unfolding role of proteasomes in familial prion disorders. *Journal of Alzheimer's disease : JAD* **5**, 15-23

432. Homma, T., Ishibashi, D., Nakagaki, T., Satoh, K., Sano, K., Atarashi, R., and Nishida, N. (2014) Increased expression of p62/SQSTM1 in prion diseases and its association with pathogenic prion protein. *Scientific reports* **4**, 4504
433. Renziehausen, J., Hiebel, C., Nagel, H., Kundu, A., Kins, S., Kogel, D., Behl, C., and Hajieva, P. (2015) The cleavage product of amyloid-beta protein precursor sAbetaPPalpha modulates BAG3-dependent aggresome formation and enhances cellular proteasomal activity. *Journal of Alzheimer's disease : JAD* **44**, 879-896
434. Viswanathan, J., Haapasalo, A., Bottcher, C., Miettinen, R., Kurkinen, K. M., Lu, A., Thomas, A., Maynard, C. J., Romano, D., Hyman, B. T., Berezovska, O., Bertram, L., Soininen, H., Dantuma, N. P., Tanzi, R. E., and Hiltunen, M. (2011) Alzheimer's disease-associated ubiquitin-1 regulates presenilin-1 accumulation and aggresome formation. *Traffic (Copenhagen, Denmark)* **12**, 330-348
435. Xia, Q., Wang, H., Zhang, Y., Ying, Z., and Wang, G. (2015) Loss of TDP-43 Inhibits Amyotrophic Lateral Sclerosis-Linked Mutant SOD1 Aggresome Formation in an HDAC6-Dependent Manner. *Journal of Alzheimer's disease : JAD* **45**, 373-386
436. Yung, C., Sha, D., Li, L., and Chin, L. S. (2015) Parkin Protects Against Misfolded SOD1 Toxicity by Promoting Its Aggresome Formation and Autophagic Clearance. *Molecular neurobiology*
437. Ardley, H. C., Scott, G. B., Rose, S. A., Tan, N. G., and Robinson, P. A. (2004) UCH-L1 aggresome formation in response to proteasome impairment indicates a role in inclusion formation in Parkinson's disease. *Journal of neurochemistry* **90**, 379-391
438. Chin, L. S., Olzmann, J. A., and Li, L. (2010) Parkin-mediated ubiquitin signalling in aggresome formation and autophagy. *Biochemical Society transactions* **38**, 144-149

439. Lan, D., Wang, W., Zhuang, J., and Zhao, Z. (2015) Proteasome inhibitor-induced autophagy in PC12 cells overexpressing A53T mutant alpha-synuclein. *Molecular medicine reports* **11**, 1655-1660
440. McNaught, K. S., Shashidharan, P., Perl, D. P., Jenner, P., and Olanow, C. W. (2002) Aggresome-related biogenesis of Lewy bodies. *The European journal of neuroscience* **16**, 2136-2148
441. Boeddrich, A., Lurz, R., and Wanker, E. E. (2003) Huntingtin fragments form aggresome-like inclusion bodies in mammalian cells. *Methods Mol Biol* **232**, 217-229
442. Nagaoka, U., Kim, K., Jana, N. R., Doi, H., Maruyama, M., Mitsui, K., Oyama, F., and Nukina, N. (2004) Increased expression of p62 in expanded polyglutamine-expressing cells and its association with polyglutamine inclusions. *Journal of neurochemistry* **91**, 57-68
443. Bjorkoy, G., Lamark, T., Brech, A., Outzen, H., Perander, M., Overvatn, A., Stenmark, H., and Johansen, T. (2005) p62/SQSTM1 forms protein aggregates degraded by autophagy and has a protective effect on huntingtin-induced cell death. *The Journal of cell biology* **171**, 603-614
444. Wigley, W. C., Fabunmi, R. P., Lee, M. G., Marino, C. R., Muallem, S., DeMartino, G. N., and Thomas, P. J. (1999) Dynamic association of proteasomal machinery with the centrosome. *The Journal of cell biology* **145**, 481-490
445. Wojcik, C., Schroeter, D., Wilk, S., Lamprecht, J., and Paweletz, N. (1996) Ubiquitin-mediated proteolysis centers in HeLa cells: indication from studies of an inhibitor of the chymotrypsin-like activity of the proteasome. *European journal of cell biology* **71**, 311-318

446. Wojcik, C. (1997) On the spatial organization of ubiquitin-dependent proteolysis in HeLa cells. *Folia histochemica et cytobiologica* **35**, 117-118
447. Weiss, A., Klein, C., Woodman, B., Sathasivam, K., Bibel, M., Regulier, E., Bates, G. P., and Paganetti, P. (2008) Sensitive biochemical aggregate detection reveals aggregation onset before symptom development in cellular and murine models of Huntington's disease. *Journal of neurochemistry* **104**, 846-858
448. Wojcik, C. (1997) An inhibitor of the chymotrypsin-like activity of the proteasome (PSI) induces similar morphological changes in various cell lines. *Folia histochemica et cytobiologica* **35**, 211-214
449. Wojcik, C., Yano, M., and DeMartino, G. N. (2004) RNA interference of valosin-containing protein (VCP/p97) reveals multiple cellular roles linked to ubiquitin/proteasome-dependent proteolysis. *Journal of cell science* **117**, 281-292
450. Salemi, L. M., Almawi, A. W., Lefebvre, K. J., and Schild-Poulter, C. (2014) Aggresome formation is regulated by RanBPM through an interaction with HDAC6. *Biology open* **3**, 418-430
451. Bang, Y., Kang, B. Y., and Choi, H. J. (2014) Preconditioning stimulus of proteasome inhibitor enhances aggresome formation and autophagy in differentiated SH-SY5Y cells. *Neuroscience letters* **566**, 263-268
452. Rusten, T. E., and Stenmark, H. (2010) p62, an autophagy hero or culprit? *Nature cell biology* **12**, 207-209
453. Lee, B. L., Singh, A., Mark Glover, J. N., Hendzel, M. J., and Spyropoulos, L. (2017) Molecular Basis for K63-Linked Ubiquitination Processes in Double-Strand DNA Break Repair: A Focus on Kinetics and Dynamics. *Journal of molecular biology* **429**, 3409-3429

454. Erpapazoglou, Z., Walker, O., and Haguenaue-Tsapis, R. (2014) Versatile roles of k63-linked ubiquitin chains in trafficking. *Cells* **3**, 1027-1088
455. Piper, R. C., and Lehner, P. J. (2011) Endosomal transport via ubiquitination. *Trends in cell biology* **21**, 647-655
456. Huebner, A. R., Cheng, L., Somparn, P., Knepper, M. A., Fenton, R. A., and Pisitkun, T. (2016) Deubiquitylation of Protein Cargo Is Not an Essential Step in Exosome Formation. *Molecular & cellular proteomics : MCP* **15**, 1556-1571
457. Dowlatshahi, D. P., Sandrin, V., Vivona, S., Shaler, T. A., Kaiser, S. E., Melandri, F., Sundquist, W. I., and Kopito, R. R. (2012) ALIX is a Lys63-specific polyubiquitin binding protein that functions in retrovirus budding. *Developmental cell* **23**, 1247-1254
458. Kegel, K. B., Kim, M., Sapp, E., McIntyre, C., Castano, J. G., Aronin, N., and DiFiglia, M. (2000) Huntingtin expression stimulates endosomal-lysosomal activity, endosome tubulation, and autophagy. *The Journal of neuroscience : the official journal of the Society for Neuroscience* **20**, 7268-7278
459. Ravikumar, B., Vacher, C., Berger, Z., Davies, J. E., Luo, S., Oroz, L. G., Scaravilli, F., Easton, D. F., Duden, R., O'Kane, C. J., and Rubinsztein, D. C. (2004) Inhibition of mTOR induces autophagy and reduces toxicity of polyglutamine expansions in fly and mouse models of Huntington disease. *Nature genetics* **36**, 585-595
460. Korolchuk, V. I., Menzies, F. M., and Rubinsztein, D. C. (2010) Mechanisms of cross-talk between the ubiquitin-proteasome and autophagy-lysosome systems. *FEBS letters* **584**, 1393-1398

461. Orthaber, D., and Glatter, O. (1998) Time and temperature dependent aggregation behaviour of the ganglioside GM1 in aqueous solution. *Chemistry and physics of lipids* **92**, 53-62
462. Lu, Q., Wu, F., and Zhang, H. (2013) Aggrephagy: lessons from *C. elegans*. *The Biochemical journal* **452**, 381-390
463. Hyttinen, J. M., Amadio, M., Viiri, J., Pascale, A., Salminen, A., and Kaarniranta, K. (2014) Clearance of misfolded and aggregated proteins by aggrephagy and implications for aggregation diseases. *Ageing research reviews* **18**, 16-28
464. Lamb, C. A., Yoshimori, T., and Tooze, S. A. (2013) The autophagosome: origins unknown, biogenesis complex. *Nature reviews. Molecular cell biology* **14**, 759-774
465. Cuervo, A. M., Bergamini, E., Brunk, U. T., Droge, W., Ffrench, M., and Terman, A. (2005) Autophagy and aging: the importance of maintaining "clean" cells. *Autophagy* **1**, 131-140
466. Tsujimoto, Y., and Shimizu, S. (2005) Another way to die: autophagic programmed cell death. *Cell death and differentiation* **12 Suppl 2**, 1528-1534
467. Giordano, S., Darley-Usmar, V., and Zhang, J. (2014) Autophagy as an essential cellular antioxidant pathway in neurodegenerative disease. *Redox biology* **2**, 82-90
468. Rubinsztein, D. C., DiFiglia, M., Heintz, N., Nixon, R. A., Qin, Z. H., Ravikumar, B., Stefanis, L., and Tolkovsky, A. (2005) Autophagy and its possible roles in nervous system diseases, damage and repair. *Autophagy* **1**, 11-22
469. Du, Y., Yang, D., Li, L., Luo, G., Li, T., Fan, X., Wang, Q., Zhang, X., Wang, Y., and Le, W. (2009) An insight into the mechanistic role of p53-mediated autophagy induction in response to proteasomal inhibition-induced neurotoxicity. *Autophagy* **5**, 663-675

470. Taylor, J. M., Brody, K. M., and Lockhart, P. J. (2012) Parkin co-regulated gene is involved in aggresome formation and autophagy in response to proteasomal impairment. *Experimental cell research* **318**, 2059-2070
471. Ding, W. X., Ni, H. M., Gao, W., Yoshimori, T., Stolz, D. B., Ron, D., and Yin, X. M. (2007) Linking of autophagy to ubiquitin-proteasome system is important for the regulation of endoplasmic reticulum stress and cell viability. *The American journal of pathology* **171**, 513-524
472. Fimia, G. M., Kroemer, G., and Piacentini, M. (2013) Molecular mechanisms of selective autophagy. *Cell death and differentiation* **20**, 1-2
473. Zaffagnini, G., and Martens, S. (2016) Mechanisms of Selective Autophagy. *Journal of molecular biology* **428**, 1714-1724
474. Mari, M., Tooze, S. A., and Reggiori, F. (2011) The puzzling origin of the autophagosomal membrane. *F1000 biology reports* **3**, 25
475. Xie, Z., and Klionsky, D. J. (2007) Autophagosome formation: core machinery and adaptations. *Nature cell biology* **9**, 1102-1109
476. Hosokawa, N., Hara, T., Kaizuka, T., Kishi, C., Takamura, A., Miura, Y., Iemura, S., Natsume, T., Takehana, K., Yamada, N., Guan, J. L., Oshiro, N., and Mizushima, N. (2009) Nutrient-dependent mTORC1 association with the ULK1-Atg13-FIP200 complex required for autophagy. *Mol Biol Cell* **20**, 1981-1991
477. Jung, C. H., Jun, C. B., Ro, S. H., Kim, Y. M., Otto, N. M., Cao, J., Kundu, M., and Kim, D. H. (2009) ULK-Atg13-FIP200 complexes mediate mTOR signaling to the autophagy machinery. *Mol Biol Cell* **20**, 1992-2003

478. Sun, Q., Fan, W., Chen, K., Ding, X., Chen, S., and Zhong, Q. (2008) Identification of Barkor as a mammalian autophagy-specific factor for Beclin 1 and class III phosphatidylinositol 3-kinase. *Proceedings of the National Academy of Sciences of the United States of America* **105**, 19211-19216
479. Itakura, E., Kishi, C., Inoue, K., and Mizushima, N. (2008) Beclin 1 forms two distinct phosphatidylinositol 3-kinase complexes with mammalian Atg14 and UVRAG. *Mol Biol Cell* **19**, 5360-5372
480. Liang, C., Feng, P., Ku, B., Dotan, I., Canaani, D., Oh, B. H., and Jung, J. U. (2006) Autophagic and tumour suppressor activity of a novel Beclin1-binding protein UVRAG. *Nature cell biology* **8**, 688-699
481. Matsunaga, K., Saitoh, T., Tabata, K., Omori, H., Satoh, T., Kurotori, N., Maejima, I., Shirahama-Noda, K., Ichimura, T., Isobe, T., Akira, S., Noda, T., and Yoshimori, T. (2009) Two Beclin 1-binding proteins, Atg14L and Rubicon, reciprocally regulate autophagy at different stages. *Nature cell biology* **11**, 385-396
482. Zhong, Y., Wang, Q. J., Li, X., Yan, Y., Backer, J. M., Chait, B. T., Heintz, N., and Yue, Z. (2009) Distinct regulation of autophagic activity by Atg14L and Rubicon associated with Beclin 1-phosphatidylinositol-3-kinase complex. *Nature cell biology* **11**, 468-476
483. Takahashi, Y., Meyerkord, C. L., and Wang, H. G. (2009) Bif-1/endophilin B1: a candidate for crescent driving force in autophagy. *Cell death and differentiation* **16**, 947-955
484. Yang, Z., and Klionsky, D. J. (2009) An overview of the molecular mechanism of autophagy. *Current topics in microbiology and immunology* **335**, 1-32
485. Lamark, T., Kirkin, V., Dikic, I., and Johansen, T. (2009) NBR1 and p62 as cargo receptors for selective autophagy of ubiquitinated targets. *Cell cycle* **8**, 1986-1990

486. von Muhlinen, N., Akutsu, M., Ravenhill, B. J., Foeglein, A., Bloor, S., Rutherford, T. J., Freund, S. M., Komander, D., and Randow, F. (2012) LC3C, bound selectively by a noncanonical LIR motif in NDP52, is required for antibacterial autophagy. *Molecular cell* **48**, 329-342
487. Kirkin, V., Lamark, T., Sou, Y. S., Bjorkoy, G., Nunn, J. L., Bruun, J. A., Shvets, E., McEwan, D. G., Clausen, T. H., Wild, P., Bilusic, I., Theurillat, J. P., Overvatn, A., Ishii, T., Elazar, Z., Komatsu, M., Dikic, I., and Johansen, T. (2009) A role for NBR1 in autophagosomal degradation of ubiquitinated substrates. *Molecular cell* **33**, 505-516
488. Wild, P., Farhan, H., McEwan, D. G., Wagner, S., Rogov, V. V., Brady, N. R., Richter, B., Korac, J., Waidmann, O., Choudhary, C., Dotsch, V., Bumann, D., and Dikic, I. (2011) Phosphorylation of the autophagy receptor optineurin restricts Salmonella growth. *Science* **333**, 228-233
489. Novak, I., Kirkin, V., McEwan, D. G., Zhang, J., Wild, P., Rozenknop, A., Rogov, V., Lohr, F., Popovic, D., Occhipinti, A., Reichert, A. S., Terzic, J., Dotsch, V., Ney, P. A., and Dikic, I. (2010) Nix is a selective autophagy receptor for mitochondrial clearance. *EMBO reports* **11**, 45-51
490. Lim, J., Lachenmayer, M. L., Wu, S., Liu, W., Kundu, M., Wang, R., Komatsu, M., Oh, Y. J., Zhao, Y., and Yue, Z. (2015) Proteotoxic stress induces phosphorylation of p62/SQSTM1 by ULK1 to regulate selective autophagic clearance of protein aggregates. *PLoS genetics* **11**, e1004987
491. Matsumoto, G., Wada, K., Okuno, M., Kurosawa, M., and Nukina, N. (2011) Serine 403 phosphorylation of p62/SQSTM1 regulates selective autophagic clearance of ubiquitinated proteins. *Molecular cell* **44**, 279-289

492. Wurzer, B., Zaffagnini, G., Fracchiolla, D., Turco, E., Abert, C., Romanov, J., and Martens, S. (2015) Oligomerization of p62 allows for selection of ubiquitinated cargo and isolation membrane during selective autophagy. *eLife* **4**, e08941
493. Seibenhener, M. L., Babu, J. R., Geetha, T., Wong, H. C., Krishna, N. R., and Wooten, M. W. (2004) Sequestosome 1/p62 is a polyubiquitin chain binding protein involved in ubiquitin proteasome degradation. *Molecular and cellular biology* **24**, 8055-8068
494. Long, J., Gallagher, T. R., Cavey, J. R., Sheppard, P. W., Ralston, S. H., Layfield, R., and Searle, M. S. (2008) Ubiquitin recognition by the ubiquitin-associated domain of p62 involves a novel conformational switch. *The Journal of biological chemistry* **283**, 5427-5440
495. Olzmann, J. A., and Chin, L. S. (2008) Parkin-mediated K63-linked polyubiquitination: a signal for targeting misfolded proteins to the aggresome-autophagy pathway. *Autophagy* **4**, 85-87
496. Tan, J. M., Wong, E. S., Kirkpatrick, D. S., Pletnikova, O., Ko, H. S., Tay, S. P., Ho, M. W., Troncoso, J., Gygi, S. P., Lee, M. K., Dawson, V. L., Dawson, T. M., and Lim, K. L. (2008) Lysine 63-linked ubiquitination promotes the formation and autophagic clearance of protein inclusions associated with neurodegenerative diseases. *Human molecular genetics* **17**, 431-439
497. Pankiv, S., Clausen, T. H., Lamark, T., Brech, A., Bruun, J. A., Outzen, H., Overvatn, A., Bjorkoy, G., and Johansen, T. (2007) p62/SQSTM1 binds directly to Atg8/LC3 to facilitate degradation of ubiquitinated protein aggregates by autophagy. *The Journal of biological chemistry* **282**, 24131-24145

498. Janen, S. B., Chaachouay, H., and Richter-Landsberg, C. (2010) Autophagy is activated by proteasomal inhibition and involved in aggresome clearance in cultured astrocytes. *Glia* **58**, 1766-1774
499. Glick, D., Barth, S., and Macleod, K. F. (2010) Autophagy: cellular and molecular mechanisms. *The Journal of pathology* **221**, 3-12
500. Webb, J. L., Ravikumar, B., and Rubinsztein, D. C. (2004) Microtubule disruption inhibits autophagosome-lysosome fusion: implications for studying the roles of aggresomes in polyglutamine diseases. *The international journal of biochemistry & cell biology* **36**, 2541-2550
501. Tanaka, Y., Guhde, G., Suter, A., Eskelinen, E. L., Hartmann, D., Lullmann-Rauch, R., Janssen, P. M., Blanz, J., von Figura, K., and Saftig, P. (2000) Accumulation of autophagic vacuoles and cardiomyopathy in LAMP-2-deficient mice. *Nature* **406**, 902-906
502. Jager, S., Bucci, C., Tanida, I., Ueno, T., Kominami, E., Saftig, P., and Eskelinen, E. L. (2004) Role for Rab7 in maturation of late autophagic vacuoles. *Journal of cell science* **117**, 4837-4848
503. Butler, D., Brown, Q. B., Chin, D. J., Batey, L., Karim, S., Mutneja, M. S., Karanian, D. A., and Bahr, B. A. (2005) Cellular responses to protein accumulation involve autophagy and lysosomal enzyme activation. *Rejuvenation research* **8**, 227-237
504. Sardiello, M., Palmieri, M., di Ronza, A., Medina, D. L., Valenza, M., Gennarino, V. A., Di Malta, C., Donaudy, F., Embrione, V., Polishchuk, R. S., Banfi, S., Parenti, G., Cattaneo, E., and Ballabio, A. (2009) A gene network regulating lysosomal biogenesis and function. *Science* **325**, 473-477

505. Rocznik-Ferguson, A., Petit, C. S., Froehlich, F., Qian, S., Ky, J., Angarola, B., Walther, T. C., and Ferguson, S. M. (2012) The transcription factor TFEB links mTORC1 signaling to transcriptional control of lysosome homeostasis. *Science signaling* **5**, ra42
506. Settembre, C., Zoncu, R., Medina, D. L., Vetrini, F., Erdin, S., Erdin, S., Huynh, T., Ferron, M., Karsenty, G., Vellard, M. C., Facchinetti, V., Sabatini, D. M., and Ballabio, A. (2012) A lysosome-to-nucleus signalling mechanism senses and regulates the lysosome via mTOR and TFEB. *The EMBO journal* **31**, 1095-1108
507. Medina, D. L., Di Paola, S., Peluso, I., Armani, A., De Stefani, D., Venditti, R., Montefusco, S., Scotto-Rosato, A., Prezioso, C., Forrester, A., Settembre, C., Wang, W., Gao, Q., Xu, H., Sandri, M., Rizzuto, R., De Matteis, M. A., and Ballabio, A. (2015) Lysosomal calcium signalling regulates autophagy through calcineurin and TFEB. *Nature cell biology* **17**, 288-299
508. Chauhan, S., Goodwin, J. G., Chauhan, S., Manyam, G., Wang, J., Kamat, A. M., and Boyd, D. D. (2013) ZKSCAN3 is a master transcriptional repressor of autophagy. *Molecular cell* **50**, 16-28
509. Menzies, F. M., Fleming, A., Caricasole, A., Bento, C. F., Andrews, S. P., Ashkenazi, A., Fullgrabe, J., Jackson, A., Jimenez Sanchez, M., Karabiyik, C., Licitra, F., Lopez Ramirez, A., Pavel, M., Puri, C., Renna, M., Ricketts, T., Schlotawa, L., Vicinanza, M., Won, H., Zhu, Y., Skidmore, J., and Rubinsztein, D. C. (2017) Autophagy and Neurodegeneration: Pathogenic Mechanisms and Therapeutic Opportunities. *Neuron* **93**, 1015-1034
510. Lim, K. L., and Lim, G. G. (2011) K63-linked ubiquitination and neurodegeneration. *Neurobiology of disease* **43**, 9-16

511. Lim, K. L., Dawson, V. L., and Dawson, T. M. (2006) Parkin-mediated lysine 63-linked polyubiquitination: a link to protein inclusions formation in Parkinson's and other conformational diseases? *Neurobiology of aging* **27**, 524-529
512. McKeon, J. E., Sha, D., Li, L., and Chin, L. S. (2015) Parkin-mediated K63-polyubiquitination targets ubiquitin C-terminal hydrolase L1 for degradation by the autophagy-lysosome system. *Cellular and molecular life sciences : CMLS* **72**, 1811-1824
513. Spilman, P., Podlitskaya, N., Hart, M. J., Debnath, J., Gorostiza, O., Bredesen, D., Richardson, A., Strong, R., and Galvan, V. (2010) Inhibition of mTOR by rapamycin abolishes cognitive deficits and reduces amyloid-beta levels in a mouse model of Alzheimer's disease. *PloS one* **5**, e9979
514. Vingtdeux, V., Chandakkar, P., Zhao, H., d'Abramo, C., Davies, P., and Marambaud, P. (2011) Novel synthetic small-molecule activators of AMPK as enhancers of autophagy and amyloid-beta peptide degradation. *FASEB J* **25**, 219-231
515. Tian, Y., Bustos, V., Flajolet, M., and Greengard, P. (2011) A small-molecule enhancer of autophagy decreases levels of A β and APP-CTF via Atg5-dependent autophagy pathway. *FASEB J* **25**, 1934-1942
516. Pickford, F., Masliah, E., Britschgi, M., Lucin, K., Narasimhan, R., Jaeger, P. A., Small, S., Spencer, B., Rockenstein, E., Levine, B., and Wyss-Coray, T. (2008) The autophagy-related protein beclin 1 shows reduced expression in early Alzheimer disease and regulates amyloid beta accumulation in mice. *The Journal of clinical investigation* **118**, 2190-2199
517. Kitada, T., Asakawa, S., Hattori, N., Matsumine, H., Yamamura, Y., Minoshima, S., Yokochi, M., Mizuno, Y., and Shimizu, N. (1998) Mutations in the parkin gene cause autosomal recessive juvenile parkinsonism. *Nature* **392**, 605-608

518. Valente, E. M., Abou-Sleiman, P. M., Caputo, V., Muqit, M. M., Harvey, K., Gispert, S., Ali, Z., Del Turco, D., Bentivoglio, A. R., Healy, D. G., Albanese, A., Nussbaum, R., Gonzalez-Maldonado, R., Deller, T., Salvi, S., Cortelli, P., Gilks, W. P., Latchman, D. S., Harvey, R. J., Dallapiccola, B., Auburger, G., and Wood, N. W. (2004) Hereditary early-onset Parkinson's disease caused by mutations in PINK1. *Science* **304**, 1158-1160
519. Bonifati, V., Rizzu, P., van Baren, M. J., Schaap, O., Breedveld, G. J., Krieger, E., Dekker, M. C., Squitieri, F., Ibanez, P., Joosse, M., van Dongen, J. W., Vanacore, N., van Swieten, J. C., Brice, A., Meco, G., van Duijn, C. M., Oostra, B. A., and Heutink, P. (2003) Mutations in the DJ-1 gene associated with autosomal recessive early-onset parkinsonism. *Science* **299**, 256-259
520. Matsuda, N., Sato, S., Shiba, K., Okatsu, K., Saisho, K., Gautier, C. A., Sou, Y. S., Saiki, S., Kawajiri, S., Sato, F., Kimura, M., Komatsu, M., Hattori, N., and Tanaka, K. (2010) PINK1 stabilized by mitochondrial depolarization recruits Parkin to damaged mitochondria and activates latent Parkin for mitophagy. *The Journal of cell biology* **189**, 211-221
521. Greene, J. C., Whitworth, A. J., Kuo, I., Andrews, L. A., Feany, M. B., and Pallanck, L. J. (2003) Mitochondrial pathology and apoptotic muscle degeneration in *Drosophila* parkin mutants. *Proceedings of the National Academy of Sciences of the United States of America* **100**, 4078-4083
522. Goldberg, M. S., Fleming, S. M., Palacino, J. J., Cepeda, C., Lam, H. A., Bhatnagar, A., Meloni, E. G., Wu, N., Ackerson, L. C., Klapstein, G. J., Gajendiran, M., Roth, B. L., Chesselet, M. F., Maidment, N. T., Levine, M. S., and Shen, J. (2003) Parkin-deficient

- mice exhibit nigrostriatal deficits but not loss of dopaminergic neurons. *The Journal of biological chemistry* **278**, 43628-43635
523. Palacino, J. J., Sagi, D., Goldberg, M. S., Krauss, S., Motz, C., Wacker, M., Klose, J., and Shen, J. (2004) Mitochondrial dysfunction and oxidative damage in parkin-deficient mice. *The Journal of biological chemistry* **279**, 18614-18622
524. Gispert, S., Ricciardi, F., Kurz, A., Azizov, M., Hoepken, H. H., Becker, D., Voos, W., Leuner, K., Muller, W. E., Kudin, A. P., Kunz, W. S., Zimmermann, A., Roeper, J., Wenzel, D., Jendrach, M., Garcia-Arencibia, M., Fernandez-Ruiz, J., Huber, L., Rohrer, H., Barrera, M., Reichert, A. S., Rub, U., Chen, A., Nussbaum, R. L., and Auburger, G. (2009) Parkinson phenotype in aged PINK1-deficient mice is accompanied by progressive mitochondrial dysfunction in absence of neurodegeneration. *PloS one* **4**, e5777
525. Pierzynowska, K., Gaffke, L., Hac, A., Mantej, J., Niedzialek, N., Brokowska, J., and Wegrzyn, G. (2018) Correction of Huntington's Disease Phenotype by Genistein-Induced Autophagy in the Cellular Model. *Neuromolecular medicine* **20**, 112-123
526. Floto, R. A., Sarkar, S., Perlstein, E. O., Kampmann, B., Schreiber, S. L., and Rubinsztein, D. C. (2007) Small molecule enhancers of rapamycin-induced TOR inhibition promote autophagy, reduce toxicity in Huntington's disease models and enhance killing of mycobacteria by macrophages. *Autophagy* **3**, 620-622
527. Ochaba, J., Lukacsovich, T., Csikos, G., Zheng, S., Margulis, J., Salazar, L., Mao, K., Lau, A. L., Yeung, S. Y., Humbert, S., Saudou, F., Klionsky, D. J., Finkbeiner, S., Zeitlin, S. O., Marsh, J. L., Housman, D. E., Thompson, L. M., and Steffan, J. S. (2014) Potential function for the Huntingtin protein as a scaffold for selective autophagy. *Proceedings of the National Academy of Sciences of the United States of America* **111**, 16889-16894

528. Rui, Y. N., Xu, Z., Patel, B., Cuervo, A. M., and Zhang, S. (2015) HTT/Huntingtin in selective autophagy and Huntington disease: A foe or a friend within? *Autophagy* **11**, 858-860
529. Mealer, R. G., Murray, A. J., Shahani, N., Subramaniam, S., and Snyder, S. H. (2014) Rhes, a striatal-selective protein implicated in Huntington disease, binds beclin-1 and activates autophagy. *The Journal of biological chemistry* **289**, 3547-3554
530. Wong, Y. C., and Holzbaur, E. L. (2014) The regulation of autophagosome dynamics by huntingtin and HAP1 is disrupted by expression of mutant huntingtin, leading to defective cargo degradation. *The Journal of neuroscience : the official journal of the Society for Neuroscience* **34**, 1293-1305
531. Hwang, J., Lee, S., Lee, J. T., Kwon, T. K., Kim, D. R., Kim, H., Park, H. C., and Suk, K. (2010) Gangliosides induce autophagic cell death in astrocytes. *British journal of pharmacology* **159**, 586-603
532. Wei, J., Fujita, M., Nakai, M., Waragai, M., Sekigawa, A., Sugama, S., Takenouchi, T., Masliah, E., and Hashimoto, M. (2009) Protective role of endogenous gangliosides for lysosomal pathology in a cellular model of synucleinopathies. *The American journal of pathology* **174**, 1891-1909
533. Wei, J., Fujita, M., Sekigawa, A., Sekiyama, K., Waragai, M., and Hashimoto, M. (2009) Gangliosides' protection against lysosomal pathology of synucleinopathies. *Autophagy* **5**, 860-861
534. Dai, R., Zhang, S., Duan, W., Wei, R., Chen, H., Cai, W., Yang, L., and Wang, Q. (2017) Enhanced Autophagy Contributes to Protective Effects of GM1 Ganglioside Against

- Abeta1-42-Induced Neurotoxicity and Cognitive Deficits. *Neurochemical research* **42**, 2417-2426
535. Li, L., Tian, J., Long, M. K., Chen, Y., Lu, J., Zhou, C., and Wang, T. (2016) Protection against Experimental Stroke by Ganglioside GM1 Is Associated with the Inhibition of Autophagy. *PloS one* **11**, e0144219
536. Yan, J., Kuroyanagi, H., Kuroiwa, A., Matsuda, Y., Tokumitsu, H., Tomoda, T., Shirasawa, T., and Muramatsu, M. (1998) Identification of mouse ULK1, a novel protein kinase structurally related to *C. elegans* UNC-51. *Biochemical and biophysical research communications* **246**, 222-227
537. Kim, J., Kundu, M., Viollet, B., and Guan, K. L. (2011) AMPK and mTOR regulate autophagy through direct phosphorylation of Ulk1. *Nature cell biology* **13**, 132-141
538. Bjorkoy, G., Lamark, T., Pankiv, S., Overvatn, A., Brech, A., and Johansen, T. (2009) Monitoring autophagic degradation of p62/SQSTM1. *Methods in enzymology* **452**, 181-197
539. Wang, Y., Tian, G., Cowan, N. J., and Cabral, F. (2006) Mutations affecting beta-tubulin folding and degradation. *The Journal of biological chemistry* **281**, 13628-13635
540. Spiegelman, B. M., Penningroth, S. M., and Kirschner, M. W. (1977) Turnover of tubulin and the N site GTP in Chinese hamster ovary cells. *Cell* **12**, 587-600
541. Lamark, T., and Johansen, T. (2012) Aggrephagy: selective disposal of protein aggregates by macroautophagy. *International journal of cell biology* **2012**, 736905
542. Ledeen, R. W., and Wu, G. (2015) The multi-tasked life of GM1 ganglioside, a true factotum of nature. *Trends in biochemical sciences* **40**, 407-418

543. Xie, X., Wu, G., Lu, Z. H., and Ledeen, R. W. (2002) Potentiation of a sodium-calcium exchanger in the nuclear envelope by nuclear GM1 ganglioside. *Journal of neurochemistry* **81**, 1185-1195
544. Xiong, J., and Zhu, M. X. (2016) Regulation of lysosomal ion homeostasis by channels and transporters. *Science China. Life sciences* **59**, 777-791
545. Gomez, N. M., Lu, W., Lim, J. C., Kiselyov, K., Campagno, K. E., Grishchuk, Y., Slaugenhaupt, S. A., Pfeffer, B. A., Fliesler, S. J., and Mitchell, C. H. (2018) Robust lysosomal calcium signaling through channel TRPML1 is impaired by lysosomal lipid accumulation. *FASEB J* **32**, 782-794
546. Zhou, S., Davidson, C., McGlynn, R., Stephney, G., Dobrenis, K., Vanier, M. T., and Walkley, S. U. (2011) Endosomal/lysosomal processing of gangliosides affects neuronal cholesterol sequestration in Niemann-Pick disease type C. *The American journal of pathology* **179**, 890-902
547. Shen, D., Wang, X., Li, X., Zhang, X., Yao, Z., Dibble, S., Dong, X. P., Yu, T., Lieberman, A. P., Showalter, H. D., and Xu, H. (2012) Lipid storage disorders block lysosomal trafficking by inhibiting a TRP channel and lysosomal calcium release. *Nature communications* **3**, 731
548. Rabouille, C. (2017) Pathways of Unconventional Protein Secretion. *Trends in cell biology* **27**, 230-240
549. Ponpuak, M., Mandell, M. A., Kimura, T., Chauhan, S., Cleyrat, C., and Deretic, V. (2015) Secretory autophagy. *Current opinion in cell biology* **35**, 106-116
550. Ejlerskov, P., Rasmussen, I., Nielsen, T. T., Bergstrom, A. L., Tohyama, Y., Jensen, P. H., and Vilhardt, F. (2013) Tubulin polymerization-promoting protein (TPPP/p25alpha)

- promotes unconventional secretion of alpha-synuclein through exophagy by impairing autophagosome-lysosome fusion. *The Journal of biological chemistry* **288**, 17313-17335
551. Nilsson, P., Loganathan, K., Sekiguchi, M., Matsuba, Y., Hui, K., Tsubuki, S., Tanaka, M., Iwata, N., Saito, T., and Saido, T. C. (2013) Abeta secretion and plaque formation depend on autophagy. *Cell reports* **5**, 61-69
552. Raposo, G., and Stoorvogel, W. (2013) Extracellular vesicles: exosomes, microvesicles, and friends. *The Journal of cell biology* **200**, 373-383
553. Iguchi, Y., Eid, L., Parent, M., Soucy, G., Bareil, C., Riku, Y., Kawai, K., Takagi, S., Yoshida, M., Katsuno, M., Sobue, G., and Julien, J. P. (2016) Exosome secretion is a key pathway for clearance of pathological TDP-43. *Brain : a journal of neurology* **139**, 3187-3201
554. Diaz-Hidalgo, L., Altuntas, S., Rossin, F., D'Eletto, M., Marsella, C., Farrace, M. G., Falasca, L., Antonioli, M., Fimia, G. M., and Piacentini, M. (2016) Transglutaminase type 2-dependent selective recruitment of proteins into exosomes under stressful cellular conditions. *Biochimica et biophysica acta* **1863**, 2084-2092
555. Zhang, X., Abels, E. R., Redzic, J. S., Margulis, J., Finkbeiner, S., and Breakefield, X. O. (2016) Potential Transfer of Polyglutamine and CAG-Repeat RNA in Extracellular Vesicles in Huntington's Disease: Background and Evaluation in Cell Culture. *Cellular and molecular neurobiology* **36**, 459-470
556. Eitan, E., Suire, C., Zhang, S., and Mattson, M. P. (2016) Impact of lysosome status on extracellular vesicle content and release. *Ageing research reviews* **32**, 65-74

557. Baixauli, F., Lopez-Otin, C., and Mittelbrunn, M. (2014) Exosomes and autophagy: coordinated mechanisms for the maintenance of cellular fitness. *Frontiers in immunology* **5**, 403
558. Croese, T., and Furlan, R. (2018) Extracellular vesicles in neurodegenerative diseases. *Molecular aspects of medicine* **60**, 52-61
559. Hessvik, N. P., Overbye, A., Brech, A., Torgersen, M. L., Jakobsen, I. S., Sandvig, K., and Llorente, A. (2016) PIKfyve inhibition increases exosome release and induces secretory autophagy. *Cellular and molecular life sciences : CMLS* **73**, 4717-4737
560. Jeon, I., Cicchetti, F., Cisbani, G., Lee, S., Li, E., Bae, J., Lee, N., Li, L., Im, W., Kim, M., Kim, H. S., Oh, S. H., Kim, T. A., Ko, J. J., Aube, B., Oueslati, A., Kim, Y. J., and Song, J. (2016) Human-to-mouse prion-like propagation of mutant huntingtin protein. *Acta neuropathologica* **132**, 577-592
561. Crawford, N. (1971) The presence of contractile proteins in platelet microparticles isolated from human and animal platelet-free plasma. *British journal of haematology* **21**, 53-69
562. Anderson, H. C. (1969) Vesicles associated with calcification in the matrix of epiphyseal cartilage. *The Journal of cell biology* **41**, 59-72
563. Dvorak, H. F., Quay, S. C., Orenstein, N. S., Dvorak, A. M., Hahn, P., Bitzer, A. M., and Carvalho, A. C. (1981) Tumor shedding and coagulation. *Science* **212**, 923-924
564. George, J. N., Thoi, L. L., McManus, L. M., and Reimann, T. A. (1982) Isolation of human platelet membrane microparticles from plasma and serum. *Blood* **60**, 834-840
565. Pan, B. T., Teng, K., Wu, C., Adam, M., and Johnstone, R. M. (1985) Electron microscopic evidence for externalization of the transferrin receptor in vesicular form in sheep reticulocytes. *The Journal of cell biology* **101**, 942-948

566. Harding, C., Heuser, J., and Stahl, P. (1983) Receptor-mediated endocytosis of transferrin and recycling of the transferrin receptor in rat reticulocytes. *The Journal of cell biology* **97**, 329-339
567. Johnstone, R. M., Adam, M., Hammond, J. R., Orr, L., and Turbide, C. (1987) Vesicle formation during reticulocyte maturation. Association of plasma membrane activities with released vesicles (exosomes). *The Journal of biological chemistry* **262**, 9412-9420
568. Colombo, M., Raposo, G., and Thery, C. (2014) Biogenesis, secretion, and intercellular interactions of exosomes and other extracellular vesicles. *Annual review of cell and developmental biology* **30**, 255-289
569. Atkin-Smith, G. K., Paone, S., Zanker, D. J., Duan, M., Phan, T. K., Chen, W., Hulett, M. D., and Poon, I. K. (2017) Isolation of cell type-specific apoptotic bodies by fluorescence-activated cell sorting. *Scientific reports* **7**, 39846
570. Valencia, K., and Lecanda, F. (2016) Microvesicles: Isolation, Characterization for In Vitro and In Vivo Procedures. *Methods Mol Biol* **1372**, 181-192
571. Szatanek, R., Baj-Krzyworzeka, M., Zimoch, J., Lekka, M., Siedlar, M., and Baran, J. (2017) The Methods of Choice for Extracellular Vesicles (EVs) Characterization. *International journal of molecular sciences* **18**
572. Hanson, P. I., and Cashikar, A. (2012) Multivesicular body morphogenesis. *Annual review of cell and developmental biology* **28**, 337-362
573. Stuffers, S., Sem Wegner, C., Stenmark, H., and Brech, A. (2009) Multivesicular endosome biogenesis in the absence of ESCRTs. *Traffic (Copenhagen, Denmark)* **10**, 925-937

574. Edgar, J. R., Eden, E. R., and Futter, C. E. (2014) Hrs- and CD63-dependent competing mechanisms make different sized endosomal intraluminal vesicles. *Traffic (Copenhagen, Denmark)* **15**, 197-211
575. Trajkovic, K., Hsu, C., Chiantia, S., Rajendran, L., Wenzel, D., Wieland, F., Schwille, P., Brugger, B., and Simons, M. (2008) Ceramide triggers budding of exosome vesicles into multivesicular endosomes. *Science* **319**, 1244-1247
576. Ghossoub, R., Lembo, F., Rubio, A., Gaillard, C. B., Bouchet, J., Vitale, N., Slavik, J., Machala, M., and Zimmermann, P. (2014) Syntenin-ALIX exosome biogenesis and budding into multivesicular bodies are controlled by ARF6 and PLD2. *Nature communications* **5**, 3477
577. Hoshino, D., Kirkbride, K. C., Costello, K., Clark, E. S., Sinha, S., Grega-Larson, N., Tyska, M. J., and Weaver, A. M. (2013) Exosome secretion is enhanced by invadopodia and drives invasive behavior. *Cell reports* **5**, 1159-1168
578. Dreux, M., Garaigorta, U., Boyd, B., Decembre, E., Chung, J., Whitten-Bauer, C., Wieland, S., and Chisari, F. V. (2012) Short-range exosomal transfer of viral RNA from infected cells to plasmacytoid dendritic cells triggers innate immunity. *Cell host & microbe* **12**, 558-570
579. Chairoungdua, A., Smith, D. L., Pochard, P., Hull, M., and Caplan, M. J. (2010) Exosome release of beta-catenin: a novel mechanism that antagonizes Wnt signaling. *The Journal of cell biology* **190**, 1079-1091
580. Kosaka, N., Iguchi, H., Yoshioka, Y., Takeshita, F., Matsuki, Y., and Ochiya, T. (2010) Secretory mechanisms and intercellular transfer of microRNAs in living cells. *The Journal of biological chemistry* **285**, 17442-17452

581. van Niel, G., Charrin, S., Simoes, S., Romao, M., Rochin, L., Saftig, P., Marks, M. S., Rubinstein, E., and Raposo, G. (2011) The tetraspanin CD63 regulates ESCRT-independent and -dependent endosomal sorting during melanogenesis. *Developmental cell* **21**, 708-721
582. Mobius, W., Ohno-Iwashita, Y., van Donselaar, E. G., Oorschot, V. M., Shimada, Y., Fujimoto, T., Heijnen, H. F., Geuze, H. J., and Slot, J. W. (2002) Immunoelectron microscopic localization of cholesterol using biotinylated and non-cytolytic perfringolysin O. *The journal of histochemistry and cytochemistry : official journal of the Histochemistry Society* **50**, 43-55
583. White, I. J., Bailey, L. M., Aghakhani, M. R., Moss, S. E., and Futter, C. E. (2006) EGF stimulates annexin 1-dependent inward vesiculation in a multivesicular endosome subpopulation. *The EMBO journal* **25**, 1-12
584. Wubbolts, R., Leckie, R. S., Veenhuizen, P. T., Schwarzmann, G., Mobius, W., Hoernschemeyer, J., Slot, J. W., Geuze, H. J., and Stoorvogel, W. (2003) Proteomic and biochemical analyses of human B cell-derived exosomes. Potential implications for their function and multivesicular body formation. *The Journal of biological chemistry* **278**, 10963-10972
585. Brouwers, J. F., Aalberts, M., Jansen, J. W., van Niel, G., Wauben, M. H., Stout, T. A., Helms, J. B., and Stoorvogel, W. (2013) Distinct lipid compositions of two types of human prostasomes. *Proteomics* **13**, 1660-1666
586. Tricarico, C., Clancy, J., and D'Souza-Schorey, C. (2016) Biology and biogenesis of shed microvesicles. *Small GTPases*, 1-13

587. Booth, A. M., Fang, Y., Fallon, J. K., Yang, J. M., Hildreth, J. E., and Gould, S. J. (2006) Exosomes and HIV Gag bud from endosome-like domains of the T cell plasma membrane. *The Journal of cell biology* **172**, 923-935
588. Bianco, F., Perrotta, C., Novellino, L., Francolini, M., Riganti, L., Menna, E., Saglietti, L., Schuchman, E. H., Furlan, R., Clementi, E., Matteoli, M., and Verderio, C. (2009) Acid sphingomyelinase activity triggers microparticle release from glial cells. *The EMBO journal* **28**, 1043-1054
589. Savina, A., Vidal, M., and Colombo, M. I. (2002) The exosome pathway in K562 cells is regulated by Rab11. *Journal of cell science* **115**, 2505-2515
590. Savina, A., Fader, C. M., Damiani, M. T., and Colombo, M. I. (2005) Rab11 promotes docking and fusion of multivesicular bodies in a calcium-dependent manner. *Traffic (Copenhagen, Denmark)* **6**, 131-143
591. Ostrowski, M., Carmo, N. B., Krumeich, S., Fanget, I., Raposo, G., Savina, A., Moita, C. F., Schauer, K., Hume, A. N., Freitas, R. P., Goud, B., Benaroch, P., Hacohen, N., Fukuda, M., Desnos, C., Seabra, M. C., Darchen, F., Amigorena, S., Moita, L. F., and Thery, C. (2010) Rab27a and Rab27b control different steps of the exosome secretion pathway. *Nature cell biology* **12**, 19-30; sup pp 11-13
592. Hsu, C., Morohashi, Y., Yoshimura, S., Manrique-Hoyos, N., Jung, S., Lauterbach, M. A., Bakhti, M., Gronborg, M., Mobius, W., Rhee, J., Barr, F. A., and Simons, M. (2010) Regulation of exosome secretion by Rab35 and its GTPase-activating proteins TBC1D10A-C. *The Journal of cell biology* **189**, 223-232
593. Hong, W., and Lev, S. (2014) Tethering the assembly of SNARE complexes. *Trends in cell biology* **24**, 35-43

594. Fader, C. M., Sanchez, D. G., Mestre, M. B., and Colombo, M. I. (2009) TI-VAMP/VAMP7 and VAMP3/cellubrevin: two v-SNARE proteins involved in specific steps of the autophagy/multivesicular body pathways. *Biochimica et biophysica acta* **1793**, 1901-1916
595. Gross, J. C., Chaudhary, V., Bartscherer, K., and Boutros, M. (2012) Active Wnt proteins are secreted on exosomes. *Nature cell biology* **14**, 1036-1045
596. Yanez-Mo, M., Siljander, P. R., Andreu, Z., Zavec, A. B., Borrás, F. E., Buzas, E. I., Buzas, K., Casal, E., Cappello, F., Carvalho, J., Colas, E., Cordeiro-da Silva, A., Fais, S., Falcon-Perez, J. M., Ghobrial, I. M., Giesel, B., Gimona, M., Graner, M., Gursel, I., Gursel, M., Heegaard, N. H., Hendrix, A., Kierulf, P., Kokubun, K., Kosanovic, M., Kralj-Iglic, V., Kramer-Albers, E. M., Laitinen, S., Lasser, C., Lener, T., Ligeti, E., Line, A., Lipps, G., Llorente, A., Lotvall, J., Mancek-Keber, M., Marcilla, A., Mittelbrunn, M., Nazarenko, I., Nolte-'t Hoen, E. N., Nyman, T. A., O'Driscoll, L., Olivan, M., Oliveira, C., Pallinger, E., Del Portillo, H. A., Reventos, J., Rigau, M., Rohde, E., Sammar, M., Sanchez-Madrid, F., Santarem, N., Schallmoser, K., Ostenfeld, M. S., Stoorvogel, W., Stukelj, R., Van der Grein, S. G., Vasconcelos, M. H., Wauben, M. H., and De Wever, O. (2015) Biological properties of extracellular vesicles and their physiological functions. *Journal of extracellular vesicles* **4**, 27066
597. Fevrier, B., Vilette, D., Archer, F., Loew, D., Faigle, W., Vidal, M., Laude, H., and Raposo, G. (2004) Cells release prions in association with exosomes. *Proceedings of the National Academy of Sciences of the United States of America* **101**, 9683-9688
598. Perez-Gonzalez, R., Gauthier, S. A., Kumar, A., and Levy, E. (2012) The exosome secretory pathway transports amyloid precursor protein carboxyl-terminal fragments from

- the cell into the brain extracellular space. *The Journal of biological chemistry* **287**, 43108-43115
599. Sharples, R. A., Vella, L. J., Nisbet, R. M., Naylor, R., Perez, K., Barnham, K. J., Masters, C. L., and Hill, A. F. (2008) Inhibition of gamma-secretase causes increased secretion of amyloid precursor protein C-terminal fragments in association with exosomes. *FASEB J* **22**, 1469-1478
600. Rajendran, L., Honsho, M., Zahn, T. R., Keller, P., Geiger, K. D., Verkade, P., and Simons, K. (2006) Alzheimer's disease beta-amyloid peptides are released in association with exosomes. *Proceedings of the National Academy of Sciences of the United States of America* **103**, 11172-11177
601. Joshi, P., Turola, E., Ruiz, A., Bergami, A., Libera, D. D., Benussi, L., Giussani, P., Magnani, G., Comi, G., Legname, G., Ghidoni, R., Furlan, R., Matteoli, M., and Verderio, C. (2014) Microglia convert aggregated amyloid-beta into neurotoxic forms through the shedding of microvesicles. *Cell death and differentiation* **21**, 582-593
602. Yuyama, K., Sun, H., Sakai, S., Mitsutake, S., Okada, M., Tahara, H., Furukawa, J., Fujitani, N., Shinohara, Y., and Igarashi, Y. (2014) Decreased amyloid-beta pathologies by intracerebral loading of glycosphingolipid-enriched exosomes in Alzheimer model mice. *The Journal of biological chemistry* **289**, 24488-24498
603. Cicchetti, F., Lacroix, S., Cisbani, G., Vallieres, N., Saint-Pierre, M., St-Amour, I., Tolouei, R., Skepper, J. N., Hauser, R. A., Mantovani, D., Barker, R. A., and Freeman, T. B. (2014) Mutant huntingtin is present in neuronal grafts in Huntington disease patients. *Annals of neurology* **76**, 31-42

604. Pearce, M. M., Spartz, E. J., Hong, W., Luo, L., and Kopito, R. R. (2015) Prion-like transmission of neuronal huntingtin aggregates to phagocytic glia in the *Drosophila* brain. *Nature communications* **6**, 6768
605. Yuyama, K., Yamamoto, N., and Yanagisawa, K. (2008) Accelerated release of exosome-associated GM1 ganglioside (GM1) by endocytic pathway abnormality: another putative pathway for GM1-induced amyloid fibril formation. *Journal of neurochemistry* **105**, 217-224
606. Momen-Heravi, F., Balaj, L., Alian, S., Mantel, P. Y., Halleck, A. E., Trachtenberg, A. J., Soria, C. E., Oquin, S., Bonebreak, C. M., Saracoglu, E., Skog, J., and Kuo, W. P. (2013) Current methods for the isolation of extracellular vesicles. *Biological chemistry* **394**, 1253-1262
607. Vella, L. J., and Hill, A. F. (2008) Generation of cell lines propagating infectious prions and the isolation and characterization of cell-derived exosomes. *Methods Mol Biol* **459**, 69-82
608. Bellingham, S. A., Guo, B. B., Coleman, B. M., and Hill, A. F. (2012) Exosomes: vehicles for the transfer of toxic proteins associated with neurodegenerative diseases? *Frontiers in physiology* **3**, 124
609. Yoshioka, Y., Konishi, Y., Kosaka, N., Katsuda, T., Kato, T., and Ochiya, T. (2013) Comparative marker analysis of extracellular vesicles in different human cancer types. *Journal of extracellular vesicles* **2**
610. Revenfeld, A. L., Baek, R., Nielsen, M. H., Stensballe, A., Varming, K., and Jorgensen, M. (2014) Diagnostic and prognostic potential of extracellular vesicles in peripheral blood. *Clinical therapeutics* **36**, 830-846

611. Mathivanan, S., Fahner, C. J., Reid, G. E., and Simpson, R. J. (2012) ExoCarta 2012: database of exosomal proteins, RNA and lipids. *Nucleic acids research* **40**, D1241-1244
612. Kalra, H., Simpson, R. J., Ji, H., Aikawa, E., Altevogt, P., Askenase, P., Bond, V. C., Borrás, F. E., Breakefield, X., Budnik, V., Buzas, E., Camussi, G., Clayton, A., Cocucci, E., Falcon-Perez, J. M., Gabrielsson, S., Gho, Y. S., Gupta, D., Harsha, H. C., Hendrix, A., Hill, A. F., Inal, J. M., Jenster, G., Kramer-Albers, E. M., Lim, S. K., Llorente, A., Lotvall, J., Marcilla, A., Mincheva-Nilsson, L., Nazarenko, I., Nieuwland, R., Nolte-'t Hoen, E. N., Pandey, A., Patel, T., Piper, M. G., Pluchino, S., Prasad, T. S., Rajendran, L., Raposo, G., Record, M., Reid, G. E., Sanchez-Madrid, F., Schiffelers, R. M., Siljander, P., Stensballe, A., Stoorvogel, W., Taylor, D., Thery, C., Valadi, H., van Balkom, B. W., Vazquez, J., Vidal, M., Wauben, M. H., Yanez-Mo, M., Zoeller, M., and Mathivanan, S. (2012) Vesiclepedia: a compendium for extracellular vesicles with continuous community annotation. *PLoS biology* **10**, e1001450
613. Kim, D. K., Kang, B., Kim, O. Y., Choi, D. S., Lee, J., Kim, S. R., Go, G., Yoon, Y. J., Kim, J. H., Jang, S. C., Park, K. S., Choi, E. J., Kim, K. P., Desiderio, D. M., Kim, Y. K., Lotvall, J., Hwang, D., and Gho, Y. S. (2013) EVpedia: an integrated database of high-throughput data for systemic analyses of extracellular vesicles. *Journal of extracellular vesicles* **2**
614. Carmichael, J., Chatellier, J., Woolfson, A., Milstein, C., Fersht, A. R., and Rubinsztein, D. C. (2000) Bacterial and yeast chaperones reduce both aggregate formation and cell death in mammalian cell models of Huntington's disease. *Proceedings of the National Academy of Sciences of the United States of America* **97**, 9701-9705

615. Perrin, V., Regulier, E., Abbas-Terki, T., Hassig, R., Brouillet, E., Aebischer, P., Luthi-Carter, R., and Deglon, N. (2007) Neuroprotection by Hsp104 and Hsp27 in lentiviral-based rat models of Huntington's disease. *Molecular therapy : the journal of the American Society of Gene Therapy* **15**, 903-911
616. Schneider, J. S., Roeltgen, D. P., Rothblat, D. S., Chapas-Crilly, J., Seraydarian, L., and Rao, J. (1995) GM1 ganglioside treatment of Parkinson's disease: an open pilot study of safety and efficacy. *Neurology* **45**, 1149-1154
617. Schneider, J. S., Roeltgen, D. P., Mancall, E. L., Chapas-Crilly, J., Rothblat, D. S., and Tatarian, G. T. (1998) Parkinson's disease: improved function with GM1 ganglioside treatment in a randomized placebo-controlled study. *Neurology* **50**, 1630-1636
618. Schneider, J. S., Sendek, S., Daskalakis, C., and Cambi, F. (2010) GM1 ganglioside in Parkinson's disease: Results of a five year open study. *Journal of the neurological sciences* **292**, 45-51
619. Sheng, Z., Otani, H., Brown, M. S., and Goldstein, J. L. (1995) Independent regulation of sterol regulatory element-binding proteins 1 and 2 in hamster liver. *Proceedings of the National Academy of Sciences of the United States of America* **92**, 935-938
620. Hua, X., Sakai, J., Brown, M. S., and Goldstein, J. L. (1996) Regulated cleavage of sterol regulatory element binding proteins requires sequences on both sides of the endoplasmic reticulum membrane. *The Journal of biological chemistry* **271**, 10379-10384
621. Theusch, E., Kim, K., Stevens, K., Smith, J. D., Chen, Y. I., Rotter, J. I., Nickerson, D. A., and Medina, M. W. (2017) Statin-induced expression change of INSIG1 in lymphoblastoid cell lines correlates with plasma triglyceride statin response in a sex-specific manner. *The pharmacogenomics journal* **17**, 222-229

622. Vock, C., Doring, F., and Nitz, I. (2008) Transcriptional regulation of HMG-CoA synthase and HMG-CoA reductase genes by human ACBP. *Cellular physiology and biochemistry : international journal of experimental cellular physiology, biochemistry, and pharmacology* **22**, 515-524
623. Sanchez, H. B., Yieh, L., and Osborne, T. F. (1995) Cooperation by sterol regulatory element-binding protein and Sp1 in sterol regulation of low density lipoprotein receptor gene. *The Journal of biological chemistry* **270**, 1161-1169

**Appendix I: Mutant HTT impairs nuclear transport of
mSREBP2 and causes a defective upregulation of
transcription of cholesterologenic genes upon culture in
lipoprotein-deficient medium**

Data presented in this appendix were generated in collaboration with Mrs. Alba Di Pardo and will be submitted for publication as a co-authored paper (Di Pardo A., Morales L.C, Maglione V., Lingrell S., Horkey M., Baker G., Kar S., Wozniak R. and Sipione S. In preparation).

Nuclear transport of mature SREBP2 is impaired in HD models

As described in chapter 3, the expression of cholesterologenic genes is affected in HD (214,287). During my graduate studies, I contributed to work aimed to determine the underlying mechanisms of such impairment. We investigated the effects of muHTT expression on SREBP2, the factor responsible for the transcription of cholesterologenic and other lipid metabolism-related genes (619,620).

Work performed by Dr. Di Pardo in the Sipione laboratory revealed that in HD cells and animal models, the mature form of SREBP2 (mSREBP2) is mislocalized to the cell cytoplasm (Figs. A1-C). It is important to mention that total levels of mSREBP2 were comparable between WT and YAC128 brain tissue (data not shown), suggesting that the processing of the precursor form of SREBP2 is not affected in HD models.

Further studies showed that the reason for mSREBP2 mislocalization in HD cells, is that muHTT binds to, and sequesters mSREBP2 in a complex with importin β , the protein that shuttles mSREBP2 to the nucleus, preventing its nuclear entry and causing the transcriptional defects observed in cell and animal models of HD (214,287).

HD cells have impaired regulation of transcription of cholesterologenic genes upon culture in lipoprotein-deficient medium

To determine the extent to which impaired nuclear localization of mSREBP2 affects transcription of cholesterologenic genes, I measured the expression of two mSREBP2 gene targets, hydroxymethylglutaryl CoA reductase (*HMGCR*) and 24-dehydrocholesterol reductase (*DHCR24*) in HD cells, in basal conditions, as well as during treatments that are known to activate the mevalonate pathway. There was no difference in the mean basal expression of either *HMGCR*

or *DHCR24* genes between human primary HD fibroblasts and controls (Fig. A2-A). When control fibroblasts were cultured in lipoprotein-deficient medium (LPDM) for 48 h, expression of *HMGCR* and *DHCR24* genes was upregulated by 2-fold, approximately. HD fibroblasts cultured under the same conditions showed reduced upregulation of the same two genes (Fig. A2-B).

Next, I used statins to inhibit HMGCR and stimulate transcription of cholesterologenic genes (621). Upon treatment with pravastatin (125 μ M for 48 h), WT fibroblasts increased the transcription of *HMGCR*, but HD fibroblasts failed to do so (Fig. A2-C).

Similar results were obtained in two clones of immortalized mouse astrocytes stably expressing an N-terminal fragment (548 a.a.) of HTT containing either 15 CAG repeats (15Q) or 128 CAG repeats (128Q). When cultured in regular medium containing cholesterol (RM), expression of *Hmgcr* was similar between cells expressing wtHTT or muHTT. However, after 48 h of culture in LPDM, both clones of astrocytes expressing muHTT had decreased upregulation of *Hmgcr* when compared to the two clones expressing wtHTT (Fig. A3). Altogether, these data suggest that in basal conditions, when cholesterol is obtained from the medium, basal transcription of genes of the mevalonate pathway is normal in HD cells. However, in conditions when the activity of the mevalonate pathway has to be increased to produce cholesterol, HD cells fail to upregulate cholesterologenic gene transcription.

Discussion

Work in the Sipione laboratory, to which I contributed, has shed light on the mechanism behind the impairment of the mevalonate pathway in HD (Di Pardo, Morales, et al. In preparation).

We have shown that muHTT interacts with the mSREBP2-importin β complex and sequesters it in the cytoplasm. My experiments showed that the consequence of this dysfunction, is that HD

cells fail to properly upregulate the transcription of cholesterologenic enzymes when cultured in conditions of low availability of cholesterol.

However, I did not observe differences in the transcription levels of cholesterologenic enzymes in basal conditions i.e. when cells were grown in the presence of lipoprotein-containing serum, which provides most of the cholesterol the cells need. A possible explanation is that other transcription factors (i.e. Sp1) may regulate the basal transcription of these genes when SREPB2 activation is limited (622,623). In these conditions, the mevalonate pathway is still active to ensure proper supply of isoprenoids, molecules that are essential for protein prenylation, mitochondrial oxidative phosphorylation and protein glycosylation.

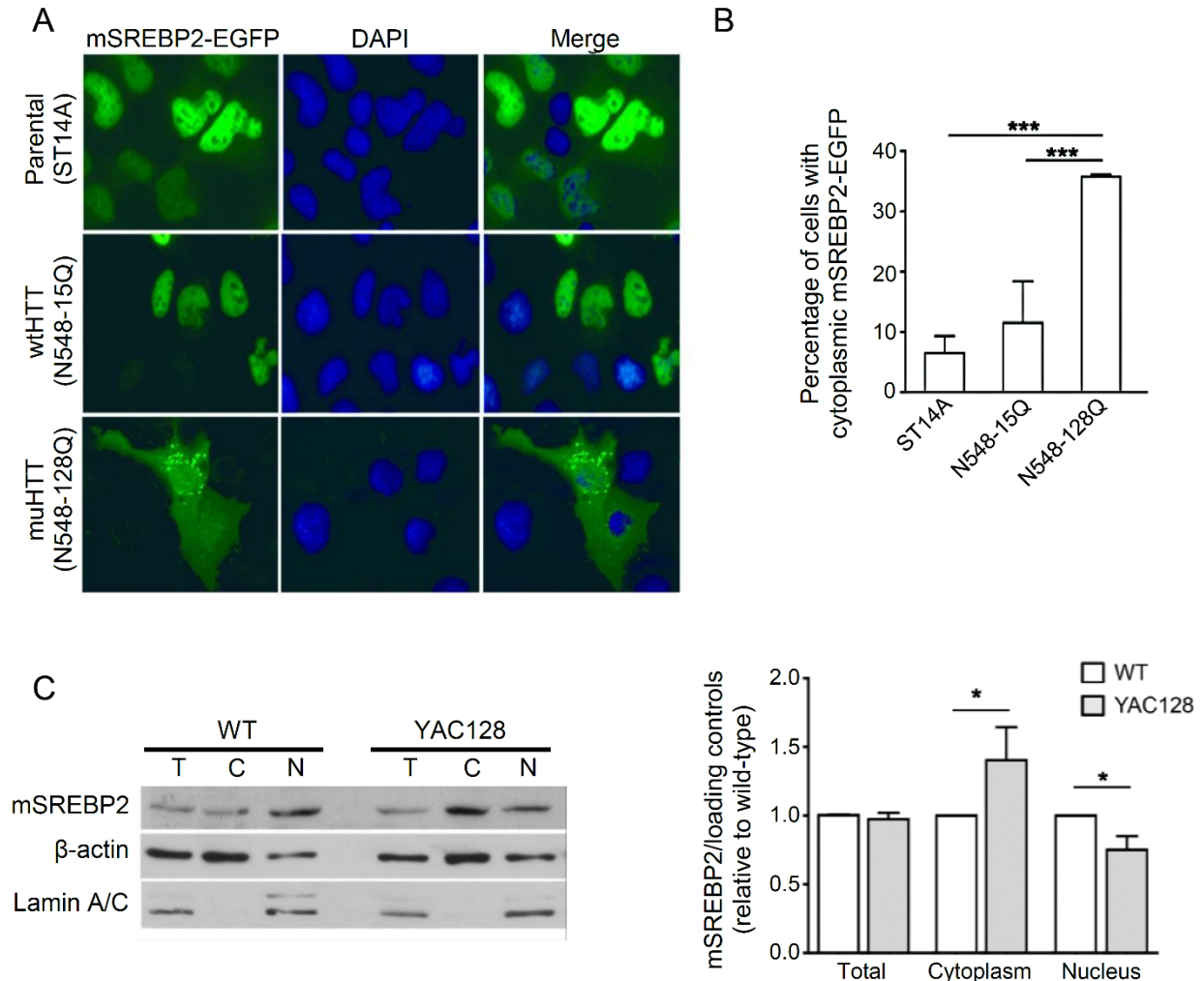
In HD, there is significant evidence of an impairment of the cholesterol biosynthetic pathway at various levels. Transcription of cholesterologenic genes is reduced in immortalized striatal cells expressing muHTT (214), as well in the brains of established HD mouse models, and even in human HD brain tissue and peripheral cells (287). It was also shown that biosynthetic precursors of cholesterol, such as lanosterol and lathosterol are reduced at early disease stages across various mouse models of HD, before any detectable motor phenotype, suggesting that the mevalonate pathway might be impaired before the onset of neuronal degeneration (287-289). A few papers have reported intracellular accumulation of cholesterol in HD cells. However, most of these observations were made by using filipin staining, a non-quantitative measure of cholesterol accumulation. In other neurodegenerative diseases in which cholesterol misdistribution may occur such as AD and NPC, cells show strong positivity for filipin in the endosomal or lysosomal compartment, in spite of the fact that total cholesterol mass remains unchanged when measured by quantitative techniques (331,344,345). In fact, total cholesterol mass is either normal, or decreased only at very late stages of the disease in HD mouse models as well (288,289). To my knowledge,

one single study reported increased amounts of cholesterol in the striatum of HdhQ111 mice measured by quantitative techniques. However, the increase was driven by esterified cholesterol and occurred concomitantly with an increase in triglycerides. Authors interpreted this phenomenon as to be secondary to defects in lipid droplet clearance due to a failure in selective autophagy (341).

It is currently unknown why levels of cholesterol remain unchanged in HD, despite the downregulation of the mevalonate pathway. It is possible that cells (or organs) may compensate any reduction in production of cholesterol by reducing its catabolism. In fact, mouse models of HD (290), as well as human patients (332,334), have reduced brain cholesterol catabolism as measured by the abundance of 24-OH-Chol in the plasma, since the origin of this hydroxylated form of cholesterol is exclusively neuronal. Although it is tempting to hypothesize that reduction of 24-OH-Chol in the plasma is secondary to a compensatory reduction in neuronal cholesterol turnover, it may be simply an indication of neuronal dysfunction/degeneration.

Figures

Figure A1. Nuclear transport of mature SREBP2 is impaired in HD models



A) Representative confocal microscopy images showing the intracellular localization of mSREBP2-EGFP transgene in transiently transfected parental striatal cells (ST14A) and in cells expressing an N-terminal fragment of wild-type (N548-15Q) or mutant (N548-128Q) HTT. Cell nuclei were counterstained with DAPI. Notice the abnormal cytoplasmic mSREBP2-EGFP localization in cells expressing the muHTT fragment.

B) Percentage of cells containing cytoplasmic mSREBP2-EGFP in parental (ST14A), and in cells expressing N548-15Q or N548-128 HTT fragments. Eighty cells were counted per group in three independent experiments. Bars show mean values \pm SD. *** p <0.001.

C) Representative blot and densitometric analysis of Total (T), cytoplasmic (C) and nuclear (N) fractions prepared from cerebral cortex of YAC128 mice and probed with anti-SREBP2 antibodies to detect the cleaved mature form of SREBP2 (mSREBP2). β -actin was used as loading control for total and cytoplasmic fractions, while lamin A/C was used as a loading control for nuclear fractions. The graph shows the densitometric analysis of 3 independent experiments. Bars show mean values \pm SD. * p <0.05.

(Figure from DiPardo A, Morales LC, et al. Manuscript in preparation)

Figure A2. HD fibroblasts do not efficiently upregulate the transcription of cholesterologenic genes upon culture in lipoprotein-deficient medium (LPDM)

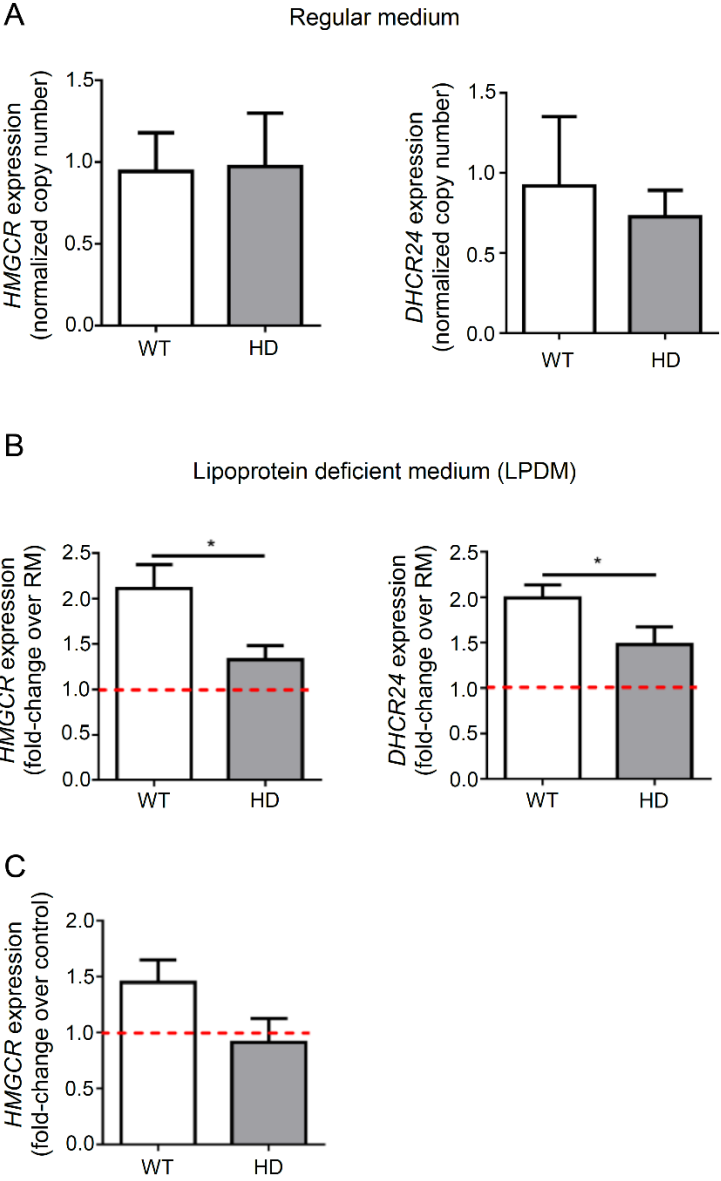


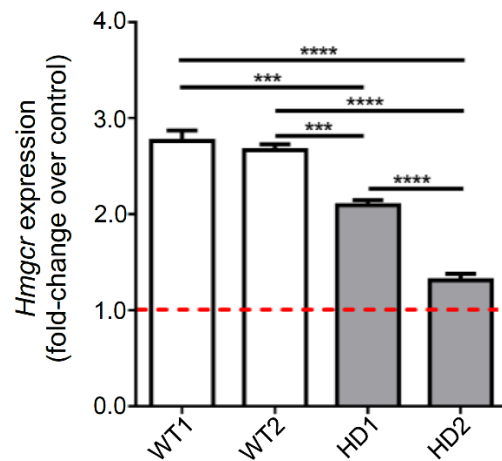
Figure A2. HD fibroblasts do not efficiently upregulate the transcription of cholesterologenic genes upon culture in lipoprotein-deficient medium (LPDM)

A) Analysis of hydroxymethylglutaryl CoA reductase (*HMGCR*) and 24-dehydrocholesterol reductase (*DHCR24*) gene expression in primary fibroblast lines obtained from healthy controls and from HD patients, cultured in medium containing 10% fetal bovine serum (regular medium, RM, WT N=3; HD N=4. Bars show mean values \pm SD.

B) Changes in gene expression of *HMGCR* and *DHCR24* in WT and HD human fibroblasts cultured in lipoprotein-deficient medium (LPDM) for 48 h. Values are expressed as fold-change compared to regular medium (red line) for each genotype. WT N=3; HD N=4. Bars show mean values \pm SD. Two-tailed Student's t-test. * $p < 0.05$.

C) Changes in expression of *HMGCR* in WT and HD human fibroblasts after treatment with Pravastatin (125 μ M, 48 h). Values are expressed as fold-change compared to untreated cells in each genotype. WT N=2; HD N=2. Bars show mean values \pm SD.

Figure A3. Decreased upregulation of *Hmgcr* gene in mouse HD astrocytes upon culture in lipoprotein-deficient medium (LPDM)



Changes in gene expression of *Hmgcr* in two clones of immortalized mouse astrocytes stably expressing N548-HTT fragment with 15 CAG repeats (WT) or 128 CAG repeats (HD). Cells were cultured in lipoprotein-deficient medium (LPDM) for 48 h. Gene expression is presented as fold-change compared to regular medium (RM, red line) for each cell clone and genotype. Bars show mean values \pm SD of technical replicates of one single experiment. One-way ANOVA with Tukey-Kramer post-hoc correction. *** $p < 0.001$, **** $p < 0.0001$.

Appendix II: Tables

Table 1. Sequence of primers used in this thesis

<u>Gene</u>	<u>Species</u>	<u>Forward</u>	<u>Reverse</u>
<i>DHCR24</i>	Human	cgc gtg tga aac act ttg aa	gca gtc ggc ata cag cat c
<i>HMGCR</i>	Human	ctg tca ttc cag cca agg tt	tgg cag agc cca cta aat tc
<i>Lamp1</i>	Mouse	aat ggc aca acg tgt ata atg g	ggc agg gaa atg ttc acg
<i>Atp6v1h</i>	Mouse	gct cac gat gtt gga gaa tat gt	gca tgt ggt tca cca act
<i>Ctsd</i>	Mouse	agc cag tgt cag agt tac tca aaa	aaa gac tgt gaa aca ctg c
<i>Rab7</i>	Mouse	cca agg cca tca atg t	cag gga att cat tgt aca gtt cc
<u>Housekeeping genes</u>			
<i>36B4</i>	Human	gat gcc cag gga aga cag	aca atg aaa cat ttc gga taa tca
<i>EIF4A2</i>	Human	aac tgg ctc aac aga tcc aaa	cct gca gtt ttt gca ttt ca
<i>ATP5B</i>	Human	ttg ctg agg tct tca cag gtc	gcc tgt tct ggg aga tgg t
<i>Atp5b</i>	Mouse	tcc agc aga ttt tag cag gtg	gct gga gtc cct cac gac
<i>Eif4a2</i>	Mouse	tcg aaa tga aat gca gaa gtt g	gct tcg tcc aaa acg aac at
<i>36b4</i>	Mouse	act ggt cta gga ccc gag aag	tcc cac ctt gtc tcc agt ct
<i>Ppia</i>	Mouse	gaa agg att tgg cta taa ggg	gat gcc agg acc tgt atg ctt

Table 2. List of antibodies used in this thesis

<u>Antibody</u>	<u>Raised in</u>	<u>Cat. No</u>	<u>Brand/Provided by</u>
AIP1 (ALIX)	Mouse	611621	BD
Calnexin	Rabbit	ADI-SPA-865	Enzo
COX IV	Mouse	ab14744	ABCAM
Flotillin-1	Mouse	610820	BD
GFP	Goat		Dr. Berthiaume/UofA
GFP	Mouse		Dr. Berthiaume/UofA
GFP	Mouse	sc-9996	Santa Cruz
GFP	Rabbit		Dr. Berthiaume/UofA
GFP	Rabbit	2956	Cell Signaling
HSP90	Rabbit	ADI-SPA-846	Enzo
HTT MAB5492	Mouse	MAB5492	Millipore
HTT N-18	Rabbit		Dr. Truant/UBC
HTT-MAB2166	Mouse	MAB2166	Millipore
HTT-PolyQ	Mouse	MAB1574	Millipore
HTT-PW0595	Rabbit	PW0595	Enzo
Lamin A/C	Rabbit	2032	Cell Signaling
LC3B	Rabbit	2775	Cell Signaling
p62	Mouse	ab56416	ABCAM
pSer403 p62	Rabbit	GTX128171	GeneTex
RAB11	Mouse	610656	BD
RAB7	Rabbit	sc-10767	Santa Cruz
RAS	Mouse	05-516	Millipore
SREBP2	Rabbit	ab30682	ABCAM
TSG101	Rabbit	ab125011	ABCAM
Tubulin	Mouse	T5201	Sigma
Tubulin	Rabbit	2125	Cell Signaling
Ubiquitin	Mouse	3936	Cell Signaling
Ubiquitin-K63	Rabbit	5621	Cell Signaling
VDAC1	Mouse	MABN504	Millipore